EARTHQUAKE ENGINEERING RESEARCH CENTER

DYNAMIC BEHAVIOR OF A PEDESTAL BASE MULTISTORY BUILDING

A Report to the
National Science Foundation

by

R. M. Stephen
E. L. Wilson
J. G. Bouwkamp
M. Button

Report No. UCB/EERC-78/13
College of Engineering
Department of Civil Engineering
University of California
Berkeley, California
July 1978

ia

TABLE OF CONTENTS

Page

Page

LIST OF FIGURES

Figure		Page

LIST OF TABLES

ABSTRACT

As a part of a continuing program to evaluate the dynamic response of actual structures and to accumulate a body of information on the dynamic properties of structures, especially when these structures have novel design features, a dynamic test program was conducted on the forty-two story Rainer Tower Building. Equally important, this program is aimed at evaluating the accuracy of computer modeling techniques and programs by comparing the experimentally derived dynamic response data with analytically predicted values.

The dynamic tests of the building included both a forced vibration study and an ambient vibration study. These results are compared and in general show very good correlation. A mathematical computer model of the Rainer Tower was formulated, and the results of the analysis are presented and compared to the experimental results. Again, in general, the results compare very favorably.

1. INTRODUCTION

1.1 General

The design of multistory structures subjected to dynamic forces resulting from foundation motions requires a consideration of both the characteristics of the ground motion and the dynamic properties of the structure. Ground motions as caused by an earthquake are random and, although not prescriptible for aseismic design, have been fairly well studied for certain well-known past earthquakes. The engineer is therefore mainly interested in the dynamic properties of the structure when designing for earthquake forces and is only indirectly concerned with the ground motion characteristics.

High speed digital computers and more sophisticated idealizations and computer model formulations of structures can predict the elastic, and in certain structural systems the inelastic, response of structures when subjected to earthquakes. However, the accuracy of the results in large measure depend upon the computer model formulation of the structure and its foundation. In order to determine the accuracy of the calculated results and to accumulate a body of information on the dynamic properties of structures, especially when these structures have novel design features, a number of dynamic tests have been conducted on full-scale structures (1).

For the above reasons, dynamic tests using forced and ambient methods were performed on the Rainer Tower Building in Seattle, Washington. Because of the potential advantages of the ambient vibration method in dynamic testing of full-scale structures, it was desirable to compare both methods in order to assess the accuracy of each method in evaluating the dynamic properties of the structural systems.

The building is described in Chapter 2, and the results of the dynamic tests, from forced, as well as ambient vibration study, are given in Chapters 3 and 4, respectively. Comparison of the dynamic properties of the building from both studies is presented in Chapter 5. A mathematical model of the structural system was formulated, and the calculated and experimental dynamic properties were compared. The formulation of the mathematical model and the analytical dynamic properties obtained are described in Chapter 6.

1.2 Acknowledgement

The authors gratefully acknowledge the financial support provided by the National Science Foundation under Grant ENV 76-04262-A02. They also wish to thank the owner, the University of Washington; the managing agent, Unico Properties, Inc., especially Mr. David C. Cortelyou; the general contractor, William Simpson Construction Co., Inc.; and the Structural Engineers, Skilling, Helle, Christiansen, Robertson, especially Mr. John B. Skilling, for their help and cooperation in coordinating and carrying out the test program.

2. THE RAINER TOWER BUILDING

2.1 General

The Rainer Tower Building is located in Seattle, Washington. The dynamic tests were performed on the Tower during April and May 1977. The building is a multistory structure, forty stories in height above the lobby level, and two below ground levels. The height of the building above the lobby level is about 514 feet. Figure 2.1 shows a general view of Rainer Square with Rainer Tower as it would be seen from the Northwest, and Fig. 2.2 shows the building from the Southeast.

2.2 Structural System and Structural Elements

The structure consists of a twelve-story pedestal rising from the basement level, above which rises a thirty-story steel frame. In overall plan, the pedestal is 68 feet 4 inches square at the base and flares out as it rises to the twelfth floor to 138 feet 10 inches square. The walls of the reinforced concrete pedestal are 5 feet 10 inches thick at the base and have a minimum thickness near the tenth floor of 1 foot 11 3/4 inches. The top of the pedestal is the twelfth floor, which is approximately 2 feet thick and is heavily reinforced with both conventional reinforcing bars and post-tensioning tendons. The pedestal rests on a 12-foot thick foundation mat that is 106 feet square in plan. Fig. 2.3 shows a cross-section of the building.

The steel frame structure extends from the twelfth floor level to the roof and consists of core frames with shear connected beams and exterior moment resistant frames with six bays at 18 feet 8 inches. The arrangement of the columns for both the core and the exterior frames is shown in Fig. 2.4.

The floor plan at the basement level is shown in Fig. 2.5. A typical floor plan of the building from the twelfth floor to the fortieth floor is given in Fig. 2.6.

The core frame columns are rolled sections of W14 shape with a minimum yield strength of 50 ksi. The core beams are, in general, rolled sections mostly wide flange shapes varying from W8 to W21. The steel being mostly A36 with some Gr50 material. The exterior columns consist of W14 shapes of A36 steel in lower floors, and above the twenty-seventh floor, they are mostly Gr50 steel. The exterior frame beams are wide flange shapes of W30 or W36, in general, of A36 steel with some beams of Gr50 steel.

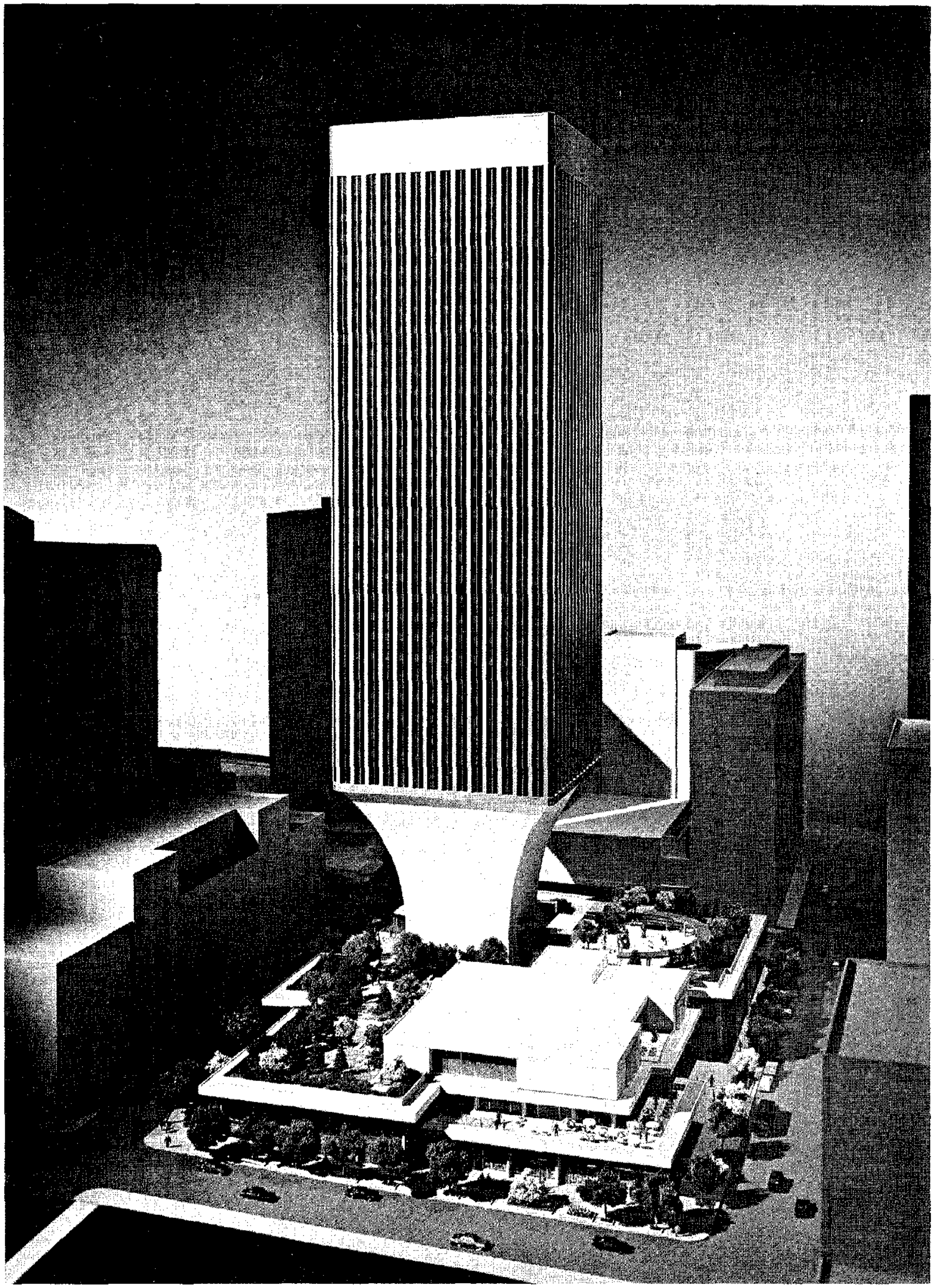

FIG. 2.1 GENERAL VIEW OF RAINER SQUARE

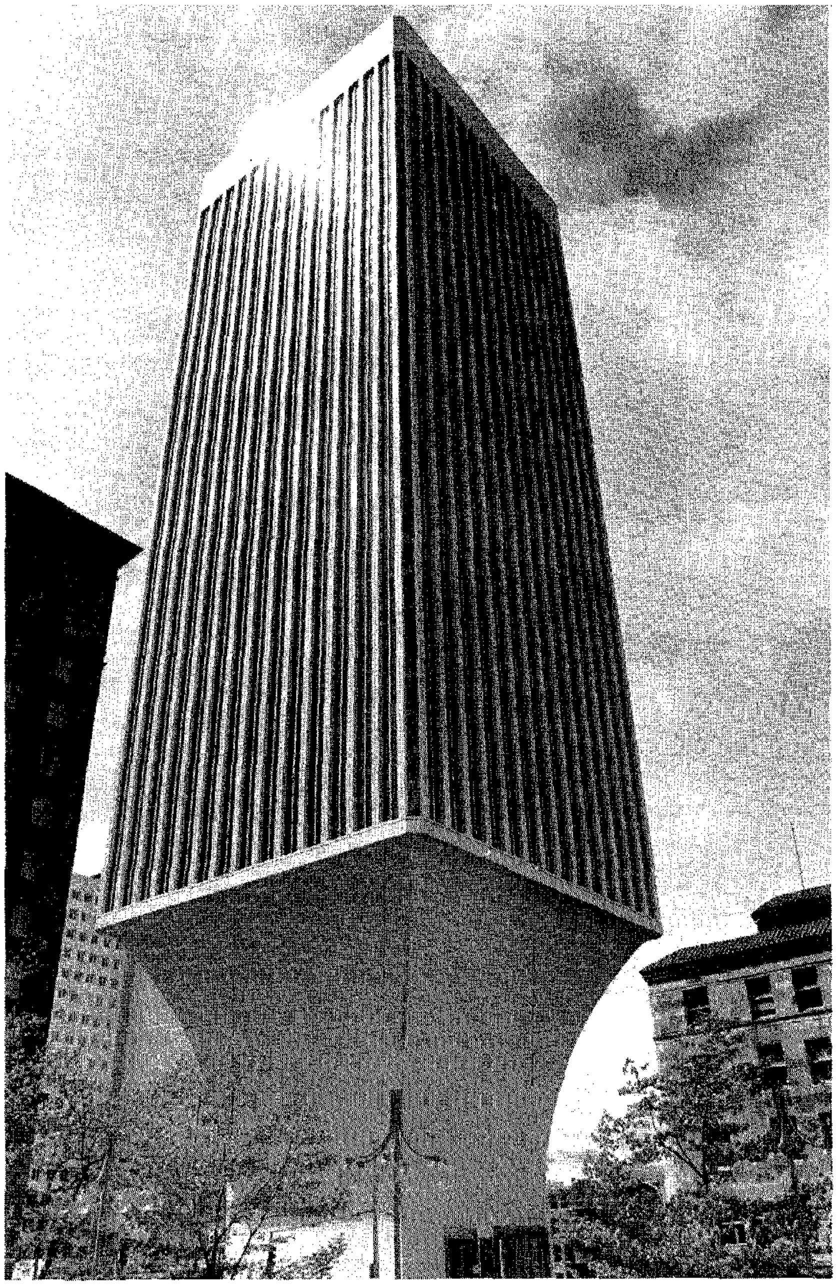

FIG. 2.2 RAINER TOWER BUILDING

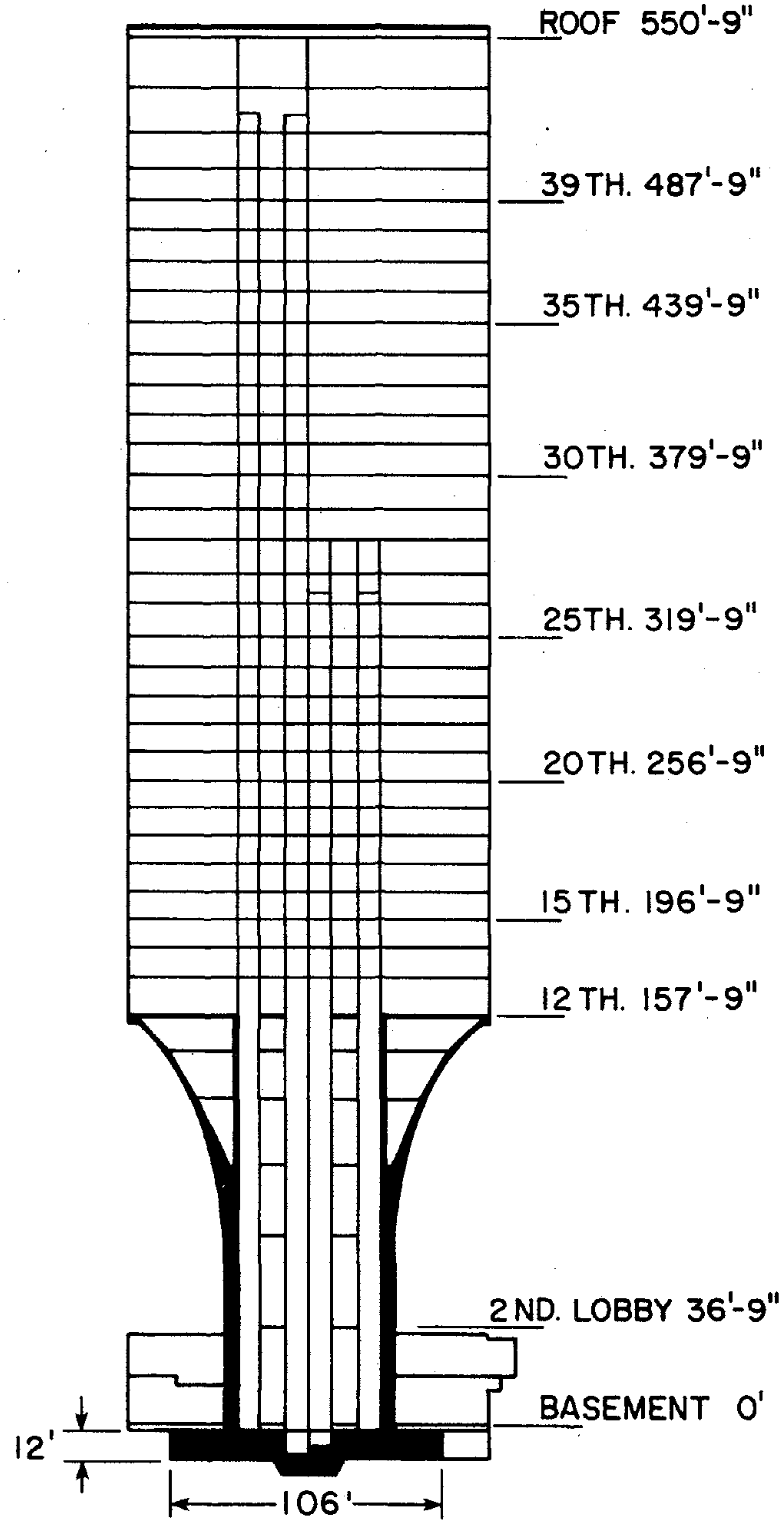

FIG. 2.3 CROSS SECTION OF THE BUILDING

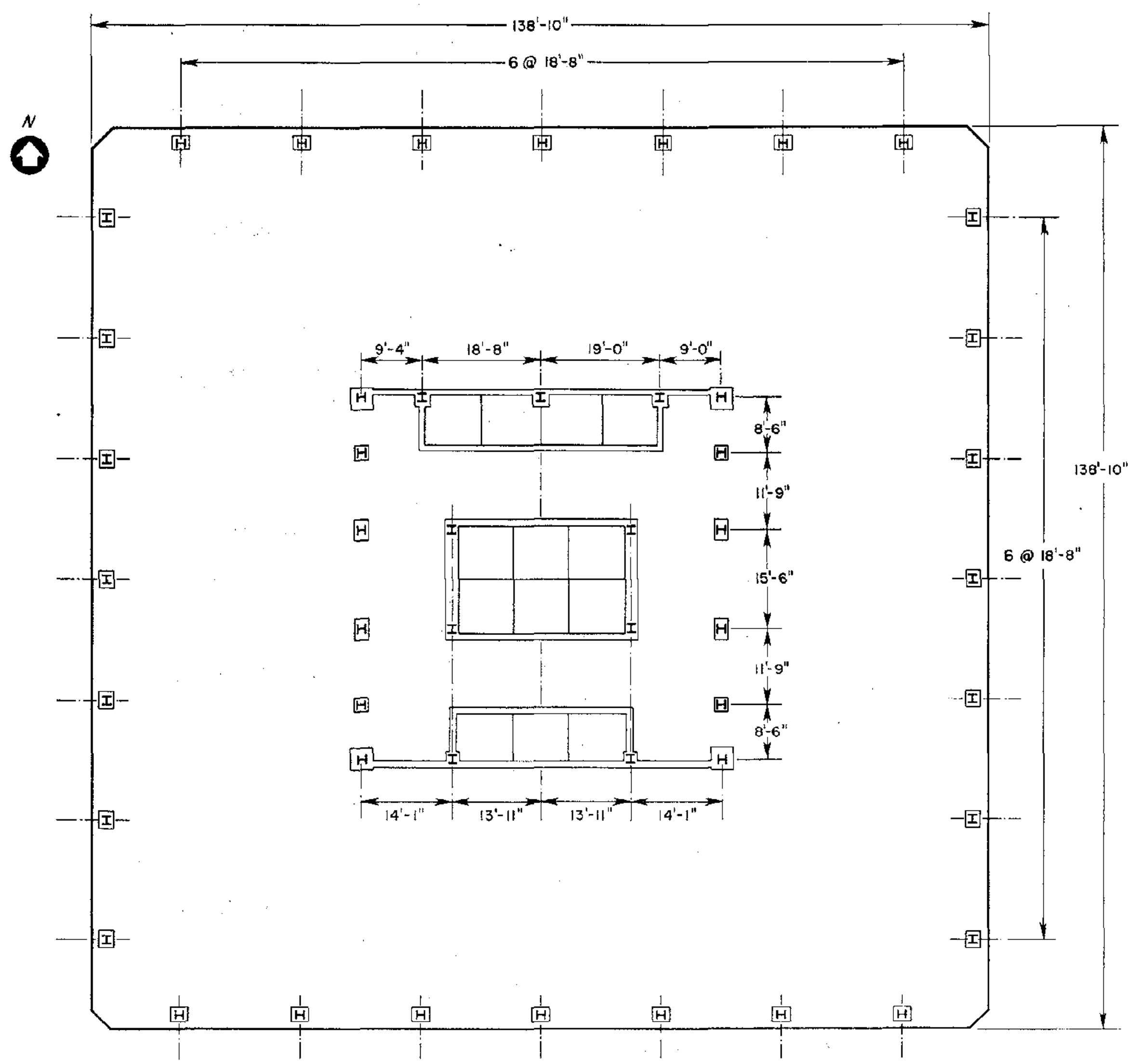

FIG. 2.4 TYPICAL FLOOR PLAN SHOWING ARRANGEMENT OF COLUMNS

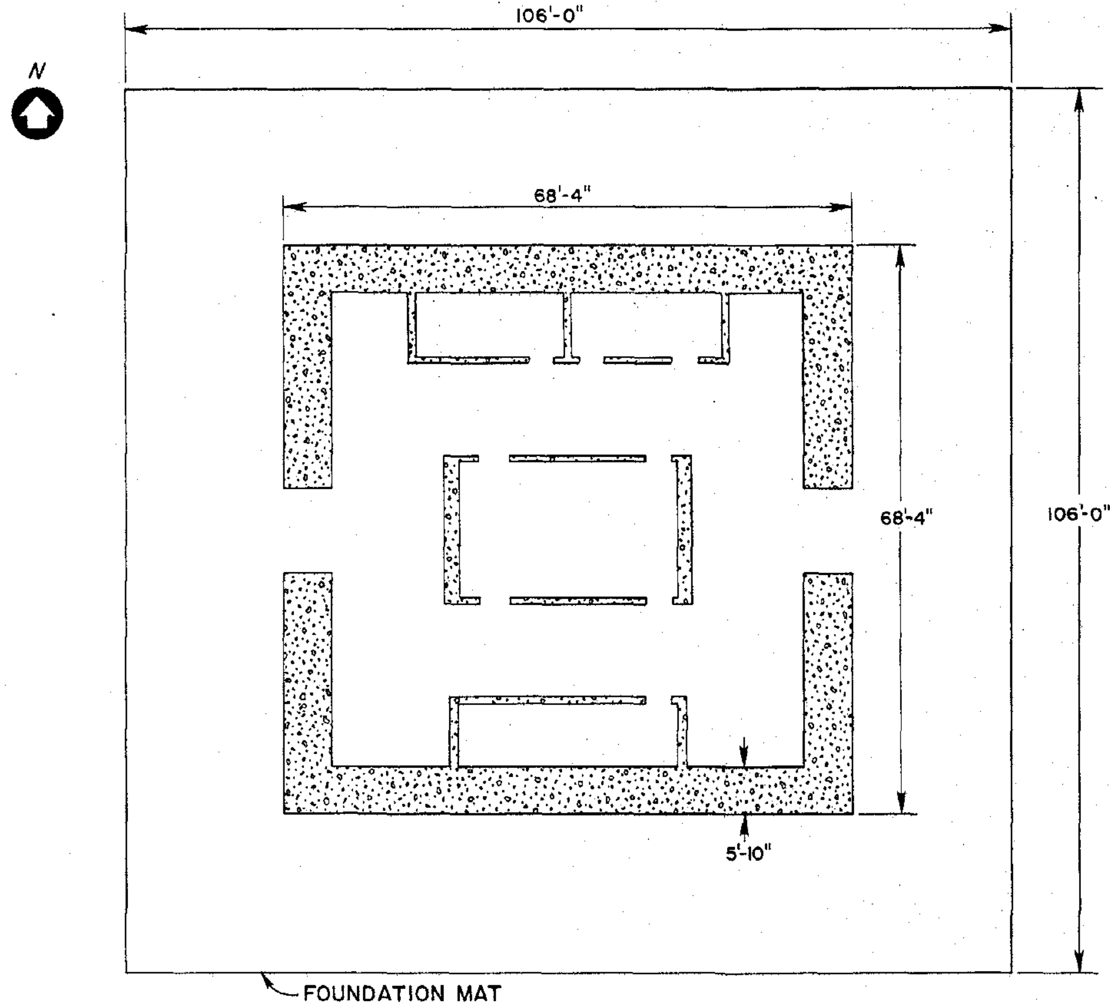

FIG. 2.5 FLOOR PLAN AT BASEMENT LEVEL

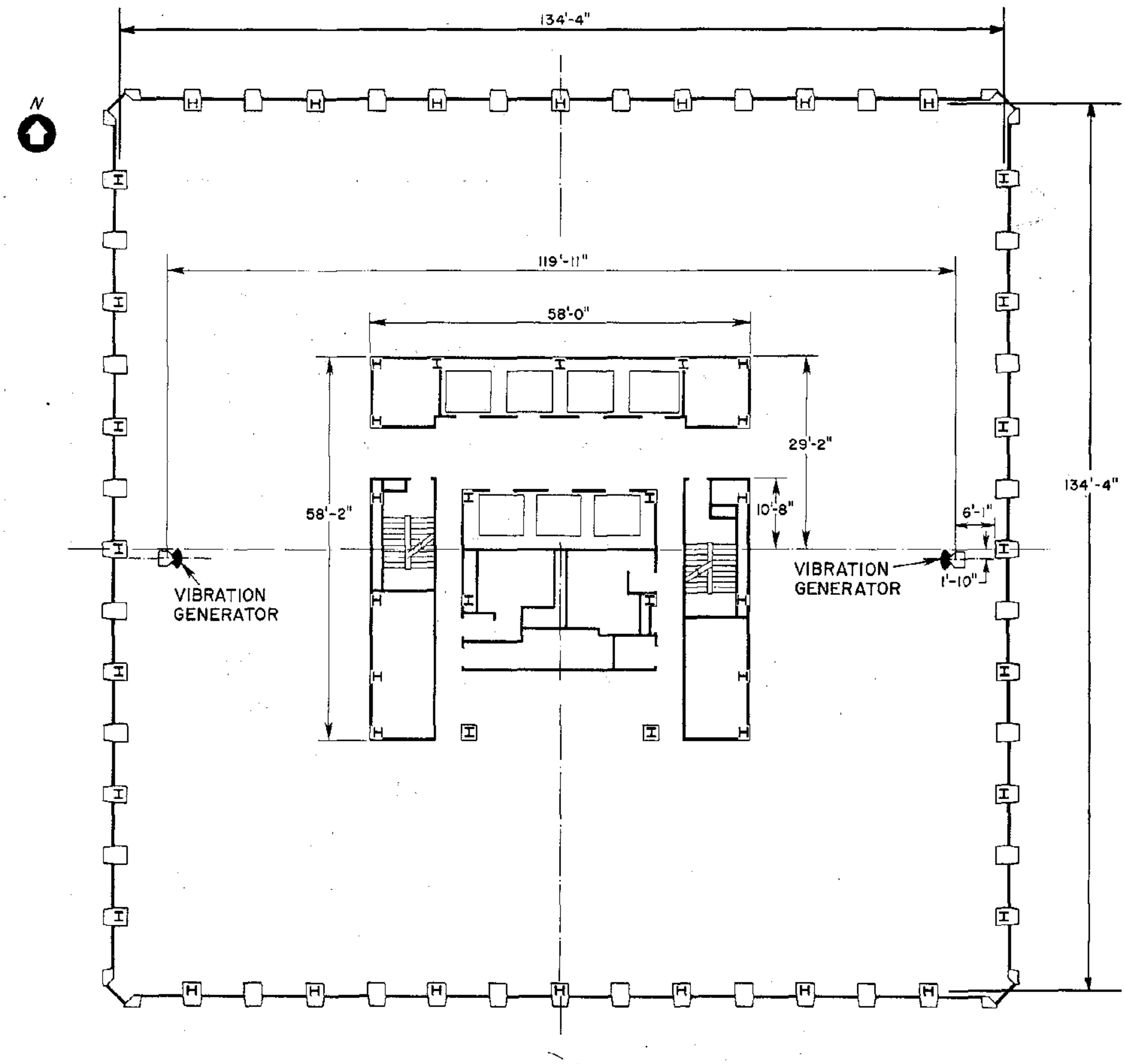

FIG. 2.6 TYPICAL FLOOR PLAN AND LOCATION OF VIBRATION GENERATORS (39th FLOOR)

3. FORCED VIBRATION STUDY

3.1 General

The forced vibration study was carried out and completed during April and May 1977. The building was structurally completed prior to the experimental work, and all of the facing cover, both glass and aluminum, as well as partition walls and installations in the core part of the building, were in place. The experimental apparatus employed in the dynamic test is described below. The general experimental procedures, equipment used, and procedures for data reduction applied, for forced vibration study conducted are also described. Finally, the experimental results are presented and discussed.

3.2 Experimental Apparatus

The experimental apparatus employed in the tests were two vibration generators, twelve accelerometers and equipment for the measurement and recording of the frequency responses. The apparatus is described in the following sections.

3.2.1 Vibration Generators

Forced vibrations were produced by two rotating-mass vibration generators or shaking machines, one of which is shown in Fig. 3.1. These machines were developed at the California Institute of Technology under the supervision of the Earthquake Engineering Research Institute for the Office of Architecture and Construction, State of California. Each machine consists of an electric motor driving two pie-shaped baskets or rotors, each of which produces a centrifugal force as a result of the rotation. The two rotors are mounted on a common vertical shaft and rotate in opposite directions so that the resultant of their centrifugal forces is a sinusoidal rectilinear force. When the baskets are lined up, a peak value of the sinusoidal force will be exerted. The structural design of the machines limits the peak value of force to 5,000 lbs. This maximum force may be attained at a number of combinations of eccentric mass and rotational speed, since the output force is proportional to the square of the rotational speed as well as the mass of the baskets and the lead plates inserted in the baskets. The maximum force of 5,000 lbs. can be reached for a minimum rotational speed of 2.5 cps when all the lead plates are placed in the baskets. At higher speeds the eccentric mass must be reduced in order not to surpass the maximum force of 5,000 lbs. The maximum operating speed is 10 cps, and the minimum practical speed is approximately 0.5 cps. At 0.5 cps with all lead plates in the baskets, a force of 200 lbs. can be generated. The relationship between output force and frequency of rotation of the baskets for different basket loads is shown in Fig. 3.2. Although the rotating mass vibration generators are very difficult to accurately control at frequencies lower than 0.5 cps and at the same time develop sufficiently large forces to record the motion of the building, in this dynamic test with extremely careful performance, it was possible to obtain frequency response for the first modes. The frequencies excited were in the range of 0.2 to 0.4 cps, and the exciting resonant force was within 81 and 114 lbs.

The speed of rotation of each motor driving the baskets is controlled by an electronic amplidyne housed in a control unit. The control unit allows the machines to be synchronized or operated 180° out-of-phase. This makes it convenient to excite, in structures with a line of symmetry, either torsional or pure translational vibrations without changing the position of either machine. A complete description of the vibration generators is given in (7).

The vibration generators were mounted on the 39th floor at the east and west sides of the building, 1 foot 10 inches off the north-south centerline and located 59 feet 11-1/2 inches on each side of the east-west centerline. Associated vibration control and recording equipment was also placed on the 39th floor (Fig. 2.6 and 3.1).

3.2.2 Accelerometers

The transducers used to detect horizontal floor accelerations of the building were Statham Model A4 linear accelerometers, with a maximum rating of ± 0.25 g.

3.2.3 Equipment for Measurement of Frequency

For the vibration generators, the vibration excitation frequencies were determined by measurement of the speed of rotation of the electric motor driving the baskets. A tachometer, attached to a rotating shaft driven by a transmission belt from the motor, generated a sinusoidal signal of frequency 300 times the frequency of rotation of the baskets. Hence, the maximum accuracy of frequency measurements was ± 1 count in the total number of counts in a period of 1 second (the gating period), i.e., ± 1/3 of 1% at 1 cps and ± 1/9 of 1% at 3 cps.

3.2.4 Recording Equipment

The electrical signals for all accelerometers were fed to amplifiers and then to a Honeywell Model 1858 Graphic Data Acquisition System with 8-in. wide chart. In frequency-response tests, the digital counter reading was observed and recorded manually on the chart alongside the associated traces.

3.3 Experimental Procedure and Data Reduction

The quantities normally determined by a dynamic test of a structure are: resonant frequencies, mode shapes, and damping capacities. The experimental procedures and reduction of data involved in determining these quantities are described in the next section.

3.3.1 Resonant Frequencies

With the equipment described on the previous page, resonant frequencies are determined by sweeping the frequency range of the vibration generators from 0.2 to 10 cps.

In the case of the vibration generators, the exciting frequency is increased slowly until acceleration traces on the recording chart are large enough for measurement. Above this level, the frequency is increased in steps until the upper speed limit of the machine is reached. Near resonance, where the slope of the frequency-response curve is changing rapidly, the frequency-interval steps are as small as the speed control permits. These steps are relatively large in regions away from resonance. Each time the frequency is set to a particular value, the vibration response is given sufficient time to become steady-state, before the acceleration traces are recorded. At the same time, the frequency of vibration, as recorded on a digital counter, is observed and written on the chart with its corresponding traces. Plotting the vibration response at each frequency step results in a frequency-response curve.

Frequency-response curves in the form of acceleration amplitude versus exciting frequency may be plotted directly from the data on the recording chart. However, the curves are for a force which increases with the square of the exciting frequency, and each acceleration amplitude should be divided by the corresponding square of its exciting frequency to obtain so-called normalized curves equivalent to those for a constant force (assuming linear stiffness and damping for the structural system).

If the original acceleration amplitudes are divided by the frequency to the fourth power, displacement frequency-response curves for constant exciting forces are obtained. In cases of fairly low damping (under 5%), there is little difference between results obtained for resonant frequencies and damping capacities measured from the different curves.

3.3.2 Mode Shapes

Once the resonant frequencies of a structure have been found, the mode shapes at each of these frequencies may be determined. In this case, with twelve accelerometers available, it was decided to use eleven floors for the measurement of the mode shapes, keeping one accelerometer as a spare.

The structure was vibrated at each of the resonant frequencies, and the vibration amplitude was determined for all accelerometers at each frequency.

It is generally necessary to make corrections to the recorded amplitudes to compensate for differences between calibration factors for each accelerometer. Absolute calibration is not required for mode shapes, and cross-calibration is sufficient. The accelerometers and all equipment associated with them in their respective recording channels are cross-calibrated simply by placing them all together and measuring the vibration amplitude of all of the accelerometers when the structure is vibrated at each of the resonant frequencies. Cross-calibration is generally carried out at the beginning and end of each day. The average calibration factors as derived from the pre- and post-test cross-calibration runs are used to adjust the recorded amplitude.

The number of points required to define a mode shape accurately depends on the mode and the number of degrees of freedom in the system.

For example, in a dynamic test on a 15-story building (12) four points were sufficient to define the first mode, whereas it required measurements of the vibration of all 14 floors and the roof to define the fifth mode shape accurately.

3.3.3 Damping Capacities

Damping capacities may be found from resonance curves in the normalized frequency-response curves by the formula:

$$\xi = \frac{\Delta f}{2f}$$

where

ξ = damping factor,

f = resonant frequency,

Δf = difference in frequency of the two points on the resonance curve with amplitudes of $1/\sqrt{2}$ times the resonant amplitude.

Strictly, the expression for ξ is only applicable to the displacement resonance curve of a linear, single degree-of-freedom system with a small amount of viscous damping. However, it has been used widely for systems differing appreciably from that for which the formula was derived, and it has become accepted as a reasonable measure of damping. In this respect, it should be remembered that in the case of full-size civil engineering structures, it is not necessary to measure damping accurately in a percentage sense. It is sufficient if the range in which an equivalent viscous damping coefficient lies is known. Meaningful ranges might be defined as: under 1%, 1-2%, 2-5%, 5-10%, over 10% (1,10).

The bandwidth method described above is extremely useful when the damping factor lies in the range of 1-10% of critical. However, if the damping lies below 1%, difficulties may be encountered in observing sufficient points on the resonance curve. Also, the small frequency difference between two relatively large frequencies becomes difficult to measure accurately. Above 10% of critical damping, resonance curves often become poorly defined due to interference between modes, and the results from the bandwidth method have little meaning.

3.4 Experimental Results

The vibration equipment was bolted to the 39th floor, as shown in Fig. 2.6; and, with the appropriate adjustments to the vibration generator equipment, it was possible to produce translational or torsional vibrations of the building. The first six translational modes, respectively in E-W and N-S directions, were excited as well as the first five torsional modes. Frequency response curves in the region of the resonant frequencies for all excited translational and torsional modes are shown successively in Figs. 3.3 through 3.19. The curves are plotted in the form of normalized displacement amplitude versus exciting frequency. The ordinates were obtained by dividing the recorded acceleration amplitude by the square of the exciting frequency to obtain acceleration amplitudes for a constant equivalent force amplitude. The values thus obtained are divided by the square of the circular frequency (rad/sec) to obtain normalized displacement amplitudes. For convenience, the actual exciting force (F_r) and displacement amplitude (u_r) for each of the excited resonancies are given in Figs. 3.3 through 3.19 as well as calculated damping factors.

The resonant frequencies and damping factors evaluated from the response curves are summarized in Tables 3.1 and 3.2, respectively. The generated exciting force by both shaking machines and the corresponding resonant displacement amplitude for each resonant frequency are given in Tables 3.3 and 3.4, respectively.

TABLE 3.1 - RESONANT FREQUENCIES (cps)

Excitation	Mode					
	1	2	3	4	5	6
E-W	0.232	0.755	1.385	1.87	2.21	2.68
N-S	0.225	0.720	1.32	1.81	2.14	2.62
Torsional	0.377	1.055	1.86	2.60	3.32	----

TABLES 3.2 - DAMPING FACTORS (%) FROM RESONANCE CURVES

Excitation	Mode					
	1	2	3	4	5	6
E-W	1.7	2.7	2.2	2.9	2.0	3.0
N-S	6.6	2.6	1.9	2.1	1.6	2.8
Torsional	2.5	1.0	1.6	2.0	2.0	---

TABLE 3.3 - RESONANT FORCE AMPLITUDES (lb)

Excitation	Mode					
	1	2	3	4	5	6
E-W	87	917	3087	5627	3338	4894
N-S	81	834	2804	5254	3115	4619
Torsional	228	1792	5549	6546	10722	----

TABLE 3.4 - RESONANT DISPLACEMENT AMPLITUDES (x 10^{-2} in) 39th FLOOR

Excitation	Mode					
	1	2	3	4	5	6
E-W	1.98	0.279	0.116	0.175	0.178	0.248
N-S	1.59	0.349	0.097	0.343	0.190	0.252
Torsional	1.44	0.43	0.178	0.437	0.776	-----

The mode shapes for the translational and torsional modes that were excited are shown in Figs. 3.20 through 3.36. Particular attention has been given to observation of inplane deformations on the 39th and 12th floors for each of the excited resonances. The horizontal inplane floor vibrational mode associated with each of the translational and torsional modes of vibration as well as the resonant displacement amplitudes of the floor center and the rotational amplitudes about the center are given in Figs. 3.20 through 3.36. Resonant rotation amplitudes for the 39th and 12th floors are summarized in Tables 3.5 and 3.6, respectively.

TABLE 3.5 - RESONANCE ROTATION AMPLITUDES
39th Floor (x 10^{-7} rad)

Excitation	Mode					
	1	2	3	4	5	6
E-W	11.6	2.2	0	0.43	0.39	0.48
N-S	20.2	2.4	0	0.55	0	0.17
Torsional	17.4	43.1	16.2	21.3	23.4	----

TABLE 3.6 - RESONANCE ROTATION AMPLITUDES
12th Floor (x 10^{-7} rad)

Excitation	Mode					
	1	2	3	4	5	6
E-W	0	0	0	0.68	0.19	0.09
N-S	0	0	0	1.10	0.62	0.17
Torsional	0	4.8	0.45	3.7	9.46	----

3.5 Discussion of Experimental Results

The forced-vibration study of the building was conducted to obtain accurate resonant frequencies for the first six translational modes of vibration in the N-S direction along one of the symmetry lines of the floor plane and the first six translation modes in the orthogonal E-W direction as well as the first five torsional modes of vibration. The resonant frequencies were well separated, and it was of interest to note the ratios of the observed higher mode frequencies with respect to the fundamental one. These ratios are given in Table 3.7 for all three directions of excited vibrations, and they indicate a type of overall structural response.

From these results, it may be concluded that the building vibration in both translational directions as well as torsional vibration are predominantly of the shear type because the determined frequency ratios follow closely the ratios 1, 3, 5, 7, 9, 11, ..., which apply for the uniform shear beam.

With the translational directions of vibration having been selected along the E-W and N-S lines of symmetry, it should be expected that the

TABLE 3.7 - RATIO OF RESONANT FREQUENCIES

Mode	Translational E-W		Translational N-S		Torsional	
	fi (cps)	fi/f_1	fi (cps)	fi/f_1	fi (cps)	fi/f_1
1	0.232	1.0	0.225	1.0	0.377	1.0
2	0.755	3.25	0.720	3.20	1.055	2.80
3	1.385	5.97	1.32	5.87	1.86	4.93
4	1.87	8.06	1.81	8.04	2.60	6.90
5	2.21	9.53	2.14	9.51	3.32	8.81
6	2.68	11.55	2.62	11.64	----	----

translational modes exist in the direction of the lines of symmetry. It was found that amplitudes of rotation on the 39th and 12th floors for both directions are on the same order of magnitude (Tables 3.5 and 3.6 and Figs. 3.20 through 3.31); and, comparing them with the amplitudes of rotation in the torsional modes, they are from one to two orders of magnitude smaller. Thus, it could be concluded that the modes of vibration excited along the lines of symmetry are actual translational modes, with practically the same resonant frequencies and mode shapes (Table 3.1 and Figs. 3.20 through 3.31). In the torsional modes of vibration, it appears that in general the line of rotation is crossing the floor plane centroid (Figs. 3.32 through 3.36). It is of interest to note that in the third torsional mode there was some N-S translational motion, and this, no doubt, was due to the close coupling of the frequencies of the fourth N-S translational mode and the third torsional mode (1.81 versus 1.86, respectively). From these results it could be concluded that the mass and stiffness center coincide with the geometric center and that the floor slabs are practically rigid in their own plane.

Damping coefficients, in general, varied from 1% to 3% of critical damping in all modes, except for the first mode in the N-S direction. It should be mentioned that the damping coefficient for the first mode in the translational direction is probably higher due to difficulties in properly controlling the building vibration at such low frequencies (0.2 and 0.4 cps) and at a very low exciting force amplitude (81 lb). Similar damping values have been reported from the other full-scale forced vibration studies of steel frame high-rise buildings (13,14,15,20).

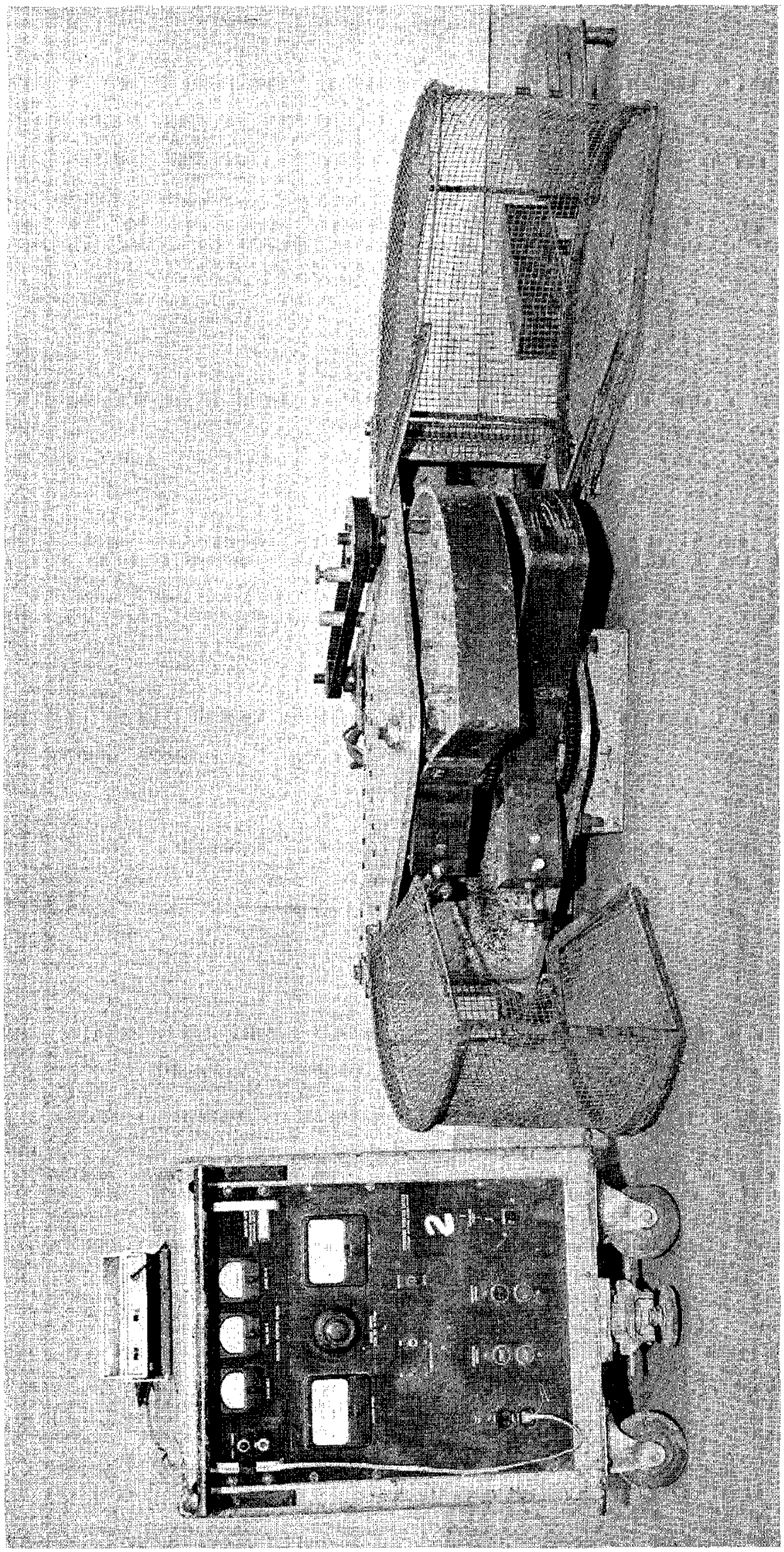

FIG. 3.1 VIBRATION GENERATOR

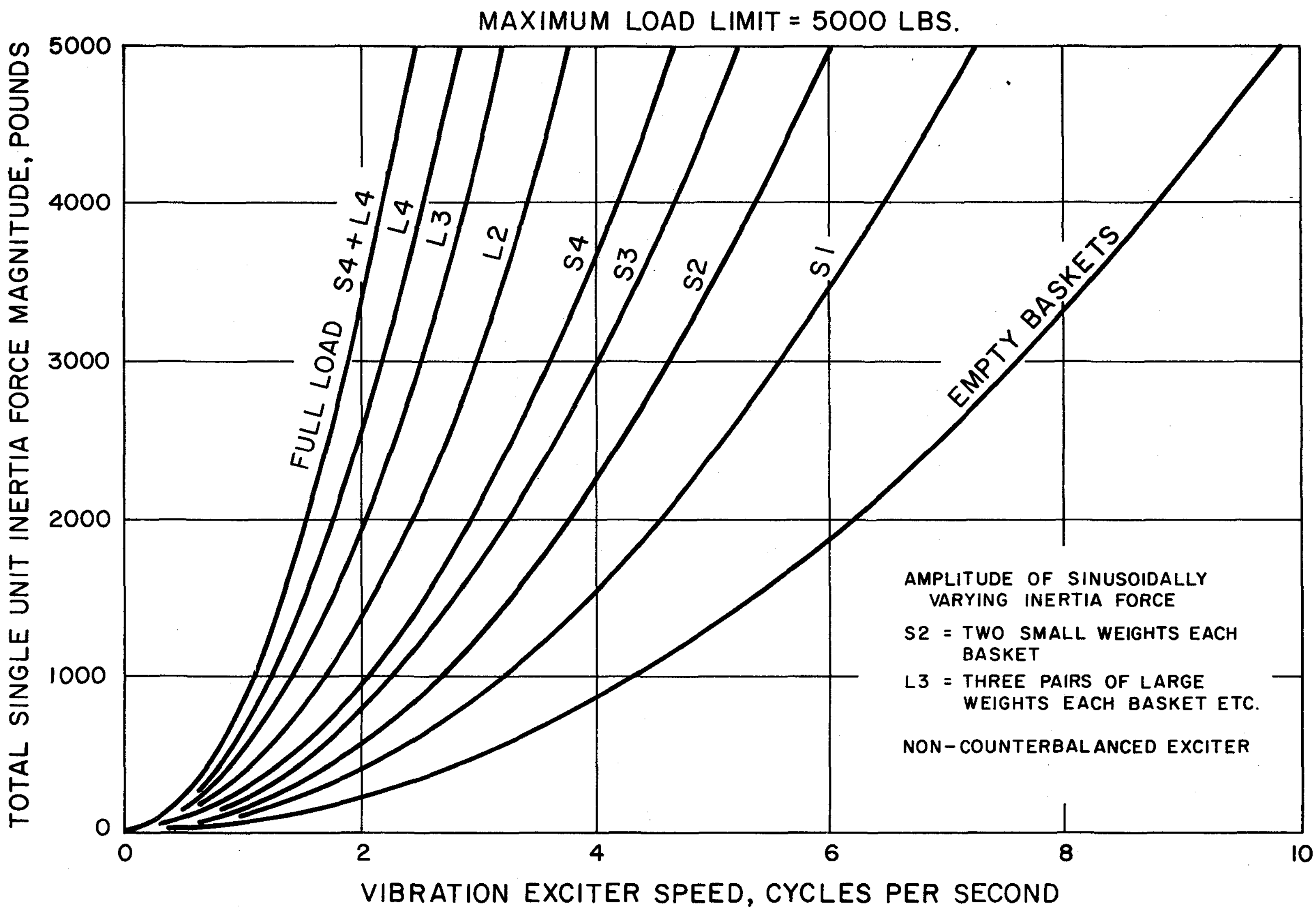

FIG. 3.2 VIBRATION FORCE OUTPUT VS. SPEED-NON-COUNTERBALANCED (After HUDSON)

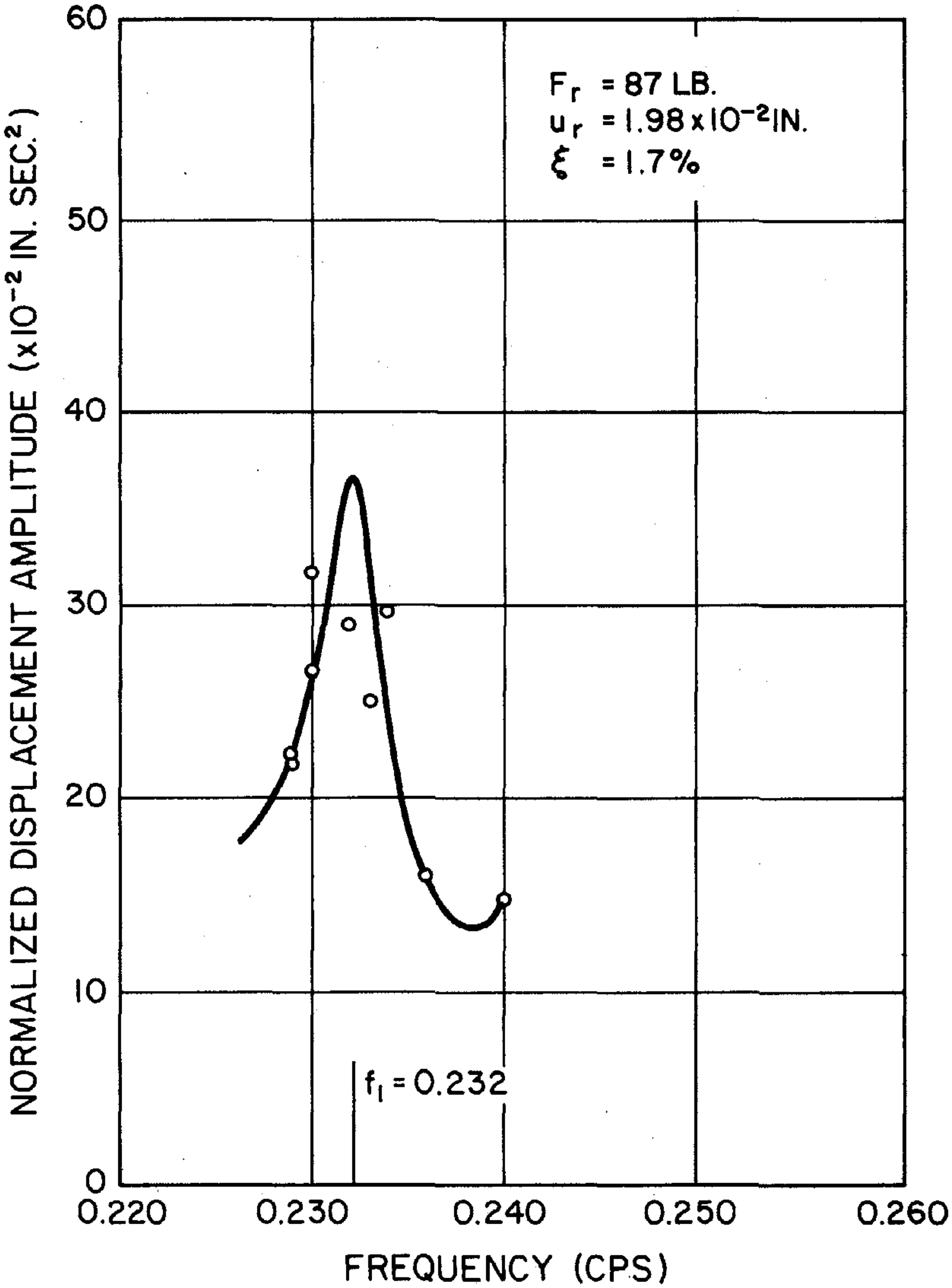

FIG. 3.3 FREQUENCY RESPONSE, FIRST MODE E-W

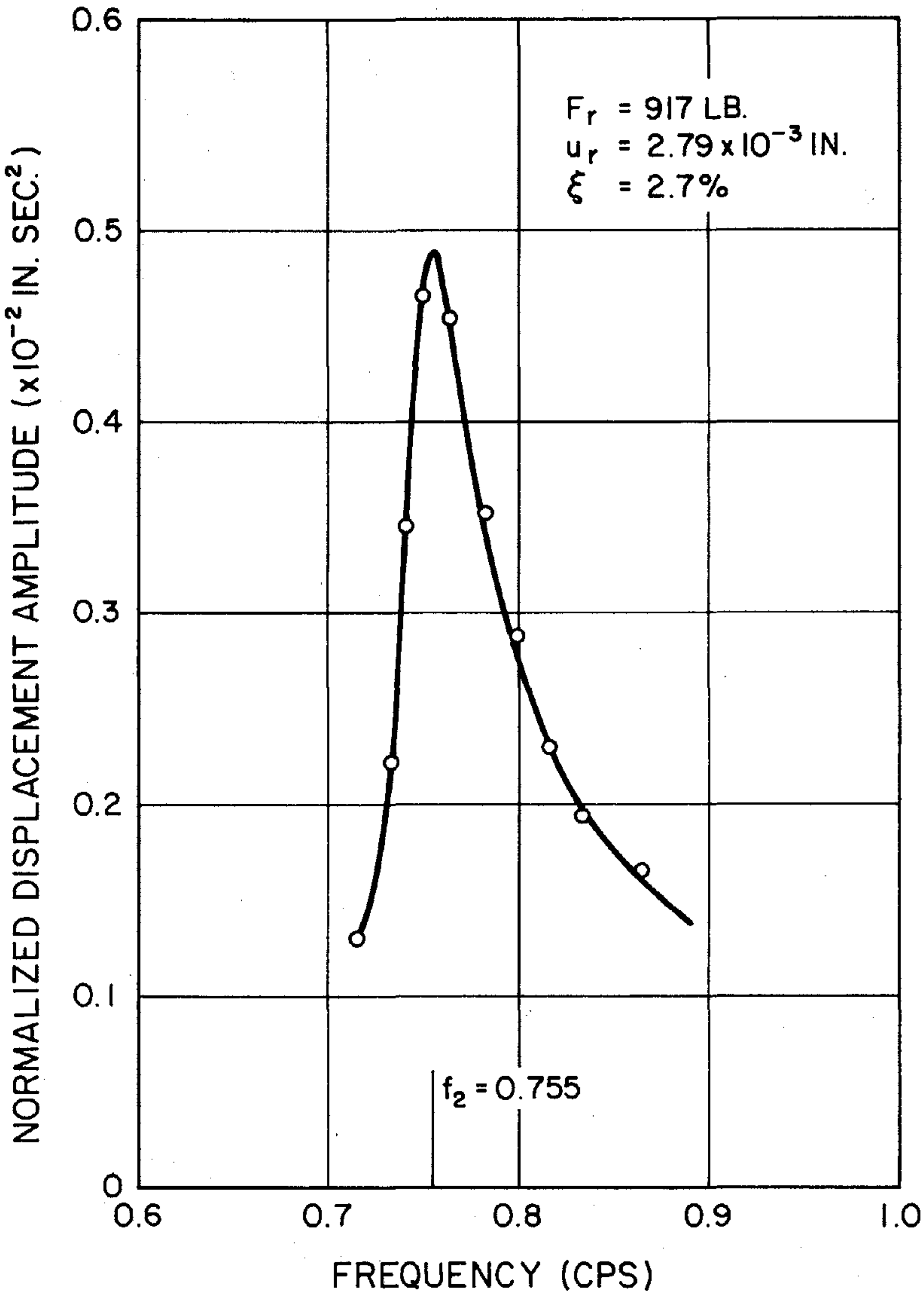

FIG. 3.4 FREQUENCY RESPONSE, SECOND MODE E-W

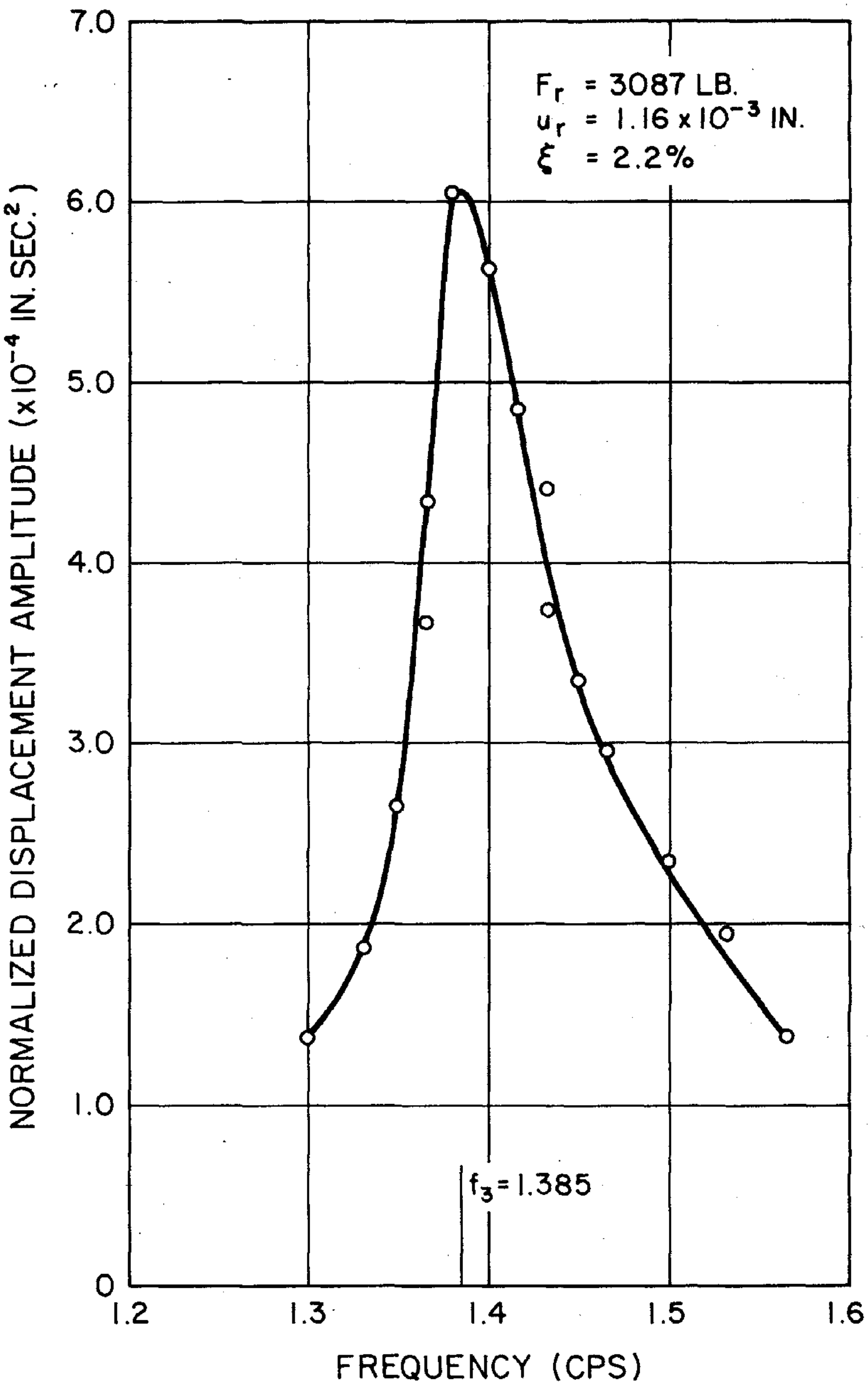

FIG. 3.5 FREQUENCY RESPONSE, THIRD MODE E-W

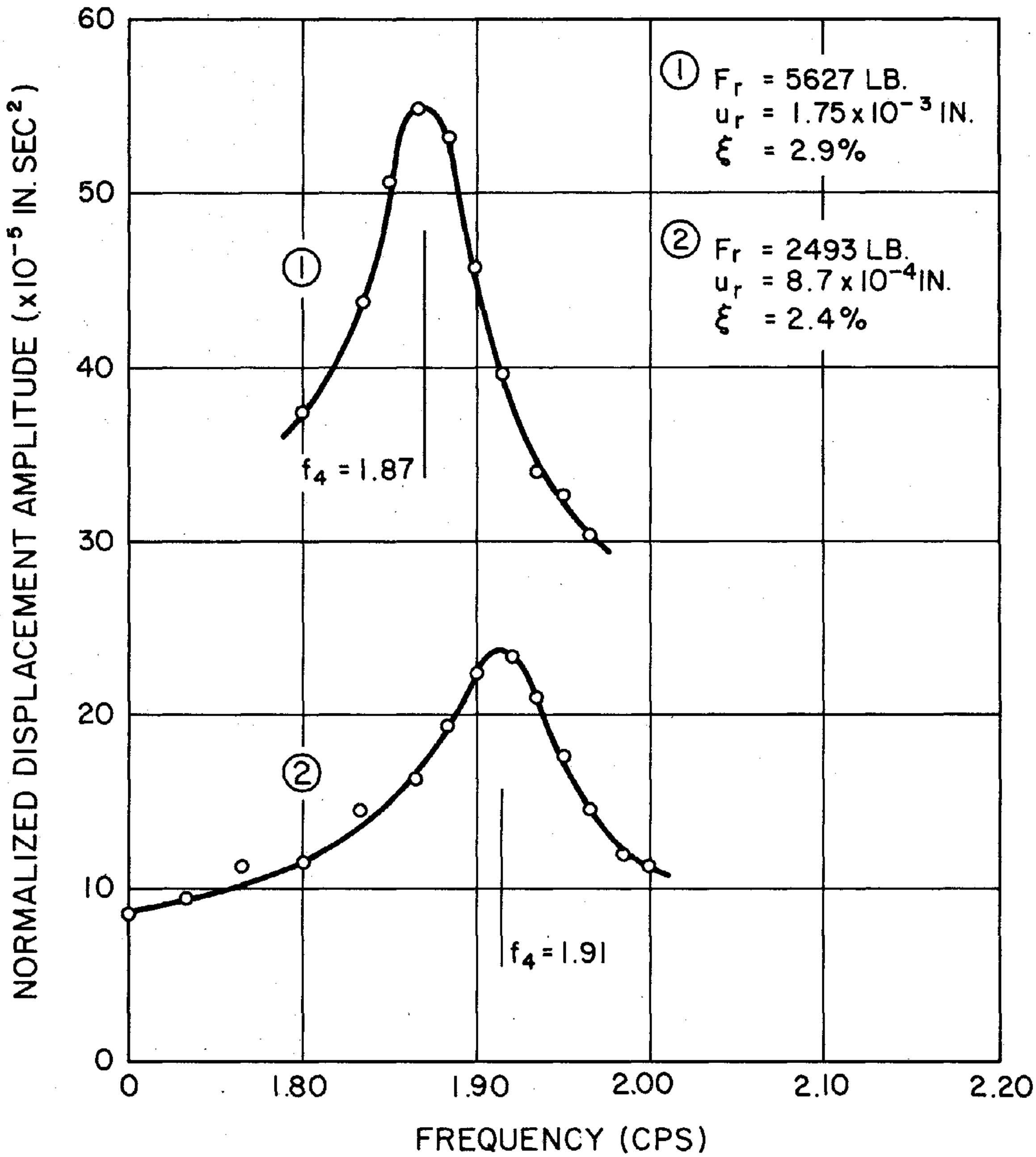

FIG. 3.6 FREQUENCY RESPONSE FOURTH MODE E-W

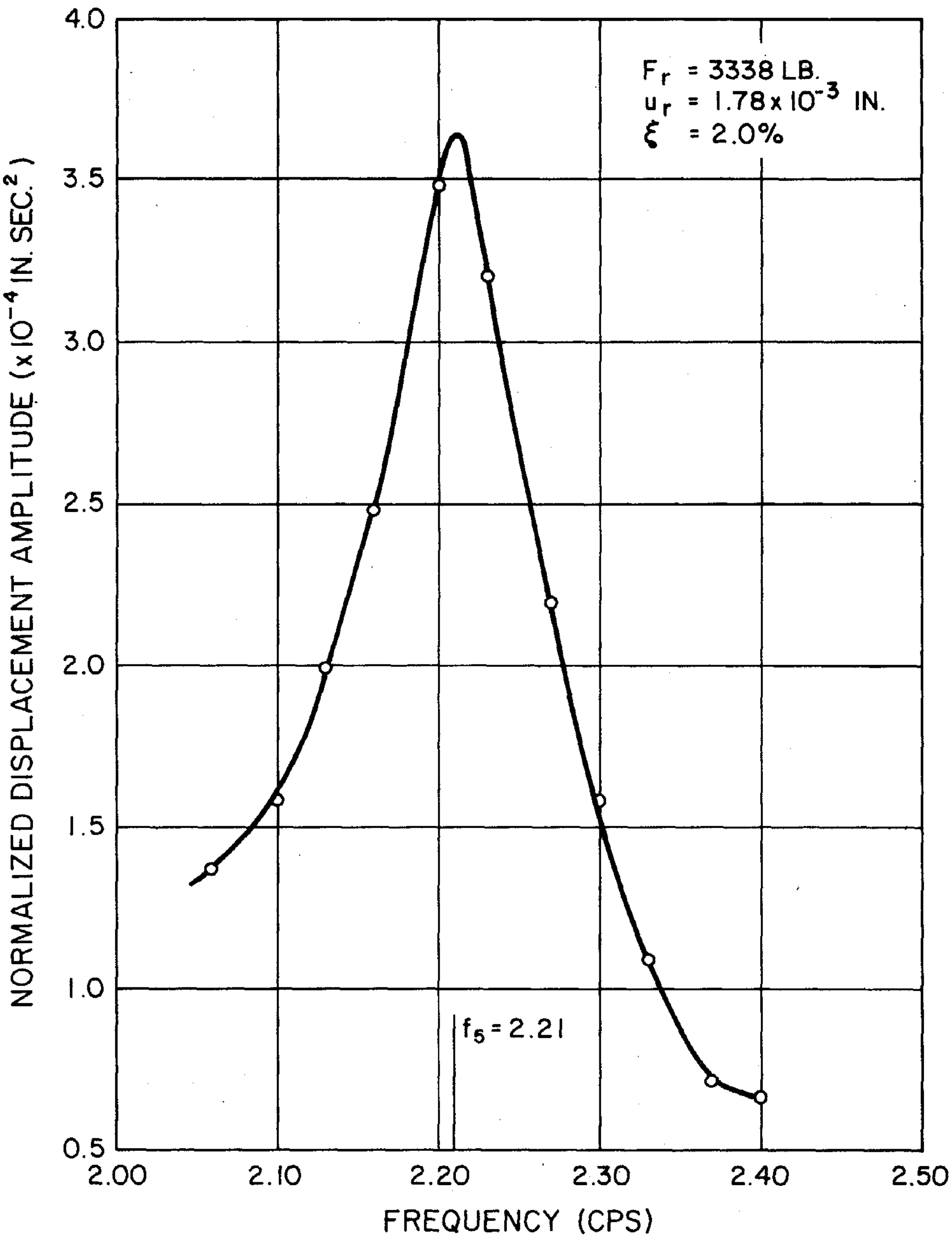

FIG. 3.7 FREQUENCY RESPONSE, FIFTH MODE E-W

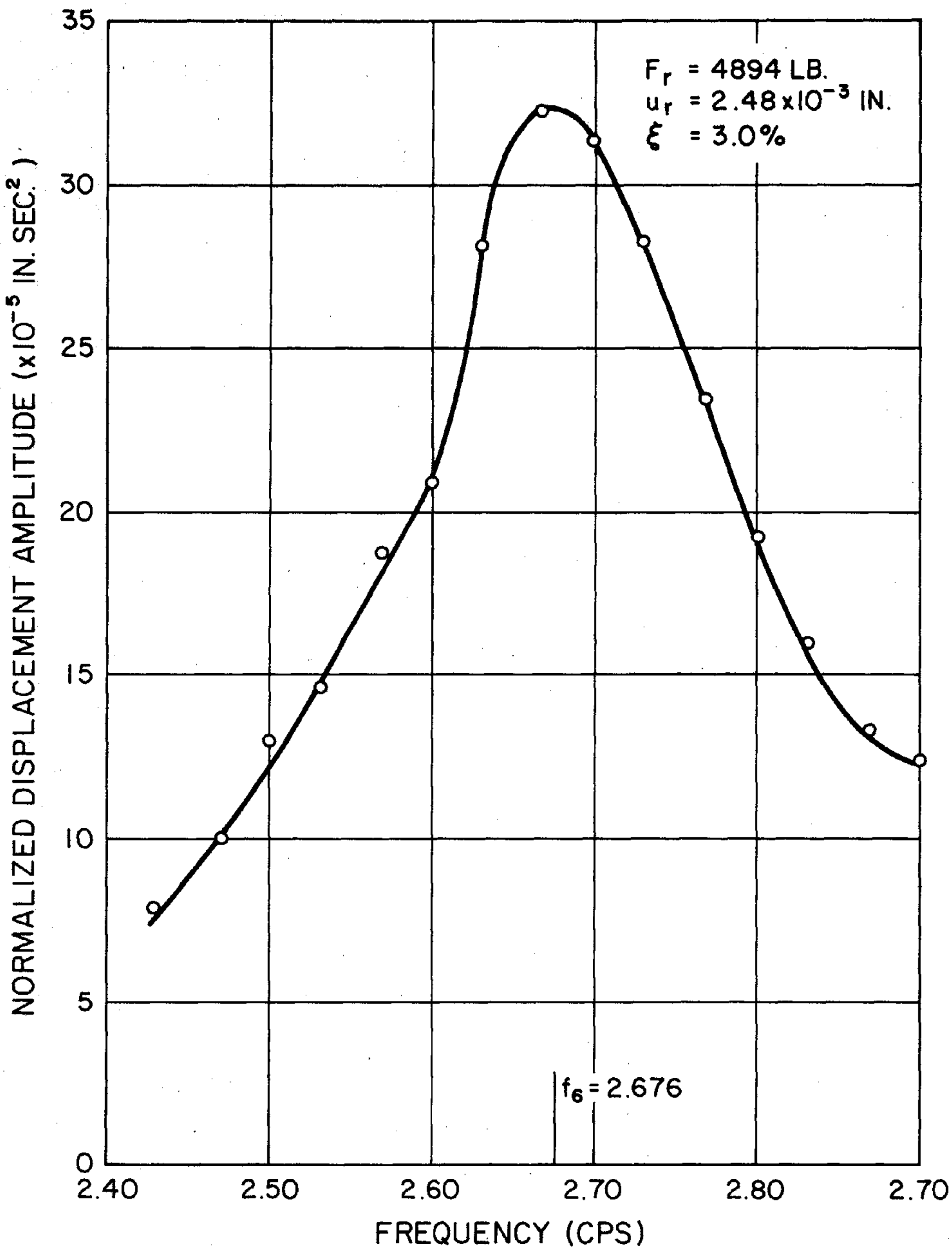

FIG. 3.8 FREQUENCY RESPONSE, SIXTH MODE E-W

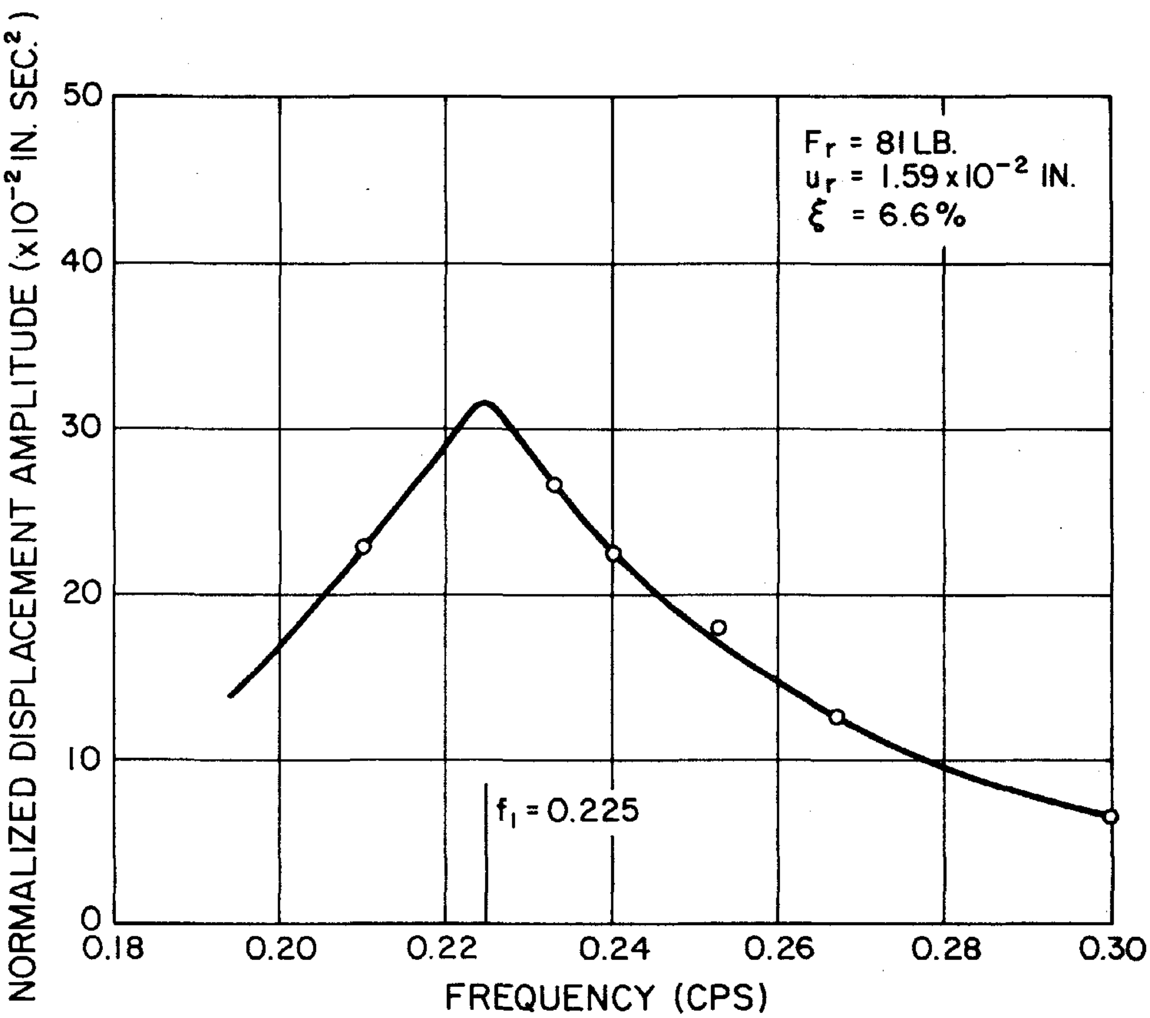

FIG. 3.9 FREQUENCY RESPONSE, FIRST MODE N-S

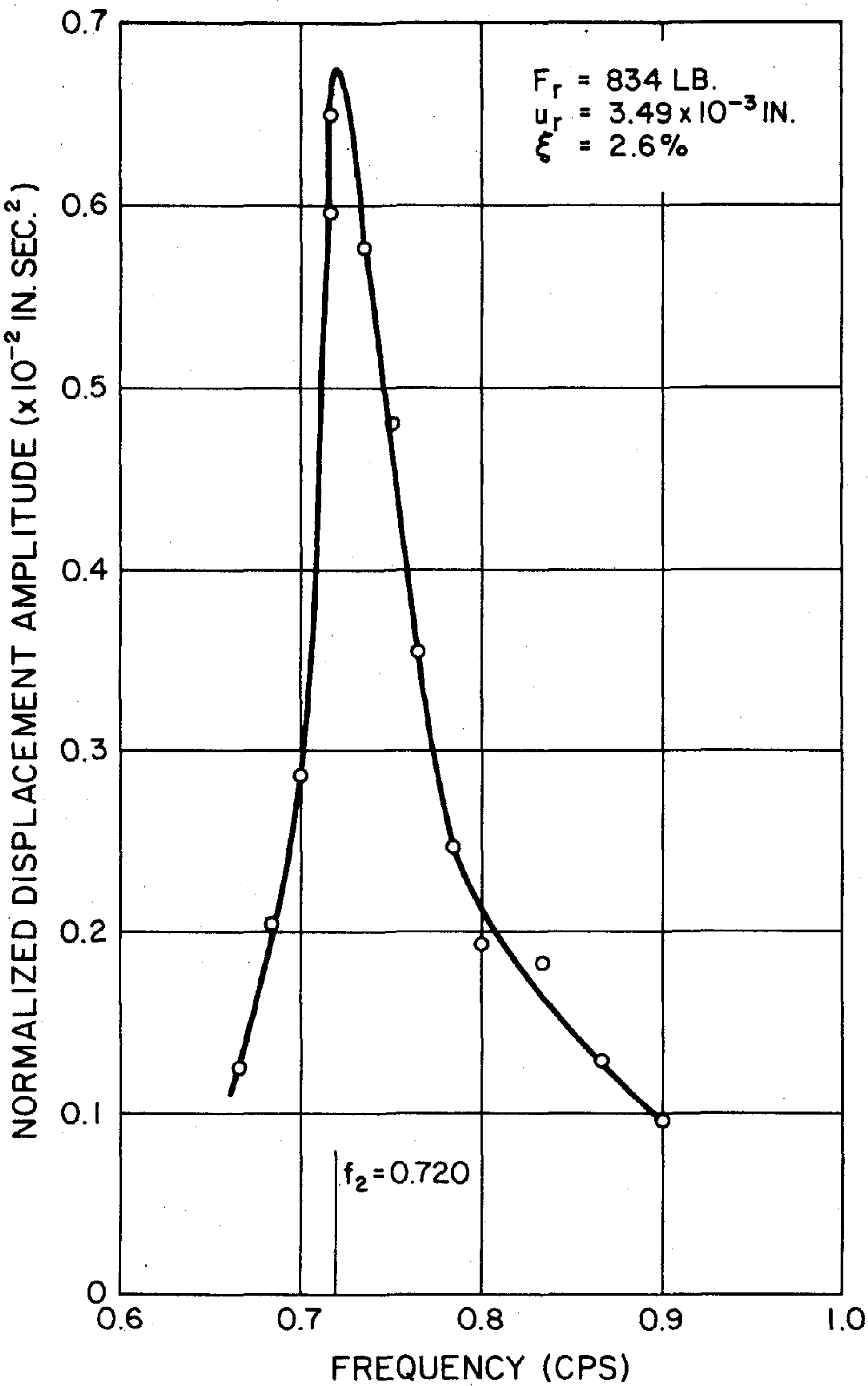

FIG. 3.10 FREQUENCY RESPONSE, SECOND MODE N-S

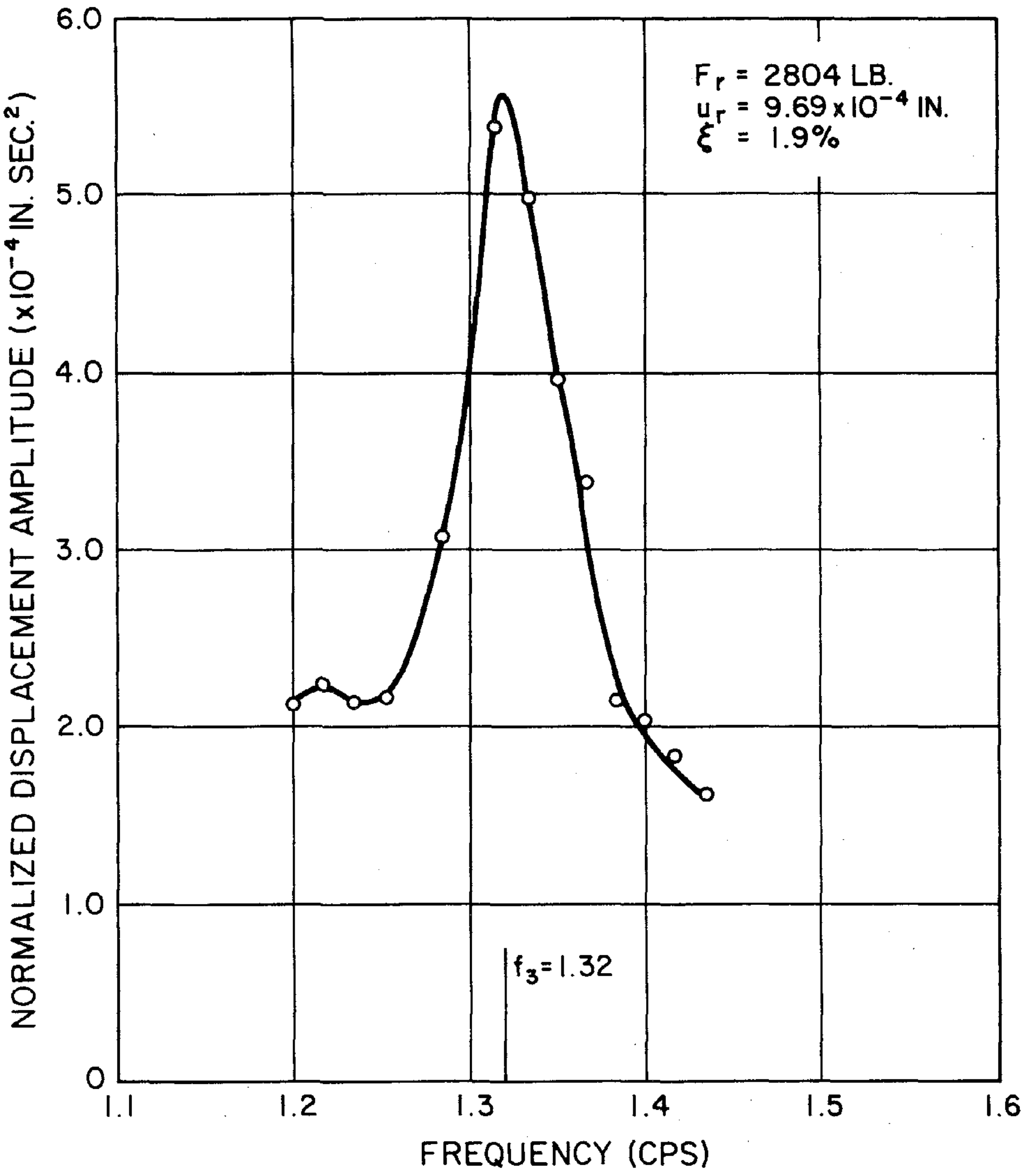

FIG. 3.11 FREQUENCY RESPONSE, THIRD MODE N-S

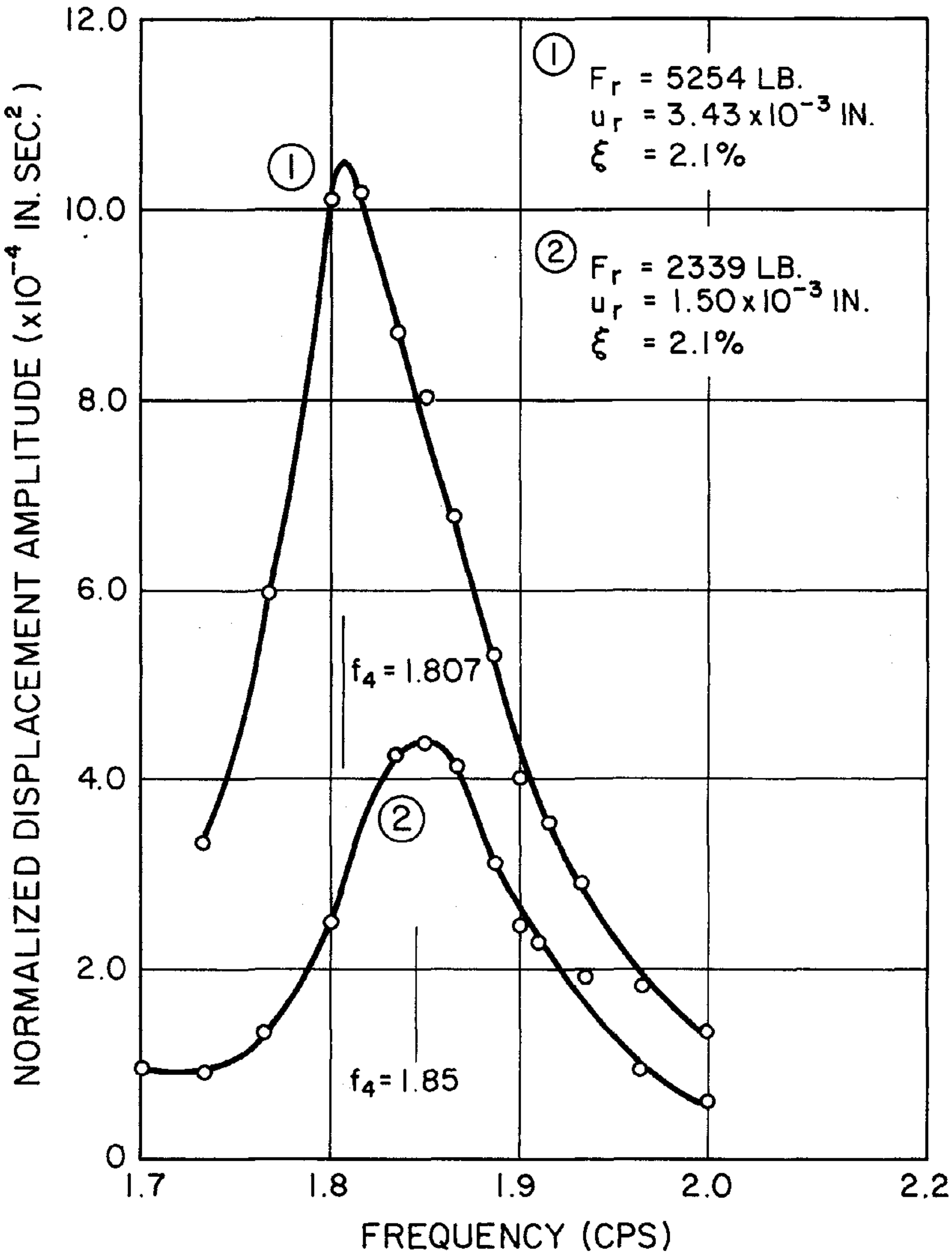

FIG. 3.12 FREQUENCY RESPONSE, FOURTH MODE N-S

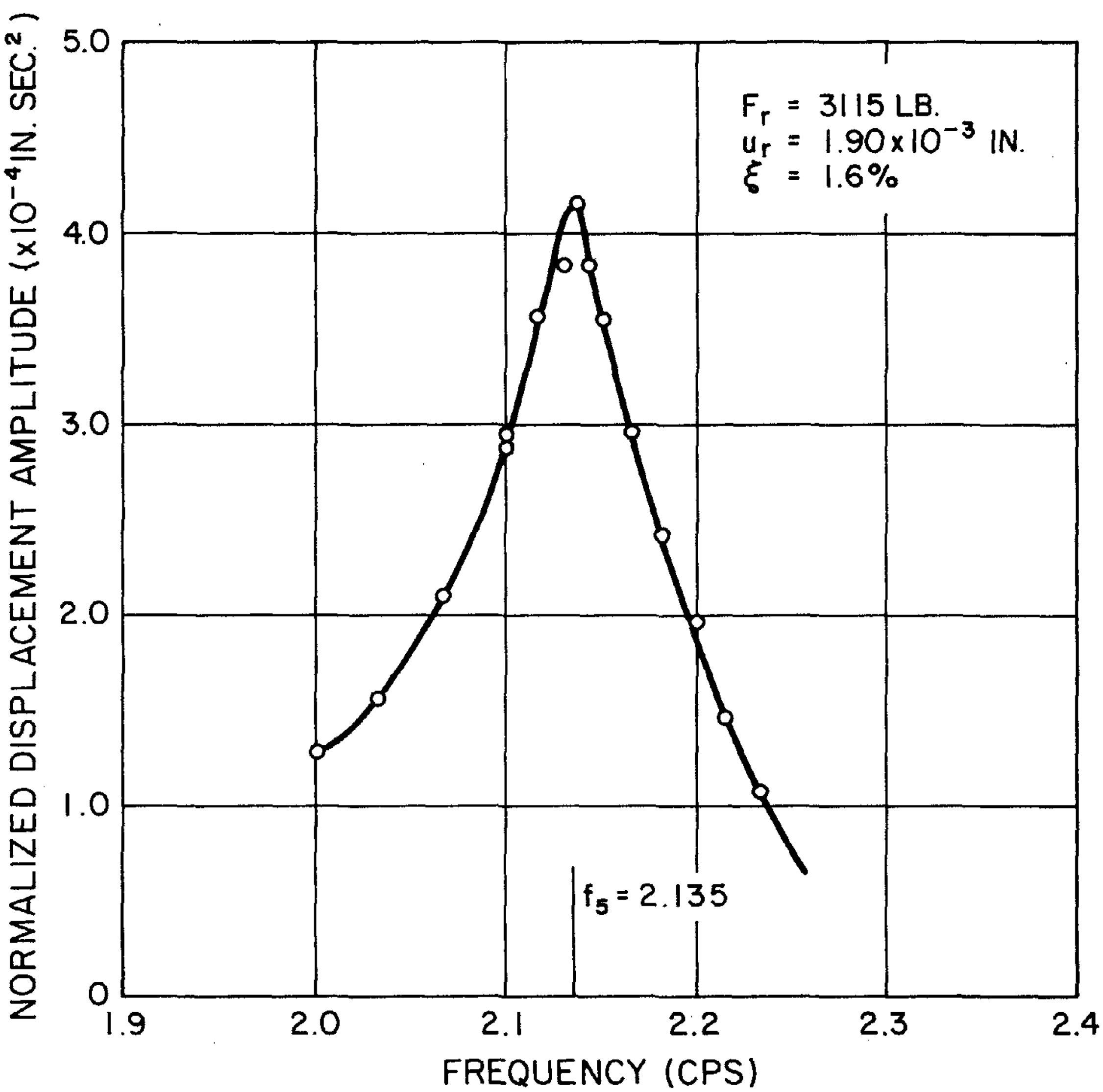

FIG. 3.13 FREQUENCY RESPONSE, FIFTH MODE N-S

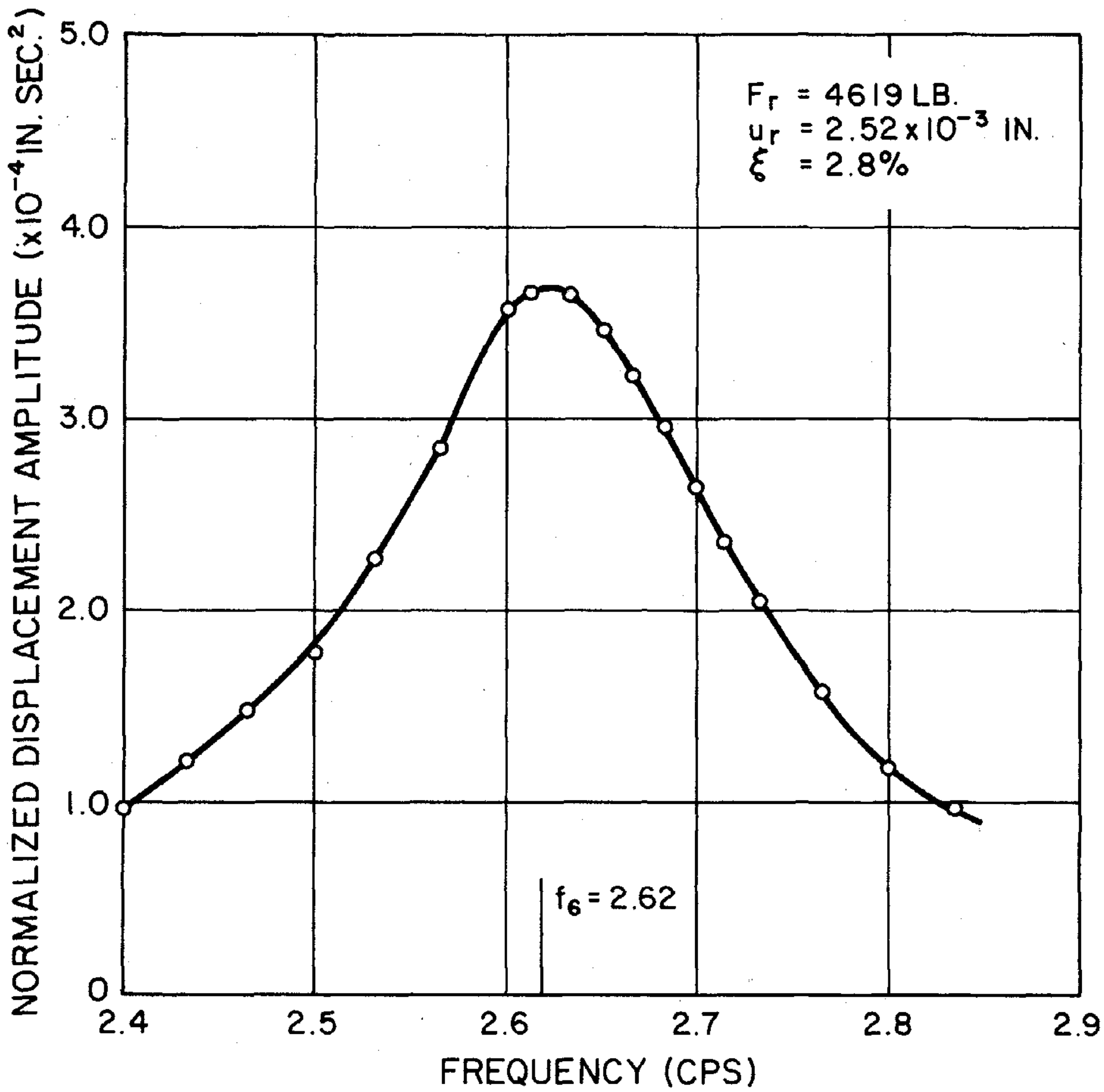

FIG. 3.14 FREQUENCY RESPONSE, SIXTH MODE N-S

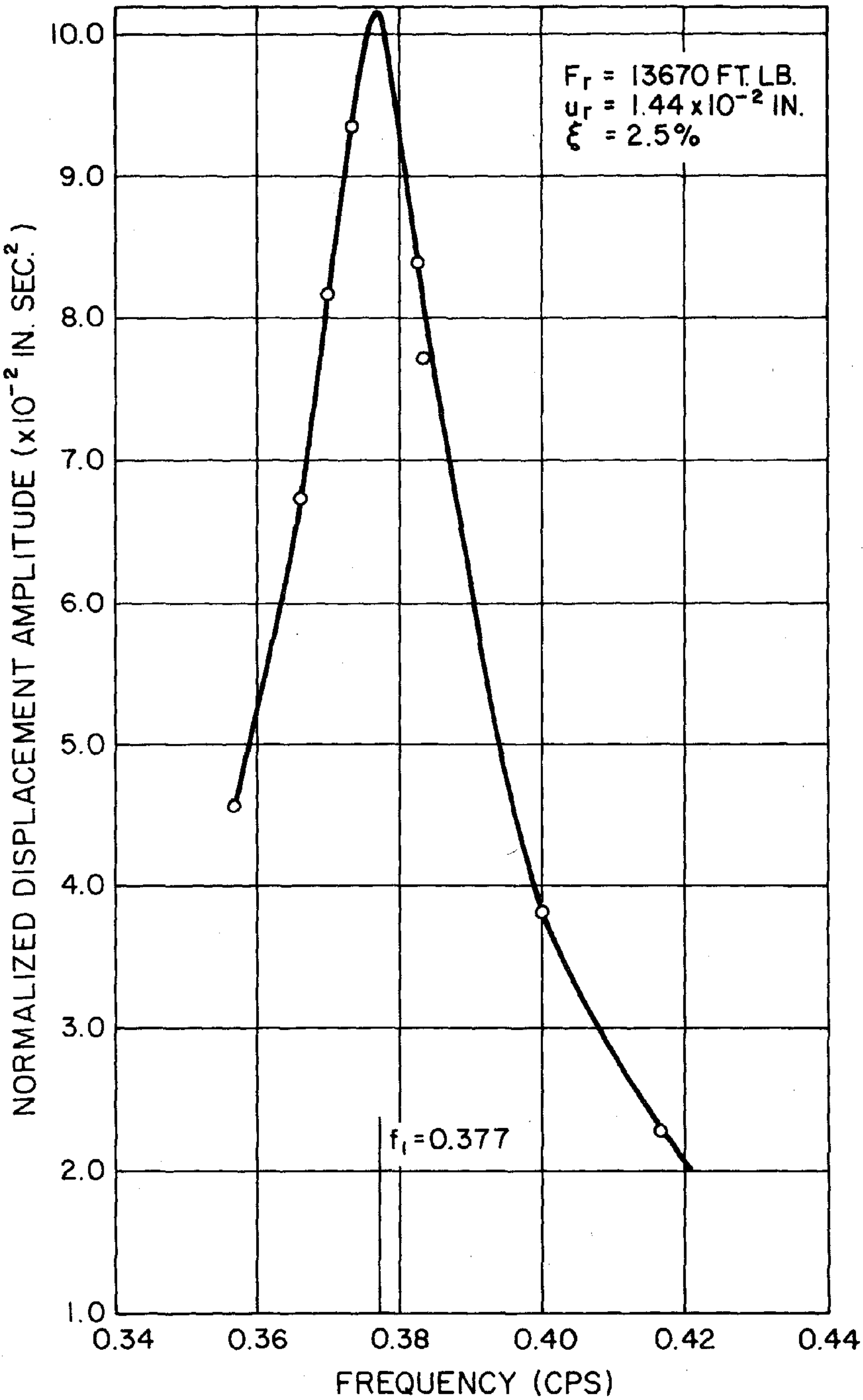

FIG. 3.15 FREQUENCY RESPONSE, FIRST TORSIONAL MODE

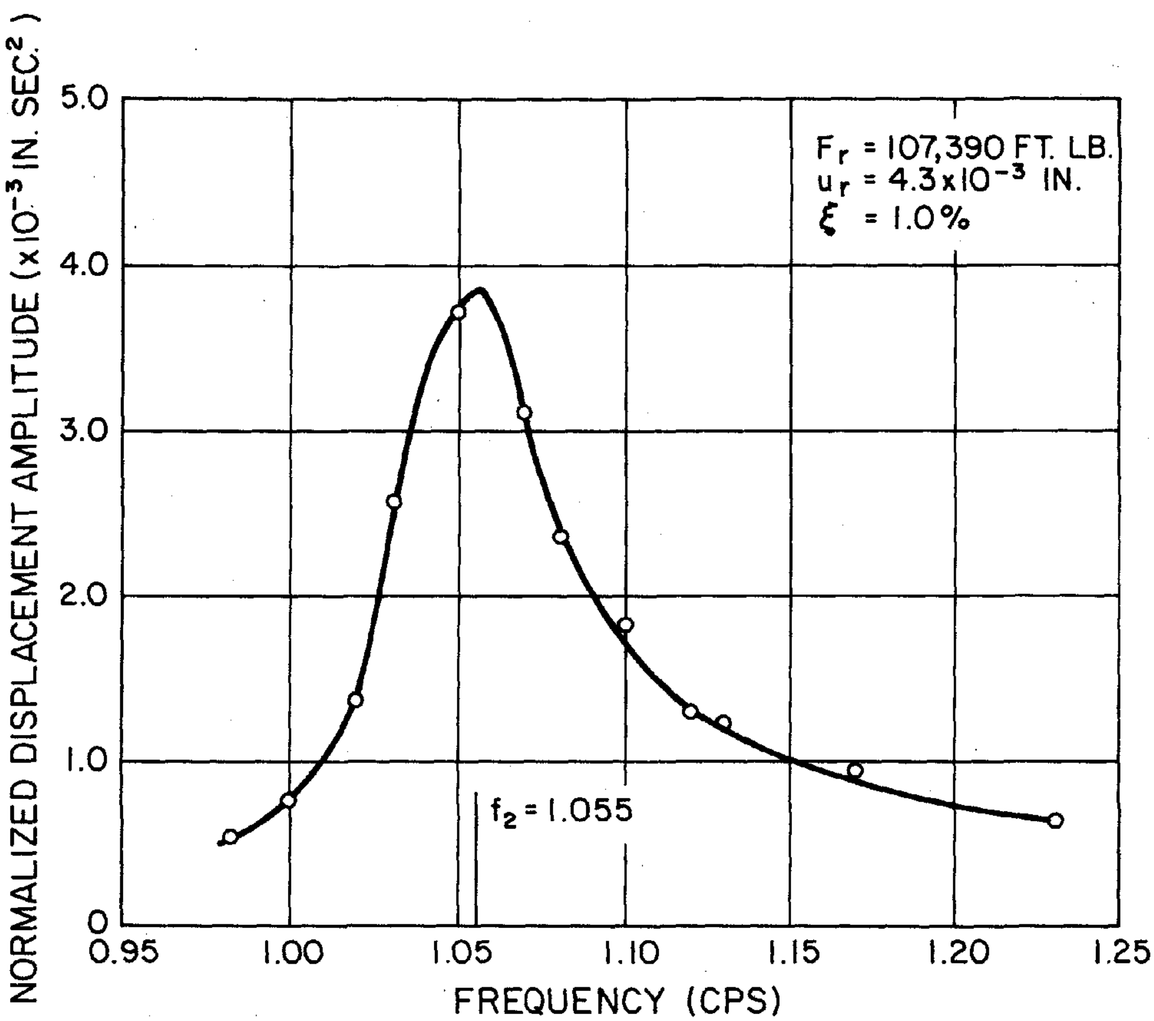

FIG. 3.16 FREQUENCY RESPONSE, SECOND TORSIONAL MODE

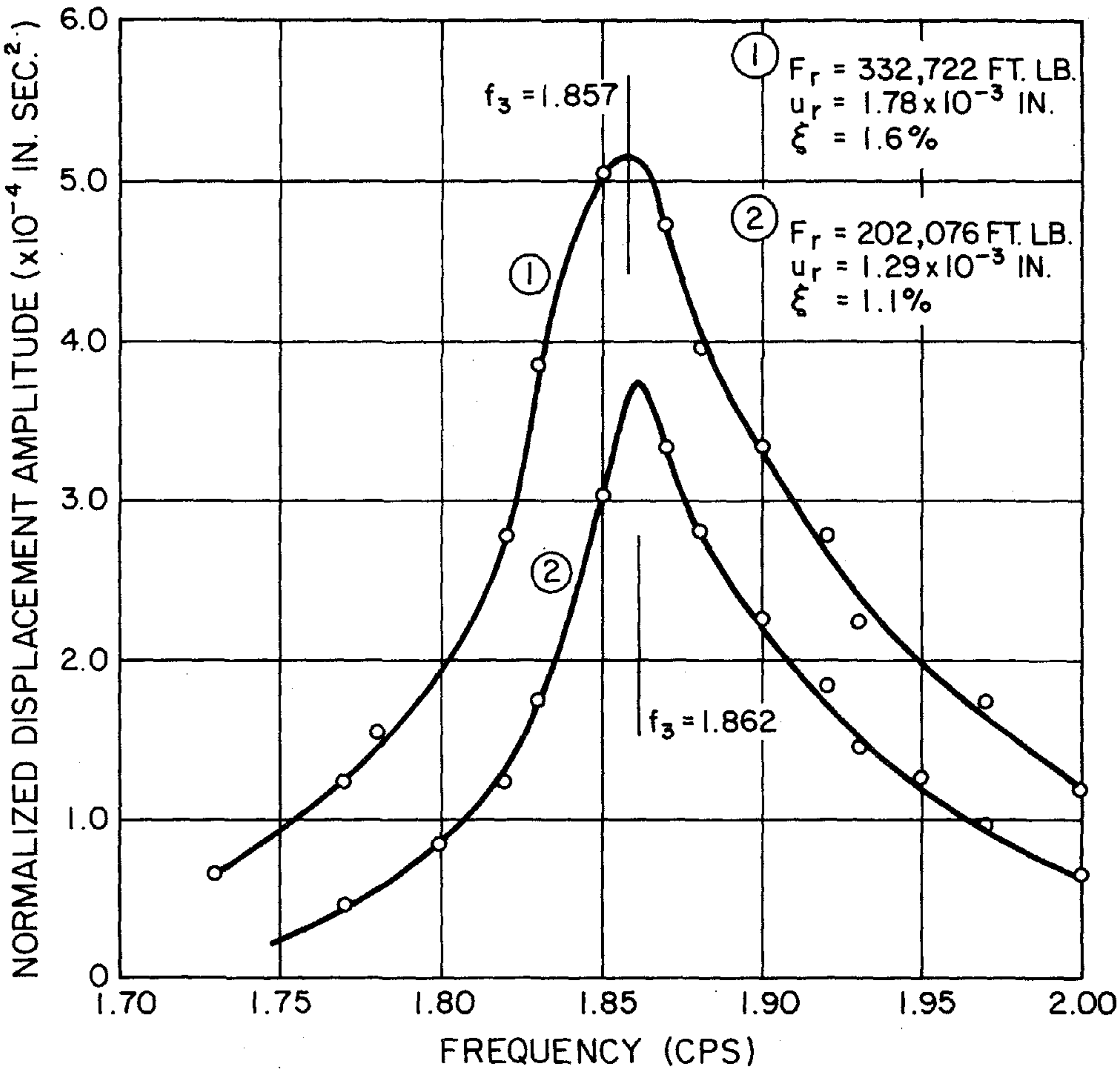

FIG. 3.17 FREQUENCY RESPONSE, THIRD TORSIONAL MODE

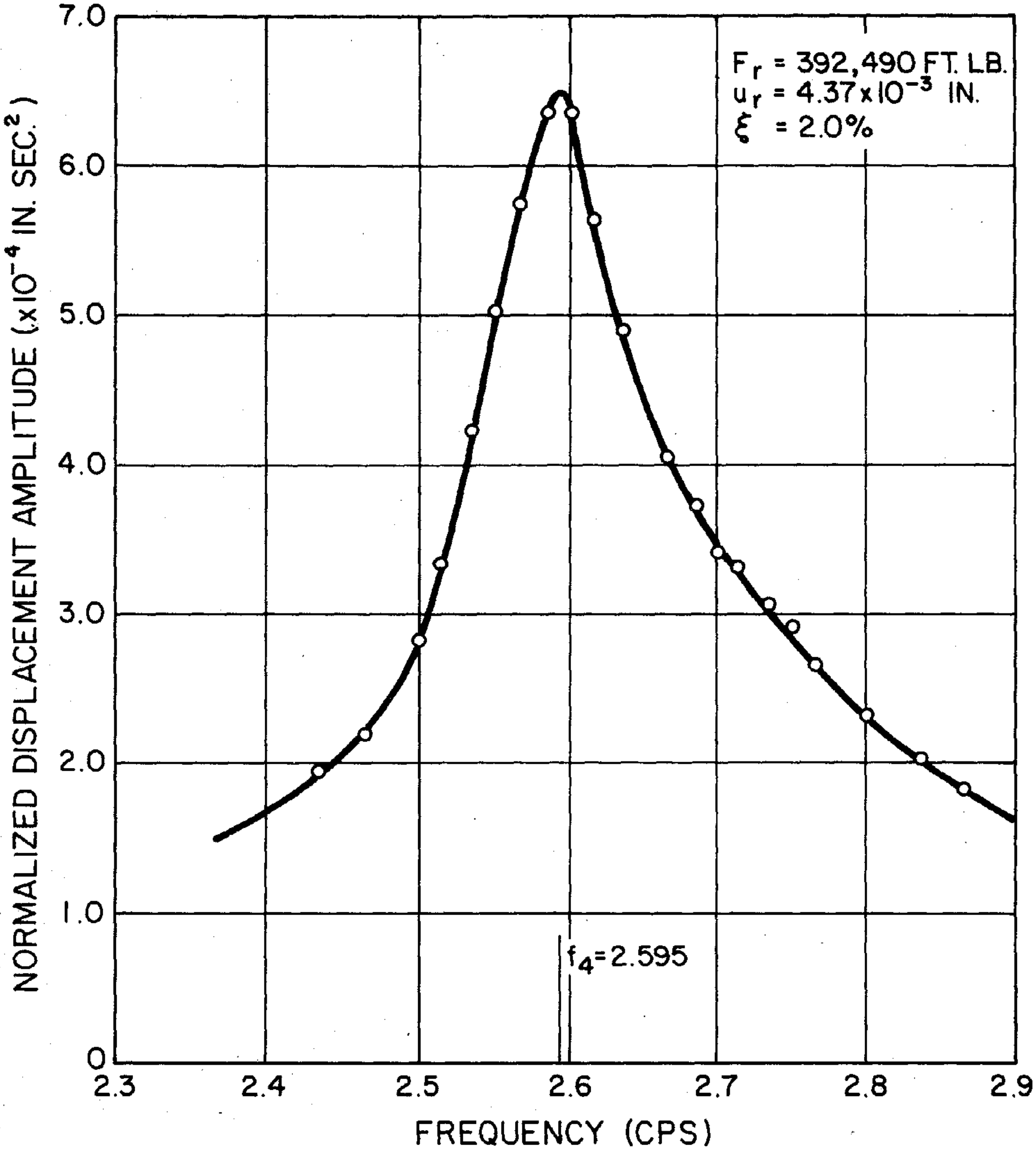

FIG. 3.18 FREQUENCY RESPONSE, FOURTH TORSIONAL MODE

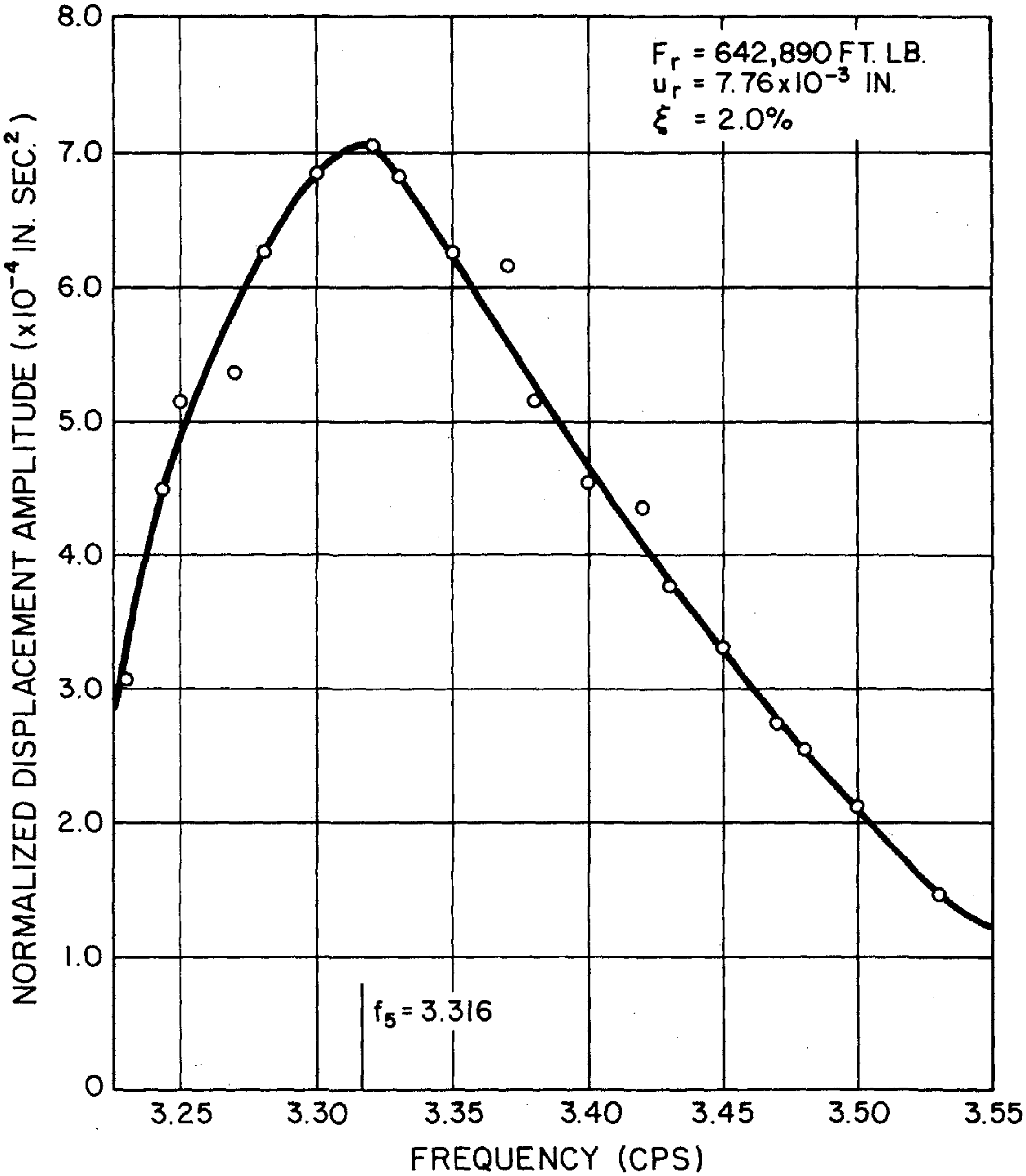

FIG. 3.19 FREQUENCY RESPONSE, FIFTH TORSIONAL MODE

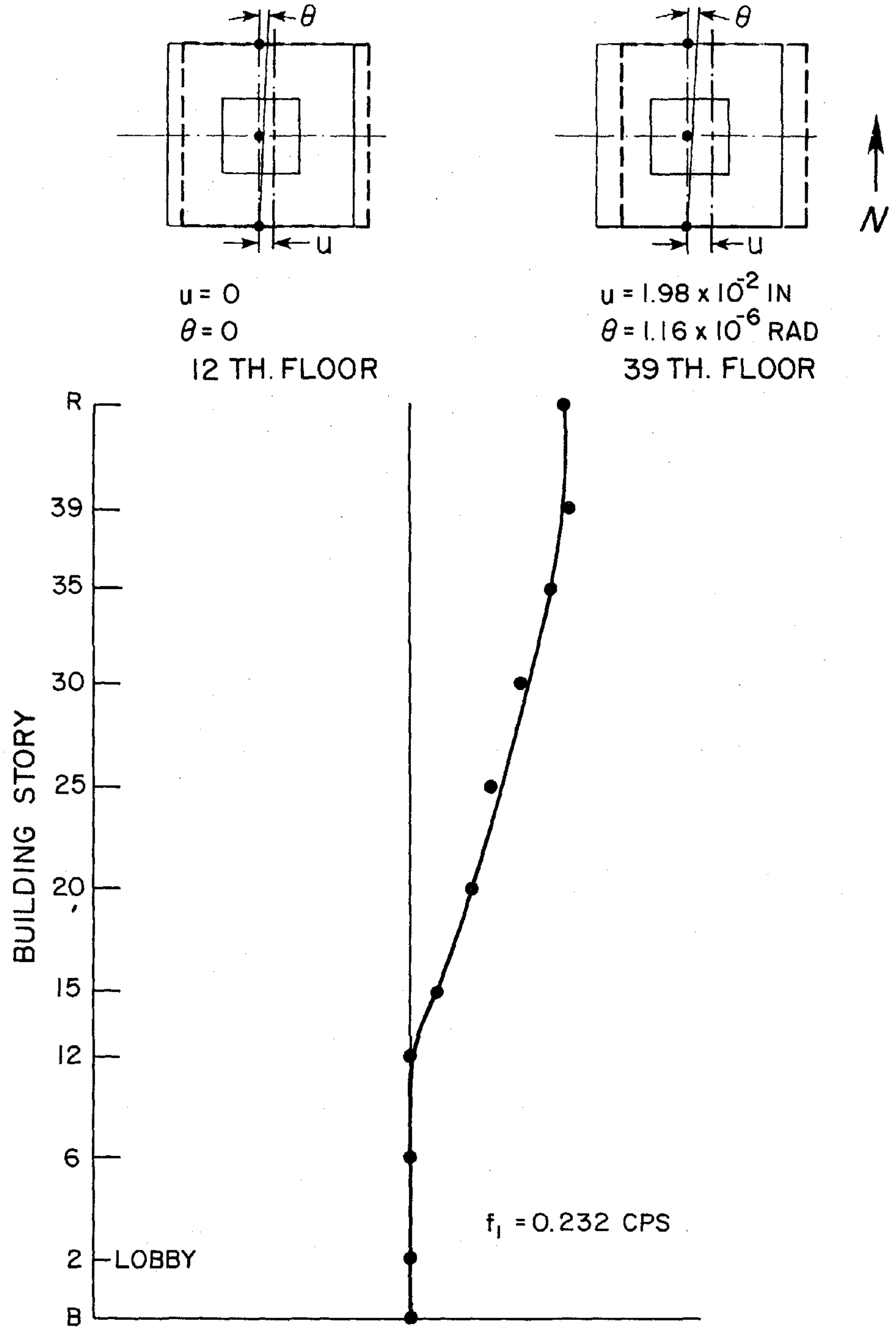

FIG. 3.20 MODE SHAPES, FIRST TRANSLATIONAL MODE E-W

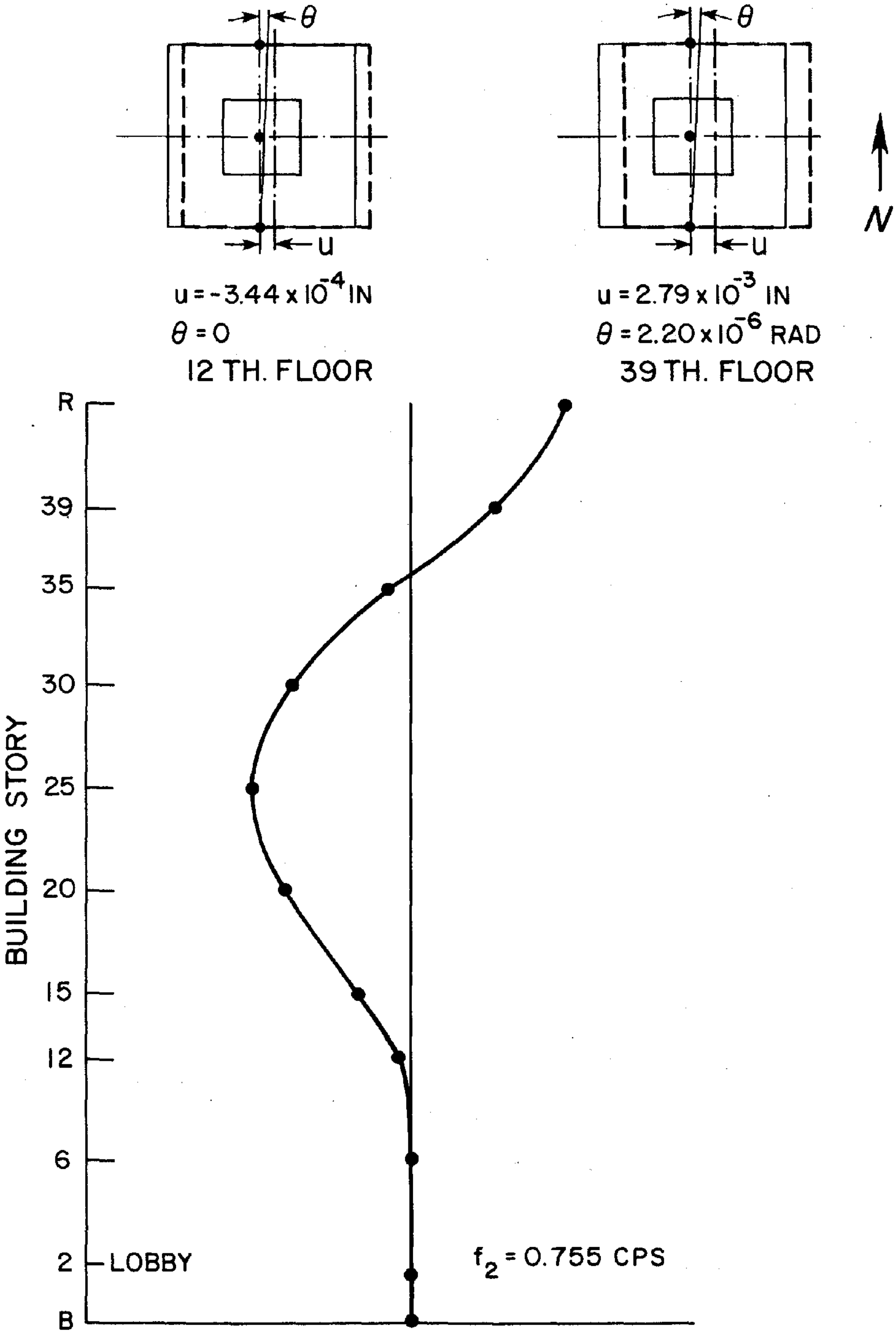

FIG. 3.21 MODE SHAPES, SECOND TRANSLATIONAL MODE E-W

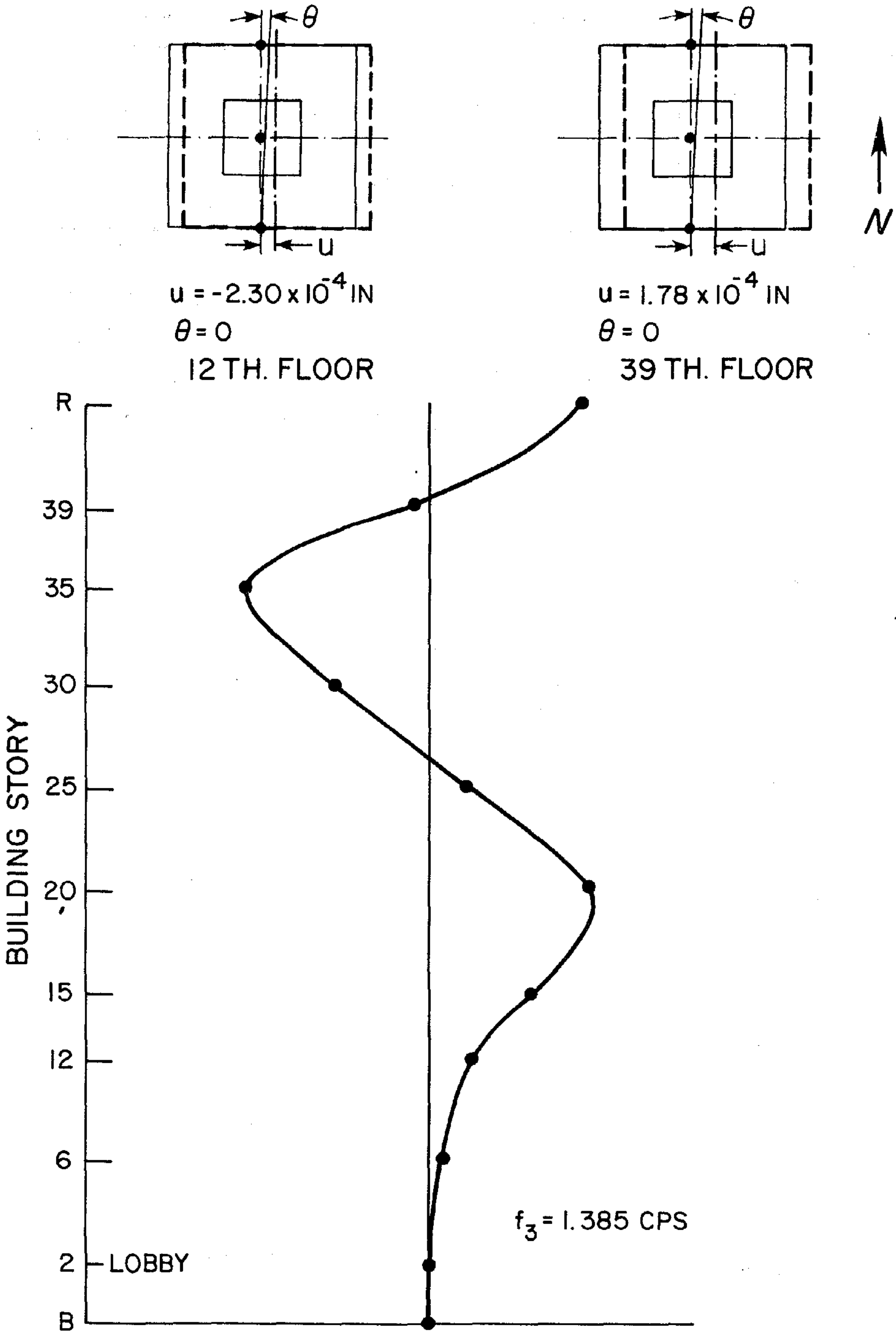

FIG. 3.22 MODE SHAPES, THIRD TRANSLATIONAL MODE E-W

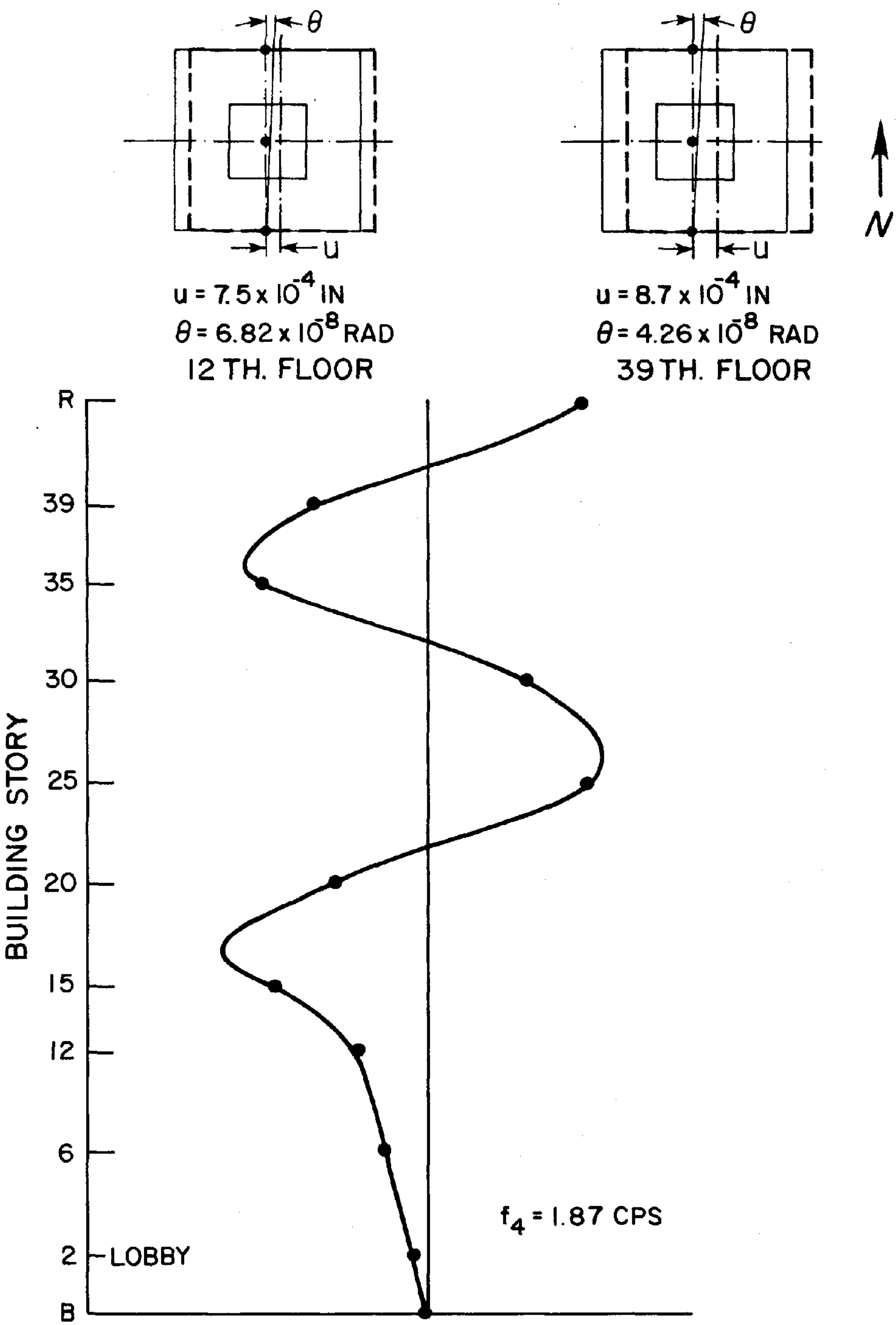

FIG. 3.23 MODE SHAPES, FOURTH TRANSLATIONAL MODE E-W

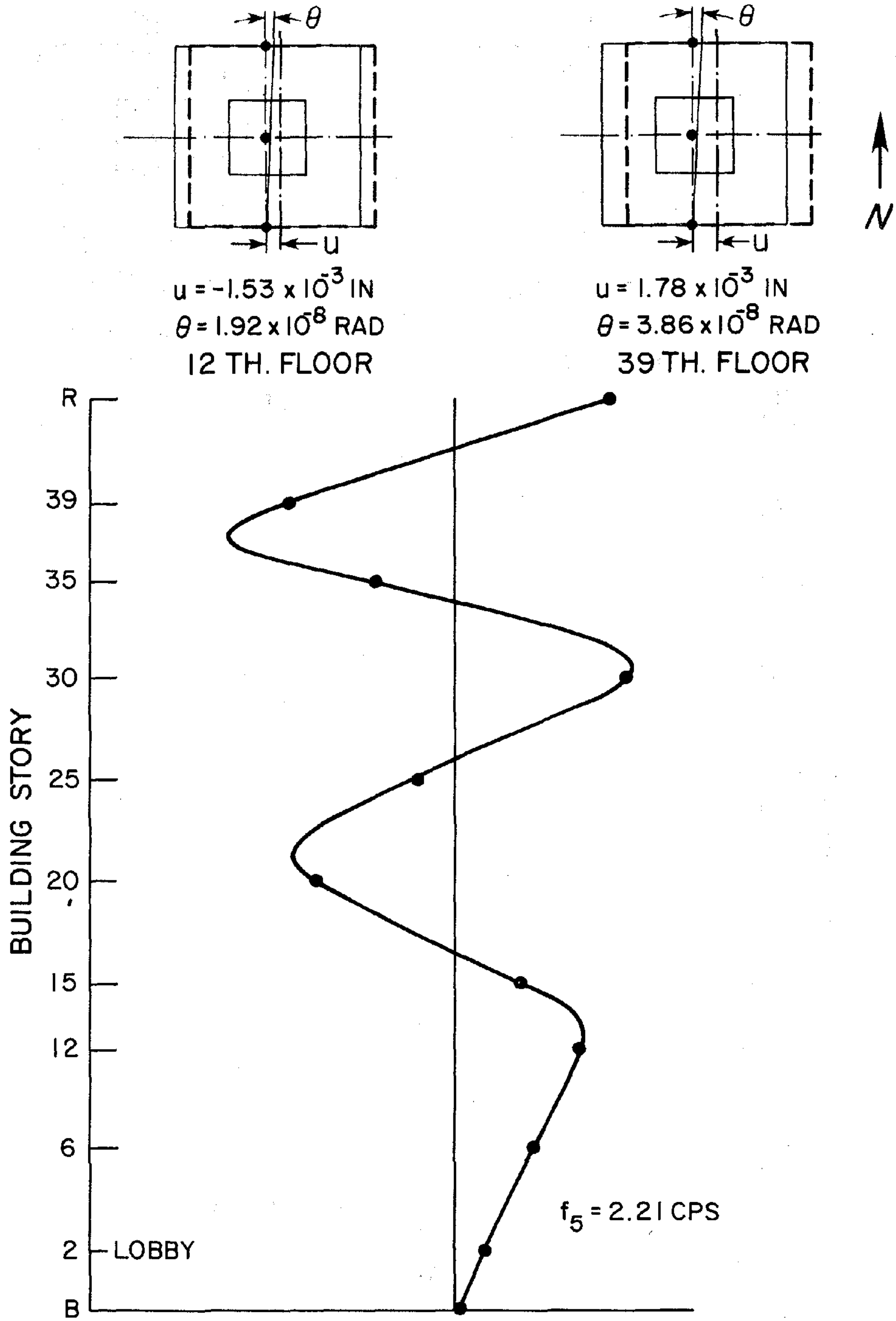

FIG. 3.24 MODE SHAPES, FIFTH TRANSLATIONAL MODE E-W

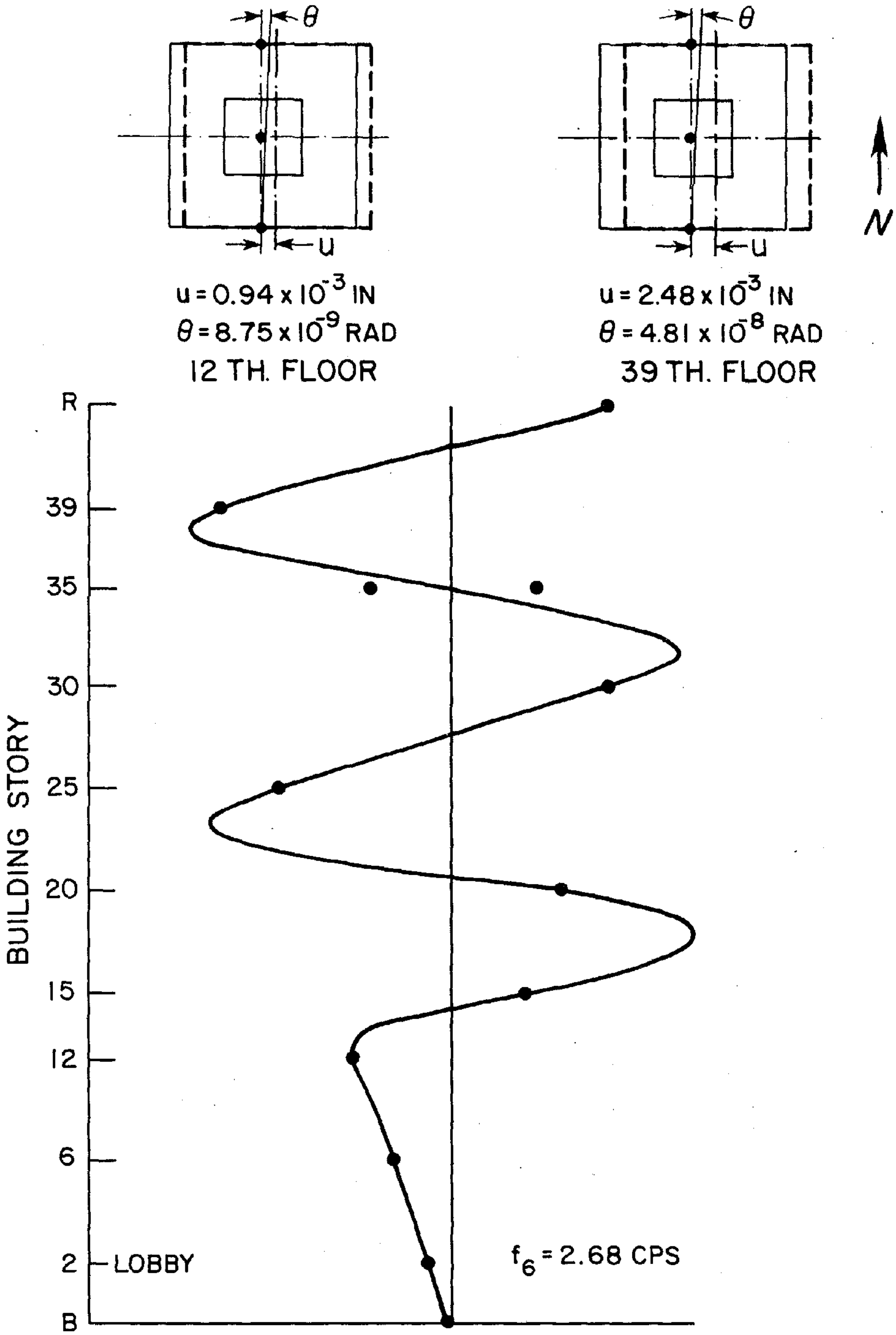

FIG. 3.25 MODE SHAPES, SIXTH TRANSLATIONAL MODE E-W

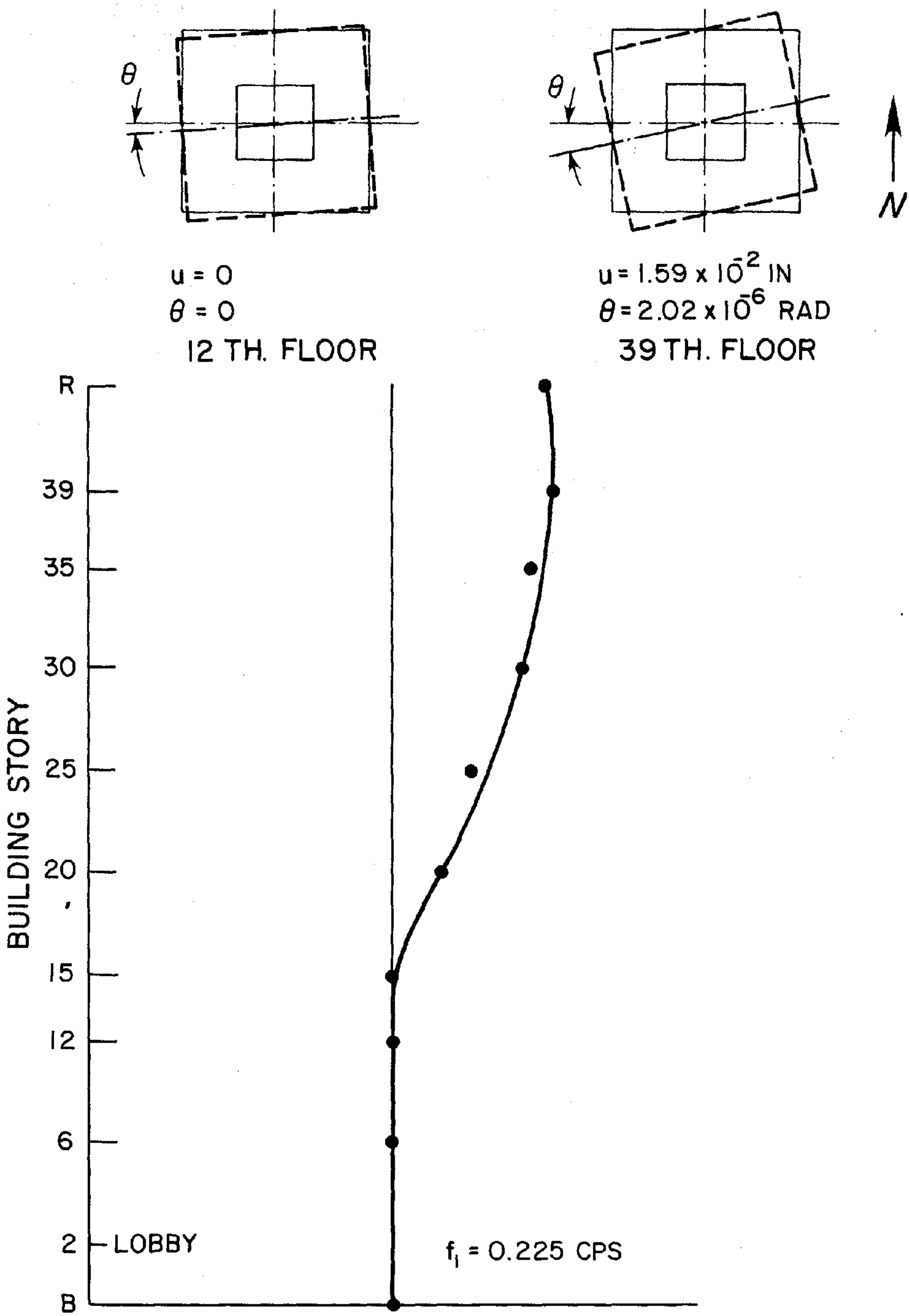

FIG. 3.26 MODE SHAPES, FIRST TRANSLATIONAL MODE N-S

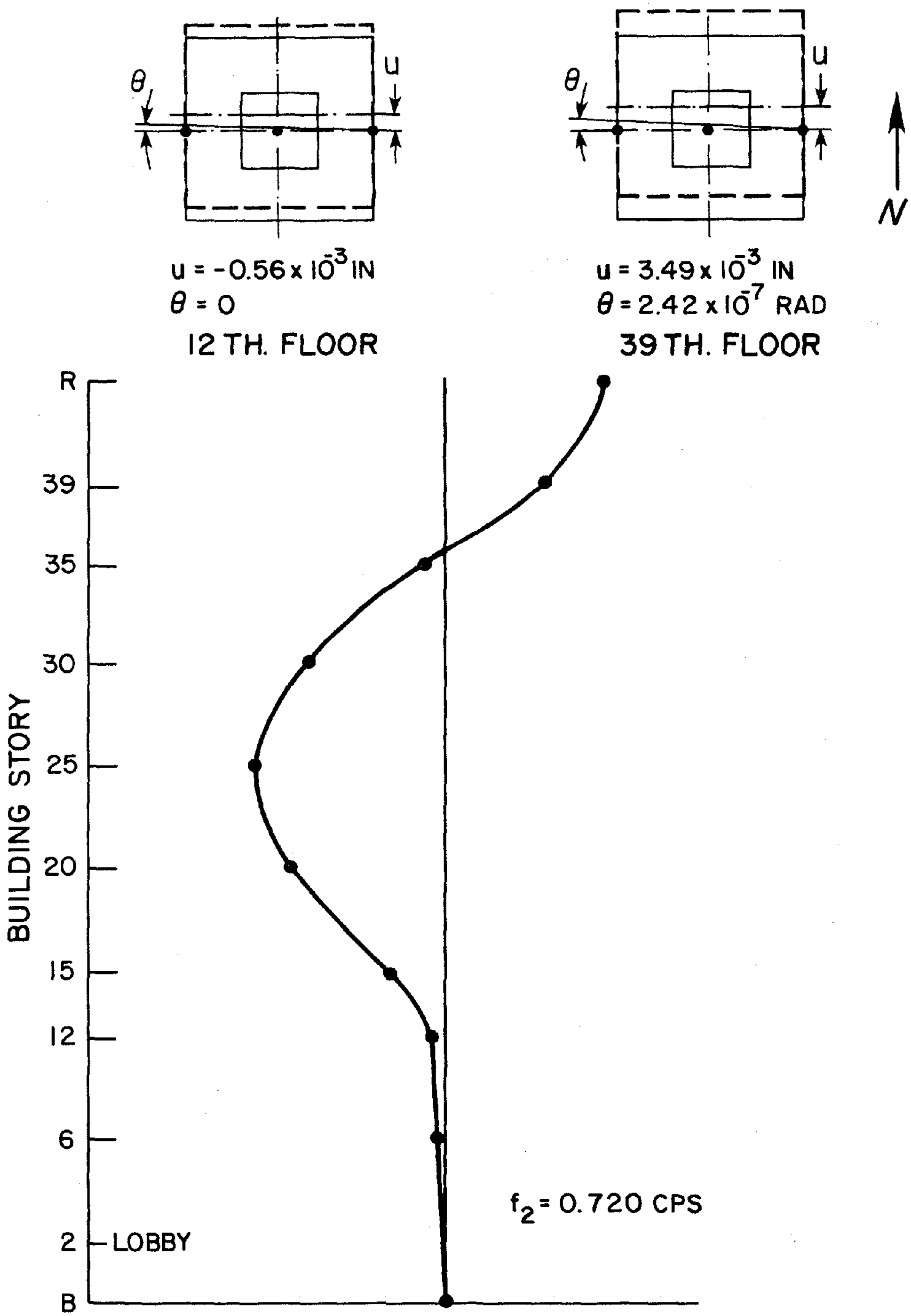

FIG. 3.27 MODE SHAPES, SECOND TRANSLATIONAL MODE N-S

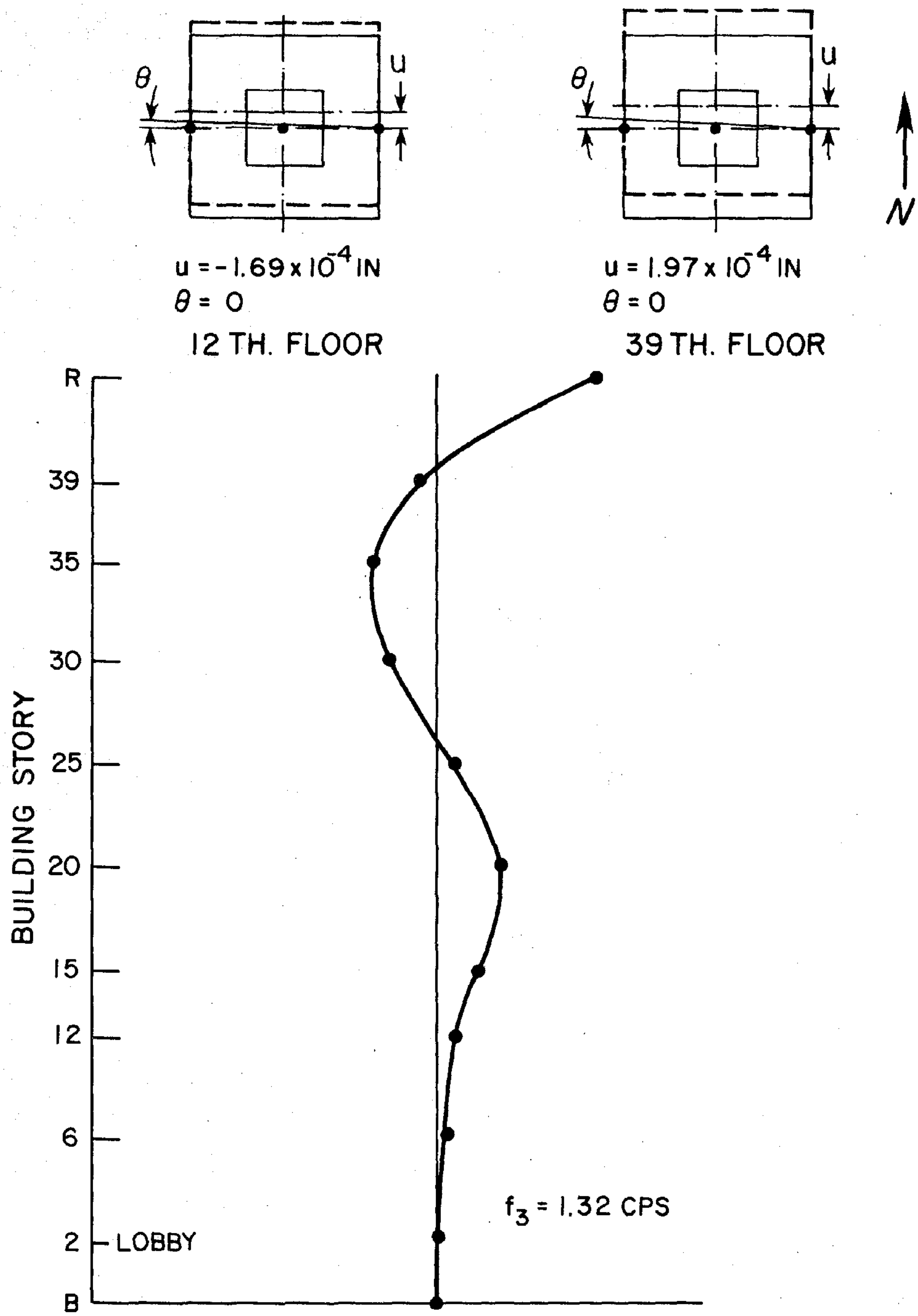

FIG. 3.28 MODE SHAPES, THIRD TRANSLATIONAL MODE N-S

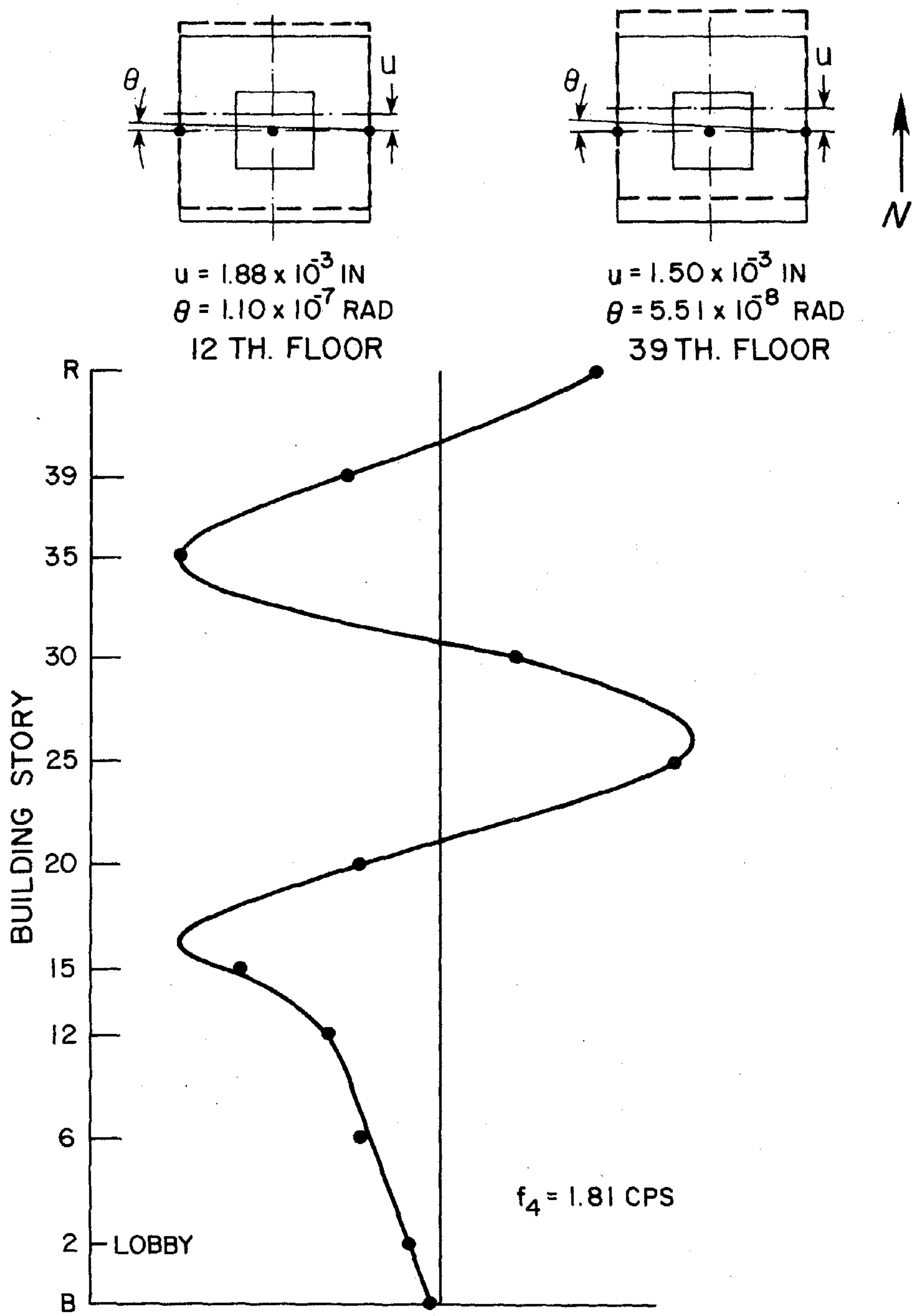

FIG. 3.29 MODE SHAPES, FOURTH TRANSLATIONAL MODE N-S

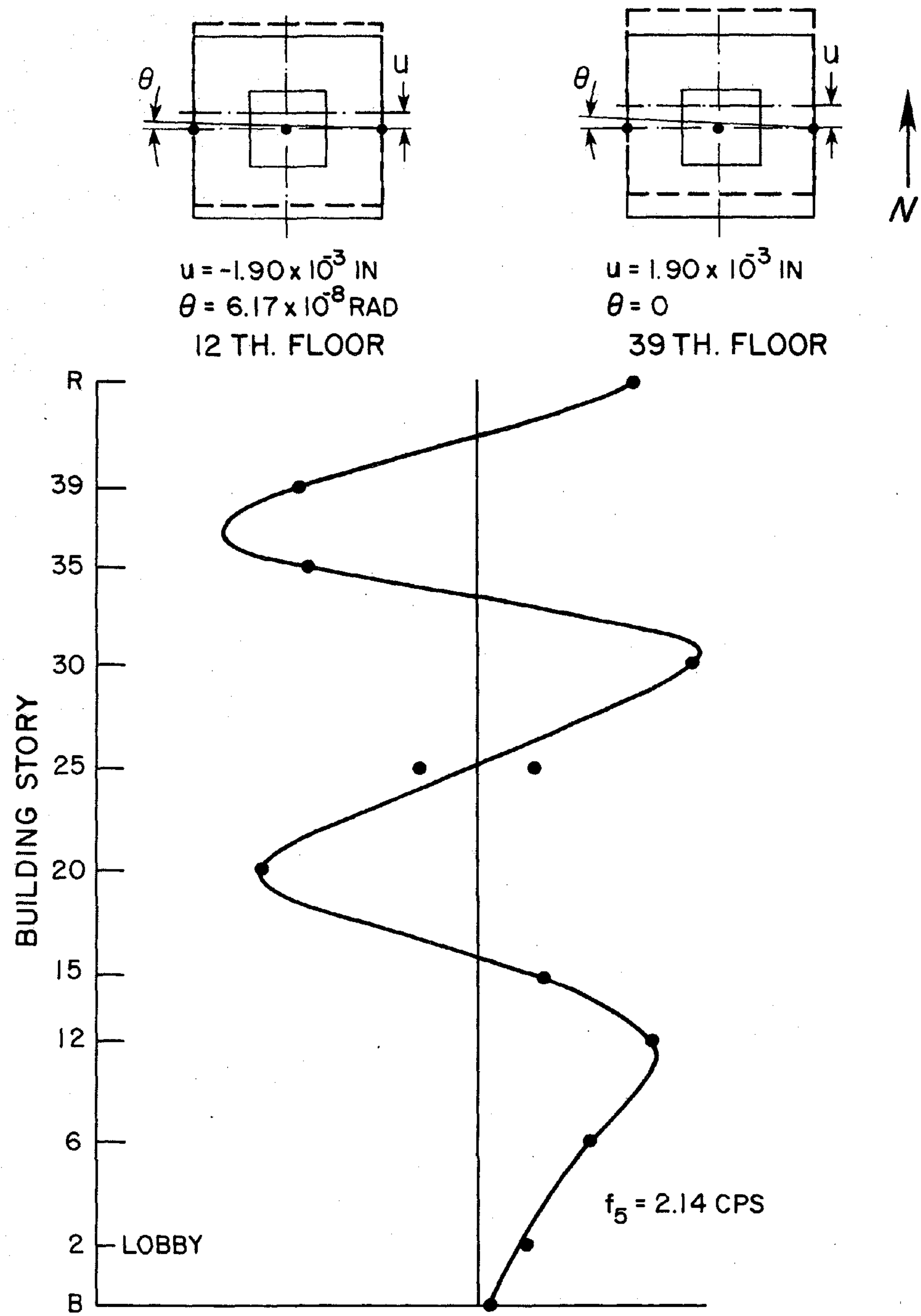

FIG. 3.30 MODE SHAPES, FIFTH TRANSLATIONAL MODE N-S

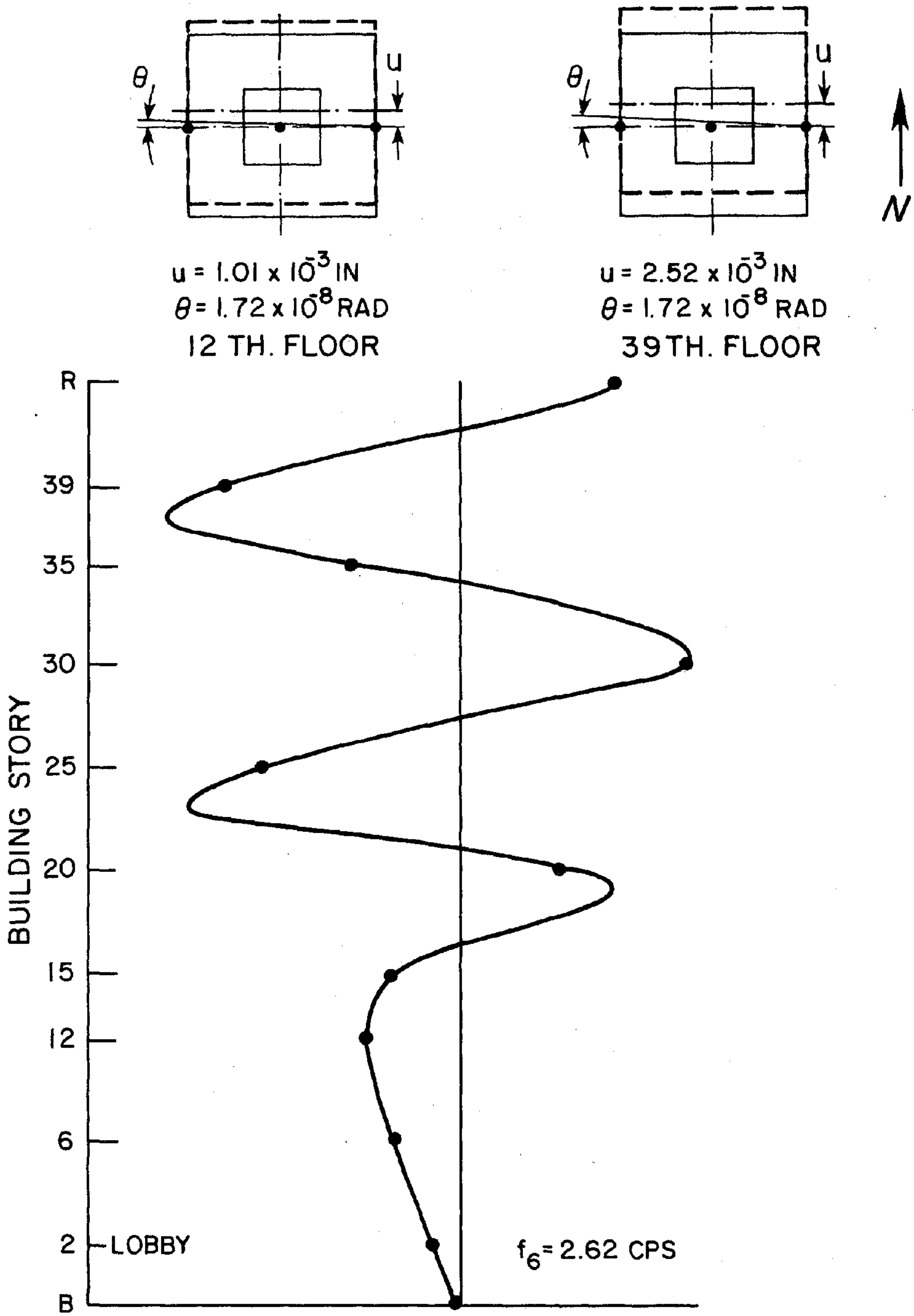

FIG. 3.31 MODE SHAPES, SIXTH TRANSLATIONAL MODE N-S

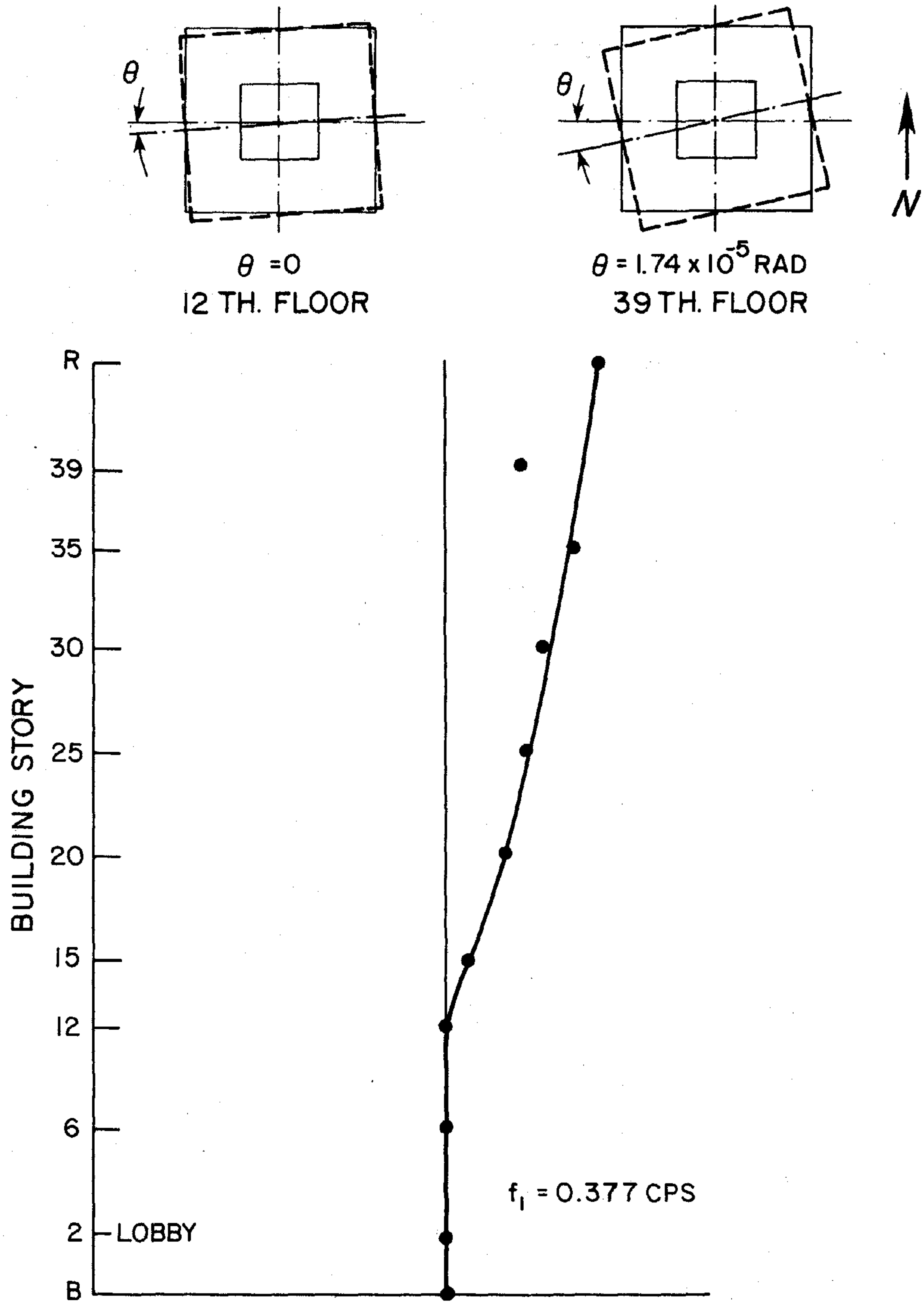

FIG. 3.32 MODE SHAPES, FIRST TORSIONAL MODE

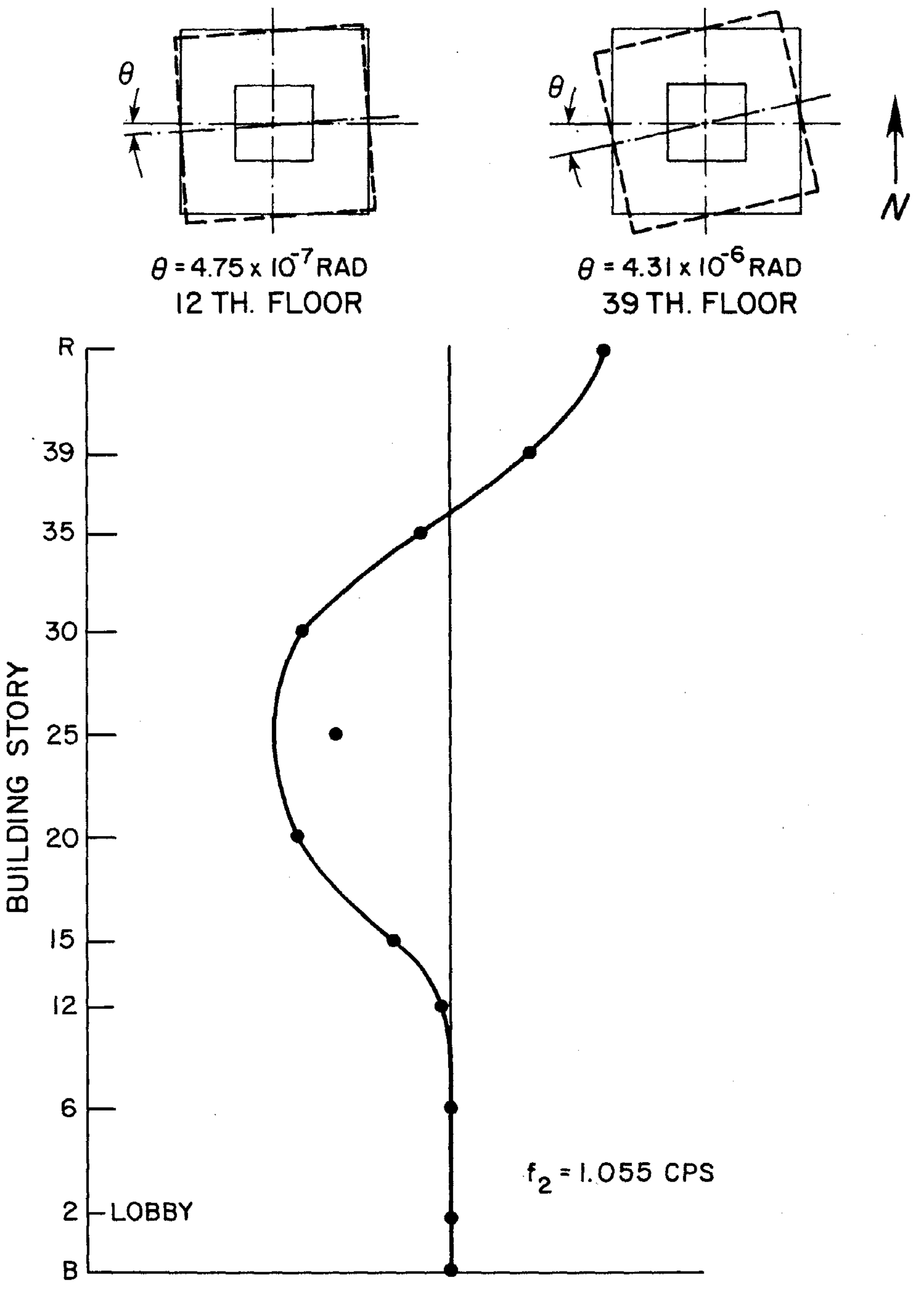

FIG. 3.33 MODE SHAPES, SECOND TORSIONAL MODE

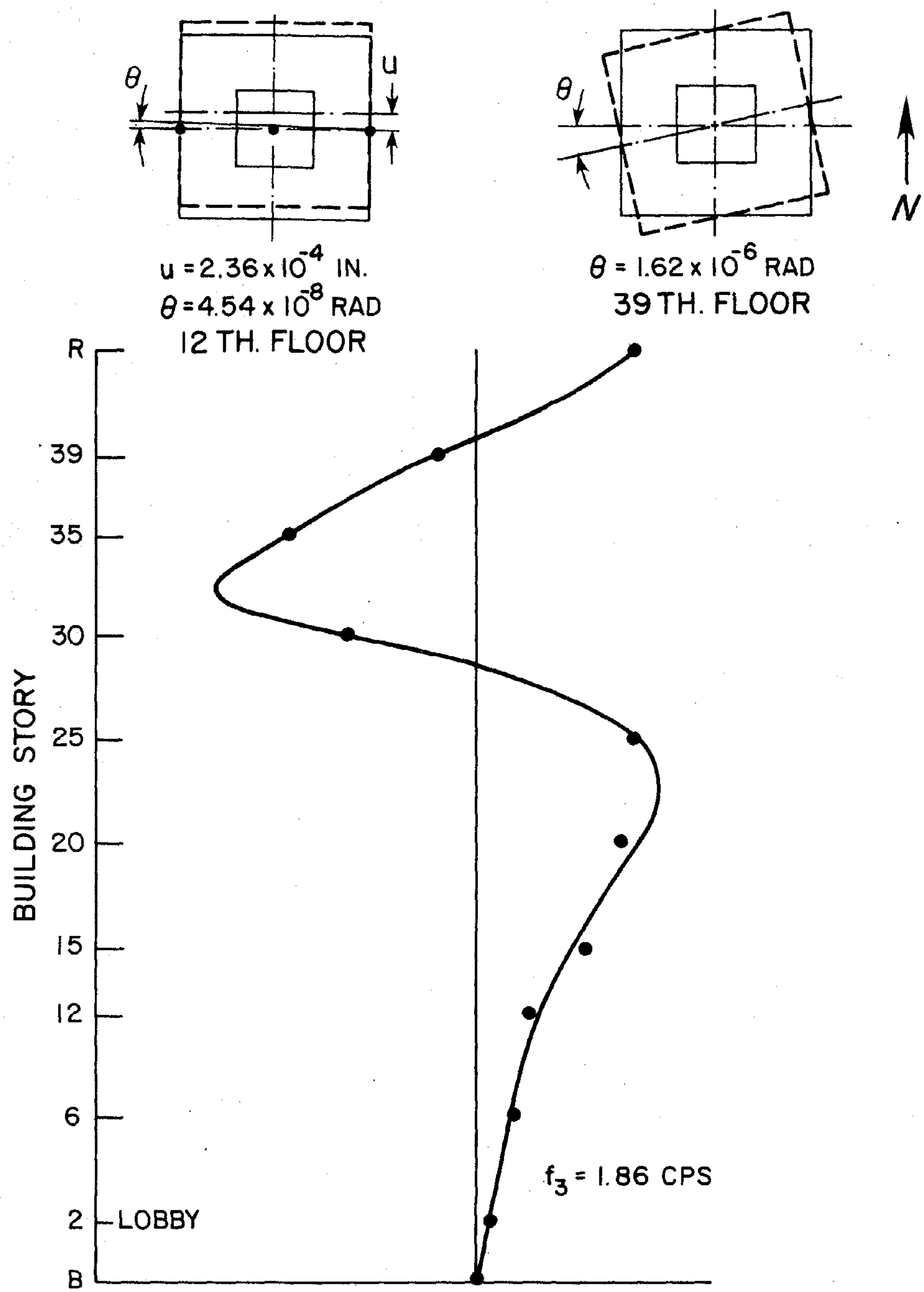

FIG. 3.34 MODE SHAPES, THIRD TORSIONAL MODE

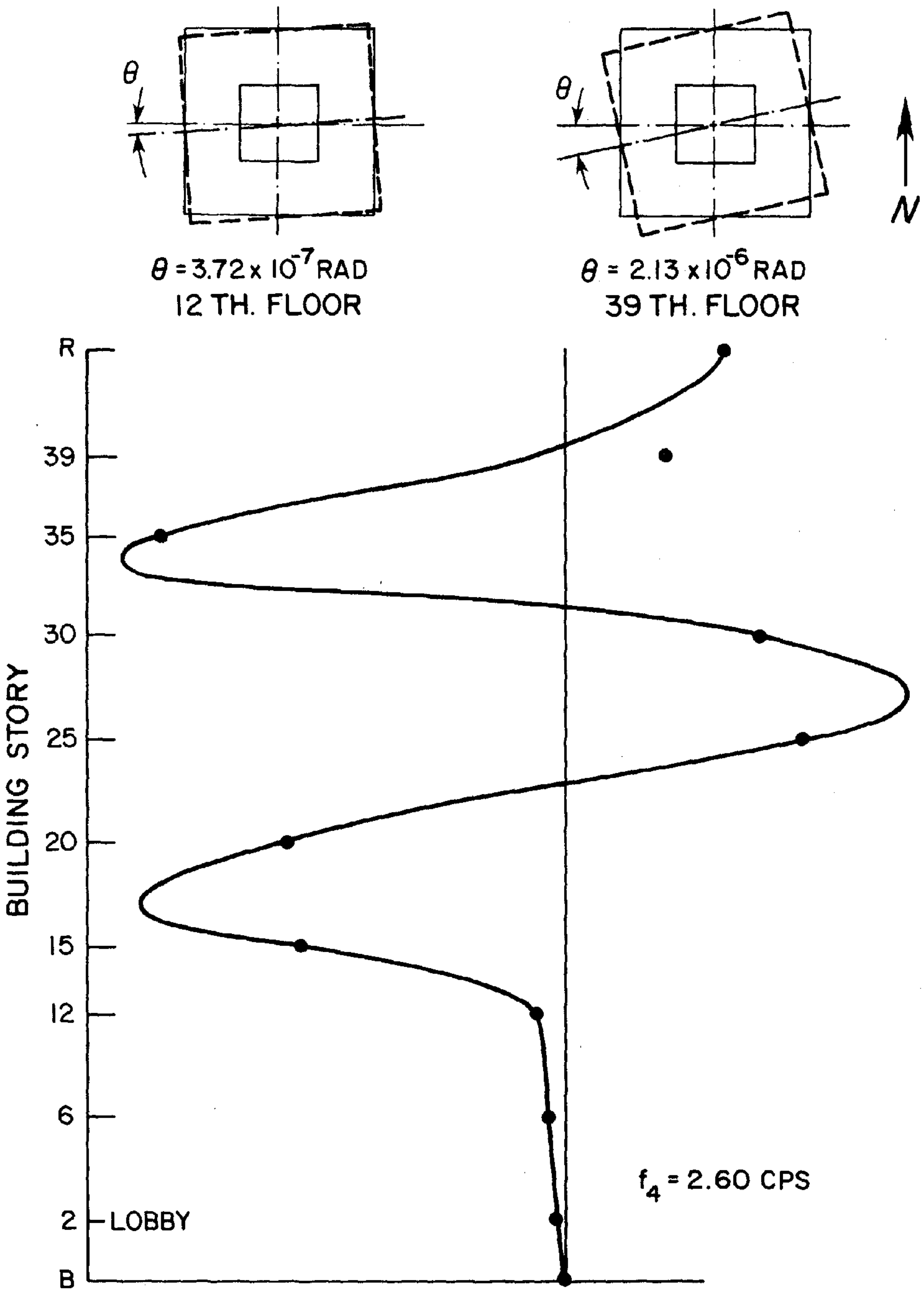

FIG. 3.35 MODE SHAPES, FOURTH TORSIONAL MODE

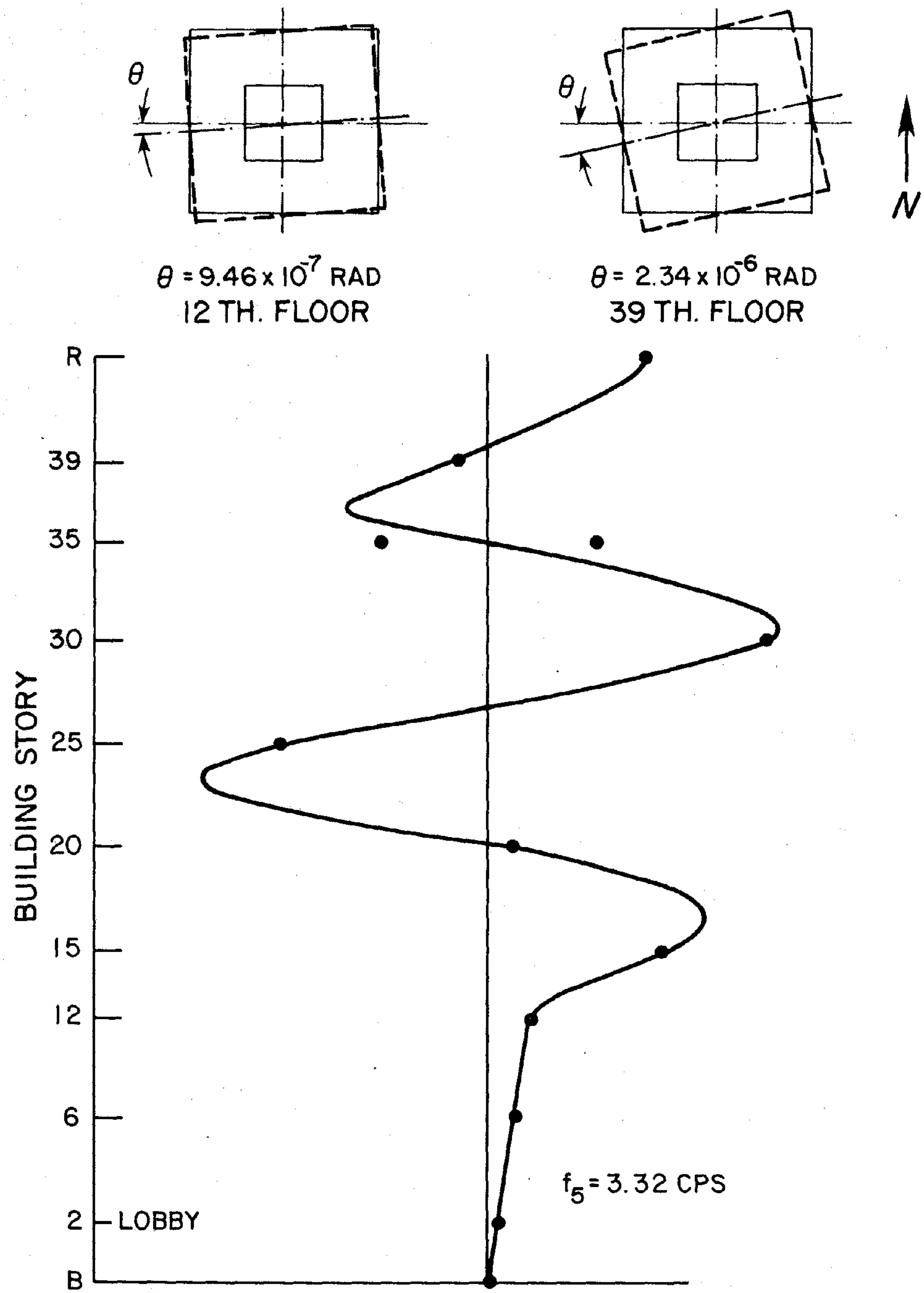

FIG. 3.36 MODE SHAPES, FIFTH TORSIONAL MODE

4. AMBIENT VIBRATION STUDY

4.1 General

In recent years a method for testing of full-scale structures based on wind and microtremor-induced vibrations has been developed. Although the method has been in use for almost 40 years by the United States Coast and Geodetic Survey (16) to measure fundamental periods of the buildings, it was not until recently that this was extended to higher modes (5,8,9, 13,14,17,20).

The ambient vibration study of the dynamic properties of the structures is a fast and relatively simple method of field measurements. It does not interfere with normal building functions, and the measuring instruments and equipment can be installed and operated by a small crew.

The objective of performing the ambient vibration study was to obtain dynamic properties of the building and then compare these results with those obtained from the forced vibration study to assess efficiency of both techniques.

The ambient vibration, experimental and analytical procedures were first suggested by Crawford and Ward (5,17). An assumption in the analysis technique is that the exciting forces are a stationary random process possessing reasonably flat frequency spectrum. For multistory buildings and other large above ground structures, the largest ambient vibrations are produced by wind. If the frequency spectrum of the vibrational exciting forces is reasonably flat, a structure subjected to this input will response in all its normal modes.

The ambient vibration study of the Rainer Tower Building was carried out on April 28, 1977. Wind direction and velocity on the day of dynamic testing measured at the Seattle-Tacoma airport are given in Table 4.1.

The direction of the wind was almost constant at aximuth 23-32° and velocity of 6-8 mph.

TABLE 4.1 - WIND DIRECTION AND VELOCITY
(at Seattle-Tacoma Airport, April 28, 1977)

Time	Wind Blowing	Direction (°)	Velocity (mph)
1 p.m.		32	6.9
4 p.m.		31	5.8
7 p.m.		23	8.0

The vibration measuring equipment employed in the ambient vibration-dynamic test is described below. The general experimental procedures and procedures for data analyses applied are also described. Finally, the experimental results are presented and discussed.

4.2 Field Measurements

4.2.1 Measuring Equipment

The wind induced vibrations were measured using Kinemetrics Ranger Seismometers, Model SS-1. The seismometer has a strong, permanent magnet as the seismic inertial mass moving within a stationary coil attached to the seismometer case. Small rod magnets at the periphery of the coil produce a reversed field which provides a destabilizing force to extend the natural period of the mass and its suspension.

The resulting seismometer frequency was 1 Hz. Damping was set at 0.7 critical. The output for a given velocity is a constant voltage at all frequencies greater than 1 Hz and falls off at 12 dB/octave for frequencies less than 1 Hz.

The Kinemetrics Signal Conditioner, Model SC-1 (Fig. 4.1) was used to amplify and control simultaneously four seismometer signals. The four input channels have isolated circuitry to integrate and differentiate the amplified input signal. All outputs are simultaneously or independently available for recording. A modification to the signal conditioner allows for outputing each channel separately or for taking the sum or difference on two channels and outputing the average of those channels. Each channel provides a nominal maximum gain of 100,000. An 18 dB/octave low pass filter is available with a cut-off frequency continuously selectable between 1 Hz and 100 Hz for each channel.

The amplified analog signals were recorded and directly converted to digital format using the Kinemetrics Digital Data System, Model DDS-1103. A direct recording oscillograph was provided to display and monitor the four signal levels during tape recordings. The data was digitized, in general, at 40 samples per second. The DDS-1103's rate of scan across multiple input channels is 40,000 Hz. This rapid scan rate is sufficient to retain the phase relationship between channels.

A Rockland FFT 512/S Real-Time Spectrum Analyzer was used in order to facilitate the rapid determination of the modal frequencies (Fig. 4.1). This unit is a single channel analyzer with 512 spectral lines calculated but only 400 lines displayed to reduce aliasing errors. Twelve analysis ranges are provided from 0-2 Hz to 0-10 KHz.

4.2.2 Measurement Procedures

When measuring ambient and forced vibrations of the buildings, it is usually assumed that the structure can be approximated by a one-dimensional, damped discrete or continuous system. In most of the cases (11,13,14), measurements indicate that for the level of excitation applied, floor structures are sufficiently stiff so that the above assumption is acceptable. In the case of the Rainer Tower Building, it is assumed that the structural behavior may be approximated by a linear one-dimensional model.

In the experimental study of building vibration which is based on the linear model, it is assumed that the resulting motions can be expressed as the superposition of modes associated with the discrete frequencies (2,3). This approach then requires a simultaneous measurement of motion in a given direction at at least two different floors to obtain their relative amplitude and phase, the two quantities needed to determine mode shapes. During the measurements of wind induced vibrations, it is not necessary to find the actual amplitudes that are recorded because all that is ever used in determining mode shapes is the relative amplitude of the same two instruments.

The modal frequencies were obtained by placing two pairs of seismometers near the outer walls on the north and south and east and west sides of the 39th floor of the building. They were oriented so that the seismometers on the north and south sides produced the east-west frequencies and those on the east and west sides produced the north-south frequencies. The signal conditioner was set so that seismometers 1 and 2 would be output as channel 1, giving the average of the sum of these two readings, and channel 2, the average of the difference of seismometers 1 and 2. The output of seismometers 3 and 4 were similarly averaged. In this way, the translational frequencies could be obtained from the average of the sum of the seismometer readings and the torsional frequencies from the average of the difference of the seismometer readings. As noted in Table 4.2, for the modal frequencies seismometers 1 and 2 were oriented to obtain the north-south frequencies and seismometers 3 and 4 to obtain the east-west frequencies. The data was recorded for a total of 900 seconds.

For measurement of the translational and torsional modes, two of the seismometers remained at the 39th floor and were placed along the building centerlines near the outer column lines and oriented south and west, respectively. The other two seismometers were oriented in the same way and relocated in approximately five floor intervals for simultaneous measurements of motion along the height of the building (Fig.4.3 and Table 4.2). As in the case for determining the modal frequencies, the sum of the two seismometers was averaged to give the translational modes and the difference of the seismometers was averaged to give the torsional modes. Each mode shape run was recorded continuously for 60 seconds. The low pass filter was set on each channel at 10 Hz to attenuate all higher frequencies, thus completely removing electrical noise and other possible high frequency vibrations. The voltage output to the recorder was adjusted to not exceed about ± 1.5 volts. The unattenuated calibration constant for the seismometers used was approximately 4.32 volts/in/sec. Corresponding first mode acceleration and displacement were about $\pm\ 0.03 \times 10^{-5}$ g and $\pm\ 5.5 \times 10^{-5}$ inches, respectively.

4.3 Data Analysis

4.3.1 Fourier Analysis

It is convenient to use Fourier transforms to analyze low level structural vibrations. They may be used to exhibit the frequency content of the recorded vibration, thus identifying modal frequencies when the input force frequency spectrum is reasonably flat. Comparing measured amplitude and phase between various points on the structure provides an estimate of the mode shape.

A measured time-series signal $x(t)$ can be transformed to the

TABLE 4.2 LOCATION OF SEISMOMETERS.

Run Number	Sample Rate (sps)	Duration (sec)	Floor, Direction Seis #1	Seis #2	Seis #3	Seis #4	Channel Data 1	2	3	4
1	20	900	39S	39S	39W	39W	T	θ	T	θ
2	40	60	39S	39S	RS	RS	T	θ	T	θ
3	40	60	39W	39W	35W	35W	T	θ	T	θ
4	40	60	39W	39W	35W	35W	T	θ	T	θ
5	40	60	39S	39S	35S	35S	T	θ	T	θ
6	40	60	39S	39S	30S	30S	T	θ	T	θ
7	40	60	39W	39W	30W	30W	T	θ	T	θ
8	40	60	39W	39W	25W	25W	T	θ	T	θ
9	40	60	39S	39S	25S	25S	T	θ	T	θ
10	40	60	39S	39S	12S	12S	T	θ	T	θ
11	40	60	39W	39W	12W	12W	T	θ	T	θ
12	40	60	39W	39W	15W	15W	T	θ	T	θ
13	40	60	39S	39S	15S	15S	T	θ	T	θ
14	40	60	39S	39S	20S	20S	T	θ	T	θ
15	40	60	39W	39W	20W	20W	T	θ	T	θ
16	40	60	39W	39W	6W	6W	T	θ	T	θ
17	40	60	39W	39S	6S	6S	T	θ	T	θ
18	40	60	39S	39S	BS Core Wall	BS Core Wall	T	θ	T	θ
19	40	60	39W	39W	BS Outer Wall	BS Outer Wall	T	θ	T	θ
20	40	60	39W	39W	BW Core Wall	BW Core Wall	T	θ	T	θ
21	40	60	39W	39W	BW Outer Wall	BW Outer Wall	T	θ	T	θ

* T = Translation θ = Torsion

frequency domain, with certain restrictions, using the integral

$$X(f) = \int_{-\infty}^{\infty} x(t)e^{-2\pi ift} \, df \qquad (4\text{-}1)$$

where $X(f)$ represents the frequency domain function, f is frequency, and $i = \sqrt{-1}$.

The time-series $x(t)$ can be recovered by the inverse transformation

$$x(t) = \int_{-\infty}^{\infty} X(f)e^{2\pi ift} \, df \qquad (4\text{-}2)$$

Equations 4-1 and 4-2 may be expressed in functional notation as

$$X(f) = F\,[x(t)] \qquad (4\text{-}3)$$

$$x(t) = F^{-1}\,[X(f)] \qquad (4\text{-}4)$$

Equation 4-3 is the direct transform and Equation 4-4 is the inverse transform. Together they are called a Fourier Transform Pair. The direct transform maps a time-series (time domain) into a function of f (frequency domain). The inverse transform reverses the process. $X(f)$ is a complex number with both amplitude and phase.

$|X(f)|$ is known as the amplitude spectrum of $x(t)$. The function $|X(f)|^2$ is known as the power spectrum of $f(t)$.

Consider the elastic structure representing a multistory building. The set of time-series $x_1(t)$, $x_2(t)$, ... $x_i(t)$, ..., $x_n(t)$ recorded for corresponding floor levels is transformed to the frequency domain,

$$\begin{aligned} X_1(f) &= F\,[x_1(t)] \\ X_2(f) &= F\,[x_2(t)] \qquad (4\text{-}5) \\ \cdot \quad & \quad \cdot \end{aligned}$$

$$\vdots \qquad \vdots$$

$$X_i(f) = F\,[x_i(t)]$$

$$\vdots \qquad \vdots$$

$$X_n(f) = F\,[x_n(t)]$$

Modal frequencies of the structure appear as peaks in the plots of amplitude spectra $|X_n(f)|$. The i'^{th} mode shape coefficient a_{ij} at each natural frequency f_j normalized to the value at coordinate 1 is simply:

$$a_{ij} = \frac{|X_i(f_j)|}{|X_1(f_j)|} \tag{4-6}$$

The relative phase of the complex product $X_1(f)\ X_i(f)$ gives the mode shape direction.

Actual calculations are based on a limited time measurement of X(t). In the time interval T, the Fourier transform (4-1) becomes

$$X(f) = \int_{-T/2}^{T/2} x(t)e^{-2\pi\ ift}\,dt \tag{4-7}$$

The Hanning time window is one of the simplest methods used to minimize the spectral spreading effect caused by the finite record length. It is used for the routine Fourier amplitude spectrum calculations in this report. The standard Fourier amplitude spectrum is smoothed by 1/4, 1/2, 1/4 weights as follows:

$$|X_i(f)|_{sm} = 1/2\ |X_i(f)| + 1/4\ \{|X_{x+1}(f)| + |X_{i-1}(f)|\} \tag{4-8}$$

In addition to the Hanning window, a number of transforms were determined using discrete sets of data along the total time history. These transforms were averaged to give a final Fourier amplitude spectra.

Estimates of equivalent viscous damping are obtained from the width of the peak corresponding to the modal frequency of interest

$$\xi = \frac{\Delta f}{2f} \tag{4-9}$$

where ξ is the critical damping ratio and Δf is the peak width (bandwidth in Hz) measured at $1/\sqrt{2}$ of the amplitude spectrum value $|X(f_i)|$.

4.3.2 Data Processing

Four simultaneous outputs were recorded on magnetic tape during each of the 21 runs listed in Table 4.2. The first run was digitized at a sample rate of 20 discrete points per second, and all the remaining runs were digitized at 40 points per second. Because of the high frequency filtering present in the field instrumentation, no significant frequencies above 10 Hz were found in the recordings. For the resonant frequency runs, 2048 data points were selected for the translational and torsional modes. A total of 20 transforms separated by 839 points were calculated and averaged over the 18,000 data points gathered.

For each mode shape run, 1024 data points were selected and a total of 10 transforms were taken. The Fourier amplitude spectrum was an average of the 10 transforms computed.

The spectral estimates were smoothed by 1/4, 1/2, 1/4 weights. The 1024 spectral estimates are uniformly distributed between 0 Hz and 40 Hz, giving a frequency resolution of 40/1024, or about 0.0391 Hz.

4.3.3 Frequencies and Modes of Vibration

The natural frequencies of vibration for six E-W and N-S translational modes and for five torsional modes are given in Table 4.3.

TABLE 4.3 - RESONANT FREQUENCIES (cps)

Excitation	Mode					
	1	2	3	4	5	6
E-W	.234	.762	1.41	1.98	2.29	2.85
N-S	.225	.732	1.35	1.87	2.16	2.76
Torsional	.381	1.07	1.86	2.64	3.47	----

The ratios of the higher mode frequencies with respect to fundamental ones are given in Table 4.4. The values obtained are close to the ratios 1, 3, 5, 7, 9, 11 ..., indicating that the building vibration in all studied directions are predominantly of the shear type.

TABLE 4.4 - RATIO OF RESONANT FREQUENCIES

Mode	Translational, E-W		Translational, N-S		Torsional	
	fi (cps)	fi/f_1	fi (cps)	fi/f_1	fi (cps)	fi/f_1
1	.234	1.00	.225	1.00	.380	1.00
2	.762	3.26	.732	3.25	1.07	2.81
3	1.41	6.03	1.35	6.00	1.86	4.88
4	1.98	8.46	1.86	8.27	2.64	6.93
5	2.29	9.79	2.16	9.6	3.47	9.10
6	2.85	12.18	2.76	12.27	----	----

Mode shapes were calculated for all six modes in the E-W and N-S translational directions as well as five torsional modes. All determined modes of vibration are given in Figs. 4.4 through 4.20.

4.3.4 Damping

In the case of force vibration study, damping in the structure can be determined in several ways: by the bandwidth method, by measuring relative peak amplitudes, or, when there is no wind, by measuring a free vibration response.

During the ambient vibrations, strictly speaking, all these methods fail unless measurements can be taken during the period when wind excitations are random and stationary in time (17). According to the criteria described in (17), during the ambient vibration study of the Rainer Tower Building, wind excitation could be considered in most of the runs as random and nearly stationary in time. There was also reasonably good separation of the translational and torsional modes and no overlapping in the peak areas was noticed.

Estimation of the equivalent viscous damping factors from this study are given in Table 4.5. The damping for the translational and torsional modes was calculated from the averaged spectra from run number one on the 39th floor.

TABLE 4.5 - DAMPING FACTORS (%)

Excitation	Mode					
	1	2	3	4	5	6
E-W	1.9	1.1	3.0	1.3	1.7	0.7
N-S	2.2	1.5	1.8	1.1	1.1	1.0
Torsional	3.3	1.6	1.7	1.4	0.6	---

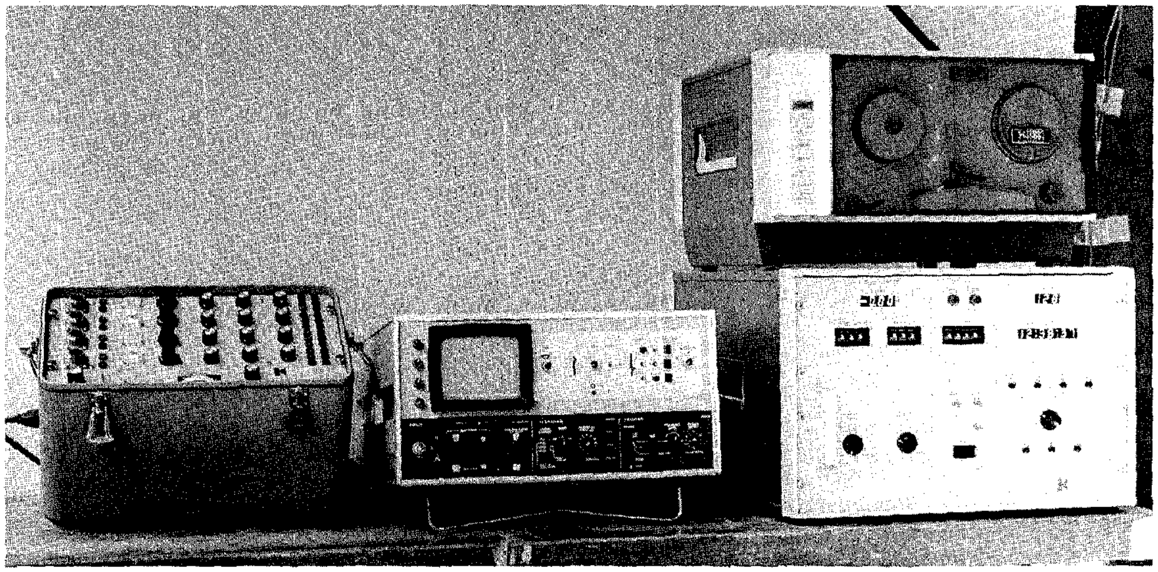

FIG. 4.1 AMBIENT VIBRATION EQUIPMENT

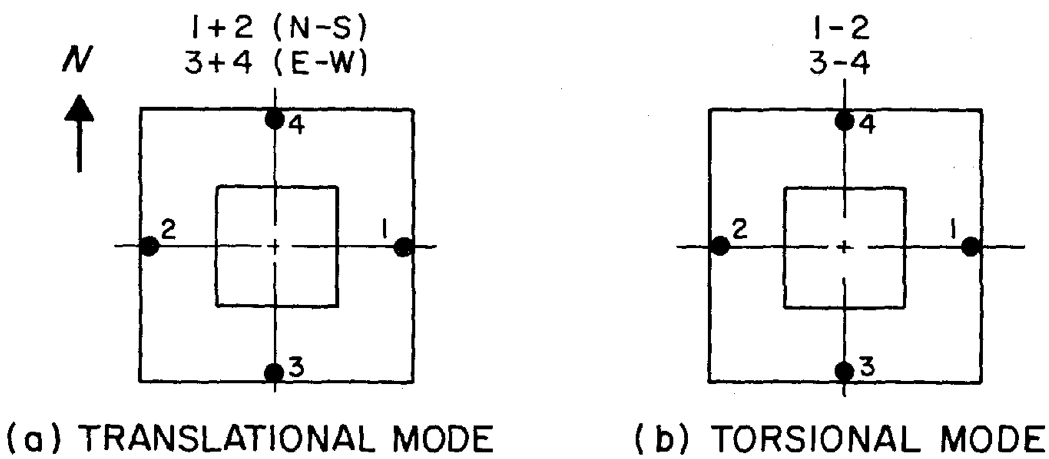

FIG. 4.2 LOCATION OF RANGER SEISMOMETERS ON THE 39TH FLOOR FOR RESONANT FREQUENCY RESPONSE

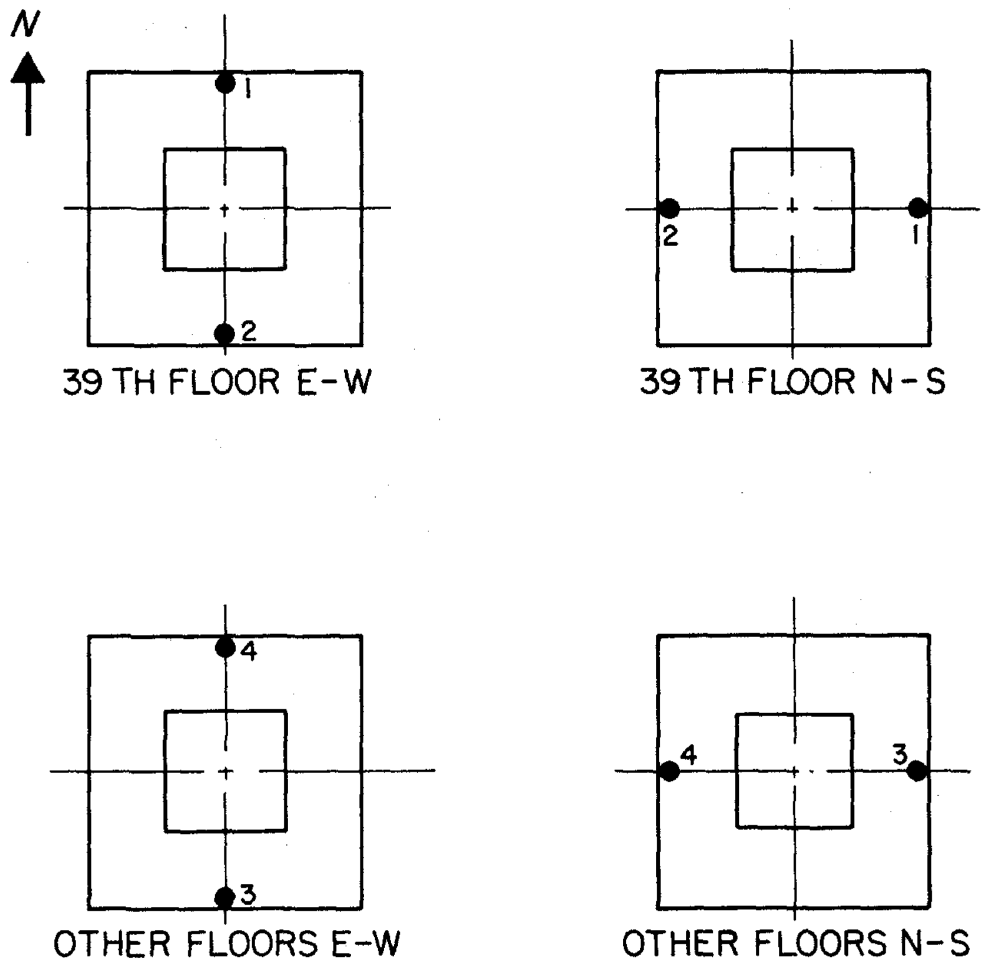

FIG. 4.3 LOCATION OF RANGER SEISMOMETERS FOR THE MODE SHAPES

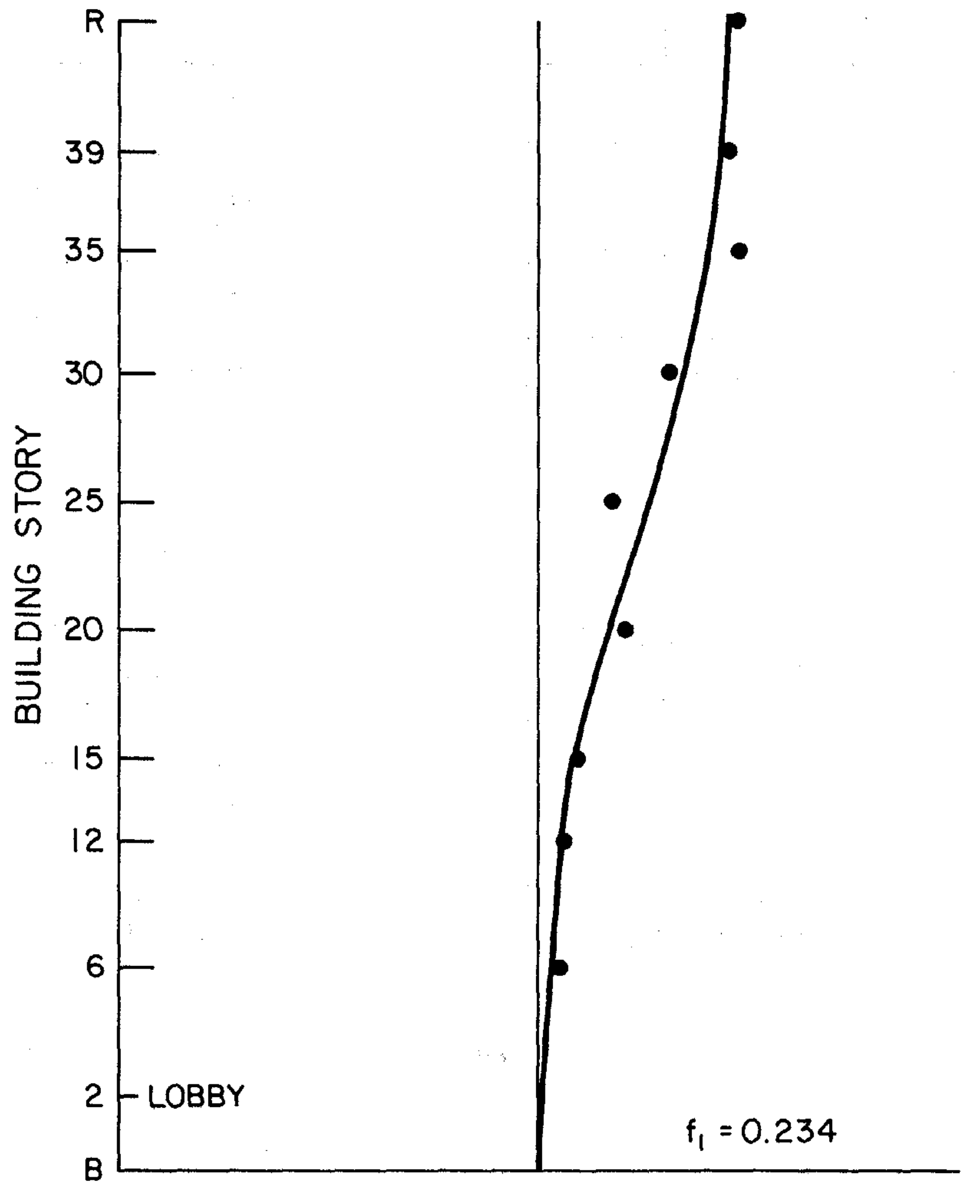

FIG. 4.4 FIRST TRANSLATIONAL MODE SHAPE, E-W

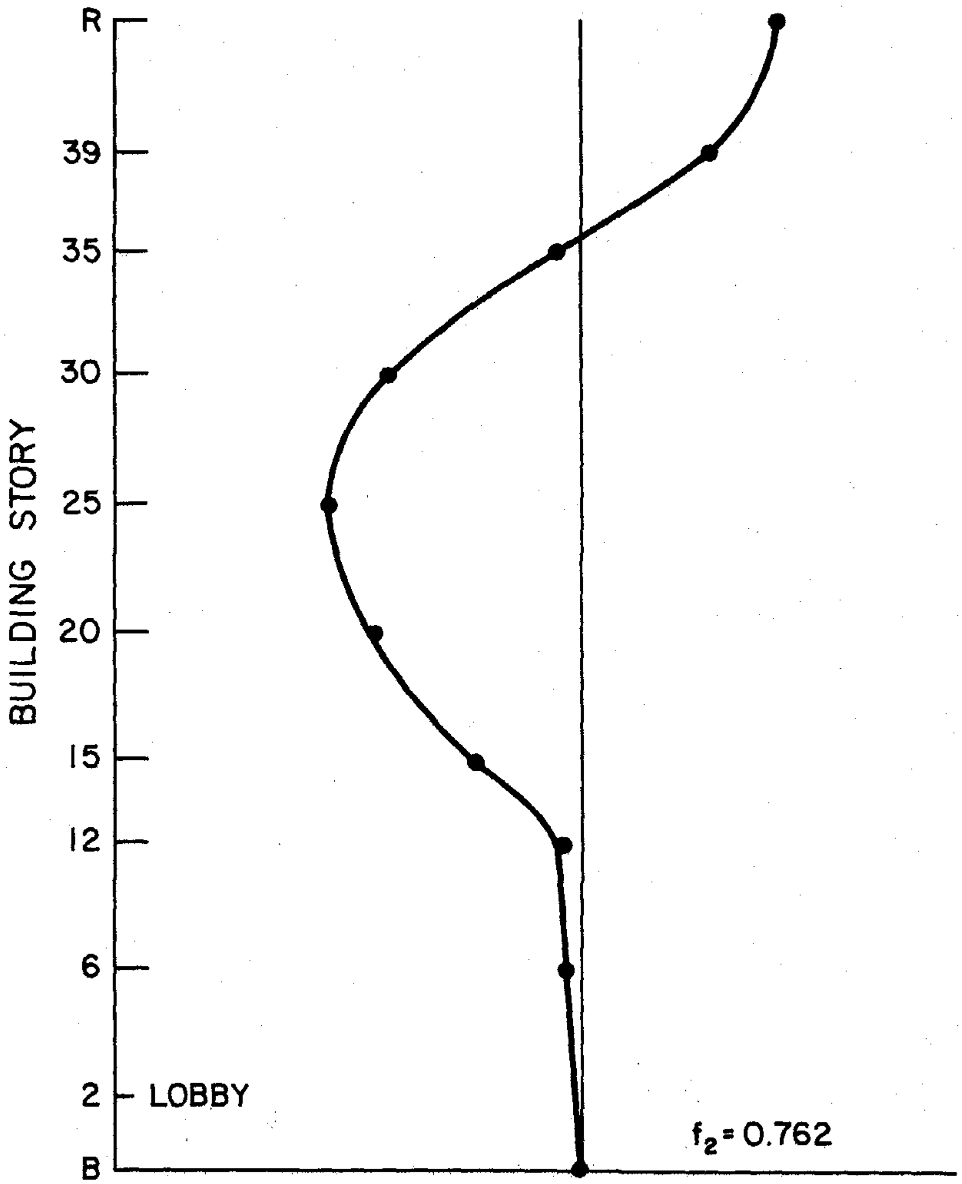

FIG. 4.5 SECOND TRANSLATIONAL MODE SHAPE, E-W

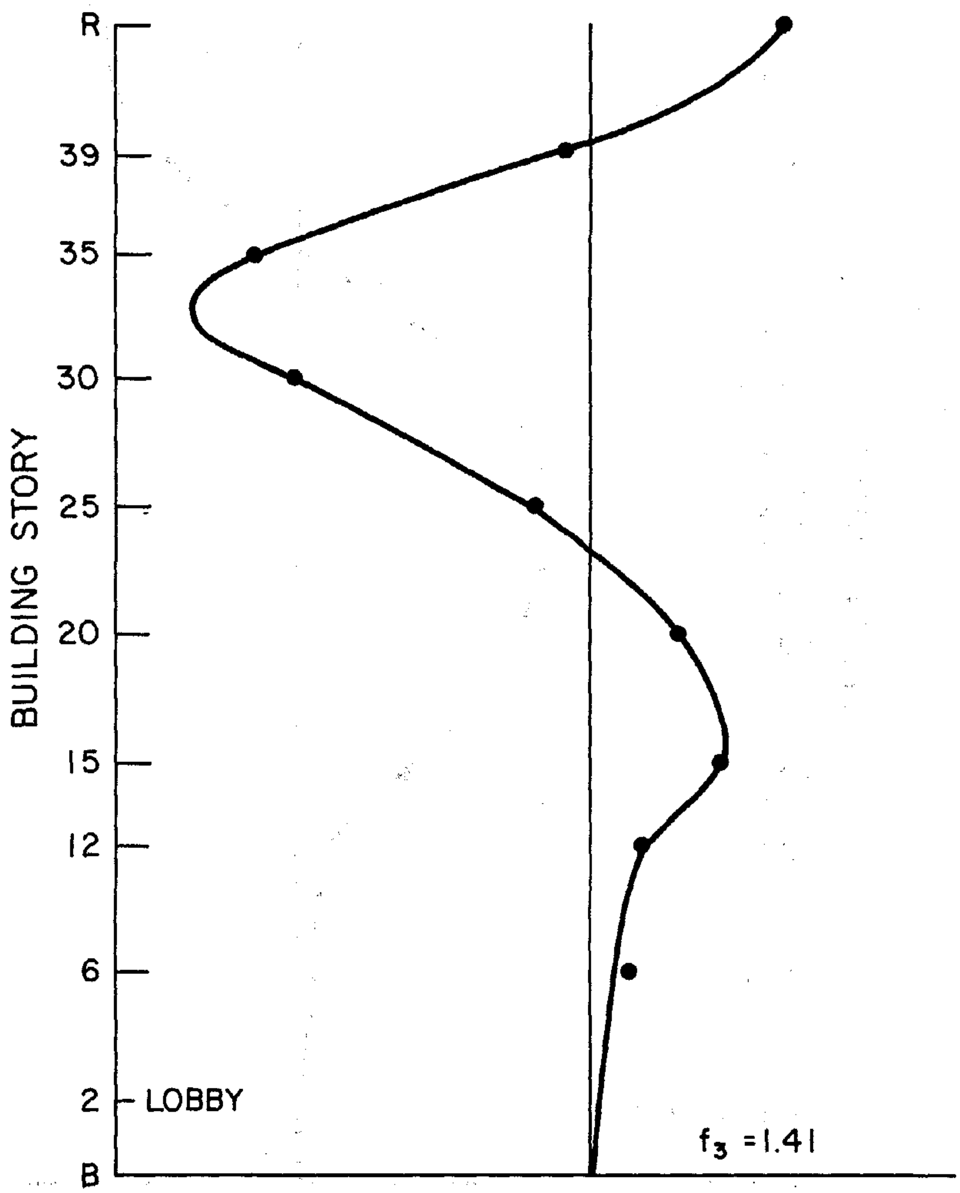

FIG. 4.6 THIRD TRANSLATIONAL MODE SHAPE, E-W

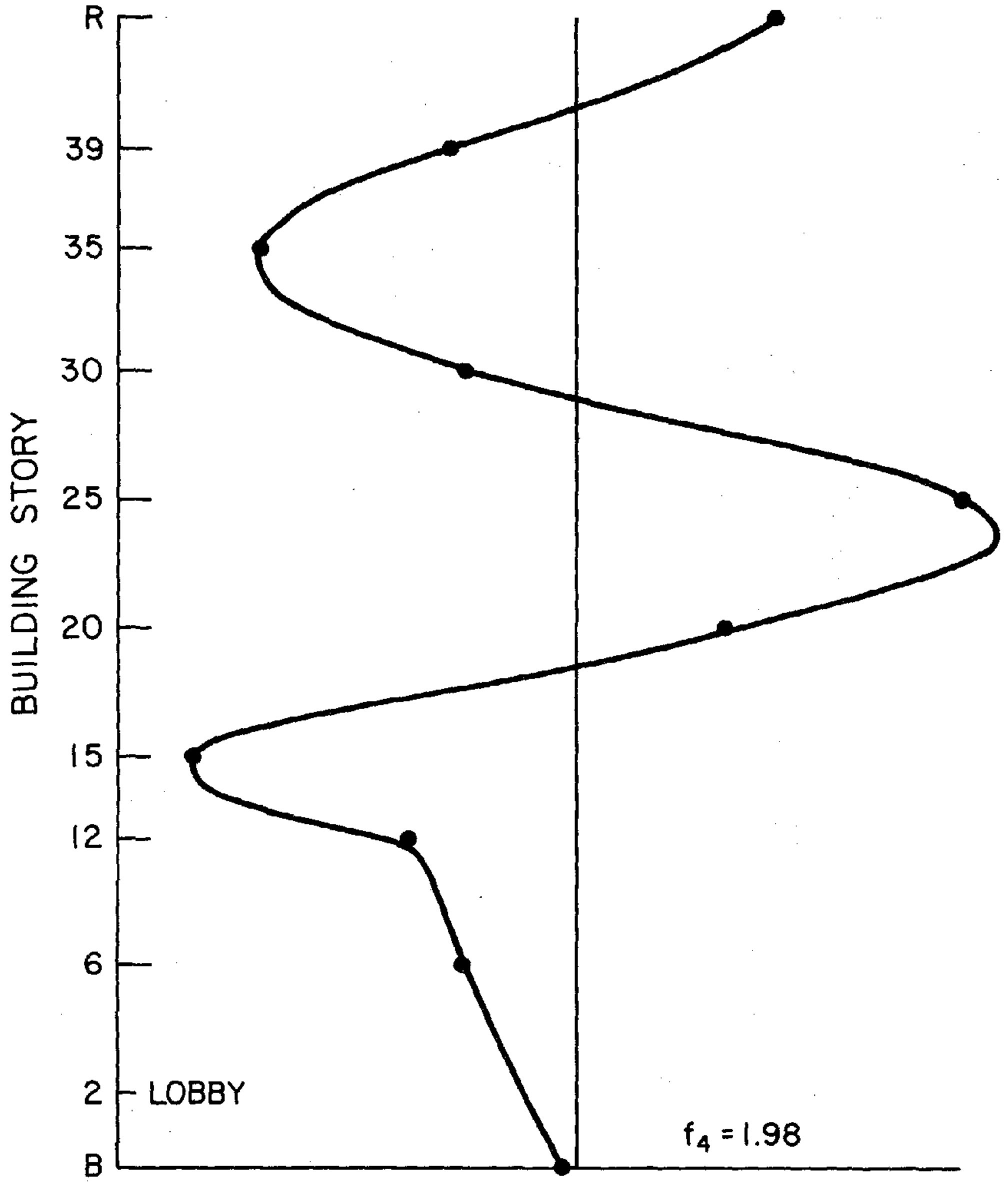

FIG. 4.7 FOURTH TRANSLATIONAL MODE SHAPE, E-W

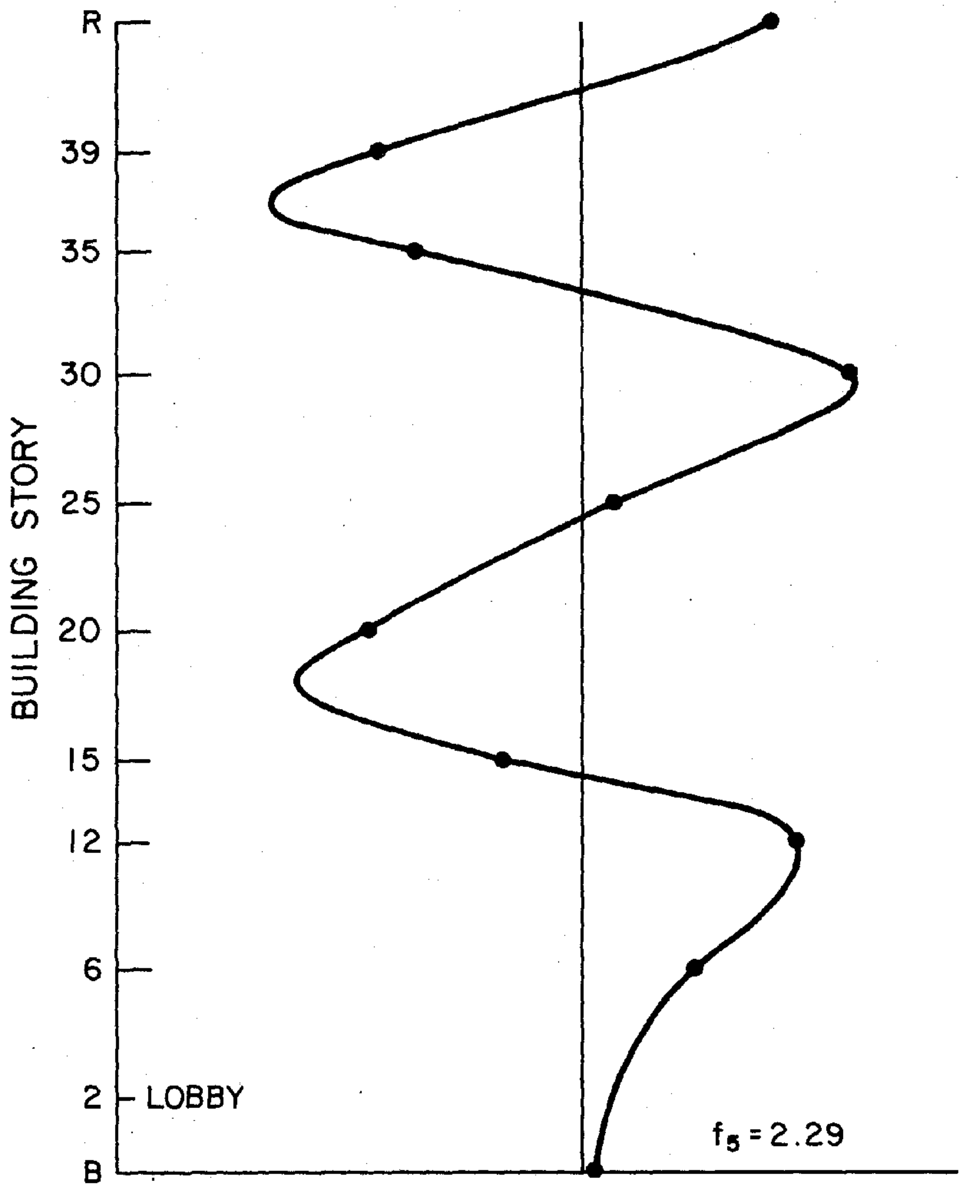

FIG. 4.8 FIFTH TRANSLATIONAL MODE SHAPE, E-W

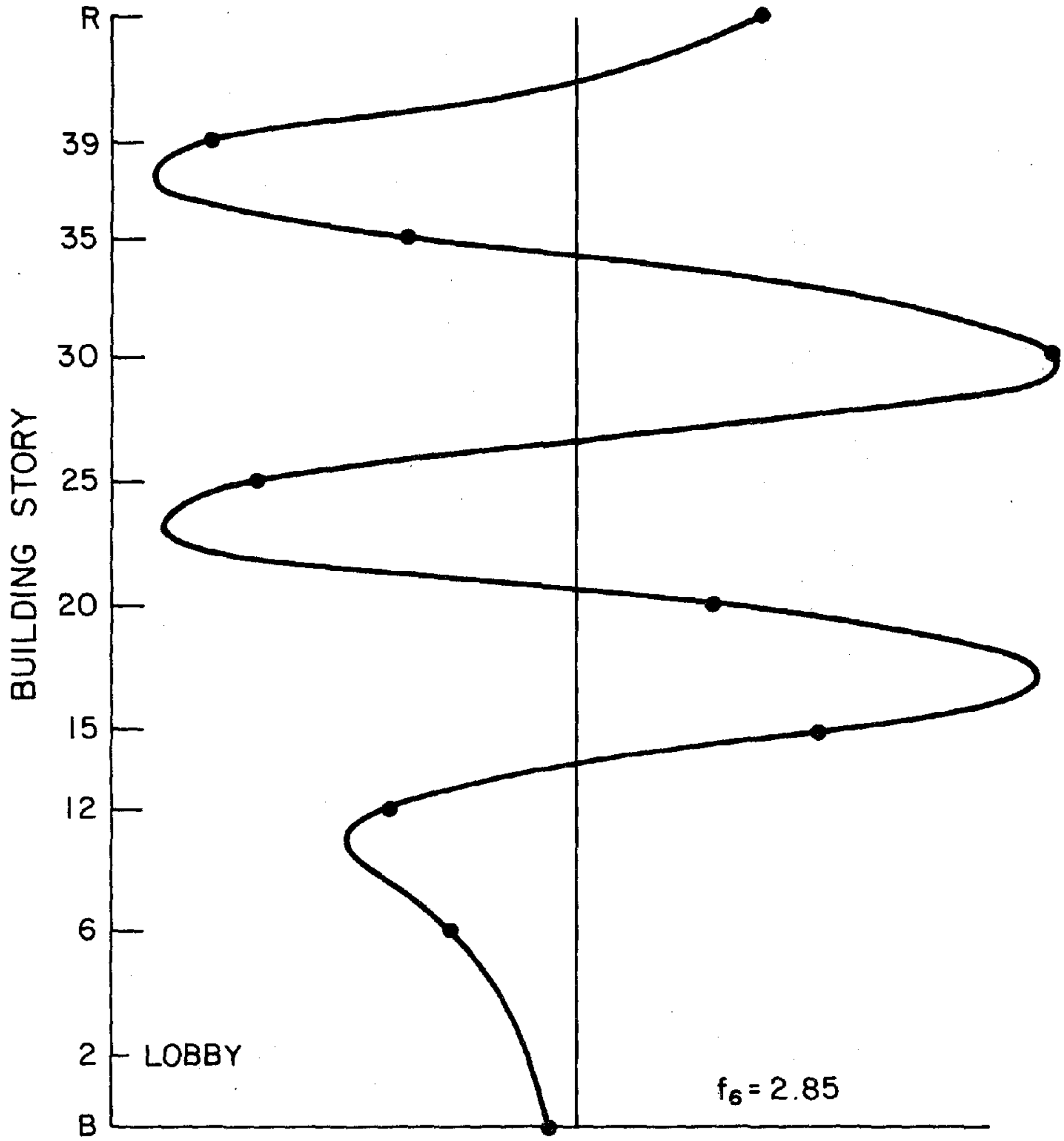

FIG. 4.9 SIXTH TRANSLATIONAL MODE SHAPE, E-W

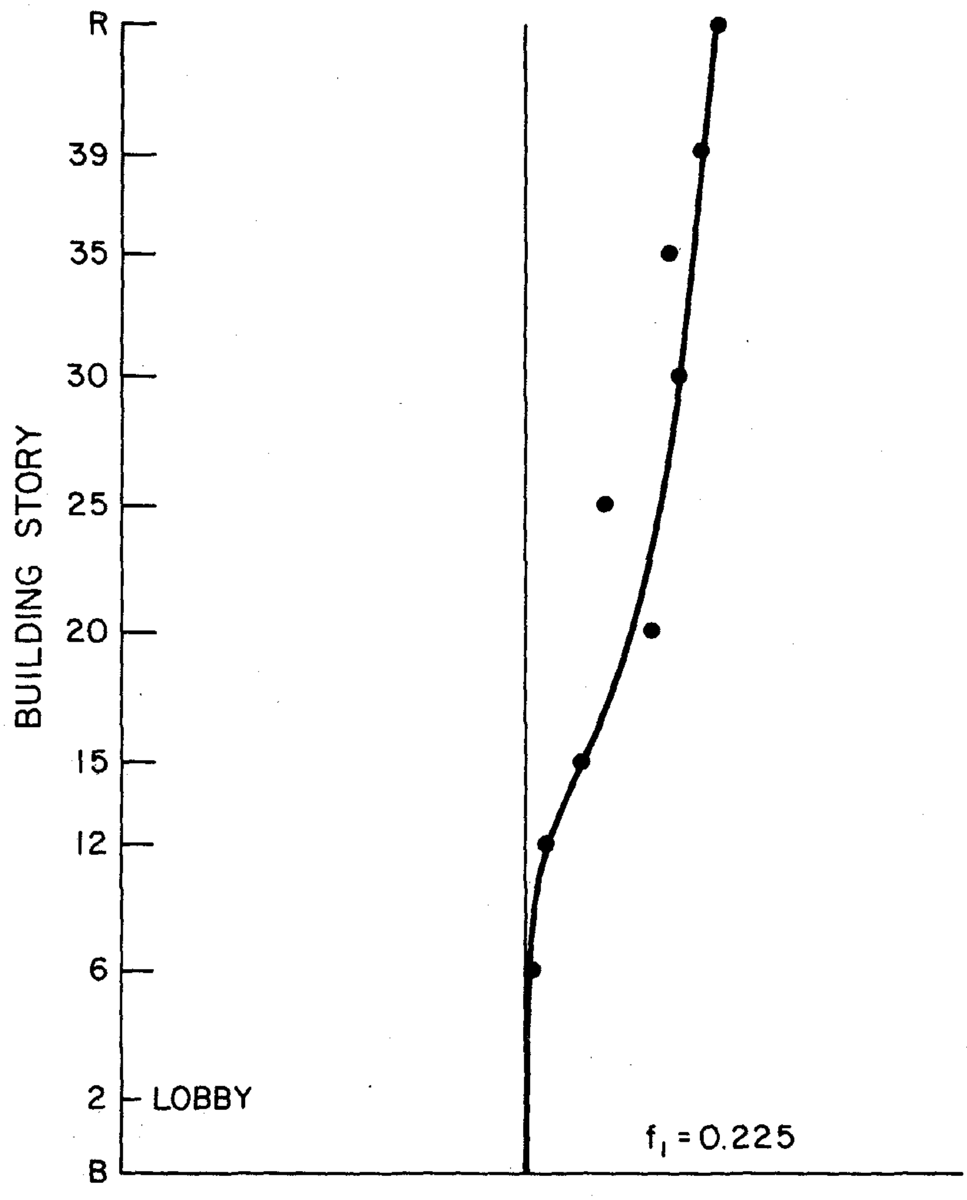

FIG. 4.10 FIRST TRANSLATIONAL MODE SHAPE, N-S

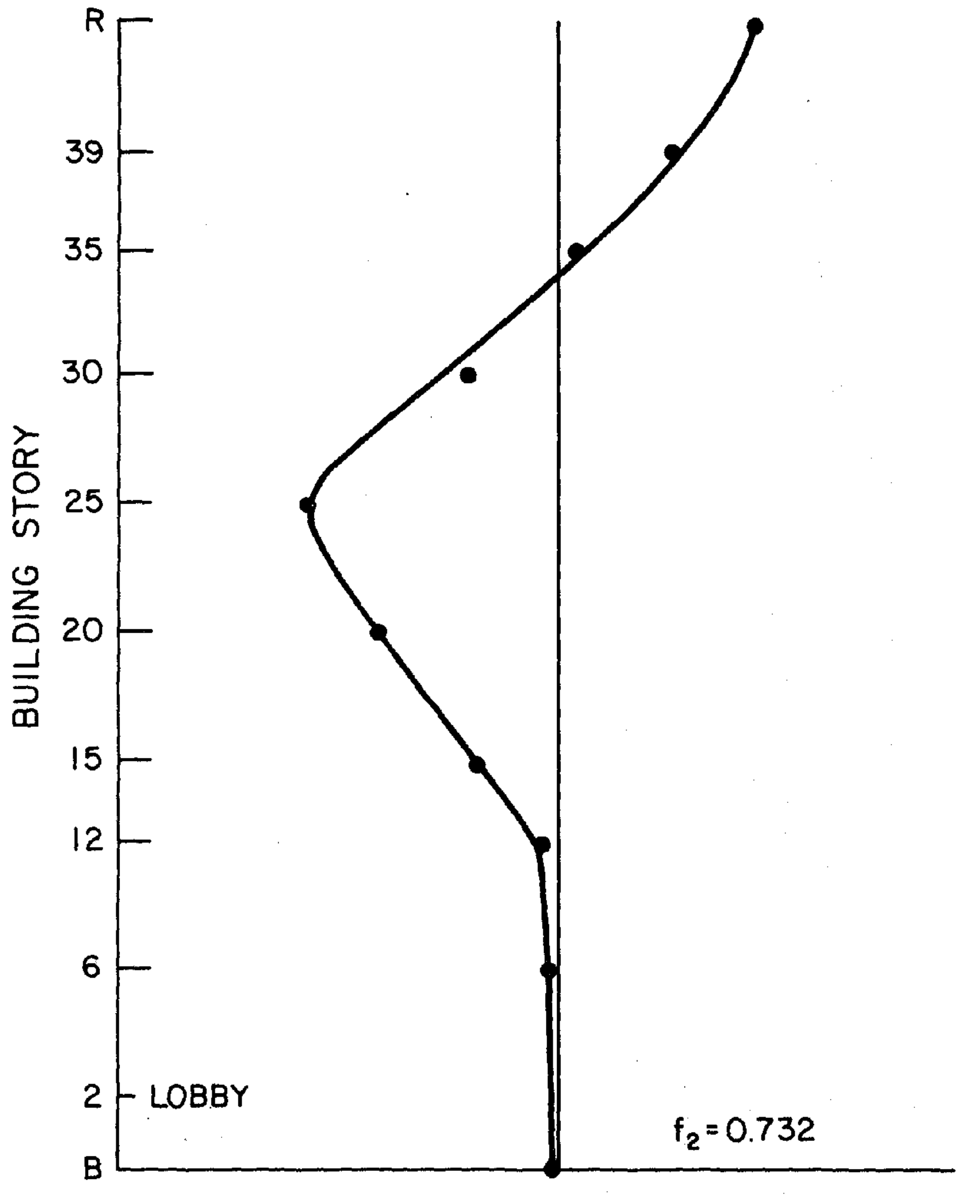

FIG. 4.11 SECOND TRANSLATIONAL MODE SHAPE, N-S

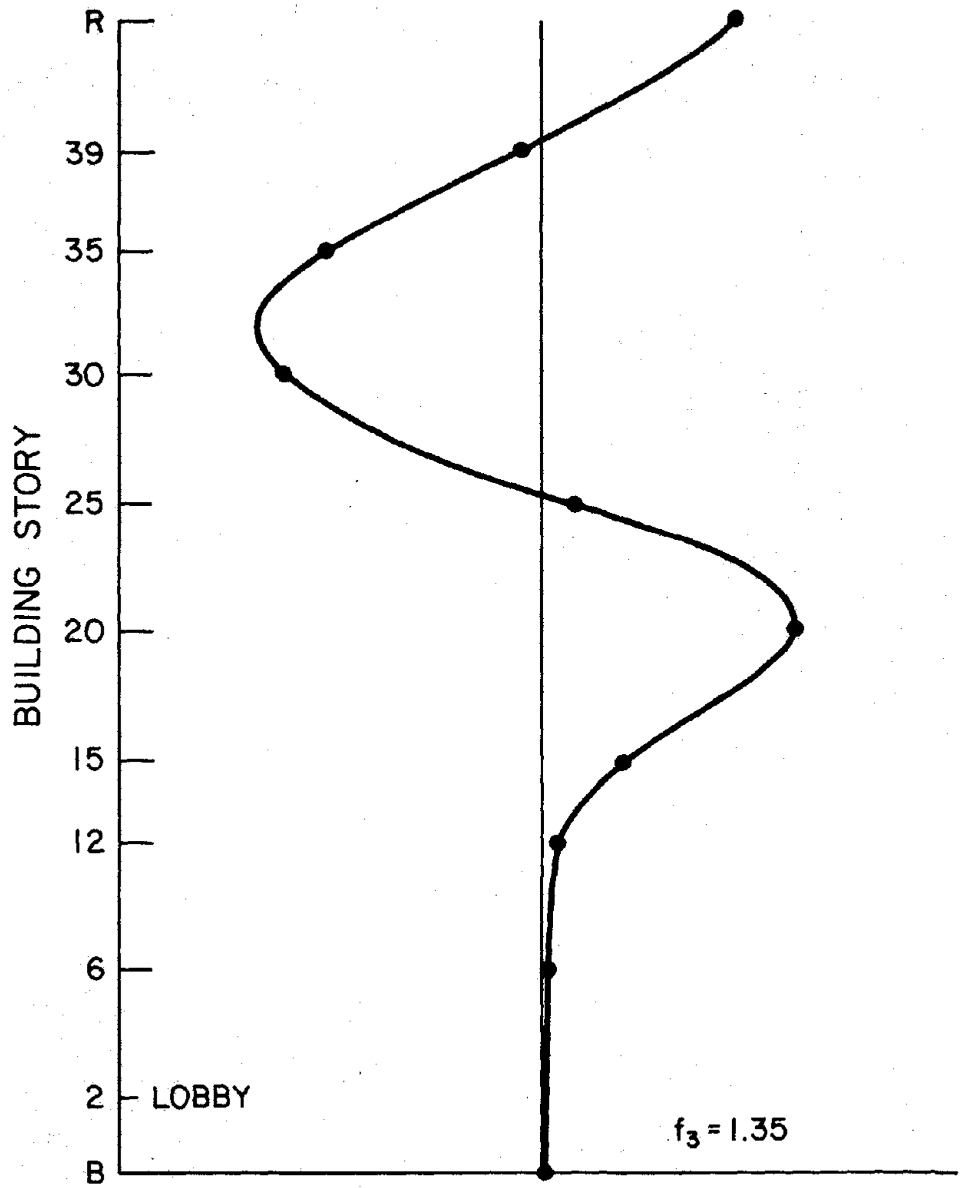

FIG. 4.12 THIRD TRANSLATIONAL MODE SHAPE, N-S

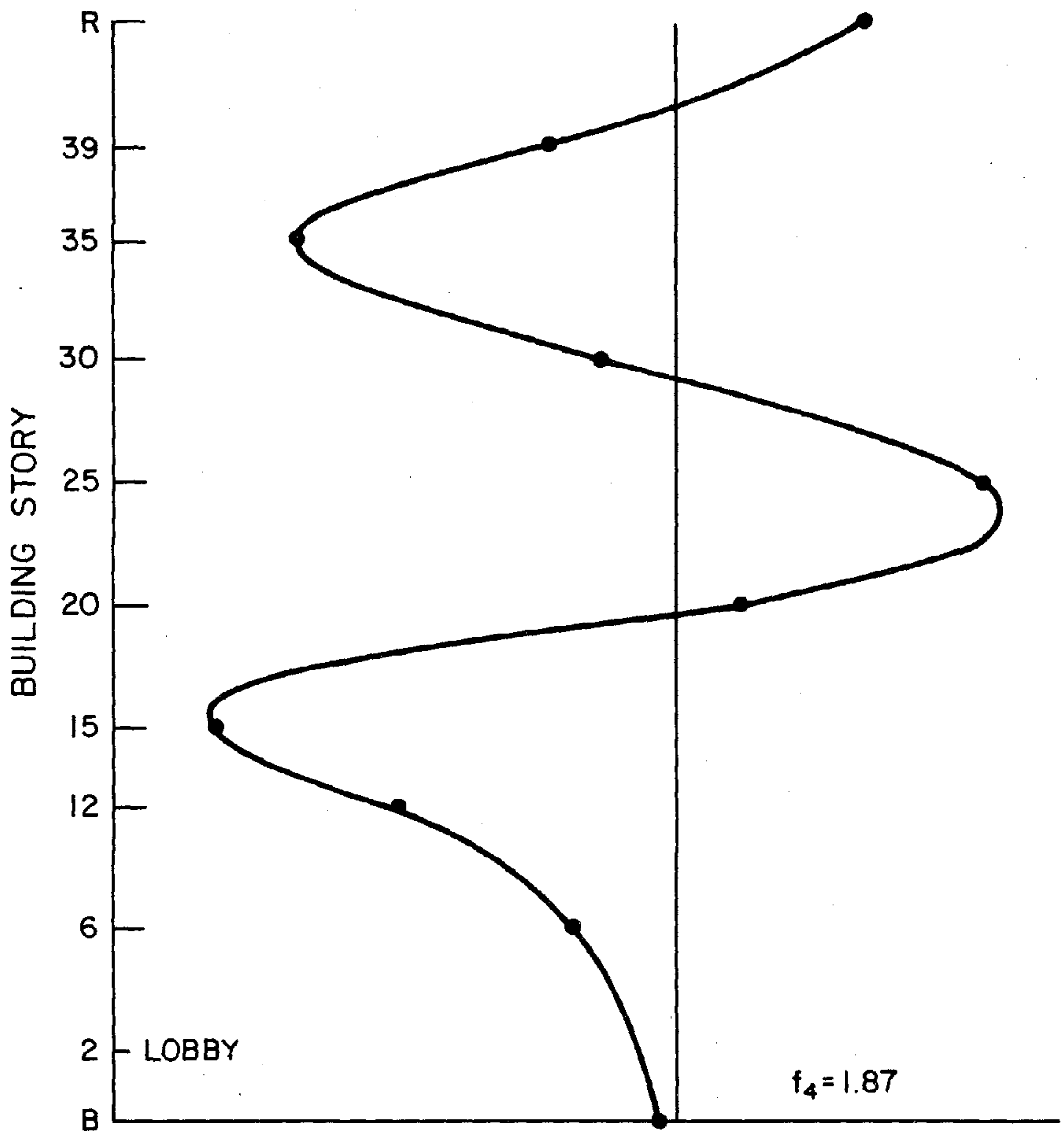

FIG. 4.13 FOURTH TRANSLATIONAL MODE SHAPE, N-S

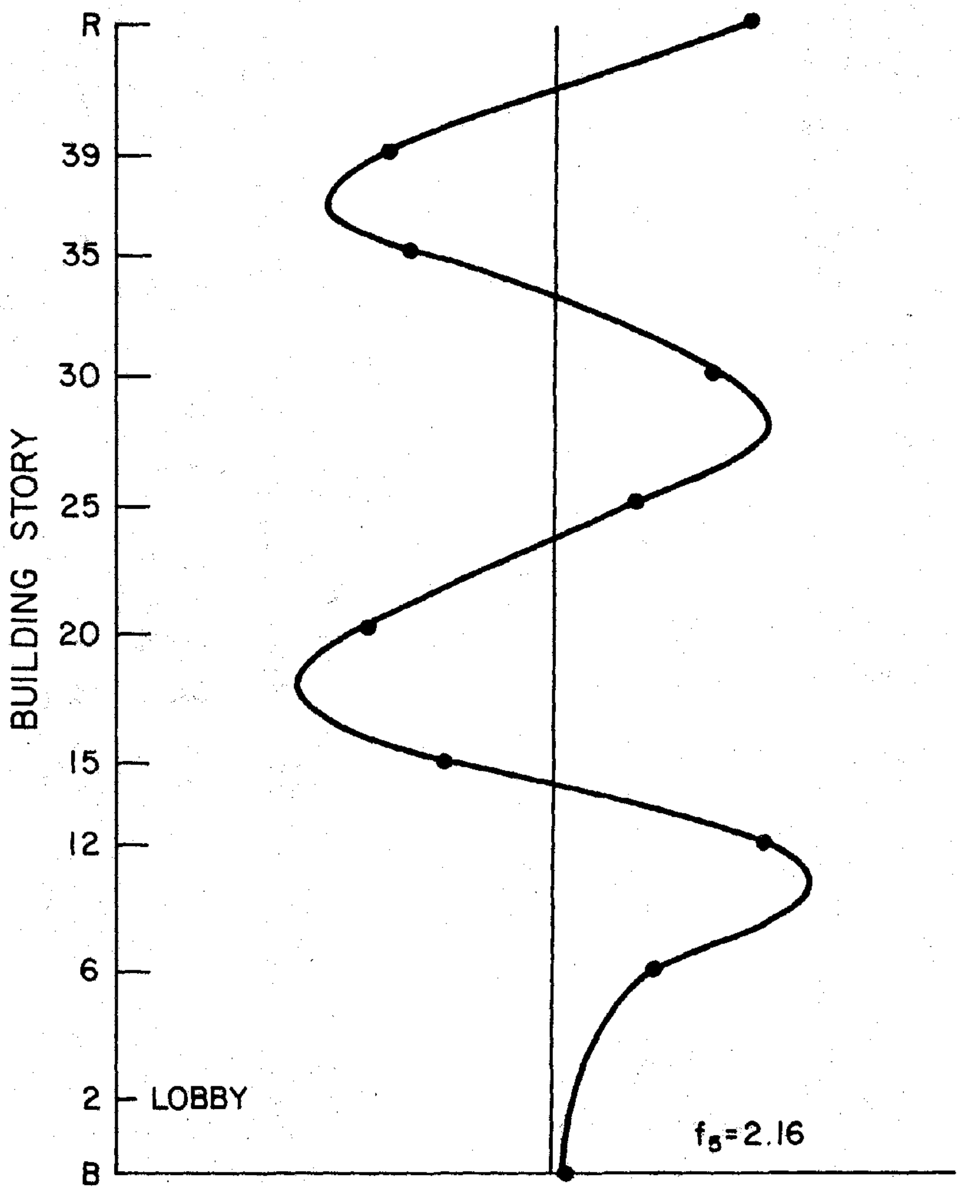

FIG. 4.14 FIFTH TRANSLATIONAL MODE SHAPE, N-S

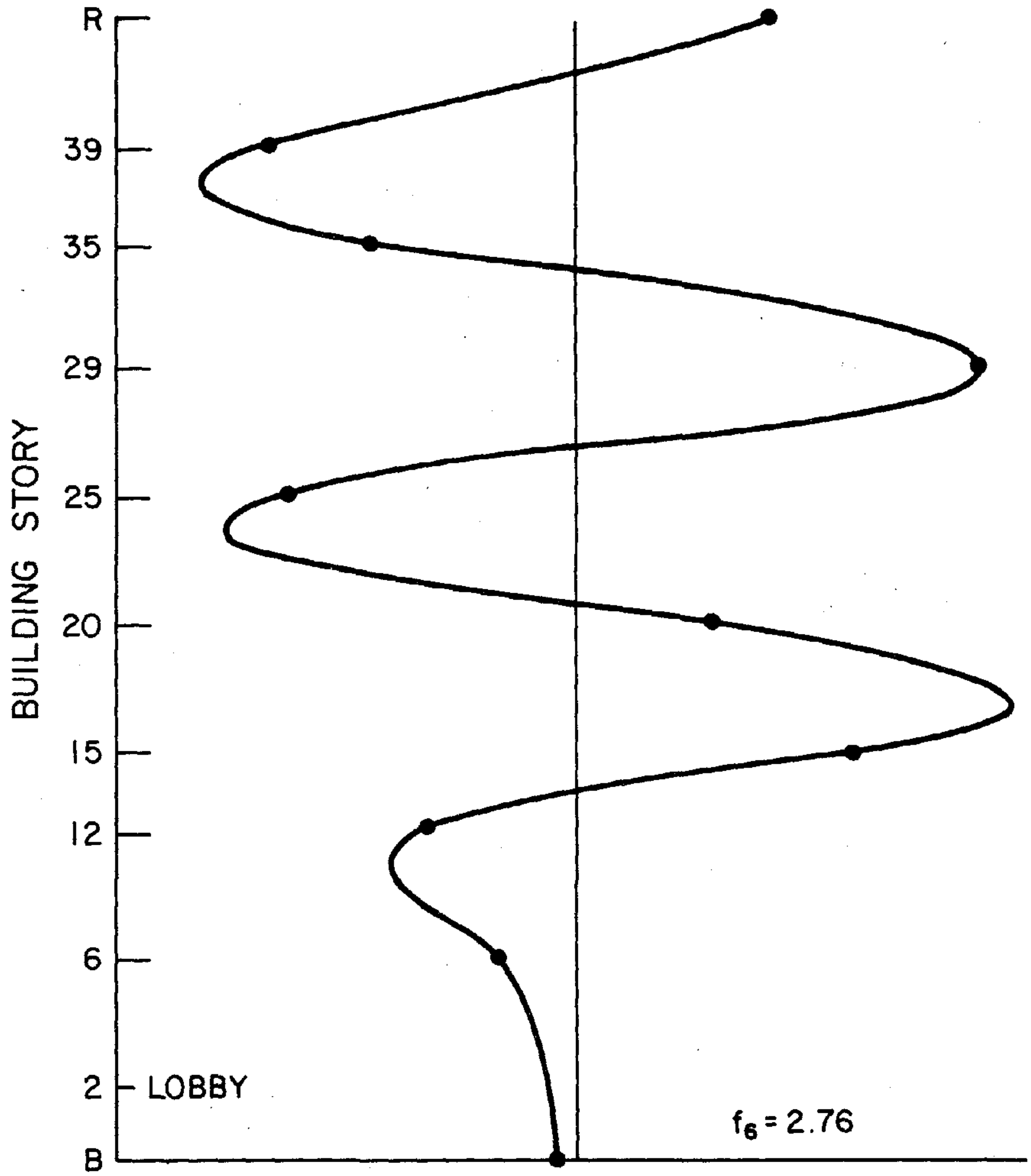

FIG. 4.15 SIXTH TRANSLATIONAL MODE SHAPE, N-S

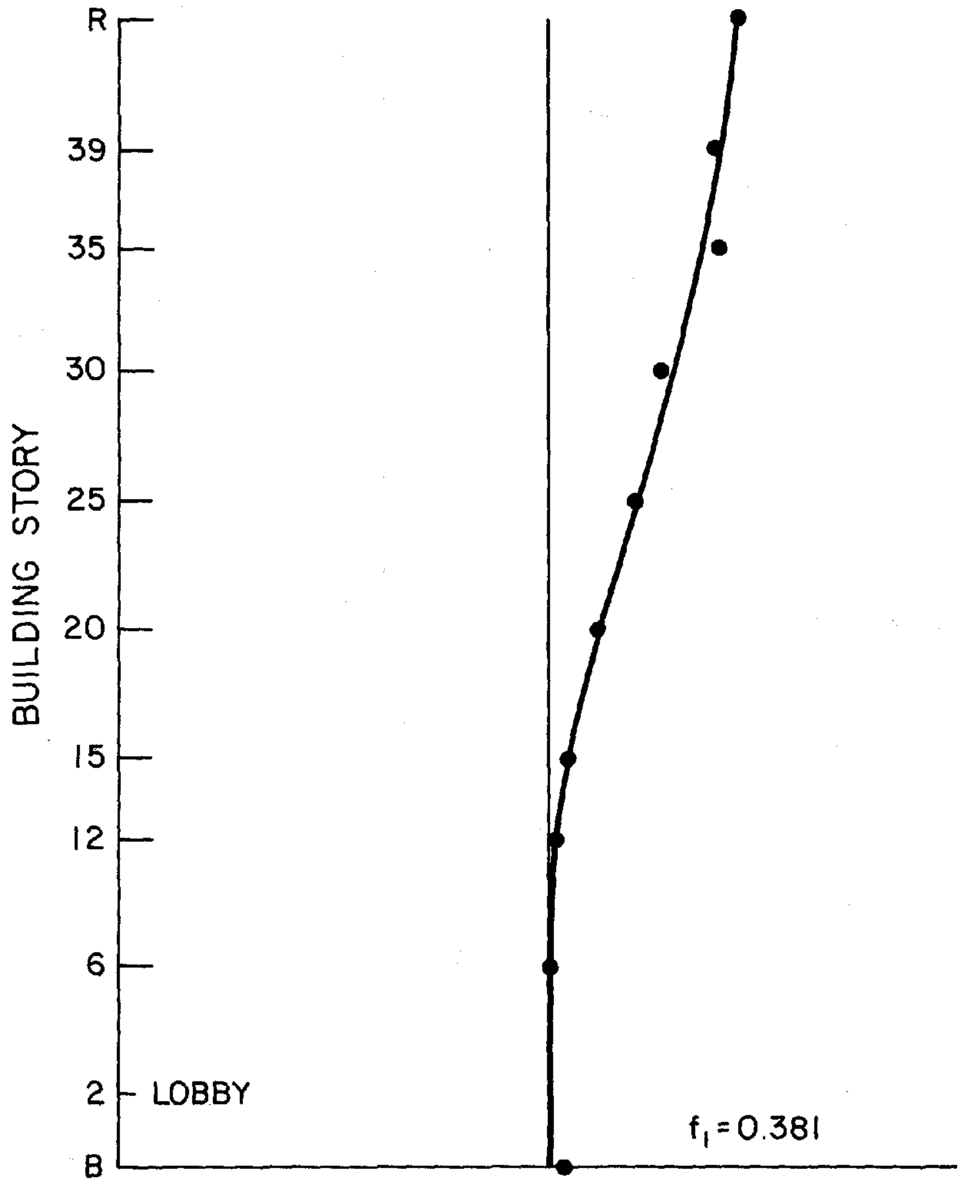

FIG. 4.16 FIRST TORSIONAL MODE SHAPE

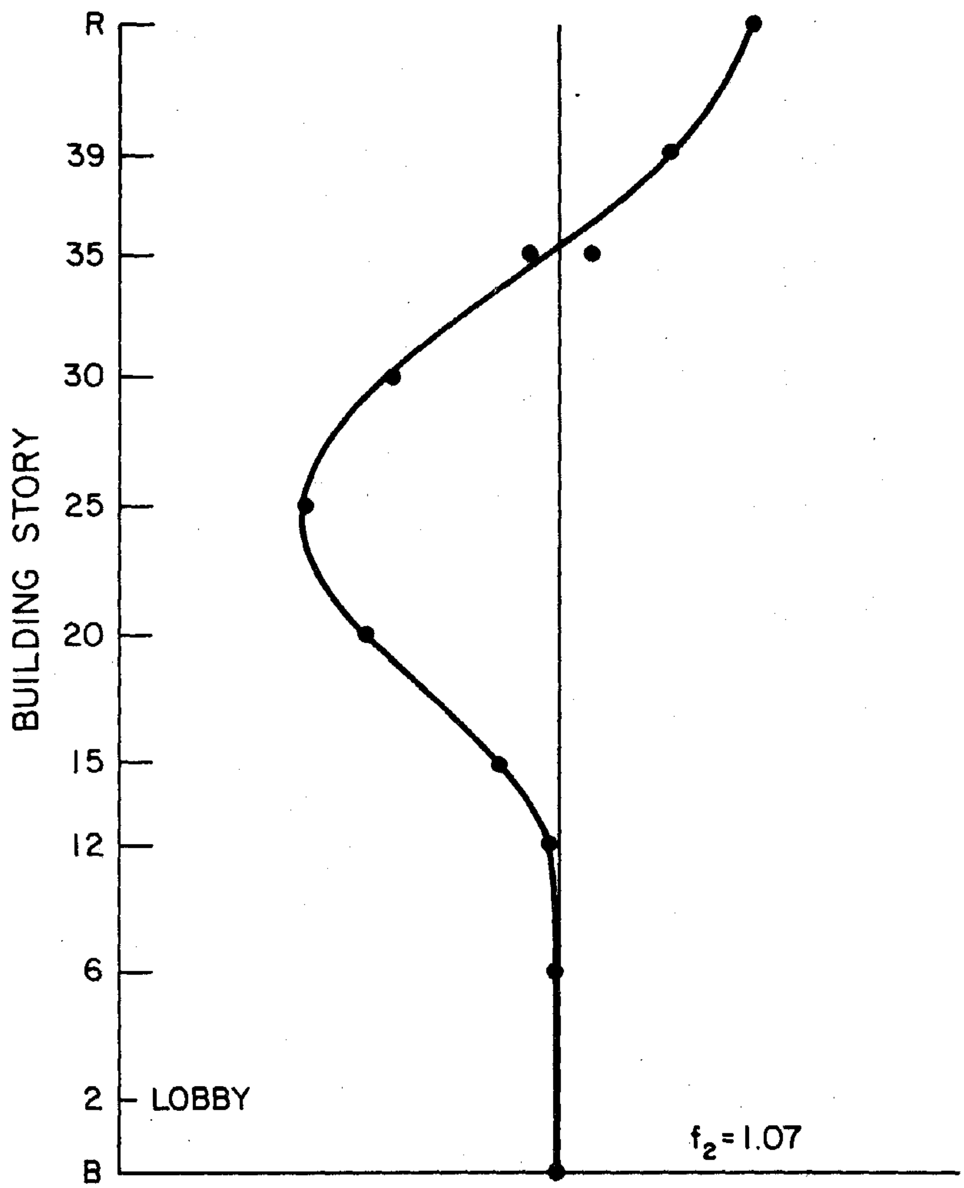

FIG. 4.17 SECOND TORSIONAL MODE SHAPE

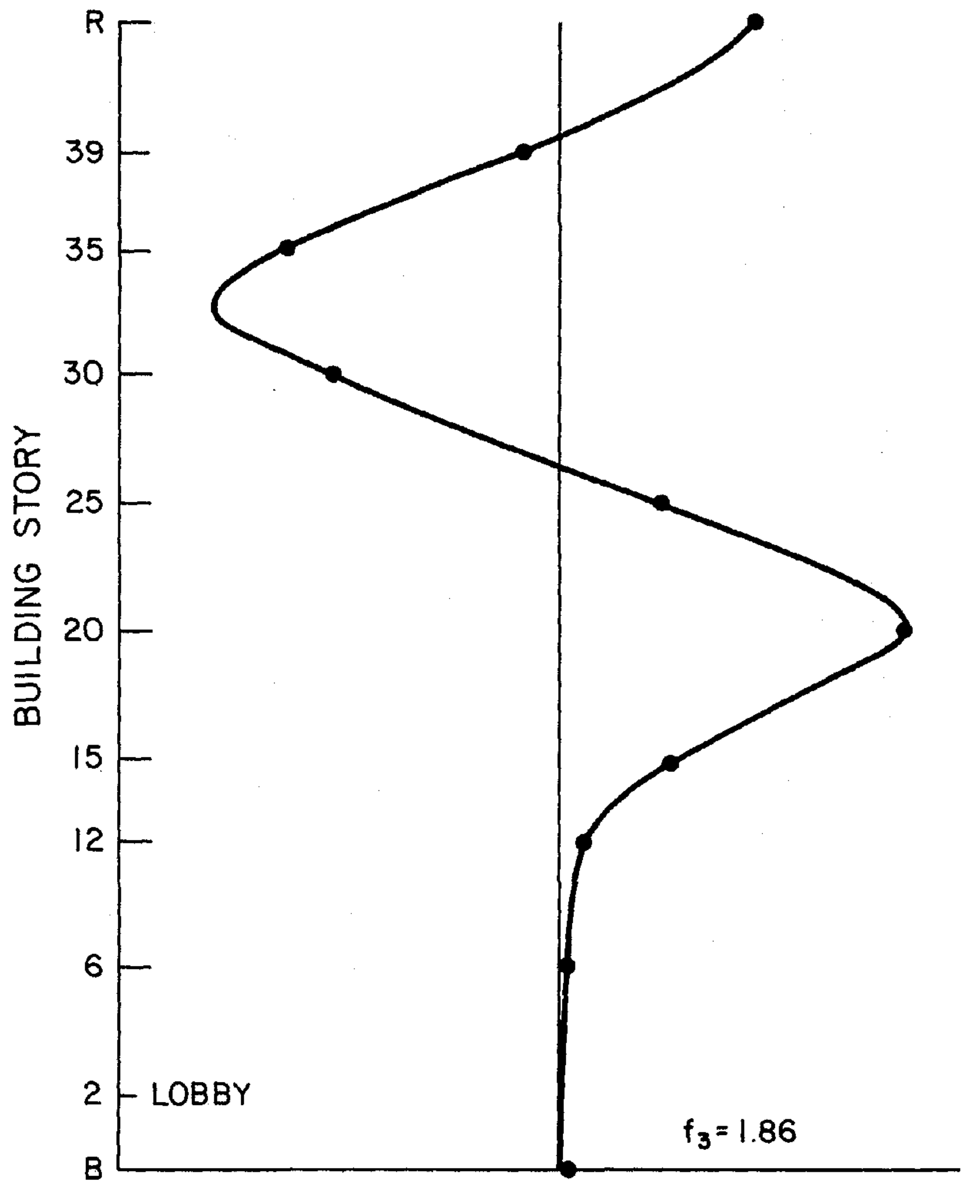

FIG. 4.18 THIRD TORSIONAL MODE SHAPE

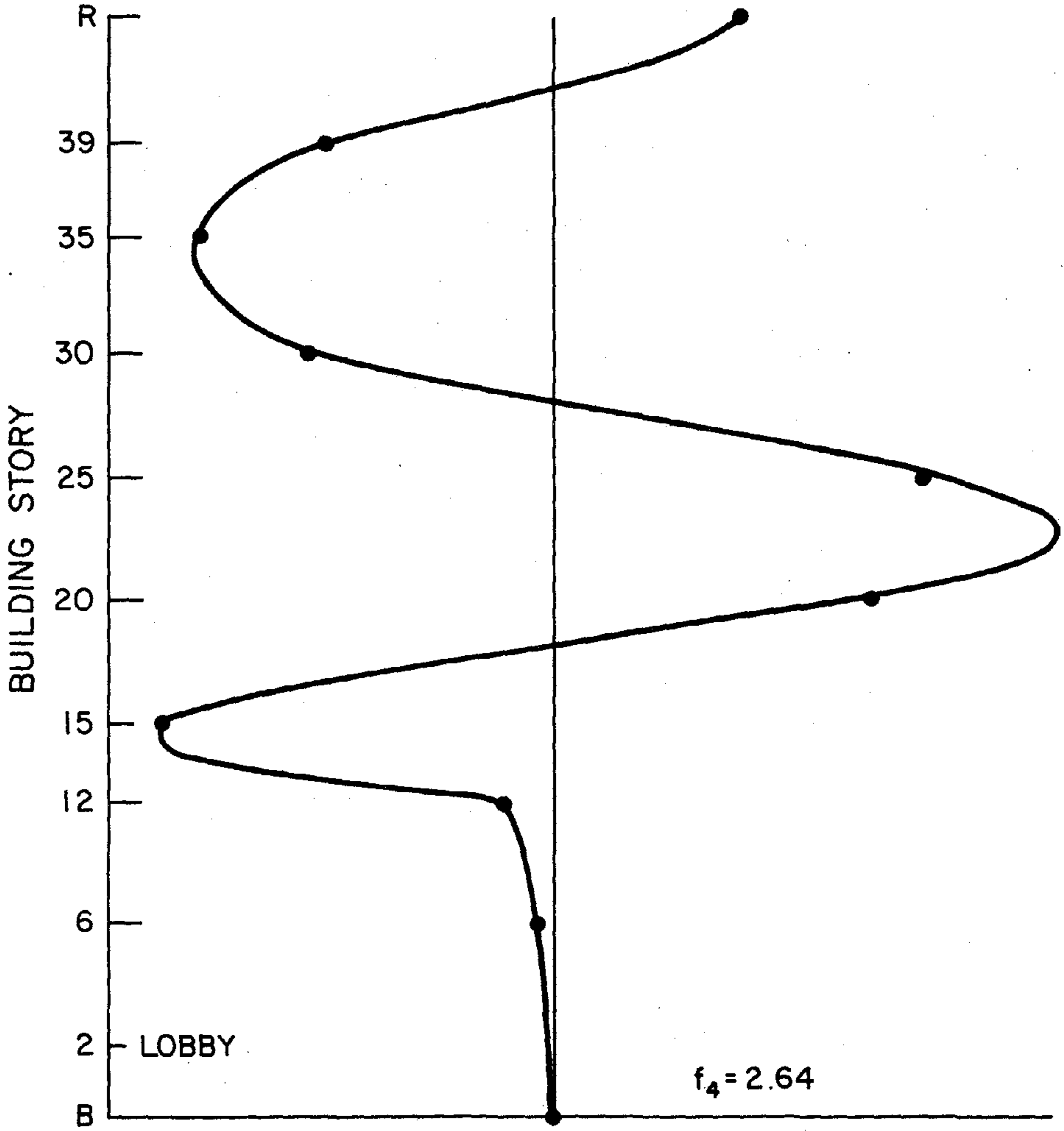

FIG. 4.19 FOURTH TORSIONAL MODE SHAPE

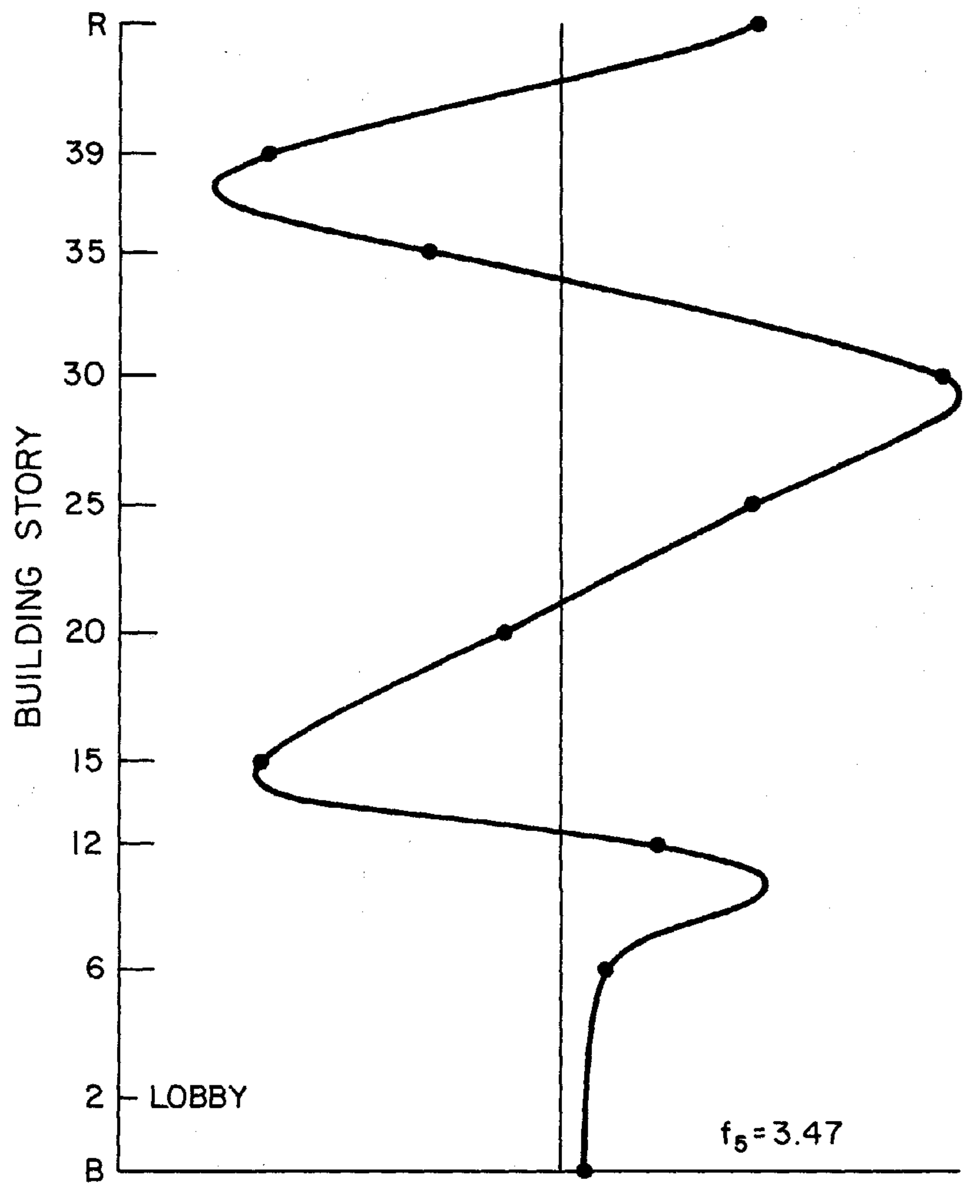

FIG. 4.20 FIFTH TORSIONAL MODE SHAPE

5. COMPARISON OF FORCED AND AMBIENT VIBRATION STUDIES

The dynamic properties (resonant frequencies, modes of vibration and damping values) were determined by full-scale dynamic test using forced and ambient vibration methods. Resonant frequencies and damping factors from both studies are summarized and compared in Table 5.1.

The resonant frequencies from both studies are in very good agreement in all separated modes of vibration, with the maximum difference about 6%. The ratios of the observed higher mode frequencies with respect to the fundamental one from both dynamic studies of the building are plotted in Fig. 5.1. These ratios for both translational directions as well as the torsional direction indicate that overall structural response is predominantly of the shear type. Equivalent viscous damping factors for the reasons discussed in Chapter 4 show some difference. It appears that it is rather difficult to obtain appropriate damping values from the ambient vibration study, particularly in cases when equivalent viscous damping is expected to be rather low.

Mode shapes for the translational (E-W and N-S) directions as well as torsional ones are compared in Figs. 5.2 through 5.13. All presented mode shapes are in good agreement from both studies.

Comparison of the forced and ambient vibration experiments of the Rainer Tower Building demonstrate the consistency of the two methods in determining with adequate accuracy the natural frequencies and mode shapes of a typical modern building. Difficulties in the evaluation of equivalent viscous damping factors from ambient vibration studies are presented, and it probably would be more realistic from this type of study to expect assessment of the range of damping factors rather than damping values associated with each mode of vibration.

The field effort involved in the ambient vibration study was significantly smaller than for the forced vibration experiment because the measuring equipment used for the ambient vibration test is much lighter and has fewer components. A group of three people required for both ambient and forced vibration experiments can perform the necessary measurements for the ambient test in one to two days. The time necessary to complete the forced vibration test was about two weeks. The total number of necessary measurements in the ambient test is significantly smaller, and, also, each individual measurement requires a shorter time interval. On the other hand, data analysis is slightly more complicated because it requires Fourier analysis using digital computers.

Both ambient and forced vibration studies may lead to the determination of up to six and more modes of vibration. The number of mode shapes resolved depends mainly on the level of the high frequency noise and the number of measuring stations in the building. Although both methods of dynamic testing of full scale structures are based on small levels of excitation, compared to strong earthquake motion, the derived dynamic properties of the structural systems are invaluable since they offer a sound basis for rational improvements of the formulation of the mathematical models in the elastic range of behavior of the structural systems.

TABLE 5.1 - COMPARISON OF RESONANT FREQUENCIES AND DAMPING FACTORS

Mode No.	Translational E-W				Translational N-S				Torsional			
	Forced		Ambient		Forced		Ambient		Forced		Ambient	
	f (Hz)	ξ (%)	f (Hz)	ξ (%)	f (Hz)	ξ (%)	f (Hz)	ξ (%)	f (Hz)	ξ (%)	f (Hz)	ξ (%)
1	0.232	1.7	0.234	1.9	0.225	6.6	0.225	2.2	0.377	2.5	0.381	3.3
2	0.755	2.7	0.762	1.1	0.720	2.6	0.732	1.5	1.055	1.0	1.07	1.6
3	1.385	2.2	1.41	3.0	1.32	1.9	1.35	1.8	1.86	1.6	1.86	1.7
4	1.87	2.9	1.98	1.3	1.81	2.1	1.87	1.1	2.60	2.0	2.64	1.4
5	2.21	2.0	2.29	1.7	2.14	1.6	2.16	1.1	3.32	3.0	3.47	0.6
6	2.68	3.0	2.85	0.7	2.62	2.8	2.76	1.0				

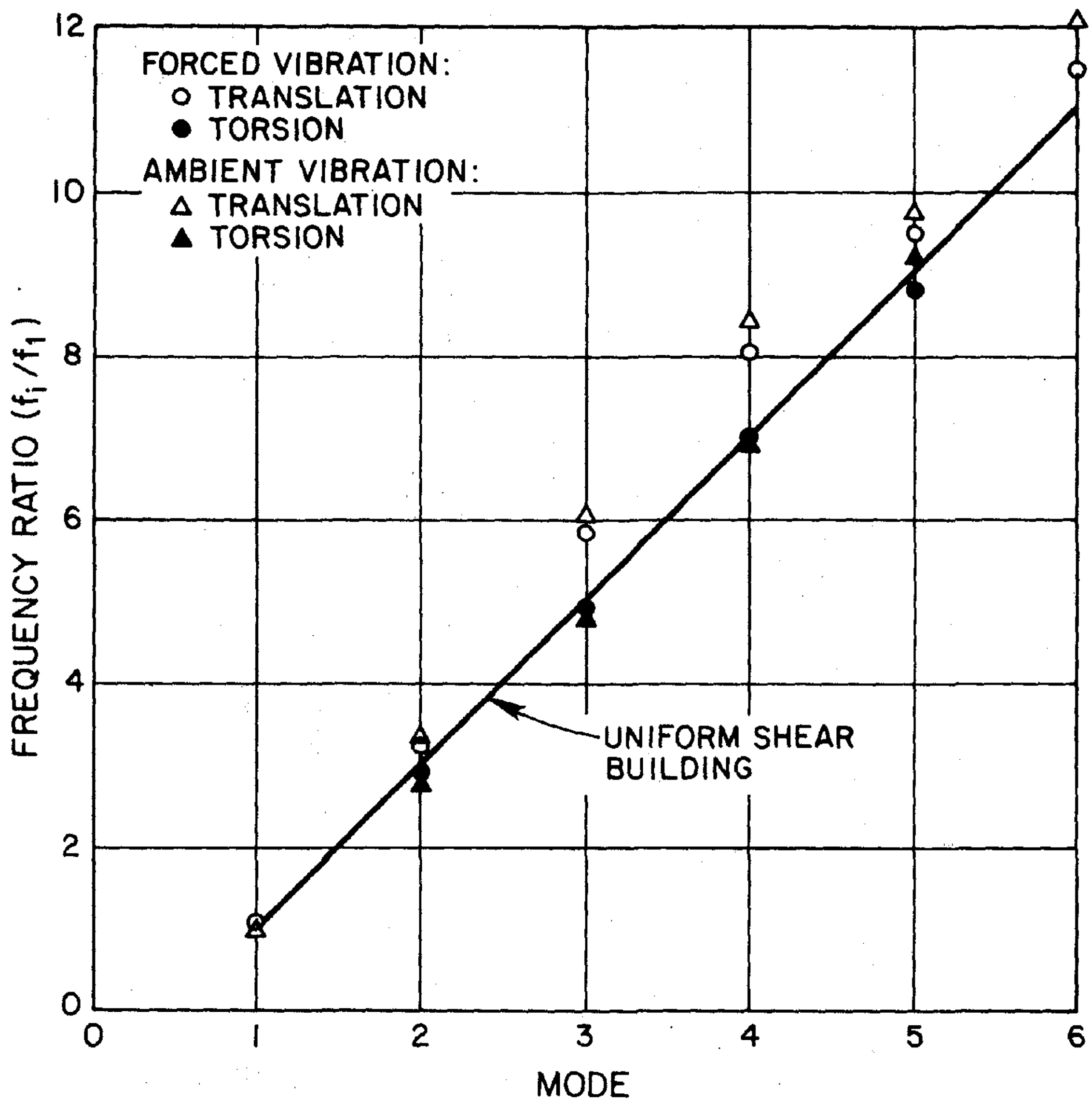

FIG. 5.1 RATIO OF RESONANT FREQUENCIES

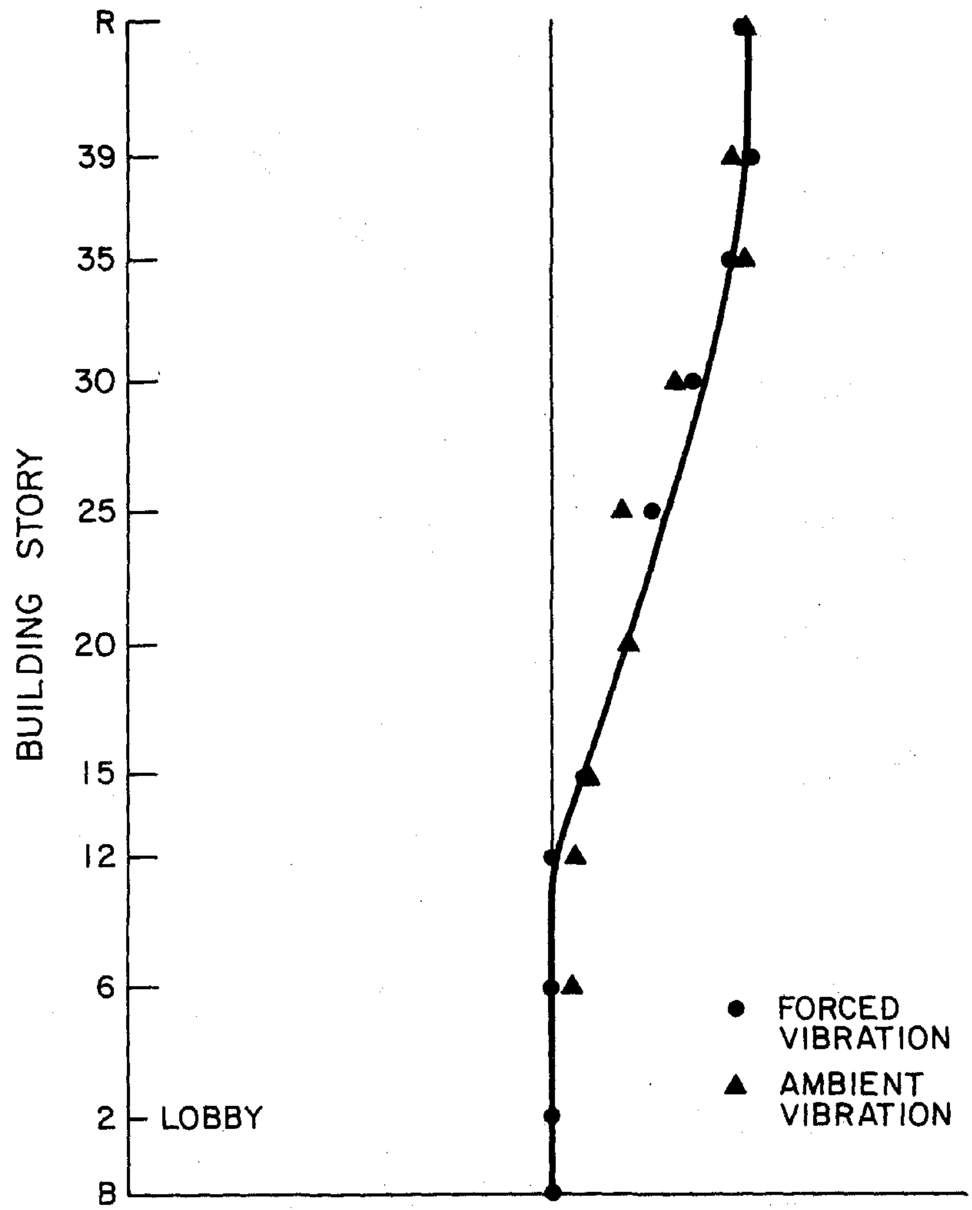

FIG. 5.2 FIRST TRANSLATIONAL MODE SHAPE, E-W

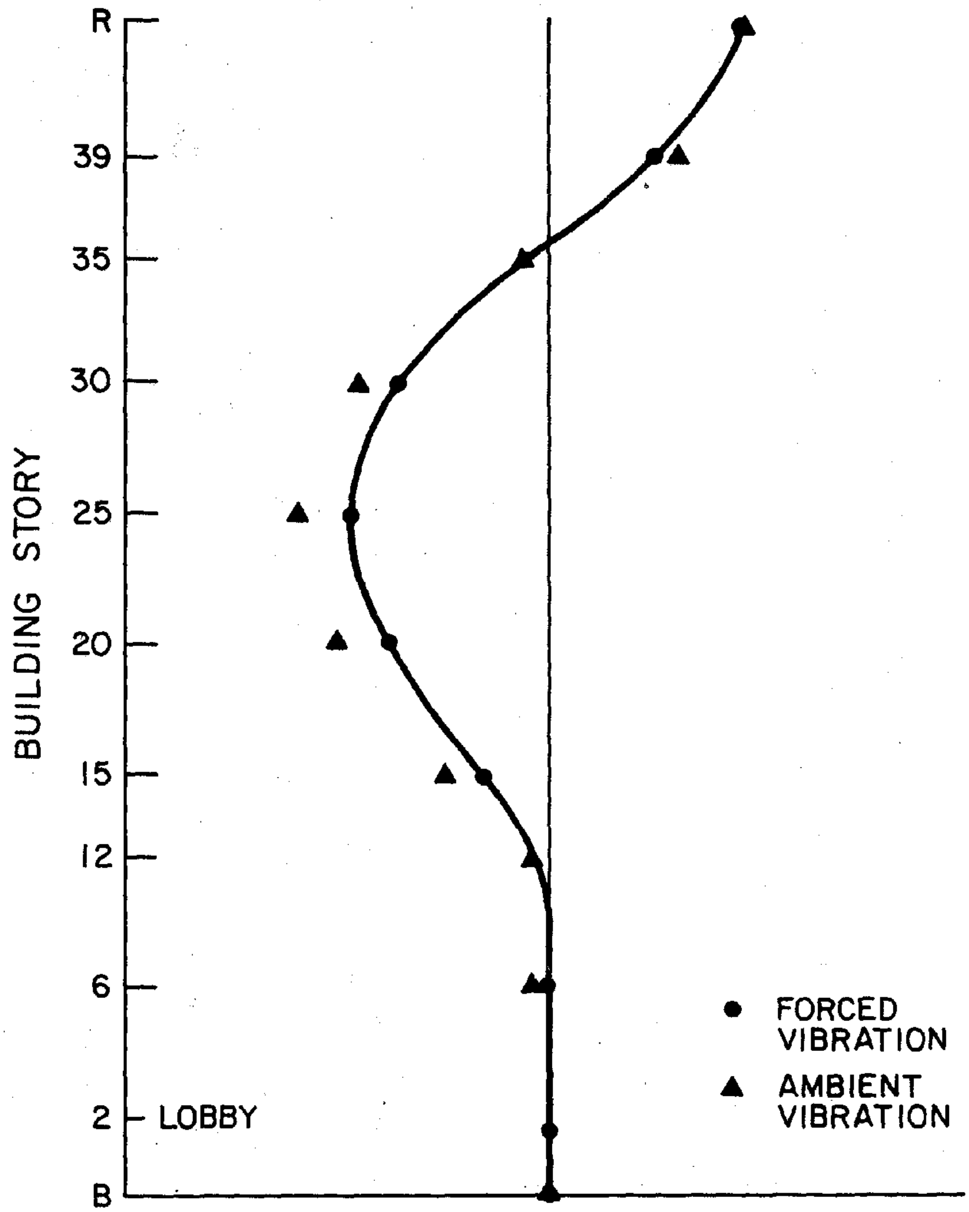

FIG. 5.3 SECOND TRANSLATIONAL MODE SHAPE, E-W

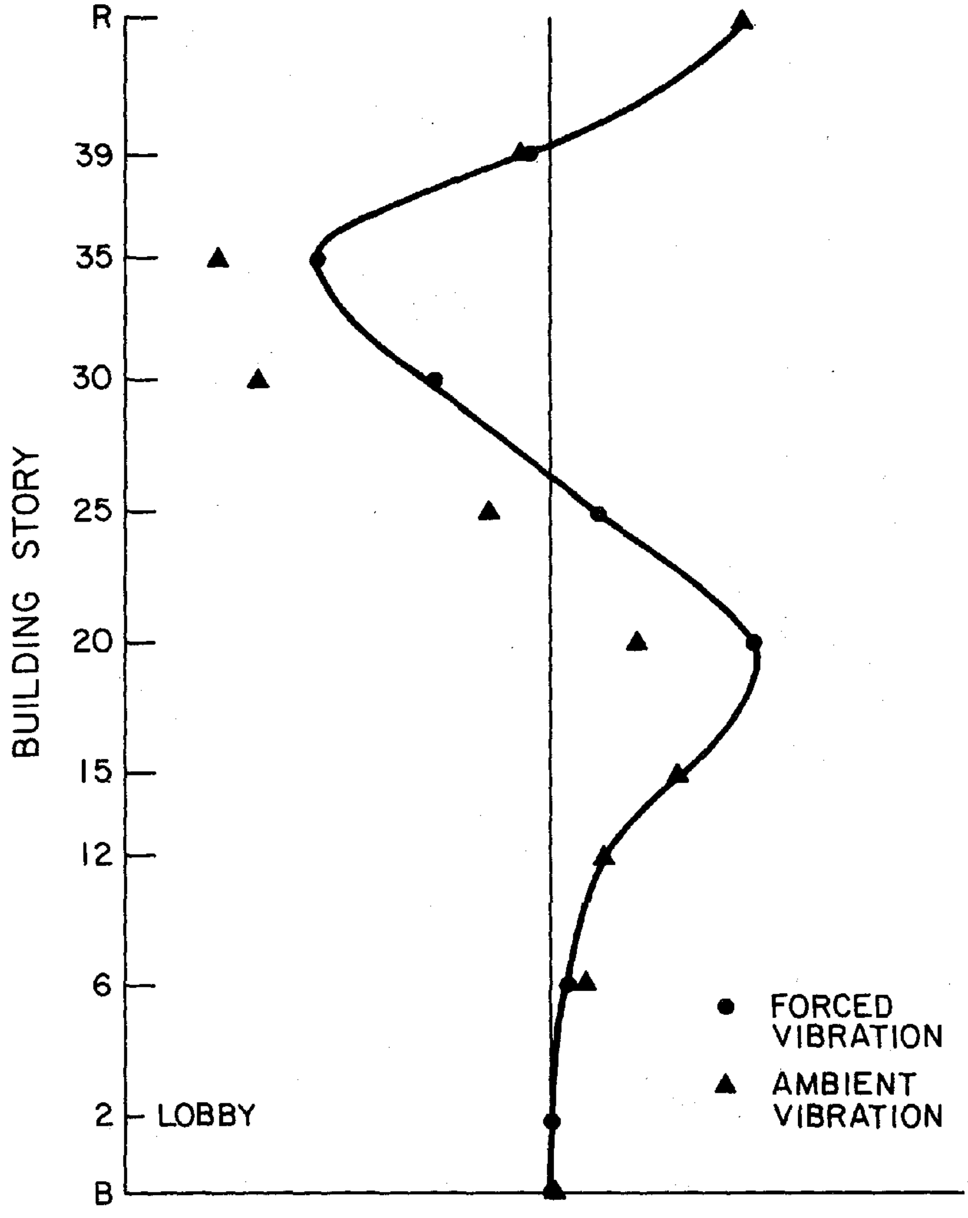

FIG. 5.4 THIRD TRANSLATIONAL MODE SHAPE, E-W

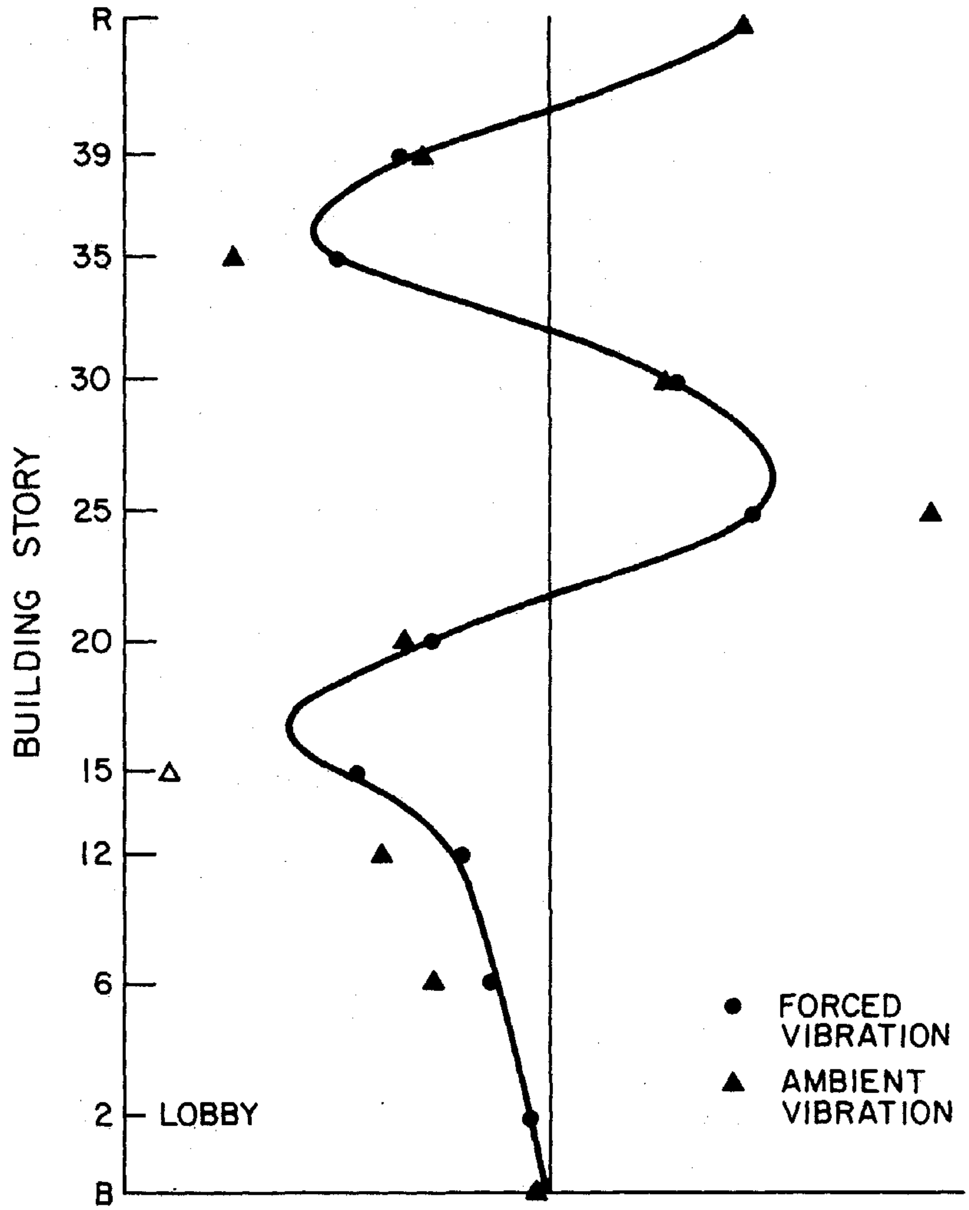

FIG. 5.5 FOURTH TRANSLATIONAL MODE SHAPE, E-W

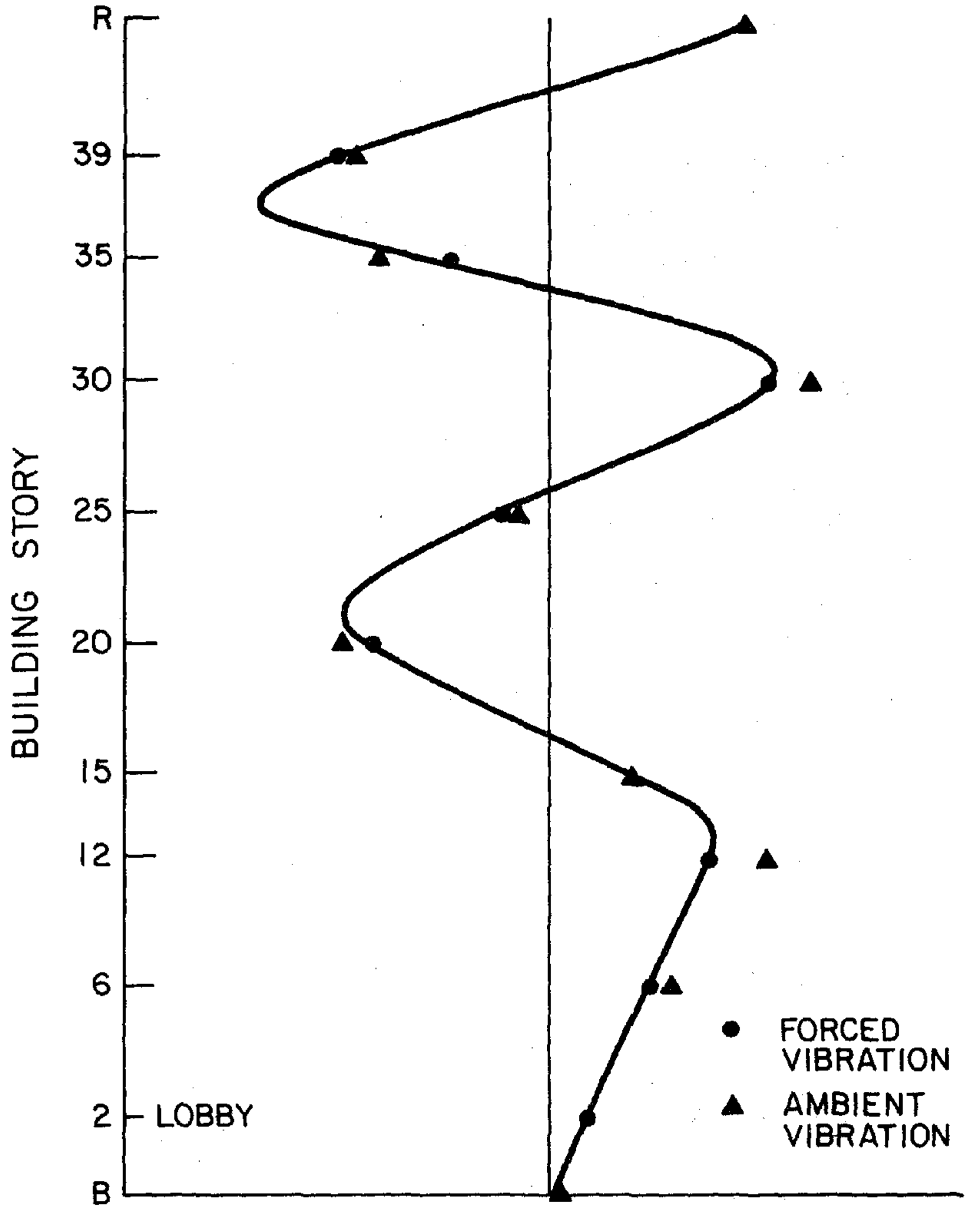

FIG. 5.6 FIFTH TRANSLATIONAL MODE SHAPE, E-W

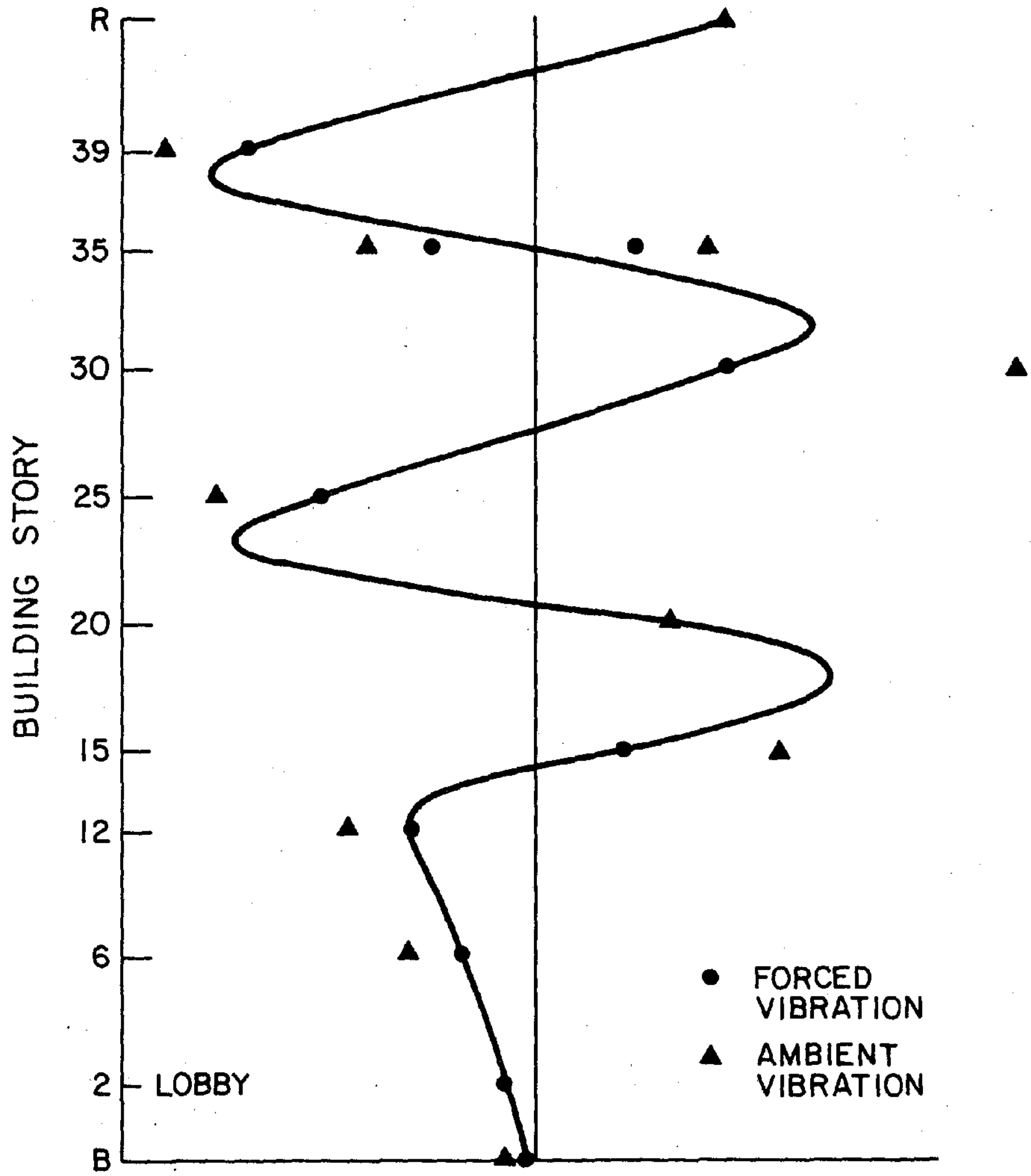

FIG. 5.7 SIXTH TRANSLATIONAL MODE SHAPE, E-W

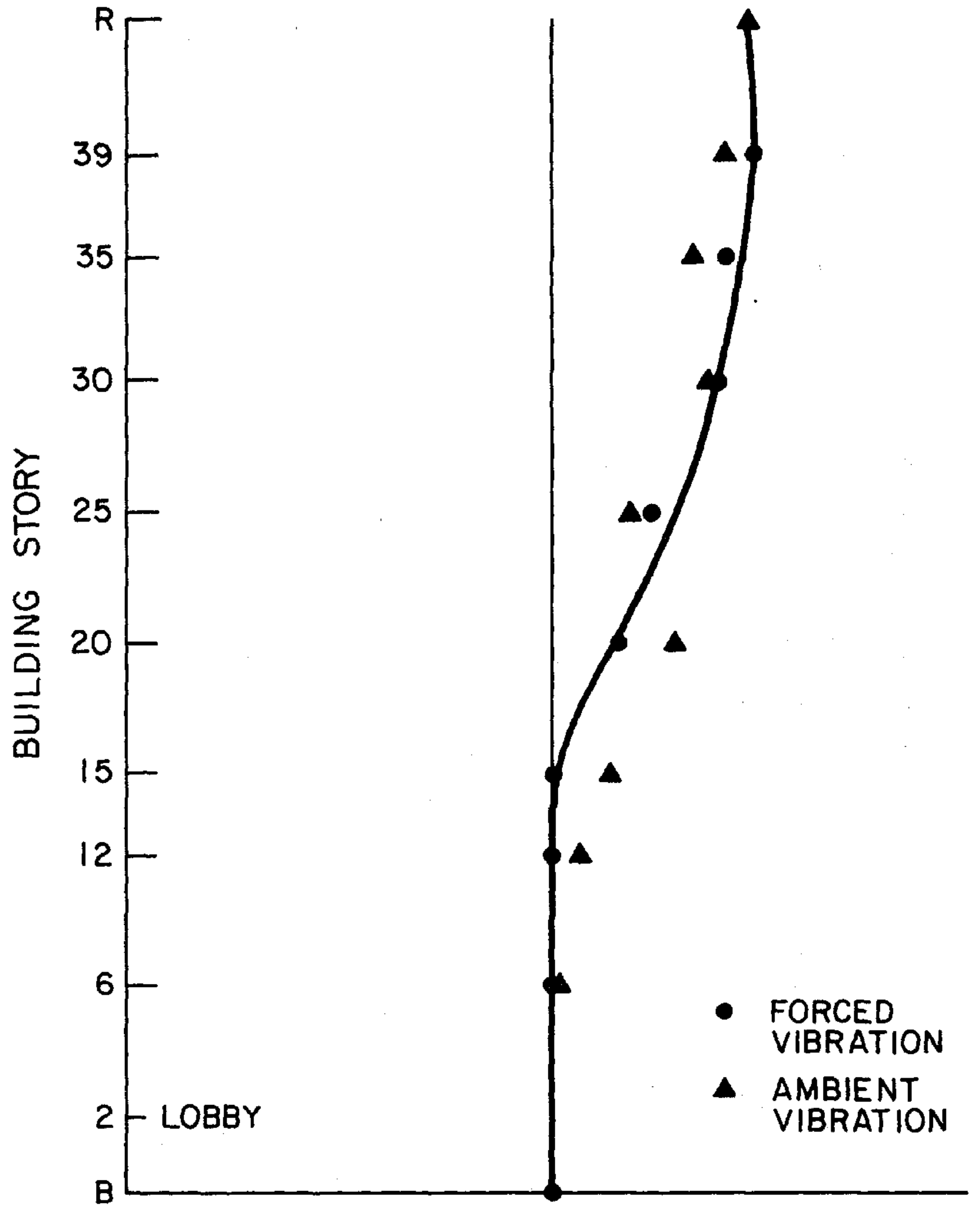

FIG. 5.8 FIRST TRANSLATIONAL MODE SHAPE, N-S

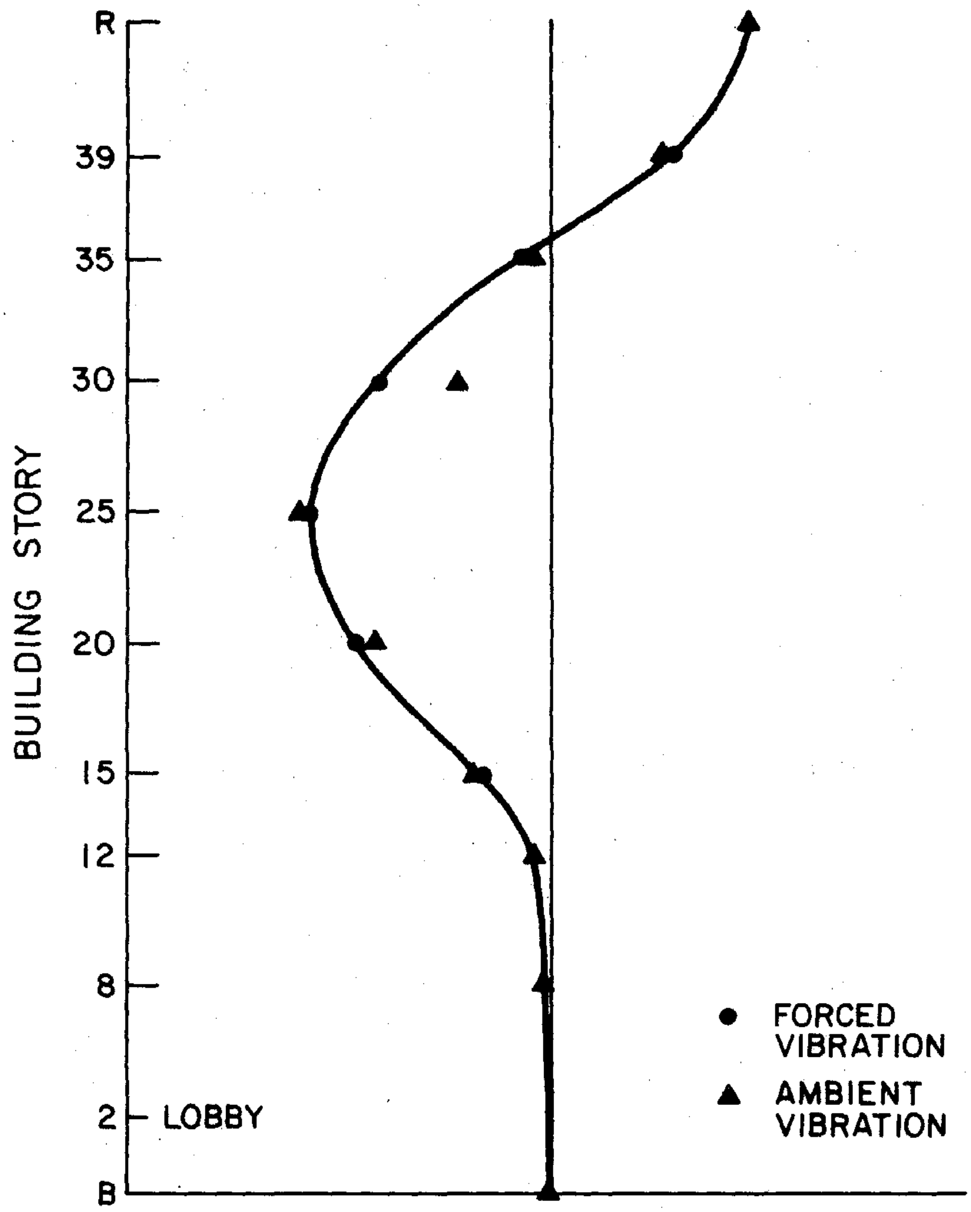

FIG. 5.9 SECOND TRANSLATIONAL MODE SHAPE, N-S

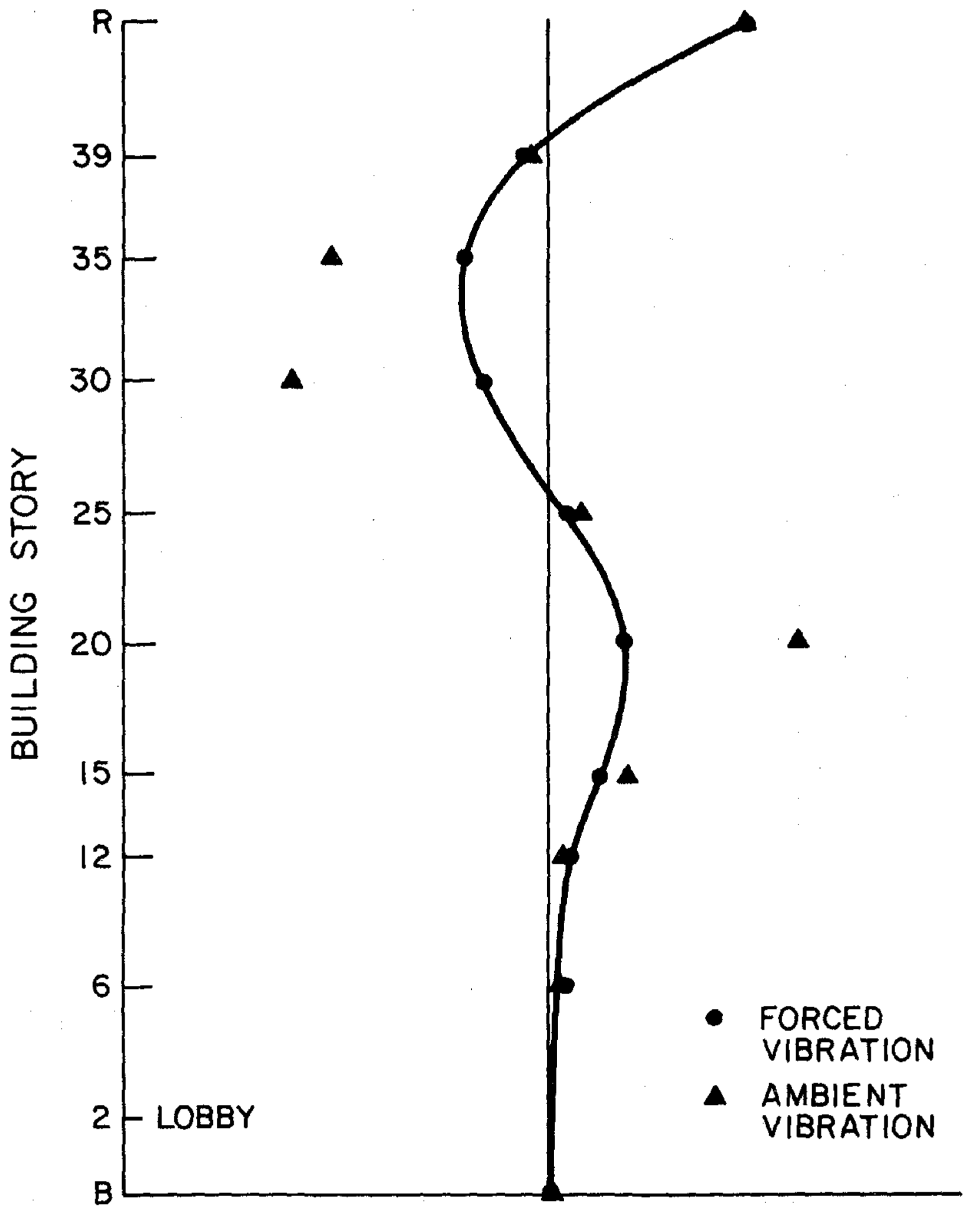

FIG. 5.10 THIRD TRANSLATIONAL MODE SHAPE, N-S

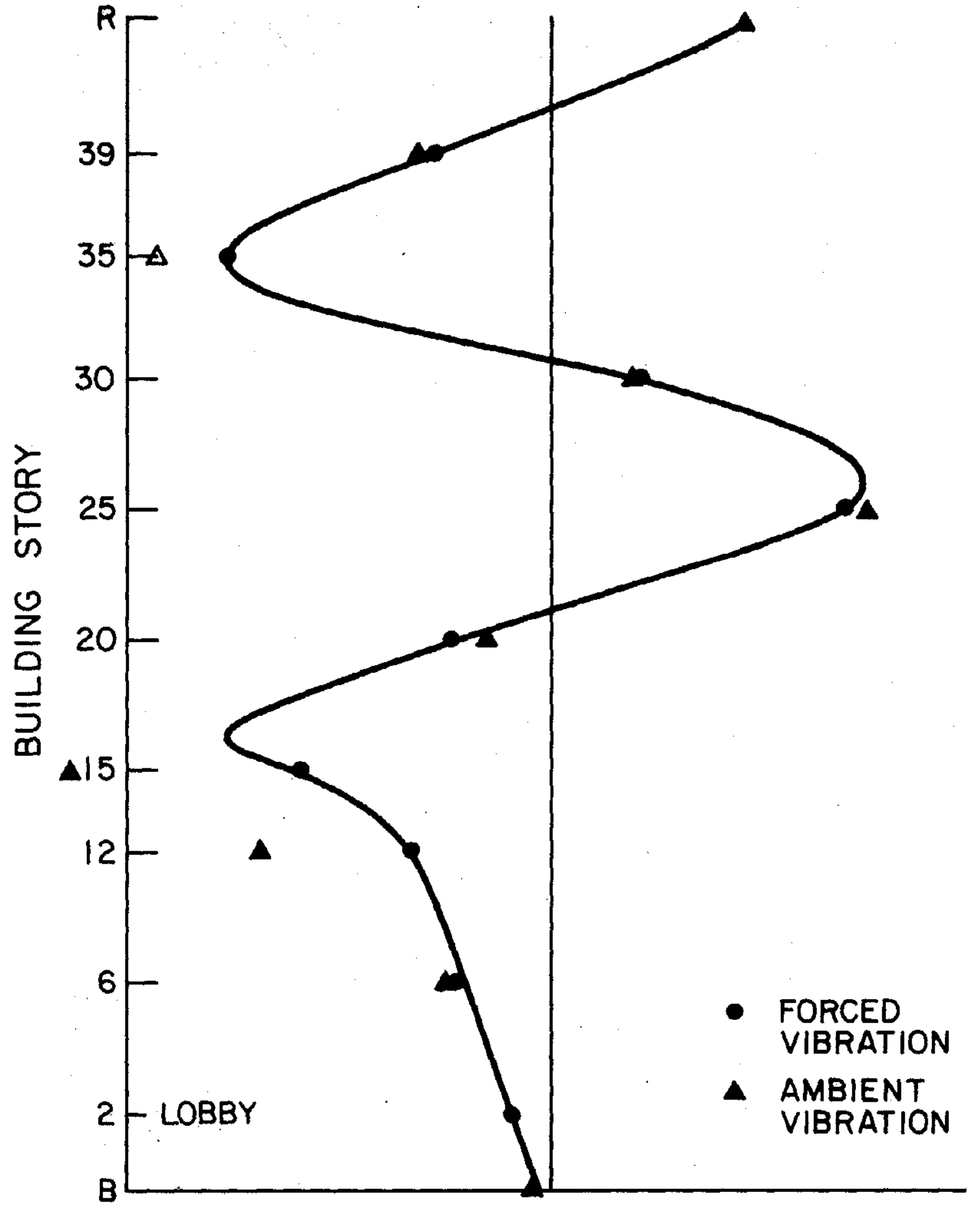

FIG. 5.11 FOURTH TRANSLATIONAL MODE SHAPE, N-S

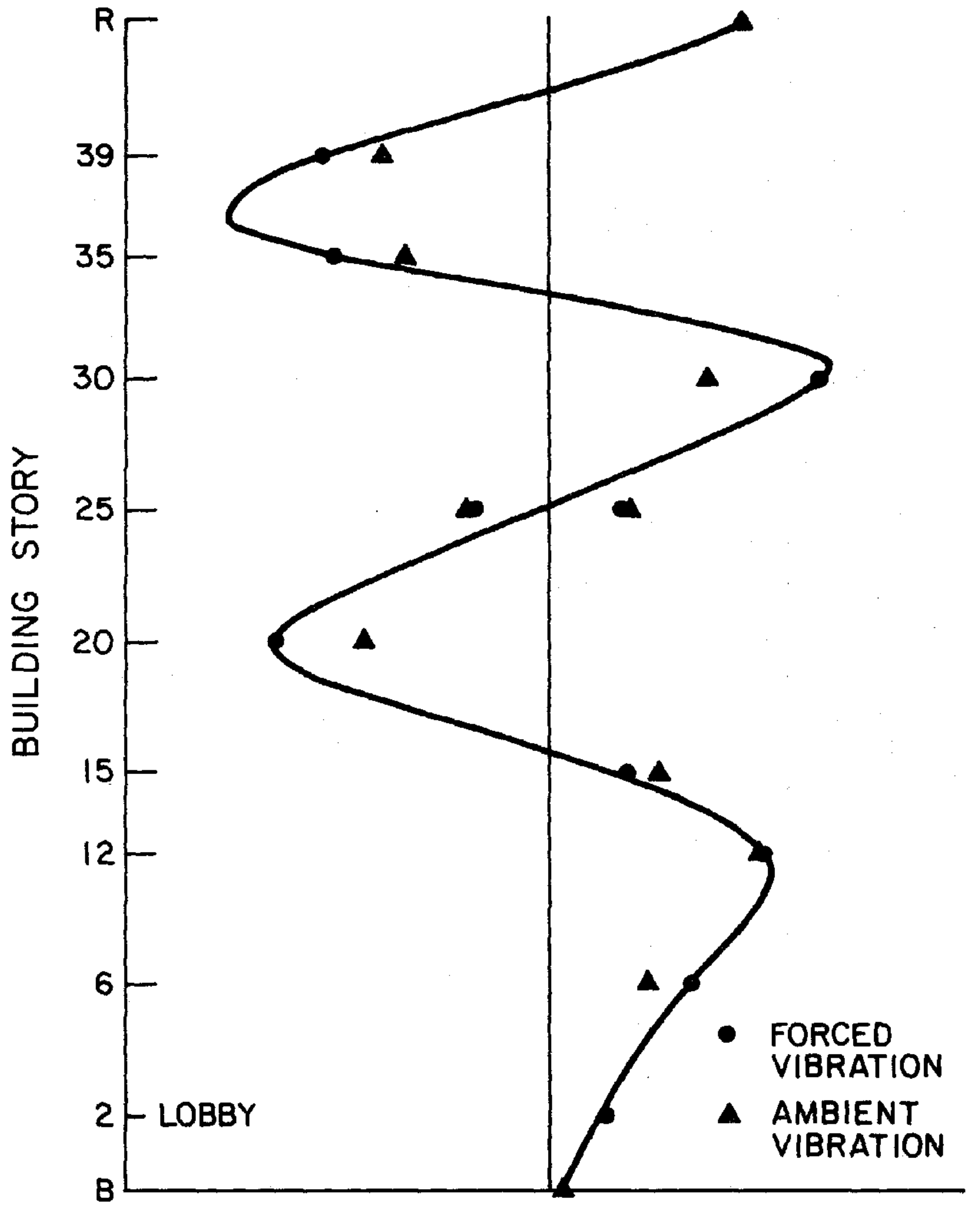

FIG. 5.12 FIFTH TRANSLATIONAL MODE SHAPE, N-S

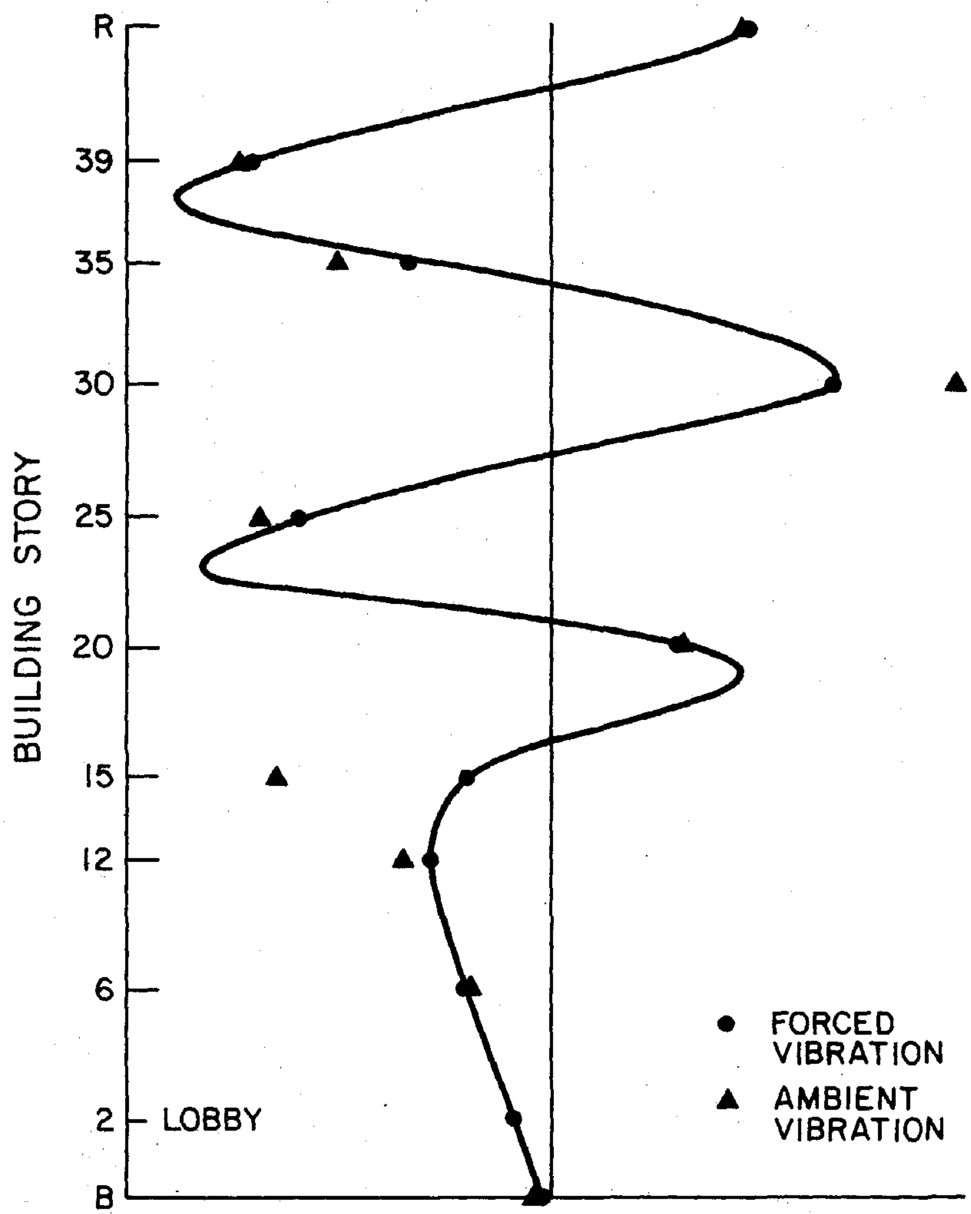

FIG. 5.13 SIXTH TRANSLATIONAL MODE SHAPE, N-S

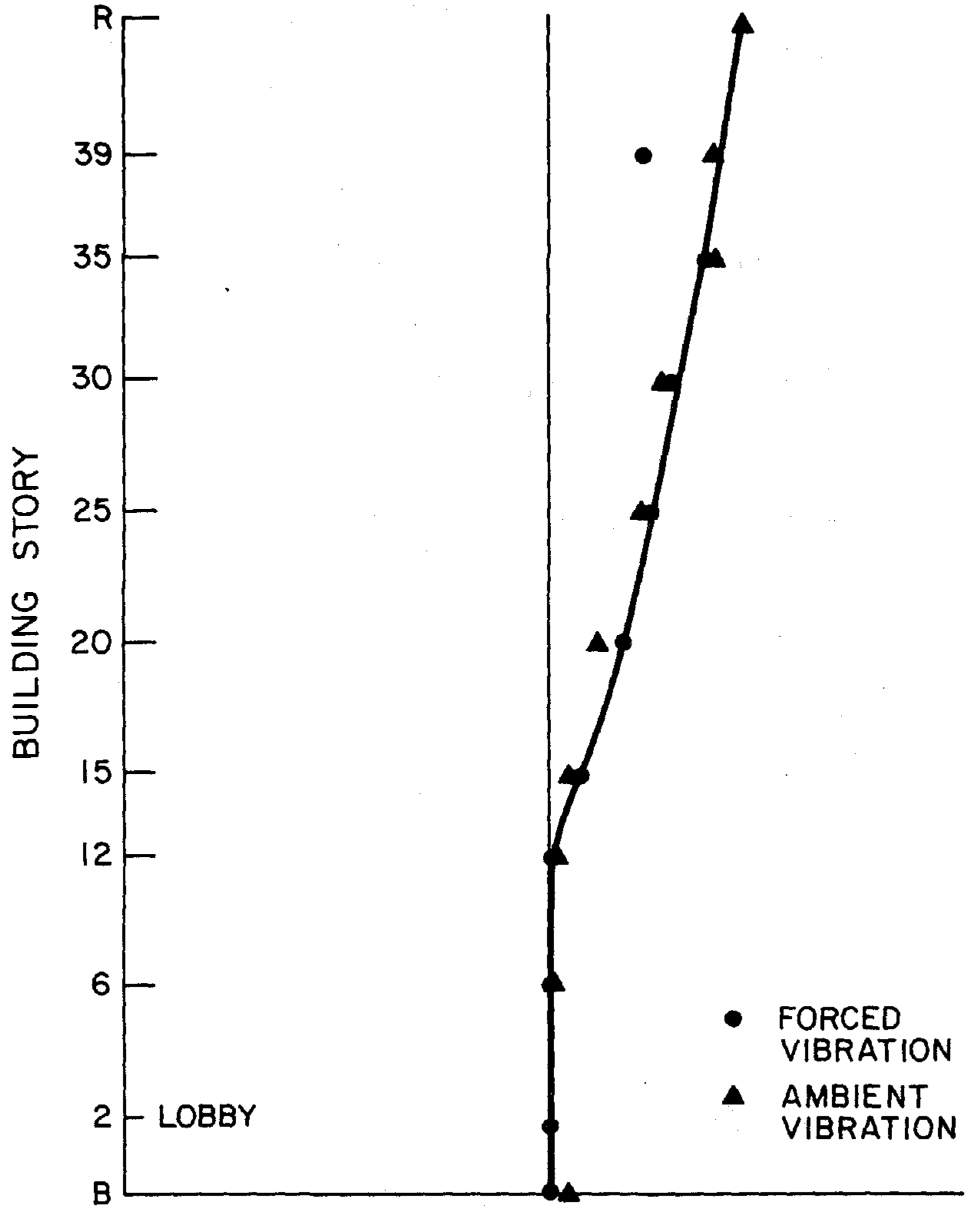

FIG. 5.14 FIRST TORSIONAL MODE SHAPE

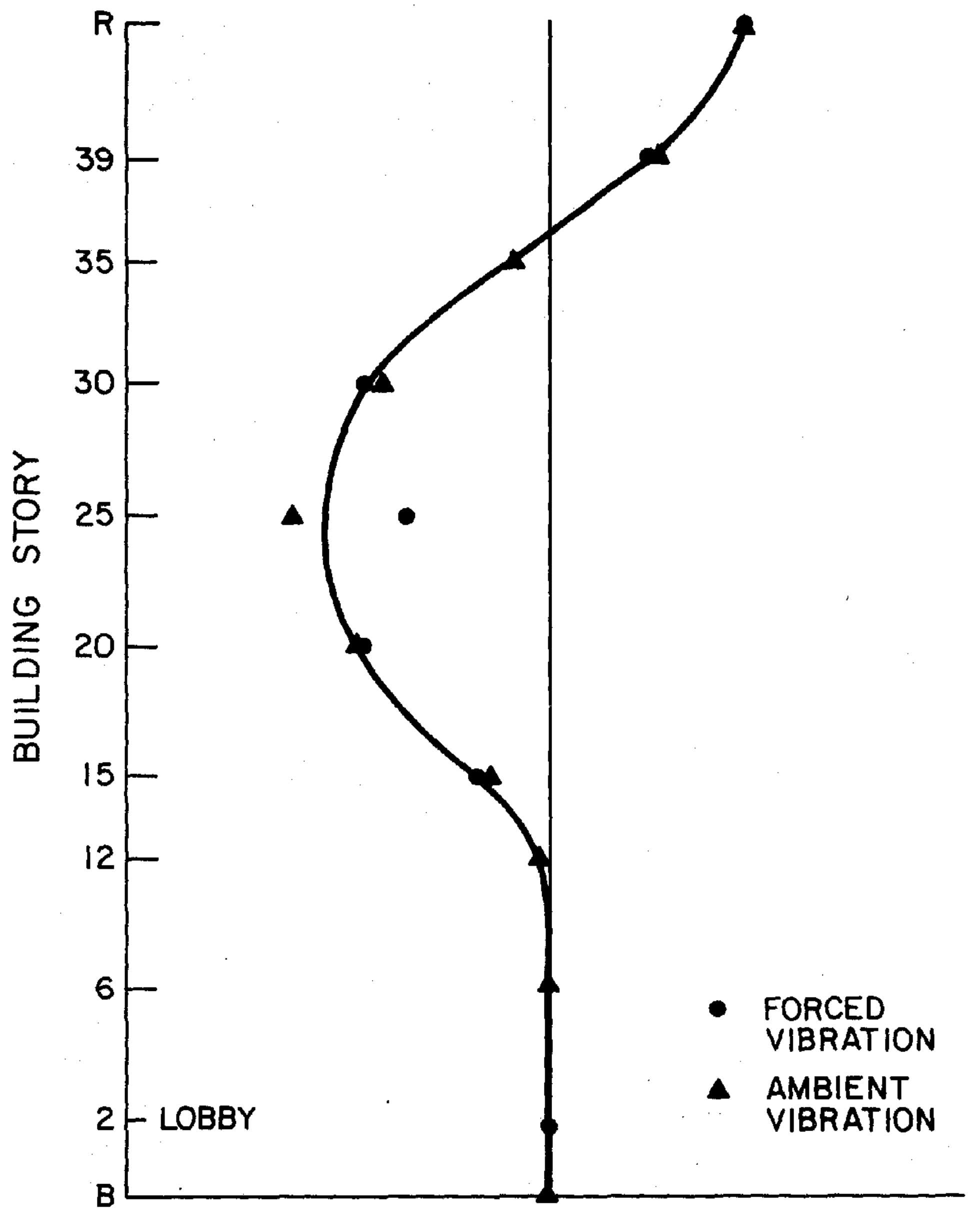

FIG. 5.15 SECOND TORSIONAL MODE SHAPE

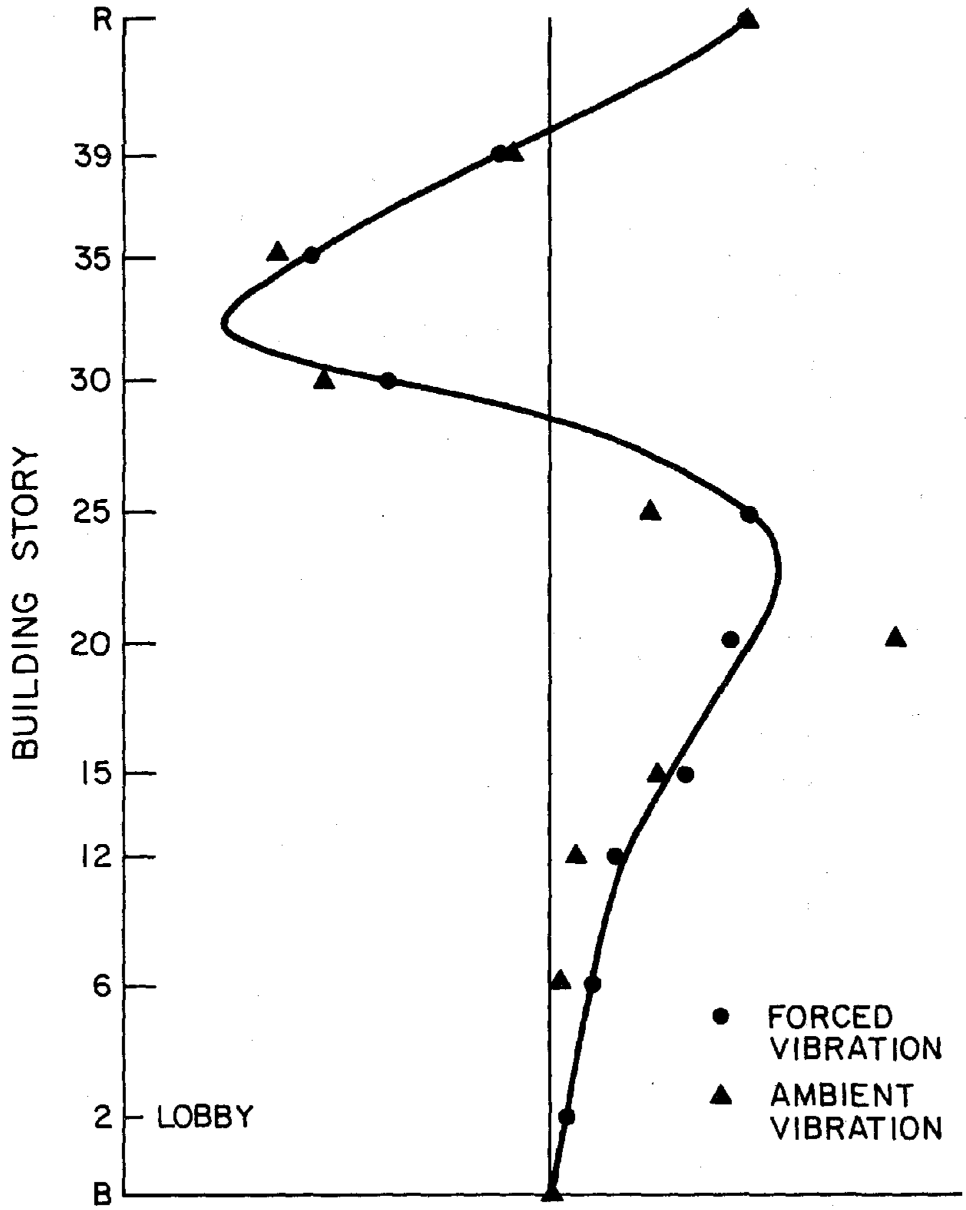

FIG. 5.16 THIRD TORSIONAL MODE SHAPE

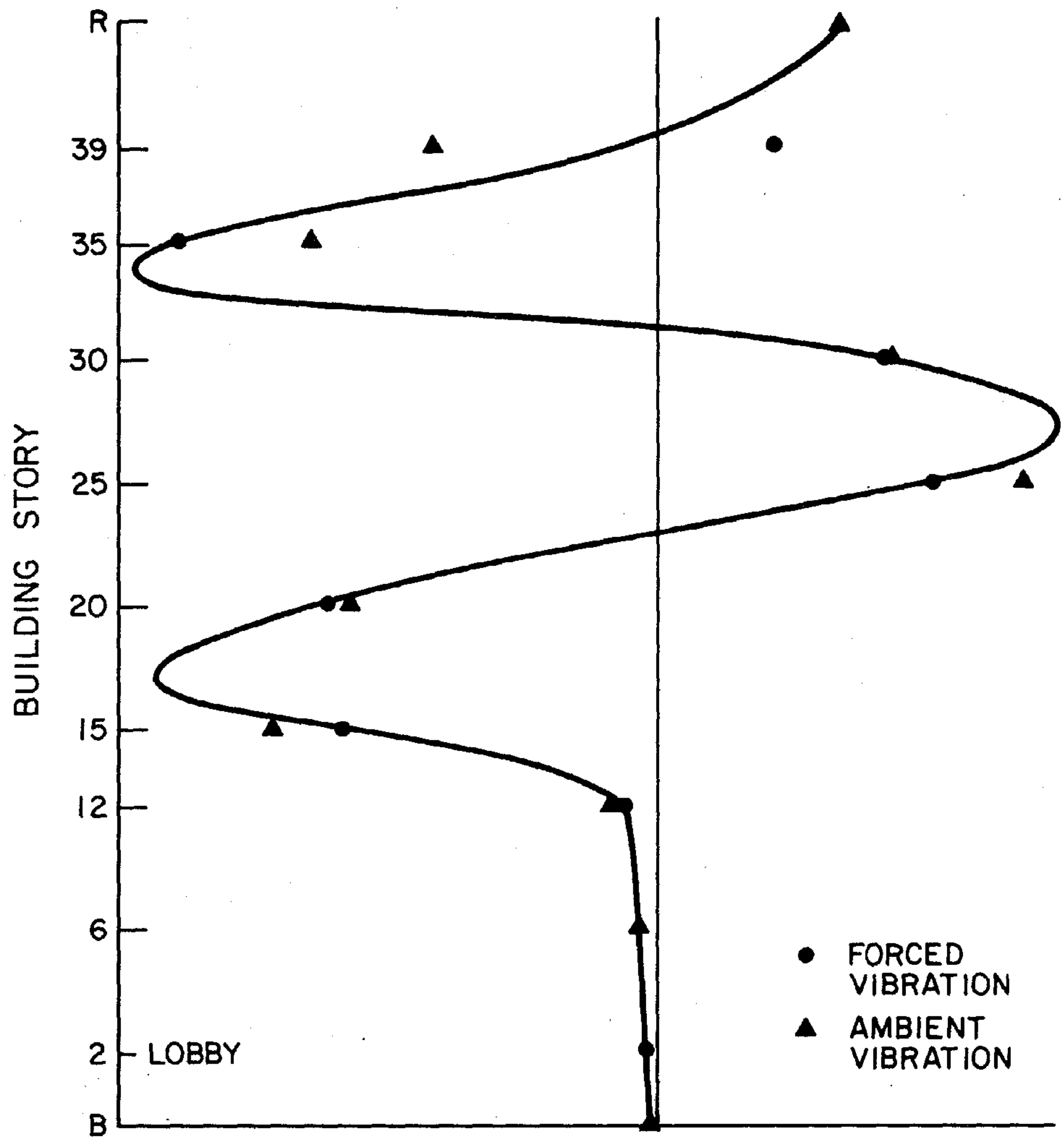

FIG. 5.17 FOURTH TORSIONAL MODE SHAPE

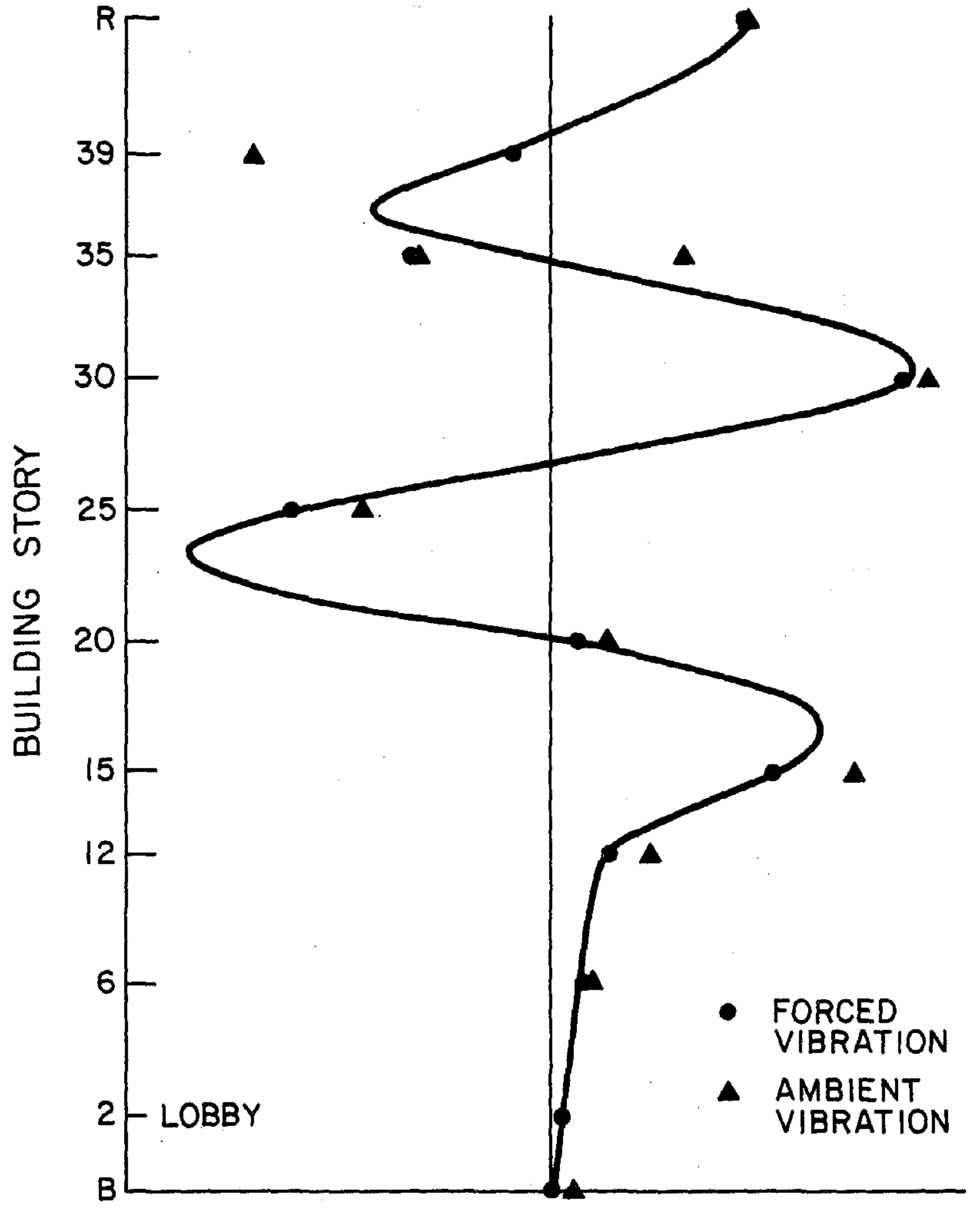

FIG. 5.18 FIFTH TORSIONAL MODE SHAPE

6. THE MATHEMATICAL MODEL

6.1 General

A model using available computer programs was set-up to analytically assess the dynamic characteristics of the building. The translational properties in two orthogonal directions and the torsional characteristics were studied and comparisons made with the observed values. The model represented one-quarter of the building above the base level. The building was represented primarily using the multipurpose program SAP, but parameter studies on the effect of rotational flexibility at the base were carried out using TABS (before that effect was incorporated in the SAP model). Both of these programs are described below, along with descriptions of the models.

6.2 Computer Programs

SAP is a multipurpose computer program developed by the Division of Structural Engineering and Structural Mechanics of the Department of Civil Engineering at the University of California, Berkeley. It was used to calculate the frequencies and mode shapes of the building. A full description of this program is given in (20).

SAP is based on the direct stiffness method, which first calculates element stiffnesses in element local coordinates and then transforms these stiffness matrices to the global system. The overall stiffness matrix is obtained by appropriate assemblage of the element stiffness matrices in global coordinates. The program evaluates the mode shapes and frequencies from the lateral stiffness matrix for the complete structure and, in this case, a diagonal matrix of its story masses, by subspace iteration.

The computer time required for a typical run for eight modes was 20 minutes. The basic computer performance data are as follows:

Typical Time Log

Nodal Point Input	11 secs
Element Stiffness Formation	125 secs
Nodal Load Input	1 sec
Total Stiffness Formation	80 secs
Eigenvalue Extraction	275 secs
	492 secs

Set-Up of Model

Number of Equations	845
Half-Bandwidth of Stiffness Matrix	46
Number of Equation Blocks	7
Number of Equations per Block	122
Number of Eigenvalues Required	8

TABS was also developed at the Berkeley campus, and a full description of it is given in (21).

TABS considers all floors to be rigid in their own plane and to have zero transverse stiffness. Initially, all elements are assembled into planar frames and their stiffnesses are transformed, using the rigid diaphragm assumption, to three degrees of freedom at the center of mass of each story level (2 translations, 1 rotation), where the story mass is lumped. Coupling between independent frames at common column lines is ignored.

The basic computer data for a very simplified one-frame idealization of the building, requiring eight modes, is as follows:

Form Frame Stiffness	2.5 secs
Mode Shapes and Frequencies	2.7 secs
	5.2 secs

A comparison of CP time between SAP and TABS indicates why the latter program was chosen for parameter studies.

Both programs used in this investigation were run on the CDC 6400 digital computer at the University of California, Berkeley campus.

6.3 Mathematical Model

6.3.1 Fixed Base Model Using SAP

The symmetrical nature of the building enabled all its characteristics to be captured by modeling only one-quarter of each floor. The obvious advantage in doing this is that storage requirements are kept to a minimum, and with logical floor-by-floor node numbering, the bandwidth of the stiffness matrix, which is the most important single factor in controlling eigenvalue solution time, can be kept down.

The response of the building in each of two translational directions and its torsional behavior were considered to be completely uncoupled, and three separate analyses were conducted to model the behavior in the N-S, E-W, and rotational modes by suitable adjustment of boundary conditions. This assumption on the independence of the degrees of freedom is considered reasonable due to the symmetry of the structure.

Three-dimensional beam elements were used to model physical beams and columns above level 12 (top of pedestal), and slaving of appropriate degrees of freedom to those of a master node at the center of each floor was used to produce an effective rigid diaphragm in its own plane, representing the inplane rigidity of the floor slab. The pedestal was modeled using two-dimensional membrane elements for both the walls and the floors. Schematics for the modeling of the pedestal and a typical upper floor are shown in Figs. 6.1 and 6.2.

The dead weights for each floor of the building were supplied by the designers, and after consultation with those who tested the building, it was decided to include 10% of the dead loads from floors 12-25 as being a reasonable estimate of the live load in the building at the time of the testing. This figure of 10% amounted to a live load of approximately

TABLE 6.1 APPROXIMATE LUMPED FLOOR WEIGHTS USED IN ANALYSIS

FLOOR	Weight Used in Program (KIPS)
Roof	2996
42	3328
41	3955
40	2133
39	2070
38	2070
37	2074
36	2074
35	2088
34	2088
33	2101
32	2110
31	2129
30	2129
29	2147
28	2147
27	2309
26	2309
25	2400
24	2484
23	2409
22	2409
21	2416
20	2416
19	2430
18	2430
17	2444
16	2444
15	2449
14	2449
13	2461
12	7560
10	6073
8	5027
6	6562
4	6454
Lobby	8734
1	4516
Base	--

15 lb/ft^2. The weights for each floor used in the analysis are indicated in Table 6.1.

In the N-S direction, several steps were taken to arrive at the final model. To begin with, just that part of the building above the pedestal was modeled. SAP uses centerline dimensions, and thus for the second run, girder depths were considered rigid and thus reduced the effective clear heights of the columns. With this inclusion, it seemed that the partial model was working satisfactorily so the pedestal was added in the next run. Finally, an accurate estimate of composite slab action with the floor girders was included. The effect of each of these additions on the first natural period is summarized in Table 6.2 below.

TABLE 6.2 - EFFECT OF STRUCTURAL MODEL ON THE FUNDAMENTAL PERIOD IN THE N-S DIRECTION

Structural Model	First Natural Period (sec)	Frequency (cps)
1. Frame above the pedestal	4.59	0.218
2. (1) plus reduced column heights	3.85	0.259
3. (2) plus addition of pedestal	4.16	0.240
4. (3) plus composite slab action	4.10	0.243
Experimental	4.44	0.225

By studying Table 6.2, the following remarks can be made:

1. The effect of the pedestal is rather small. By studying the mode shapes, it can be seen that this part of the structure is extremely stiff, and the building is behaving rather like a 30-story structure connected to the ground via an almost rigid arm.
2. The most significant effect on the fundamental period is the

reduction in clear column height due to the assumption of rigid column action over the girder depths. The reduction in period is obvious when one considers that the increase in stiffness is by the ratio $\left(\frac{L0}{L1}\right)^3$ where L1 is the clear height and L0 is the floor to floor height. This parameter is typically:

$$\left(\frac{144}{114}\right)^3 = (1.26)^3 = 2.02$$

At this point, eight modes were extracted for the N-S direction and compared to those from the forced vibration tests. The frequency values agreed well but examination of the mode shapes, especially the higher modes, suggested that there may well be some rotational flexibility due to nonrigid soil action at the base.

6.3.2 Flexible Base Model Using TABS

It was decided to use the computer program TABS, with its capability of external story stiffnesses, to arrive at some figures for the effect of base flexibility. A model using a single frame with four column lines and panel elements to represent the pedestal was established to give a fundamental frequency of 0.243 cps.

The procedure from there was to see what value of flexural inertia was needed for the dummy story in order to reduce the fundamental frequency to 0.225 cps. A value of 0.005 times that of the actual base I was found to give the appropriate reduction. A check on the higher mode shapes indicated that this value also gave better correlation with observed mode shapes. This value of I for a dummy story was then included in a SAP model.

6.3.3 Flexible Base Model Using SAP

An extra dummy story was added to the SAP model, and boundary elements were used to give external translational stiffness at the true base level. The effect on the first period is indicated in Table 6.3.

TABLE 6.3 - EFFECT OF FLEXIBLE BASE ON FUNDAMENTAL PERIOD, N-S DIRECTION

	Fundamental Period (sec)	Frequency (Hz)
Fixed Base SAP Model	4.10	0.243
Flexible Base SAP Model	4.48	0.223
Experiment	4.44	0.225

The higher mode shapes from the flexible base model were in better agreement than those from the fixed base model.

6.4 Results of the Mathematical Model

The frequencies from the model which were described in Section 6.3 are summarized in Table 6.4 below. The corresponding translational mode shapes for the flexible base model are shown in Figs. 6.3 through 6.8. The torsional mode shape from the fixed based model are shown in Figs. 6.9 through 6.14.

TABLE 6.4 - RESULTS OF MATHEMATICAL MODEL RESONANT FREQUENCIES (Hz)

Model	Mode						
	1	2	3	4	5	6	7
N-S Fixed Base	.243	.719	1.240	1.751	2.260	2.740	3.202
N-S Flexible Base	.223	.700	1.196	1.695	2.143	2.536	2.923
E-W Fixed Base	.245	.721	1.248	1.757	2.275	2.764	3.222
Torsional	.323	.857	1.439	2.020	2.615	3.196	-----

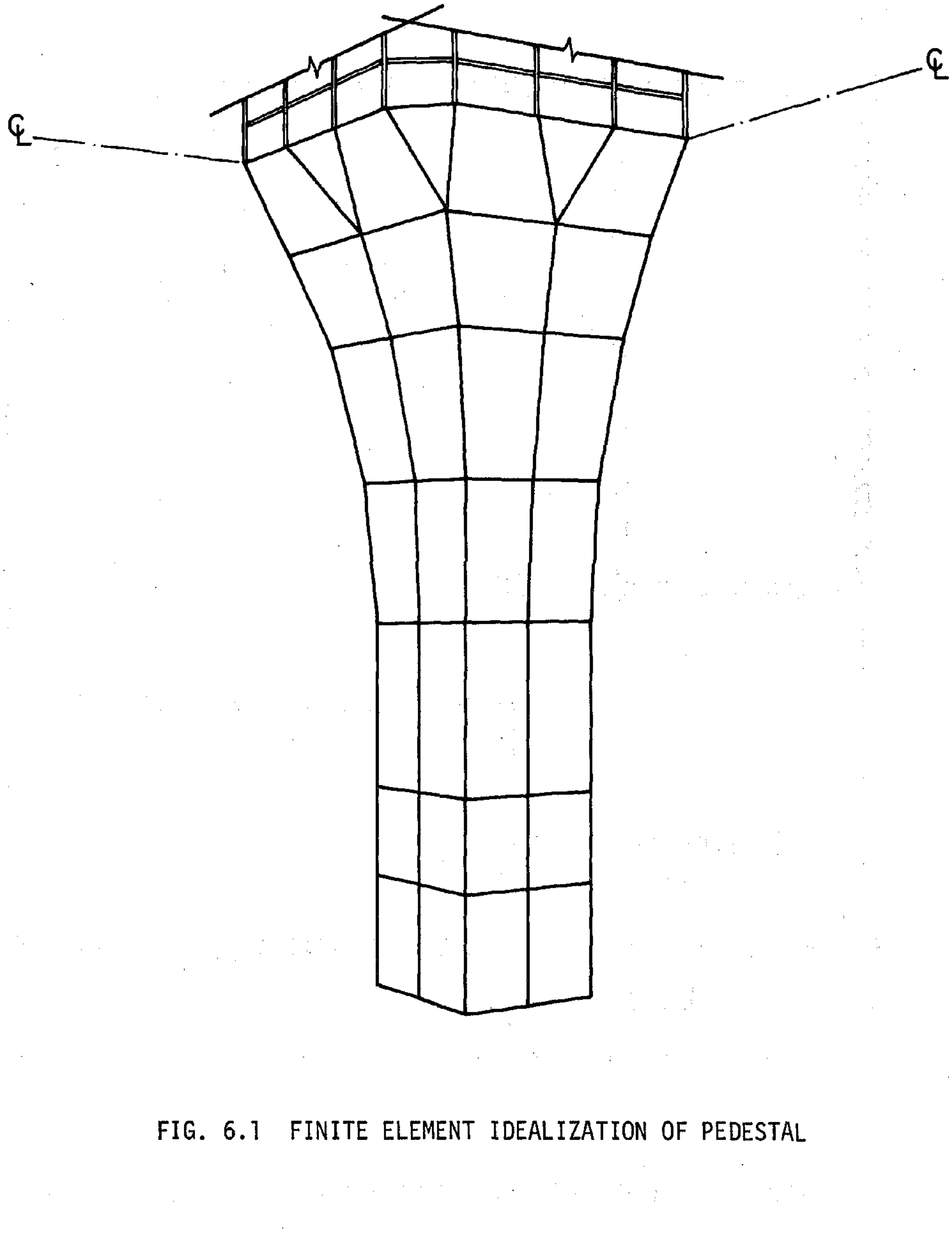

FIG. 6.1 FINITE ELEMENT IDEALIZATION OF PEDESTAL

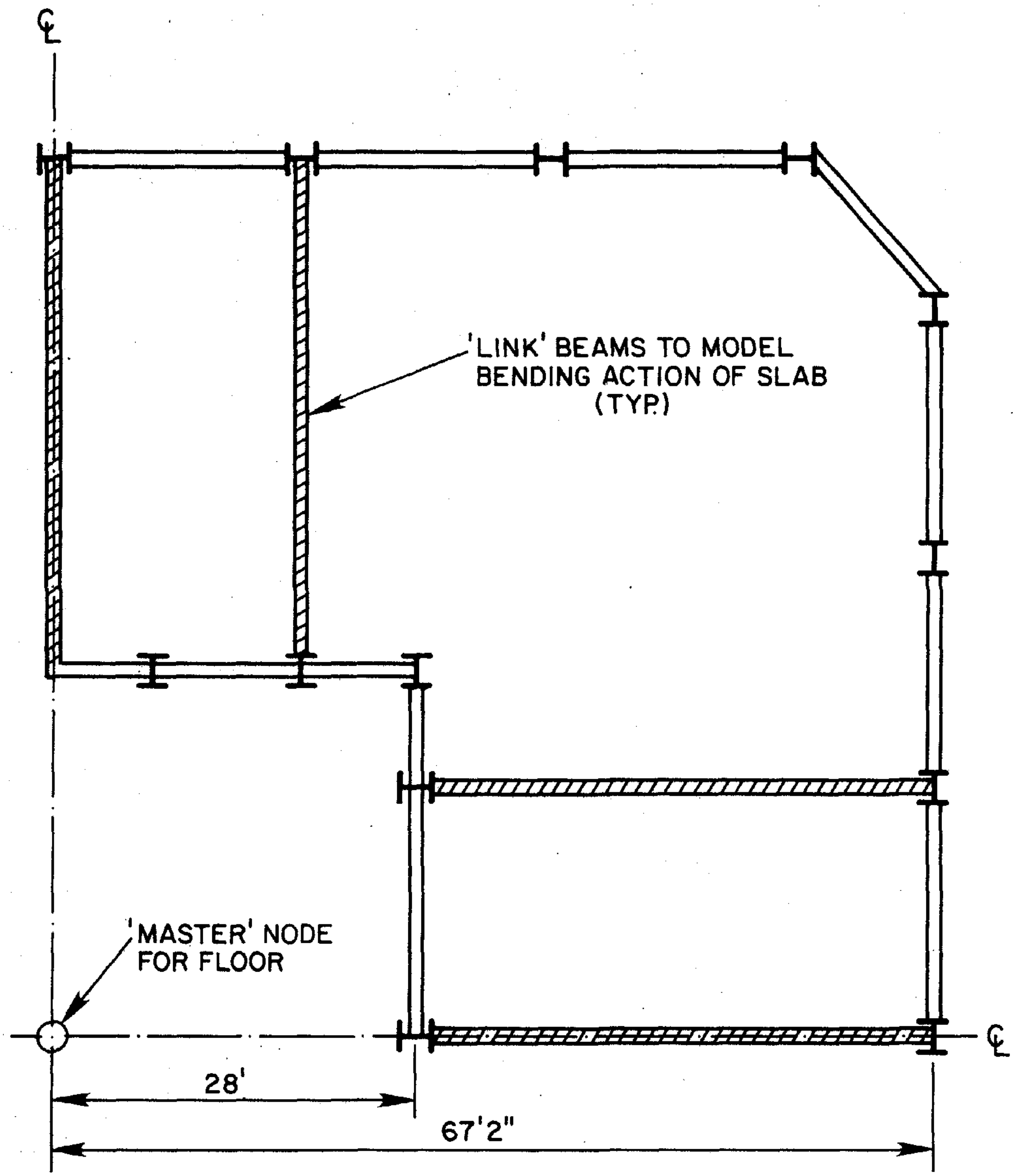

FIG. 6.2 FINITE ELEMENT IDEALIZATION OF TYPICAL UPPER FLOOR

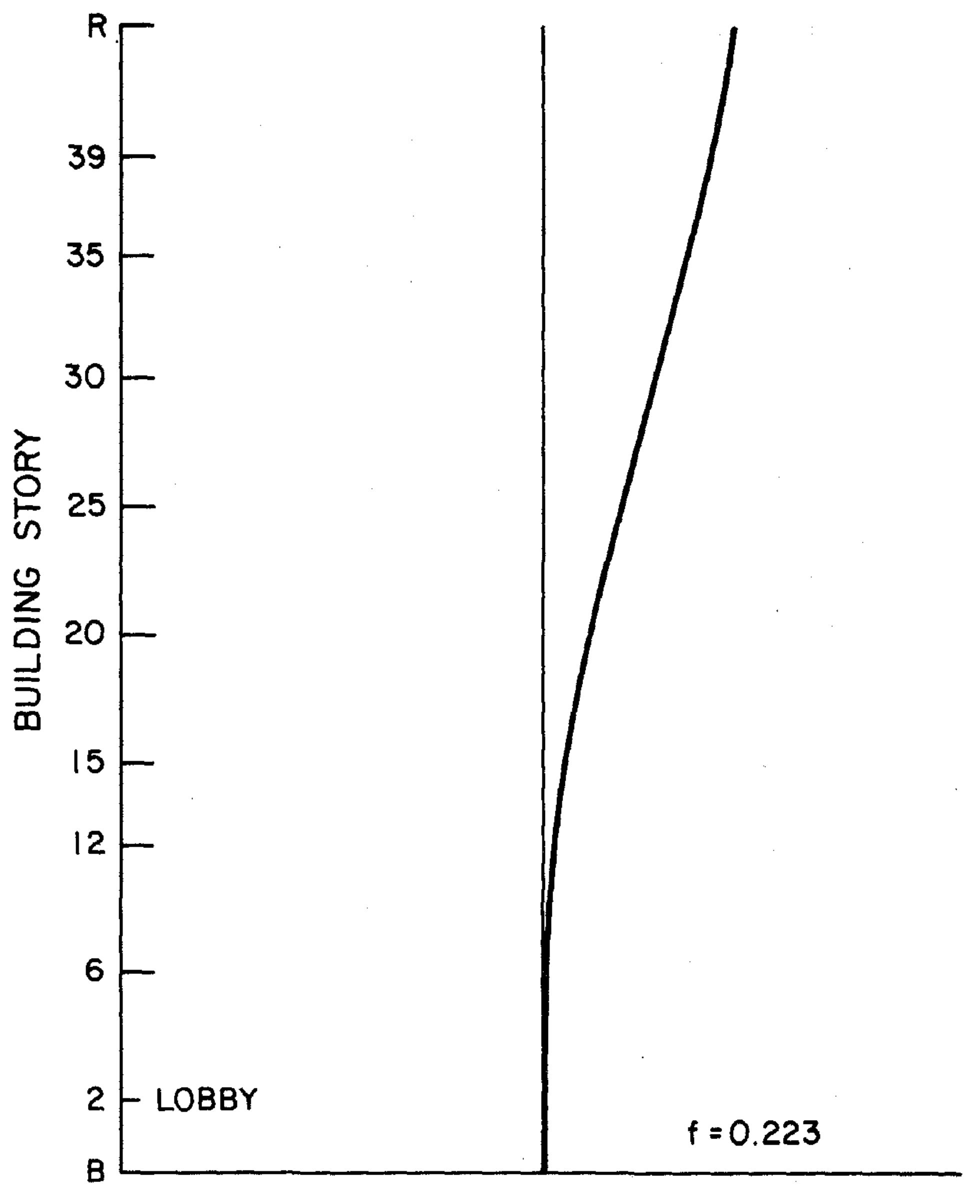

FIG. 6.3 FIRST TRANSLATIONAL MODE SHAPE FLEXIBLE BASE

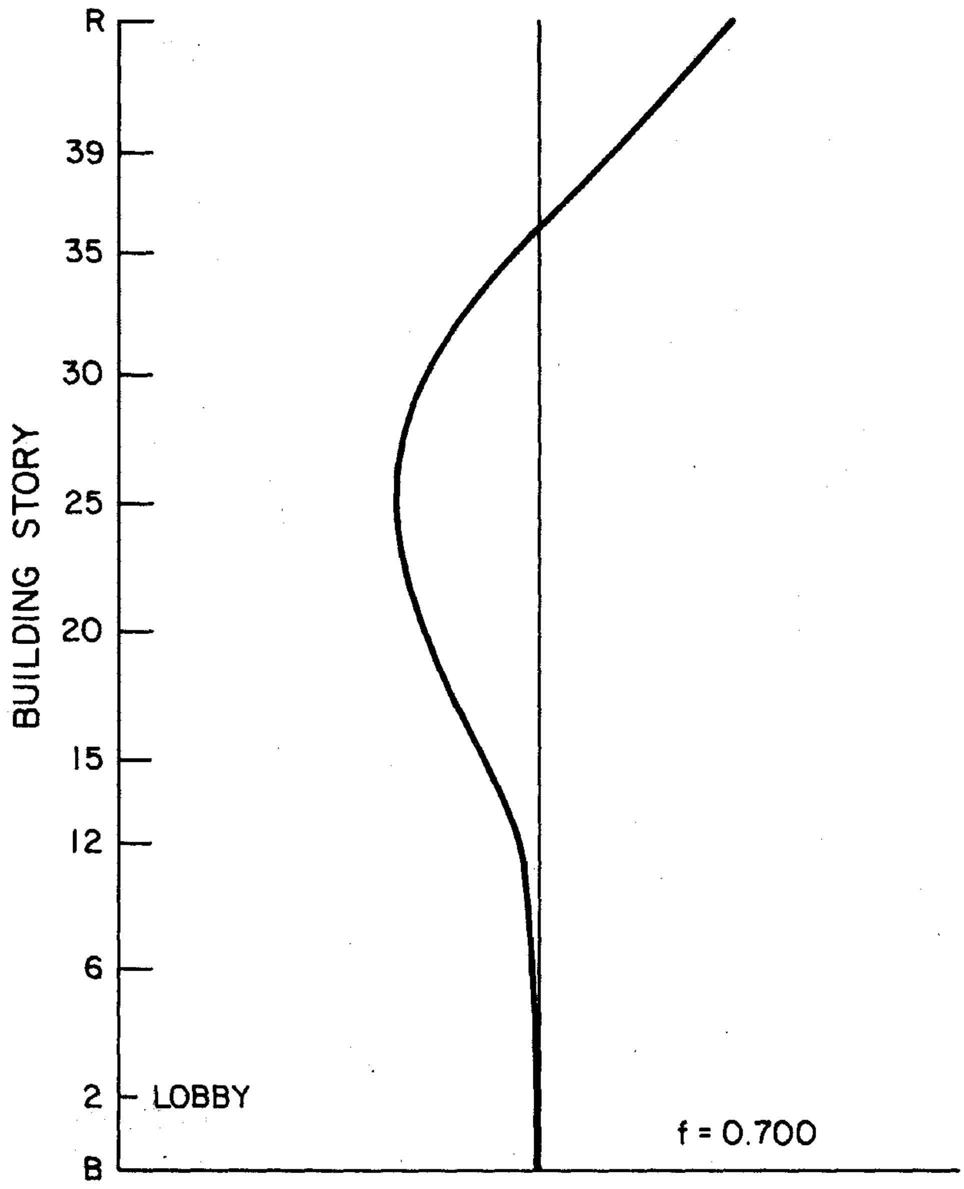

FIG. 6.4 SECOND TRANSLATIONAL MODE SHAPE FLEXIBLE BASE

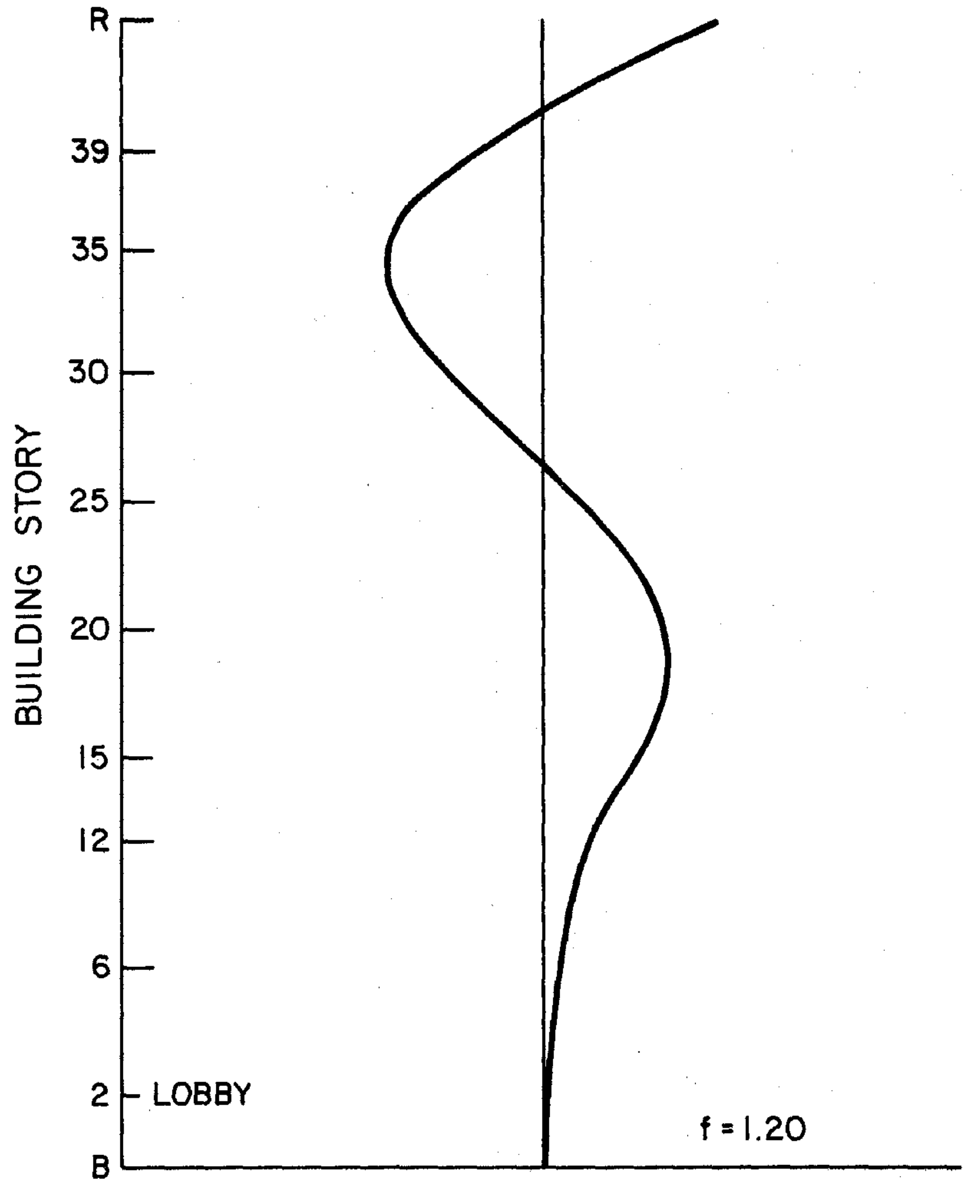

FIG. 6.5 THIRD TRANSLATIONAL MODE SHAPE FLEXIBLE BASE

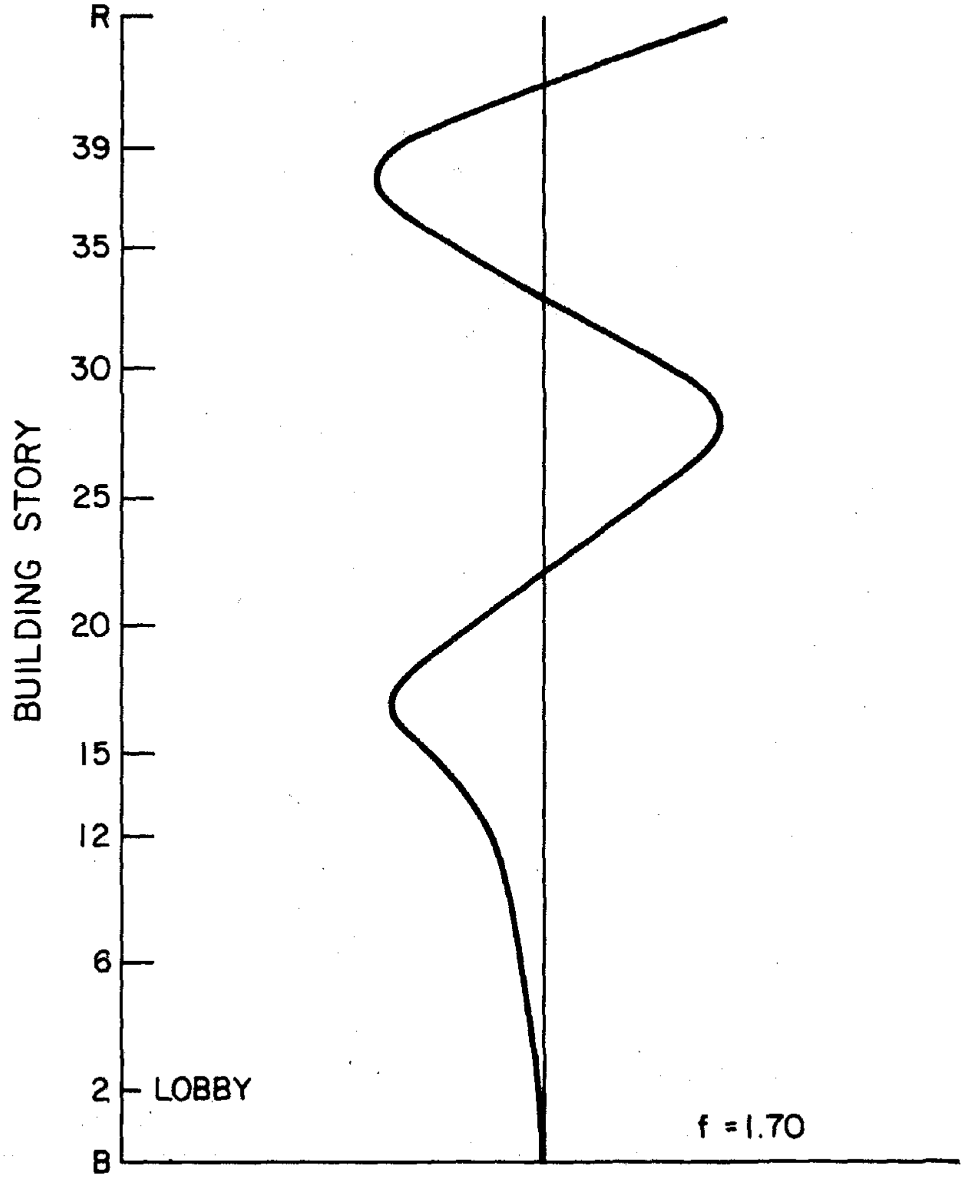

FIG. 6.6 FOURTH TRANSLATIONAL MODE SHAPE FLEXIBLE BASE

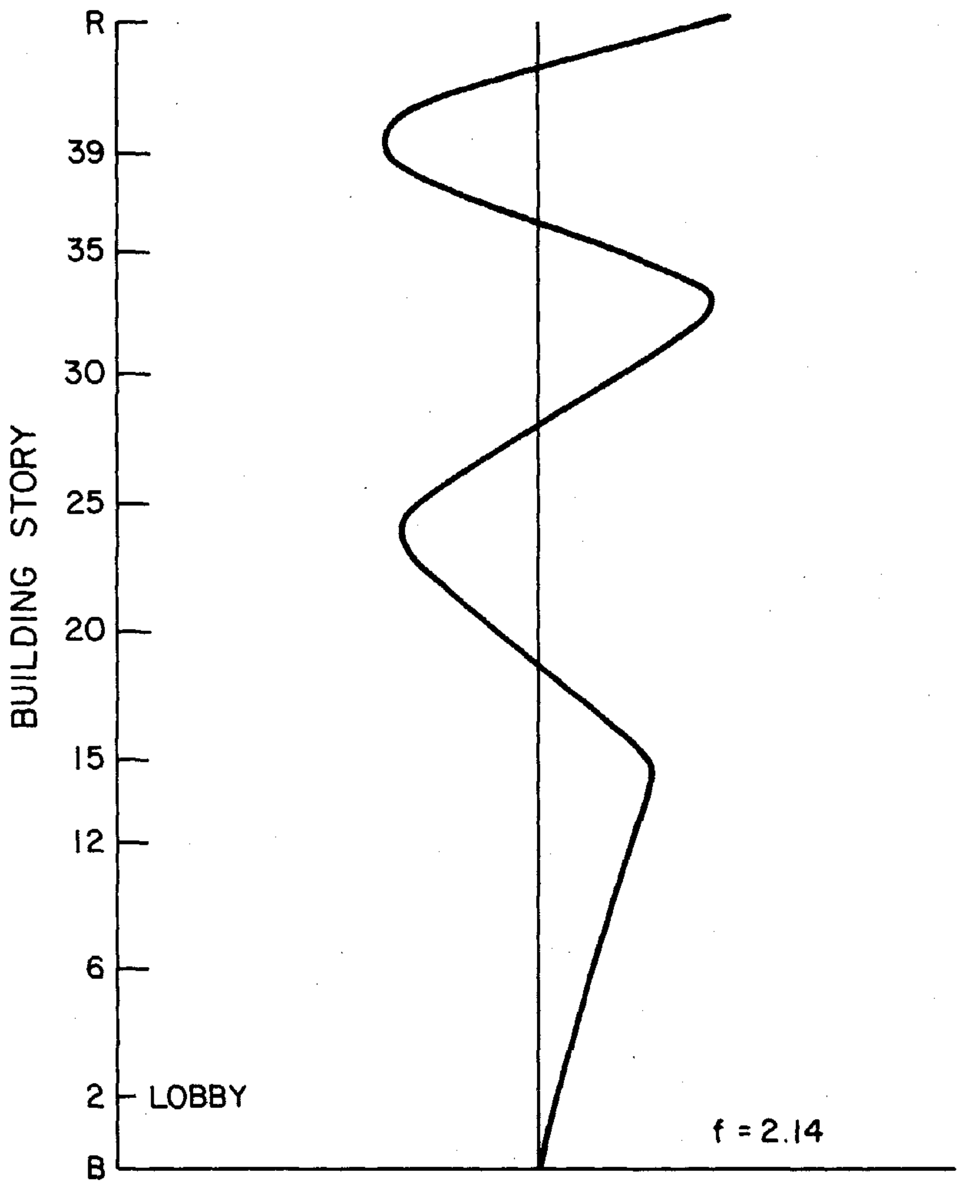

FIG. 6.7 FIFTH TRANSLATIONAL MODE SHAPE FLEXIBLE BASE

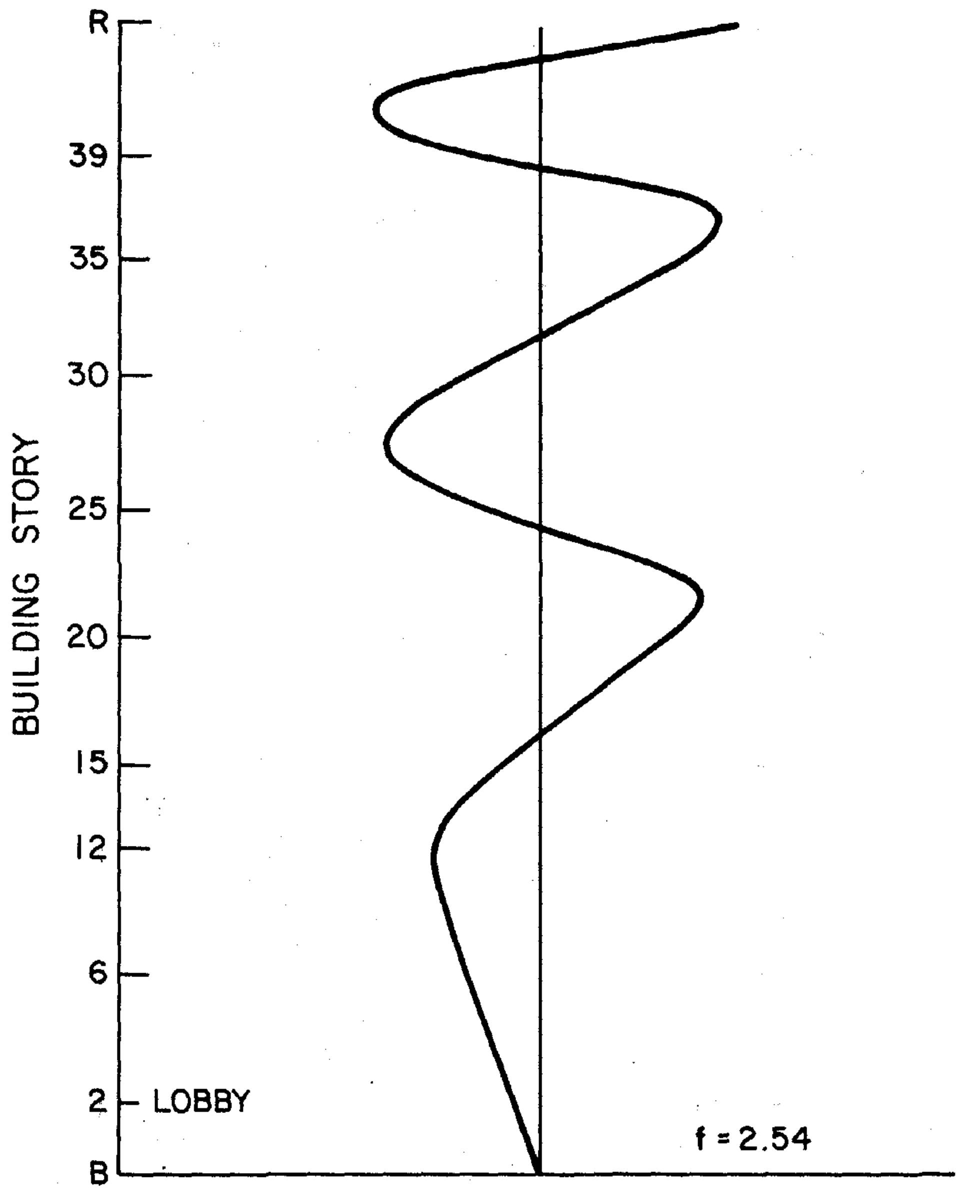

FIG. 6.8 SIXTH TRANSLATIONAL MODE SHAPE FLEXIBLE BASE

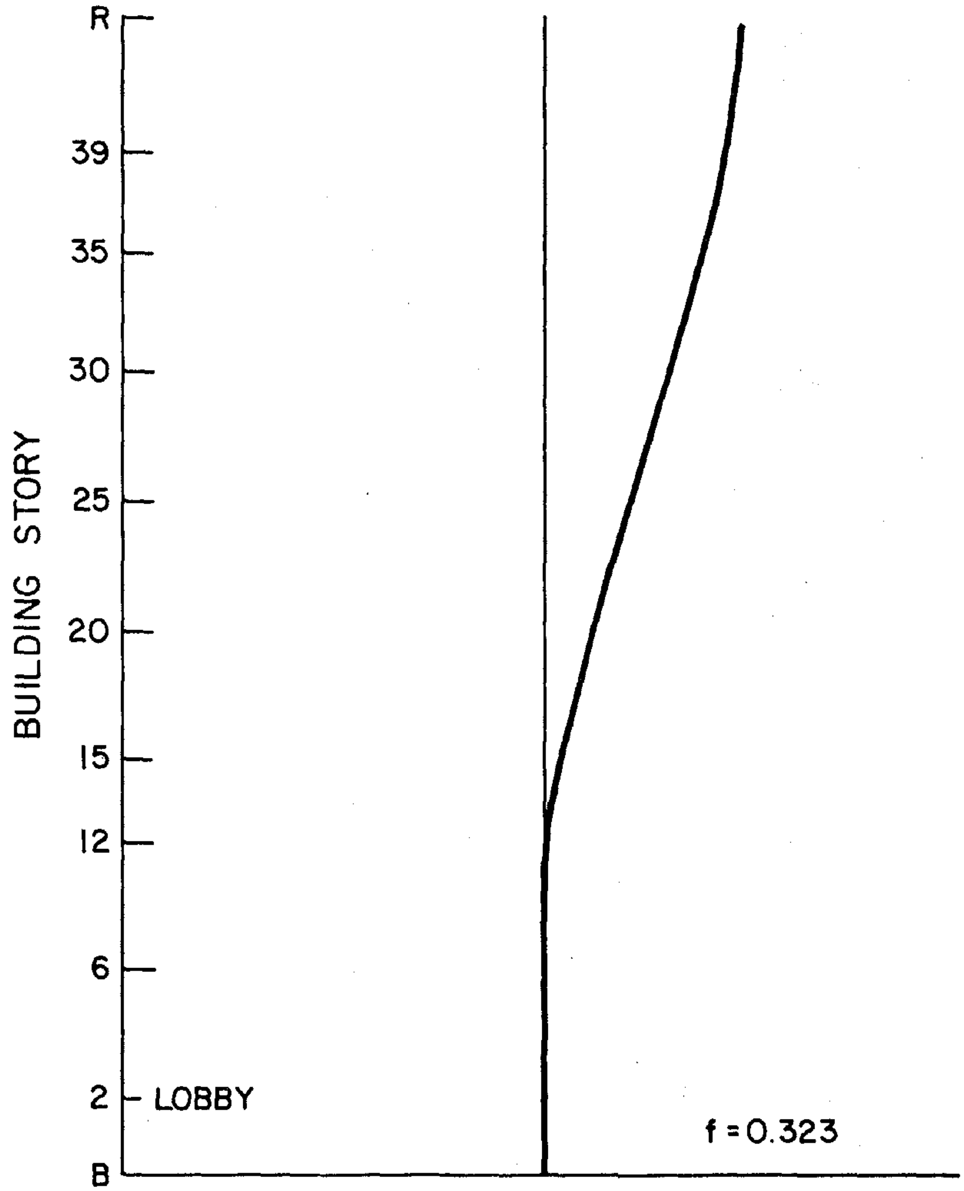

FIG. 6.9 FIRST TORSIONAL MODE SHAPE

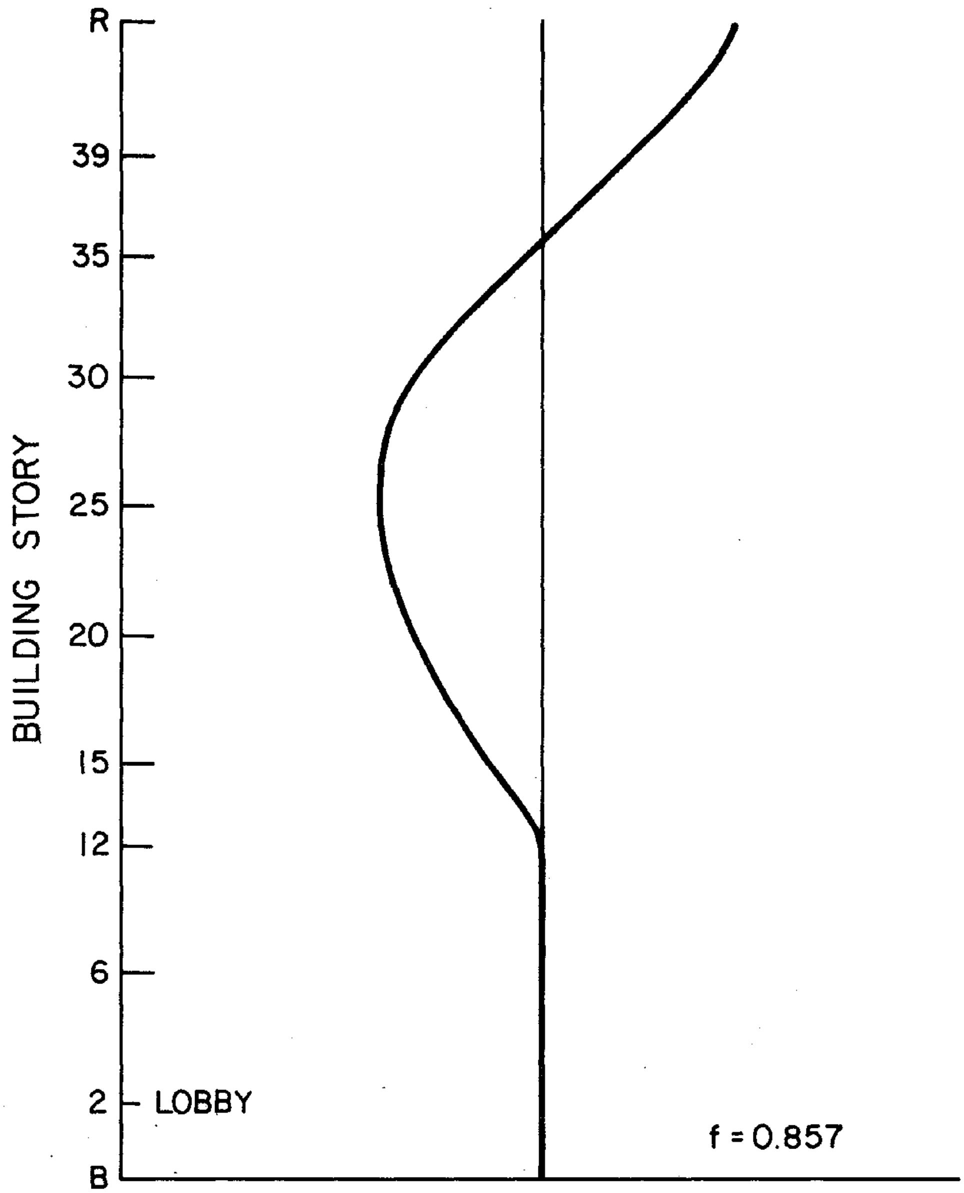

FIG. 6.10 SECOND TORSIONAL MODE SHAPE

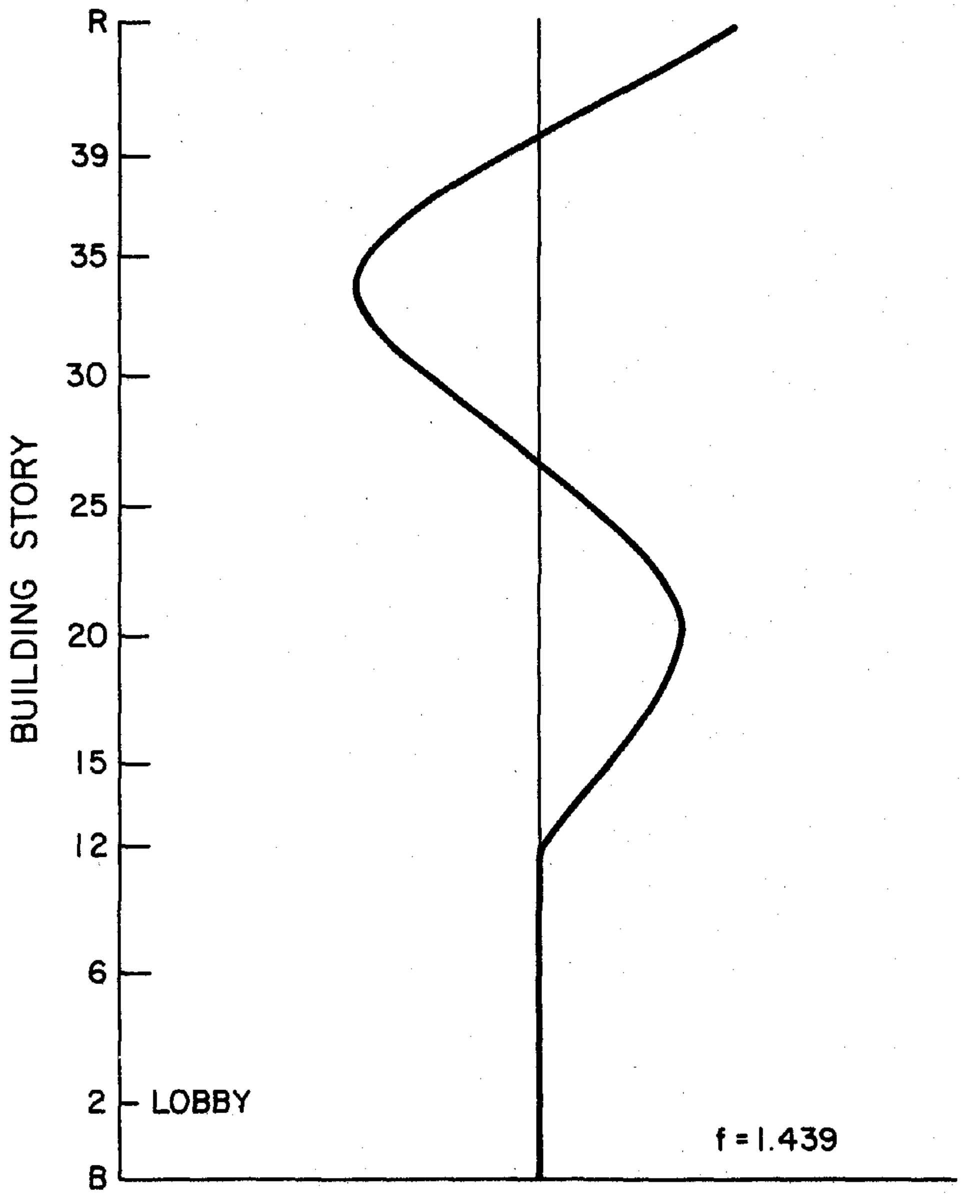

FIG. 6.11 THIRD TORSIONAL MODE SHAPE

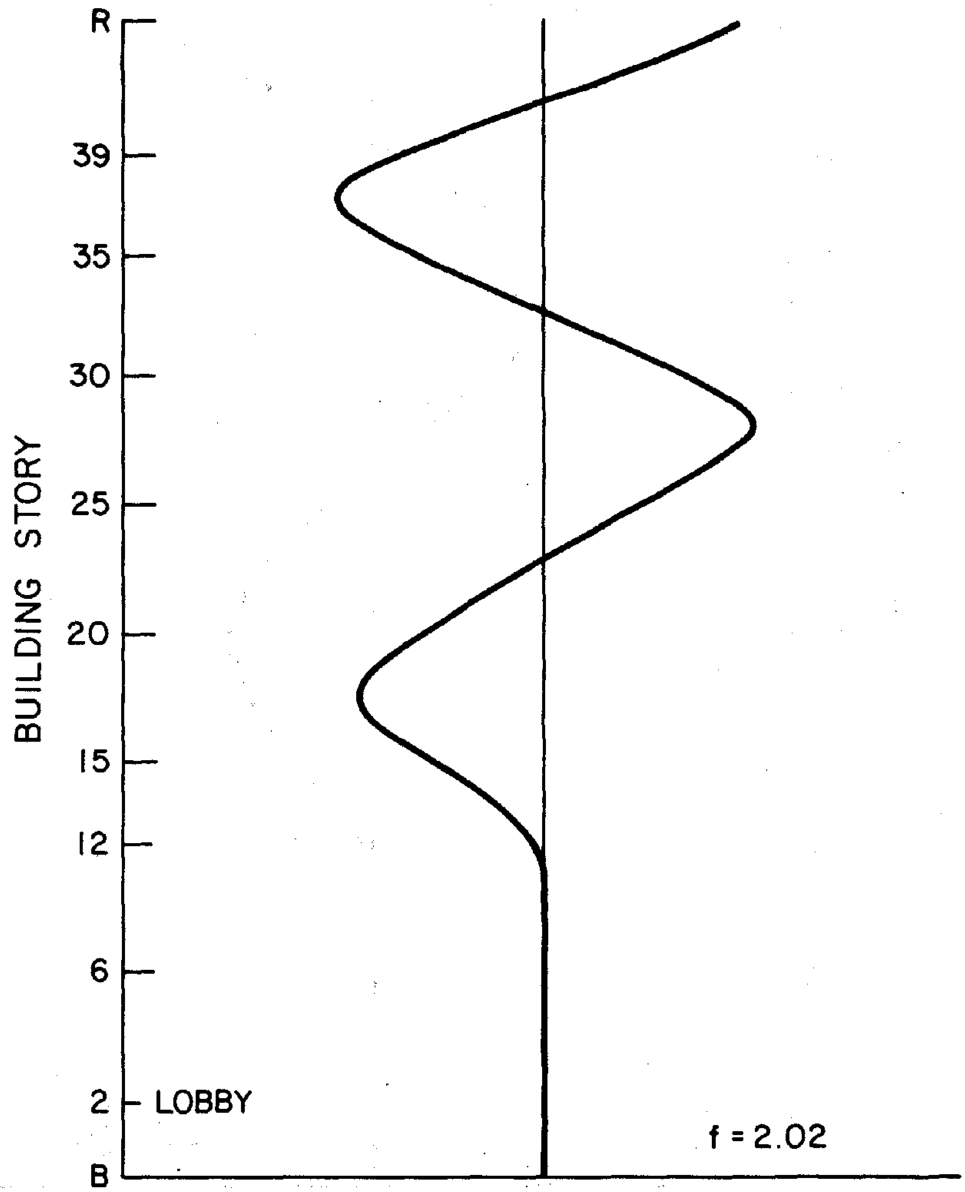

FIG. 6.12 FOURTH TORSIONAL MODE SHAPE

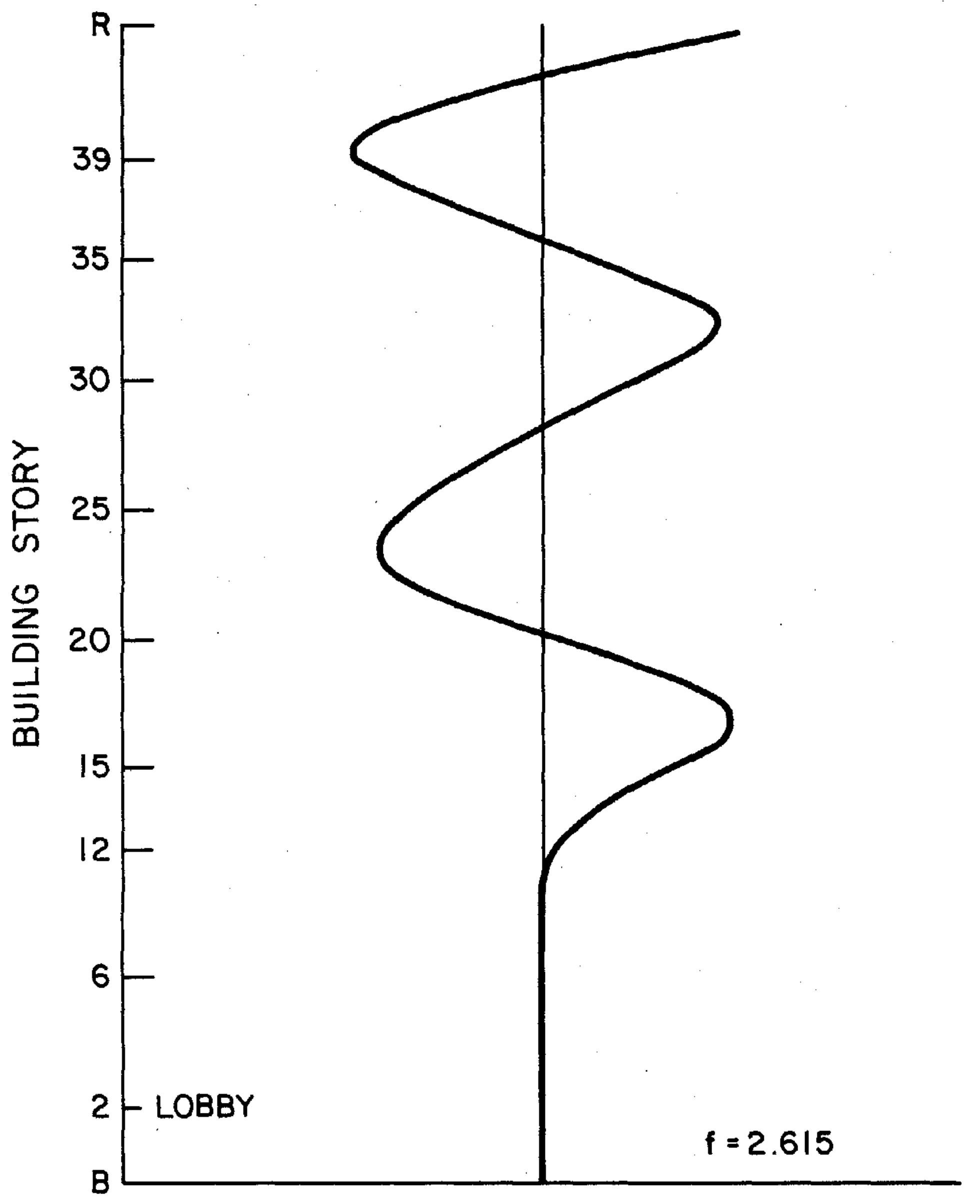

FIG. 6.13 FIFTH TORSIONAL MODE SHAPE

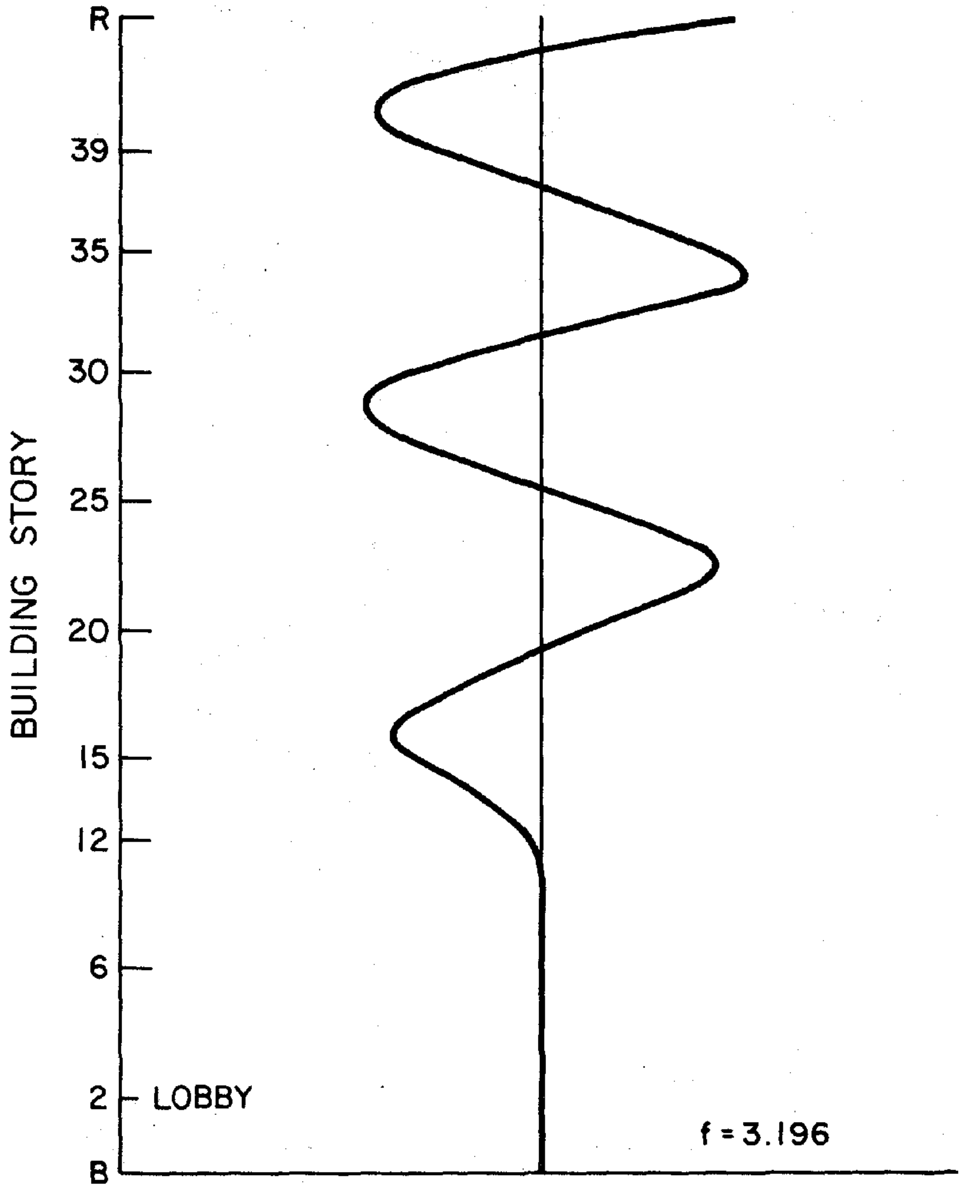

FIG. 6.14 SIXTH TORSIONAL MODE SHAPE

7. COMPARISON OF EXPERIMENTAL AND ANALYTICAL RESULTS

The resonant frequencies and damping factors obtained from the full-scale tests are summarized and compared in Table 7.1. The analytical results for the E-W translation with the fixed base and the N-S translation with the fixed and flexible base are listed. The mode shapes for the translational as well as the torsional motions are compared in Fig. 7.1. The analytical translational mode plotted is for the flexible base whereas the torsional analytical mode is for the fixed base model.

A comparison of the translational analytical flexible base model results show good agreement with the experimental studies. The fixed base analytical results vary up to about 8% of the experimental translational results. Even with the flexible base model, it would appear that the model is somewhat stiffer than the actual building. In comparing the torsional analytical results, which were for a fixed base model, with the experimental results, the actual building indicates a much more flexible structure.

TABLE 7.1 COMPARISON OF RESONANT FREQUENCIES AND DAMPING FACTORS

Mode No.	Translational E-W				
	Forced		Ambient		Analysis Fixed Base
	f (Hz)	ξ (%)	f (Hz)	ξ (%)	f (Hz)
1	0.232	1.7	0.234	1.9	0.245
2	0.755	2.7	0.762	1.1	0.721
3	1.385	2.2	1.41	3.0	1.248
4	1.87	2.9	1.98	1.3	1.757
5	2.21	2.0	2.29	1.7	2.275
6	2.68	3.0	2.85	0.7	2.764

Mode No.	Translational N-S					
	Forced		Ambient		Analysis Fixed Base	Analysis Flexible Base
	f (Hz)	ξ (%)	f (Hz)	ξ (%)	f (Hz)	f (Hz)
1	0.225	6.6	0.225	2.2	0.243	0.223
2	0.720	2.6	0.732	1.5	0.719	0.700
3	1.32	1.9	1.35	1.8	1.240	1.196
4	1.81	2.1	1.87	1.1	1.751	1.695
5	2.14	1.6	2.16	1.1	2.26	2.143
6	2.62	2.8	2.76	1.0	2.74	2.536

Mode No.	Torsional				
	Forced		Ambient		Analysis Fixed Base
	f (Hz)	ξ (%)	f (Hz)	ξ (%)	f (Hz)
1	0.377	2.5	0.381	3.3	0.322
2	1.055	1.0	1.07	1.6	0.857
3	1.86	1.6	1.86	1.7	1.439
4	2.60	2.0	2.64	1.4	2.02
5	3.32	2.0	3.47	0.6	2.615
					3.196

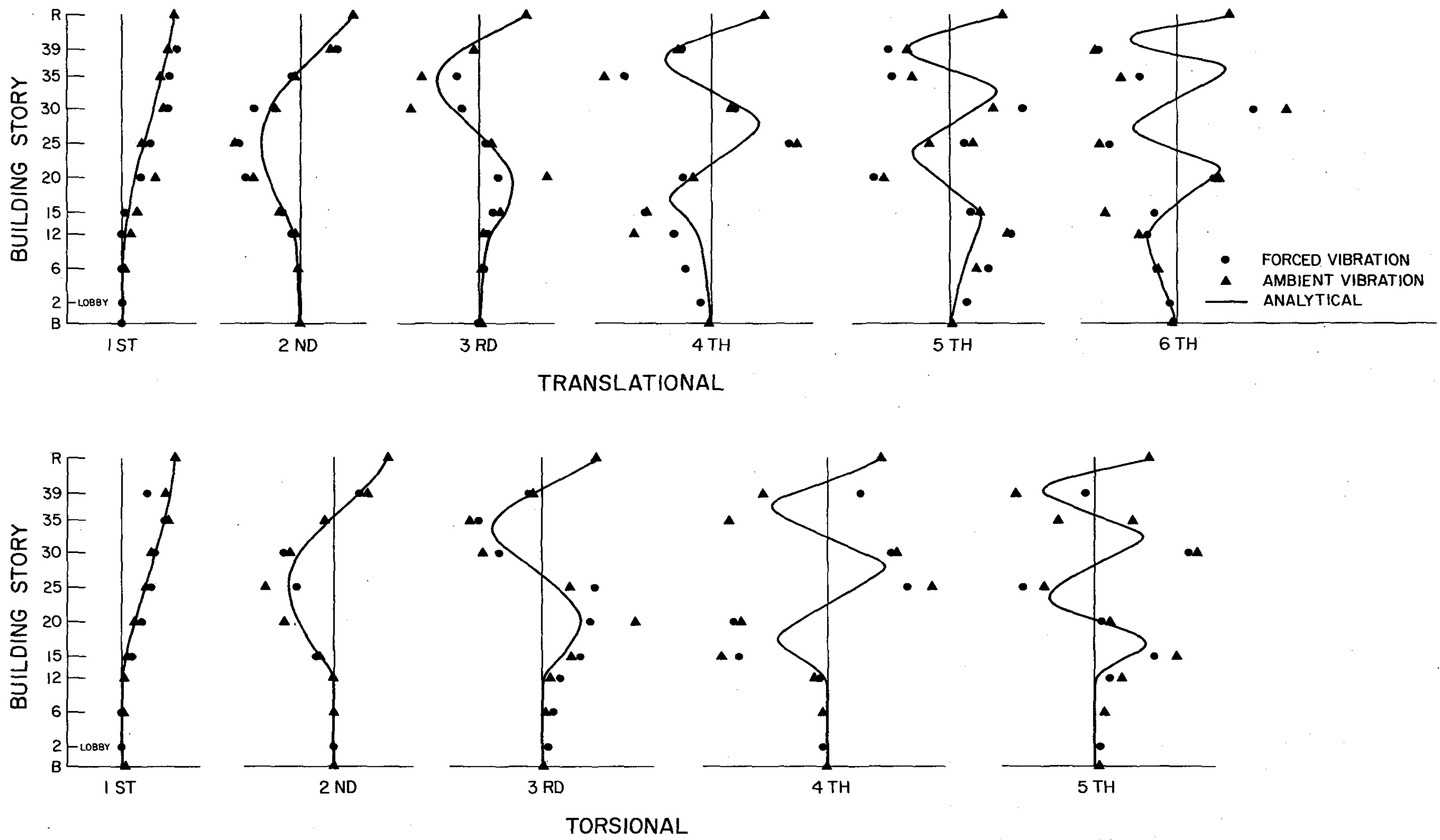

FIG. 7.1 TYPICAL MODE SHAPES

8. GENERAL CONCLUSIONS

The dynamic properties of the translational modes in the N-S and E-W directions as well as the torsional modes of the Rainer Tower Building were determined by forced vibration and ambient vibration studies.

The resonant frequencies from both studies are in very good agreement in all separated modes of vibration. The ratios of the observed higher mode frequencies with respect to the fundamental one from both dynamic studies of the building indicate that the overall structural response is predominantly of the shear type.

Comparison of the forced and ambient vibration experiments demonstrates that it is possible to determine with adequate accuracy the natural frequencies and mode shapes of typical modern buildings using the ambient vibration method. Difficulties in evaluation of equivalent viscous damping factors from ambient vibration studies are present, and it would probably be more realistic from this type of study to expect assessment of the range of damping factors rather than damping values associated with each mode of vibration.

A comparison of the analytical results with the experimental results shows good agreement in the translational motion, especially when a flexible base was incorporated into the model.

REFERENCES

1. Bouwkamp, J. G. and Rea, Dixon, "Dynamic Testing and Formulation of Mathematical Models," Chapter VIII in Earthquake Engineering, R. L. Wiegel, Editor, Prentice-Hall, 1970.

2. Caughey, T. K., "Classical Normal Modes in Damped Linear Systems," J. Appl. Mech., 27, 1960, pp. 269-271.

3. Clough, R. W. and Penzien, J., Dynamics of Structures, McGraw-Hill, 1975.

4. Cooley, J. W. and Tukey, J. W., "An Algorithm for the Machine Calculation of Complex Fourier Series," Math. of Comp., 19, pp. 297-301.

5. Crawford, R. and Ward, H. S., "Determination of the National Periods of Buildings," Bull. Seis. Soc. Am., 54, 1964, pp. 1743-1756.

6. Horner, J. B. and Jennings, P. C., "Modal Interference in Vibration Tests," J. Engrg. Mech. Div., Proc. ASCE, 95, EM4, 1965, pp. 827-839.

7. Hudson, D. E., "Synchronized Vibration Generators for Dynamic Tests of Full Scale Structures," Earthquake Engineering Research Laboratory Report, California Institute of Technology, Pasadena, 1962.

8. Kawasumi, K. and Kanai, K., "Small Amplitude Vibration of Actual Buildings," Proc. First World Conf. Earthquake Eng., Berkeley, 1956.

9. McLamore, V. R., "Ambient Vibration Survey of Chesapeake Bay Bridge," Teledyne Gestronics, Rep. No. 0370-2150, 1970.

10. Petrovski, J. and Jurukovski, D., "Dynamic Properties of Structures From Full-Scale Forced Vibration Studies and Formulation of Mathematical Models," UNESCO Interregional Seminar on Low Cost Construction Resistant to Earthquake and Hurricanes, Skopje, November 1971.

11. Petrovski, J., Jurukovski, D. and Percinkov, S., "Dynamic Properties of Multistory Trade Building and Formulation of the Mathematical Model," Publ. No. 24, Institute of Earthquake Engineering and Engineering Seismology, University of Skopje, 1971.

12. Rea, D., Bouwkamp, J. G. and Clough, R. W., "The Dynamic Behavior of Still Frame and Truss Buildings," AISI, Bull. No. 9, April 1968.

13. Stephen, R. M., Hollings, J. P. and Bouwkamp, J. G., "Dynamic Behavior of a Multistory Pyramid-Shaped Building," Report No. EERC 73-17, Earthquake Engineering Research Center, University of California, Berkeley, 1973.

14. Trifunac, M. D., "Wind and Microtremor Induced Vibrations of a Twenty-Two Story Steel Frame Building," Earthquake Engineering Research Laboratory, EERL 70-10, California Institute of Technology, Pasadena, 1970.

15. Trifunac, M. D., "Comparisons Between Ambient and Forced Vibration Experiments," Earthquake Engineering and Structural Dynamics, 1, 1972, pp. 133-150.

16. U. S. Coast and Geodetic Survey, "Earthquake Investigations in California, 1934-1935," Special Publication No. 201, U. S. Dept. of Commerce, Washington, D.C., 1936.

17. Ward, H. S. and Crawford, R., "Wind Induced Vibrations and Building Modes," Bull. Seism. Soc. Am., 56, 1966, pp. 793-813.

18. Wilson, E. L., Bathe, K. J., Peterson, F. E. and Dovey, H. H., "Computer Program for Static and Dynamic Analysis of Linear Structural Systems," Earthquake Engineering Research Center, Report No. EERC 72-10, November 1972.

19. Petrovski, J., Stephen, R. M., Gartenbaum, E., and Bouwkamp, J. G., "Dynamic Behavior of a Multistory Triangular-Shaped Building," Earthquake Engineering Research Center, Report No. EERC 76-3, October 1976.

20. Bathe, K. J., Wilson, E. L. and Peterson, F. E., "SAPIV - A Structural Analysis Program for Static and Dynamic Response of Linear Systems," Earthquake Engineering Research Center, Report No. EERC 73-11, Revised April 1974.

21. Wilson, E. L. and Dovey, H. H., "Three-Dimensional Analysis of Building Systems - TABS," Earthquake Engineering Research Center, Report No. EERC 72-8, December 1972.

EARTHQUAKE ENGINEERING RESEARCH CENTER REPORTS

EARTHQUAKE ENGINEERING RESEARCH CENTER REPORTS

NOTE: Numbers in parenthesis are Accession Numbers assigned by the National Technical Information Service; these are followed by a price code. Copies of the reports may be ordered from the National Technical Information Service, 5285 Port Royal Road, Springfield, Virginia, 22161. Accession Numbers should be quoted on orders for reports (PB --- ---) and remittance must accompany each order. Reports without this information were not available at time of printing. Upon request, EERC will mail inquirers this information when it becomes available.

EERC 67-1 "Feasibility Study Large-Scale Earthquake Simulator Facility," by J. Penzien, J.G. Bouwkamp, R.W. Clough and D. Rea - 1967 (PB 187 905)A07

EERC 68-1 Unassigned

EERC 68-2 "Inelastic Behavior of Beam-to-Column Subassemblages Under Repeated Loading," by V.V. Bertero - 1968 (PB 184 888)A05

EERC 68-3 "A Graphical Method for Solving the Wave Reflection-Refraction Problem," by H.D. McNiven and Y. Mengi - 1968 (PB 187 943)A03

EERC 68-4 "Dynamic Properties of McKinley School Buildings," by D. Rea, J.G. Bouwkamp and R.W. Clough - 1968 (PB 187 902)A07

EERC 68-5 "Characteristics of Rock Motions During Earthquakes," by H.B. Seed, I.M. Idriss and F.W. Kiefer - 1968 (PB 188 338)A03

EERC 69-1 "Earthquake Engineering Research at Berkeley," - 1969 (PB 187 906)A11

EERC 69-2 "Nonlinear Seismic Response of Earth Structures," by M. Dibaj and J. Penzien - 1969 (PB 187 904)A08

EERC 69-3 "Probabilistic Study of the Behavior of Structures During Earthquakes," by R. Ruiz and J. Penzien - 1969 (PB 187 886)A06

EERC 69-4 "Numerical Solution of Boundary Value Problems in Structural Mechanics by Reduction to an Initial Value Formulation," by N. Distefano and J. Schujman - 1969 (PB 187 942)A02

EERC 69-5 "Dynamic Programming and the Solution of the Biharmonic Equation," by N. Distefano - 1969 (PB 187 941)A03

EERC 69-6 "Stochastic Analysis of Offshore Tower Structures," by A.K. Malhotra and J. Penzien - 1969 (PB 187 903)A09

EERC 69-7 "Rock Motion Accelerograms for High Magnitude Earthquakes," by H.B. Seed and I.M. Idriss - 1969 (PB 187 940)A02

EERC 69-8 "Structural Dynamics Testing Facilities at the University of California, Berkeley," by R.M. Stephen, J.G. Bouwkamp, R.W. Clough and J. Penzien - 1969 (PB 189 111)A04

EERC 69-9 "Seismic Response of Soil Deposits Underlain by Sloping Rock Boundaries," by H. Dezfulian and H.B. Seed 1969 (PB 189 114)A03

EERC 69-10 "Dynamic Stress Analysis of Axisymmetric Structures Under Arbitrary Loading," by S. Ghosh and E.L. Wilson 1969 (PB 189 026)A10

EERC 69-11 "Seismic Behavior of Multistory Frames Designed by Different Philosophies," by J.C. Anderson and V. V. Bertero - 1969 (PB 190 662)A10

EERC 69-12 "Stiffness Degradation of Reinforcing Concrete Members Subjected to Cyclic Flexural Moments," by V.V. Bertero, B. Bresler and H. Ming Liao - 1969 (PB 202 942)A07

EERC 69-13 "Response of Non-Uniform Soil Deposits to Travelling Seismic Waves," by H. Dezfulian and H.B. Seed - 1969 (PB 191 023)A03

EERC 69-14 "Damping Capacity of a Model Steel Structure," by D. Rea, R.W. Clough and J.G. Bouwkamp - 1969 (PB 190 663)A06

EERC 69-15 "Influence of Local Soil Conditions on Building Damage Potential during Earthquakes," by H.B. Seed and I.M. Idriss - 1969 (PB 191 036)A03

EERC 69-16 "The Behavior of Sands Under Seismic Loading Conditions," by M.L. Silver and H.B. Seed - 1969 (AD 714 982)A07

EERC 70-1 "Earthquake Response of Gravity Dams," by A.K. Chopra - 1970 (AD 709 640)A03

EERC 70-2 "Relationships between Soil Conditions and Building Damage in the Caracas Earthquake of July 29, 1967," by H.B. Seed, I.M. Idriss and H. Dezfulian - 1970 (PB 195 762)A05

EERC 70-3 "Cyclic Loading of Full Size Steel Connections," by E.P. Popov and R.M. Stephen - 1970 (PB 213 545)A04

EERC 70-4 "Seismic Analysis of the Charaima Building, Caraballeda, Venezuela," by Subcommittee of the SEAONC Research Committee: V.V. Bertero, P.F. Fratessa, S.A. Mahin, J.H. Sexton, A.C. Scordelis, E.L. Wilson, L.A. Wyllie, H.B. Seed and J. Penzien, Chairman - 1970 (PB 201 455)A06

EERC 70-5 "A Computer Program for Earthquake Analysis of Dams," by A.K. Chopra and P. Chakrabarti - 1970 (AD 723 994)A05

EERC 70-6 "The Propagation of Love Waves Across Non-Horizontally Layered Structures," by J. Lysmer and L.A. Drake 1970 (PB 197 896)A03

EERC 70-7 "Influence of Base Rock Characteristics on Ground Response," by J. Lysmer, H.B. Seed and P.B. Schnabel 1970 (PB 197 897)A03

EERC 70-8 "Applicability of Laboratory Test Procedures for Measuring Soil Liquefaction Characteristics under Cyclic Loading," by H.B. Seed and W.H. Peacock - 1970 (PB 198 016)A03

EERC 70-9 "A Simplified Procedure for Evaluating Soil Liquefaction Potential," by H.B. Seed and I.M. Idriss - 1970 (PB 198 009)A03

EERC 70-10 "Soil Moduli and Damping Factors for Dynamic Response Analysis," by H.B. Seed and I.M. Idriss - 1970 (PB 197 869)A03

EERC 71-1 "Koyna Earthquake of December 11, 1967 and the Performance of Koyna Dam," by A.K. Chopra and P. Chakrabarti 1971 (AD 731 496)A06

EERC 71-2 "Preliminary In-Situ Measurements of Anelastic Absorption in Soils Using a Prototype Earthquake Simulator," by R.D. Borcherdt and P.W. Rodgers - 1971 (PB 201 454)A03

EERC 71-3 "Static and Dynamic Analysis of Inelastic Frame Structures," by F.L. Porter and G.H. Powell - 1971 (PB 210 135)A06

EERC 71-4 "Research Needs in Limit Design of Reinforced Concrete Structures," by V.V. Bertero - 1971 (PB 202 943)A04

EERC 71-5 "Dynamic Behavior of a High-Rise Diagonally Braced Steel Building," by D. Rea, A.A. Shah and J.G. Bouwkamp 1971 (PB 203 584)A06

EERC 71-6 "Dynamic Stress Analysis of Porous Elastic Solids Saturated with Compressible Fluids," by J. Ghaboussi and E. L. Wilson - 1971 (PB 211 396)A06

EERC 71-7 "Inelastic Behavior of Steel Beam-to-Column Subassemblages," by H. Krawinkler, V.V. Bertero and E.P. Popov 1971 (PB 211 335)A14

EERC 71-8 "Modification of Seismograph Records for Effects of Local Soil Conditions," by P. Schnabel, H.B. Seed and J. Lysmer - 1971 (PB 214 450)A03

EERC 72-1 "Static and Earthquake Analysis of Three Dimensional Frame and Shear Wall Buildings," by E.L. Wilson and H.H. Dovey - 1972 (PB 212 904)A05

EERC 72-2 "Accelerations in Rock for Earthquakes in the Western United States," by P.B. Schnabel and H.B. Seed - 1972 (PB 213 100)A03

EERC 72-3 "Elastic-Plastic Earthquake Response of Soil-Building Systems," by T. Minami - 1972 (PB 214 868)A08

EERC 72-4 "Stochastic Inelastic Response of Offshore Towers to Strong Motion Earthquakes," by M.K. Kaul - 1972 (PB 215 713)A05

EERC 72-5 "Cyclic Behavior of Three Reinforced Concrete Flexural Members with High Shear," by E.P. Popov, V.V. Bertero and H. Krawinkler - 1972 (PB 214 555)A05

EERC 72-6 "Earthquake Response of Gravity Dams Including Reservoir Interaction Effects," by P. Chakrabarti and A.K. Chopra - 1972 (AD 762 330)A08

EERC 72-7 "Dynamic Properties of Pine Flat Dam," by D. Rea, C.Y. Liaw and A.K. Chopra - 1972 (AD 763 928)A05

EERC 72-8 "Three Dimensional Analysis of Building Systems," by E.L. Wilson and H.H. Dovey - 1972 (PB 222 438)A06

EERC 72-9 "Rate of Loading Effects on Uncracked and Repaired Reinforced Concrete Members," by S. Mahin, V.V. Bertero, D. Rea and M. Atalay - 1972 (PB 224 520)A08

EERC 72-10 "Computer Program for Static and Dynamic Analysis of Linear Structural Systems," by E.L. Wilson, K.-J. Bathe, J.E. Peterson and H.H.Dovey - 1972 (PB 220 437)A04

EERC 72-11 "Literature Survey - Seismic Effects on Highway Bridges," by T. Iwasaki, J. Penzien and R.W. Clough - 1972 (PB 215 613)A19

EERC 72-12 "SHAKE-A Computer Program for Earthquake Response Analysis of Horizontally Layered Sites," by P.B. Schnabel and J. Lysmer - 1972 (PB 220 207)A06

EERC 73-1 "Optimal Seismic Design of Multistory Frames," by V.V. Bertero and H. Kamil - 1973

EERC 73-2 "Analysis of the Slides in the San Fernando Dams During the Earthquake of February 9, 1971," by H.B. Seed, K.L. Lee, I.M. Idriss and F. Makdisi - 1973 (PB 223 402)A14

EERC 73-3 "Computer Aided Ultimate Load Design of Unbraced Multistory Steel Frames," by M.B. El-Hafez and G.H. Powell 1973 (PB 248 315)A09

EERC 73-4 "Experimental Investigation into the Seismic Behavior of Critical Regions of Reinforced Concrete Components as Influenced by Moment and Shear," by M. Celebi and J. Penzien - 1973 (PB 215 884)A09

EERC 73-5 "Hysteretic Behavior of Epoxy-Repaired Reinforced Concrete Beams," by M. Celebi and J. Penzien - 1973 (PB 239 568)A03

EERC 73-6 "General Purpose Computer Program for Inelastic Dynamic Response of Plane Structures," by A. Kanaan and G.H. Powell - 1973 (PB 221 260)A08

EERC 73-7 "A Computer Program for Earthquake Analysis of Gravity Dams Including Reservoir Interaction," by P. Chakrabarti and A.K. Chopra - 1973 (AD 766 271)A04

EERC 73-8 "Behavior of Reinforced Concrete Deep Beam-Column Subassemblages Under Cyclic Loads," by O. Küstü and J.G. Bouwkamp - 1973 (PB 246 117)A12

EERC 73-9 "Earthquake Analysis of Structure-Foundation Systems," by A.K. Vaish and A.K. Chopra - 1973 (AD 766 272)A07

EERC 73-10 "Deconvolution of Seismic Response for Linear Systems," by R.B. Reimer - 1973 (PB 227 179)A08

EERC 73-11 "SAP IV: A Structural Analysis Program for Static and Dynamic Response of Linear Systems," by K.-J. Bathe, E.L. Wilson and F.E. Peterson - 1973 (PB 221 967)A09

EERC 73-12 "Analytical Investigations of the Seismic Response of Long, Multiple Span Highway Bridges," by W.S. Tseng and J. Penzien - 1973 (PB 227 816)A10

EERC 73-13 "Earthquake Analysis of Multi-Story Buildings Including Foundation Interaction," by A.K. Chopra and J.A. Gutierrez - 1973 (PB 222 970)A03

EERC 73-14 "ADAP: A Computer Program for Static and Dynamic Analysis of Arch Dams," by R.W. Clough, J.M. Raphael and S. Mojtahedi - 1973 (PB 223 763)A09

EERC 73-15 "Cyclic Plastic Analysis of Structural Steel Joints," by R.B. Pinkney and R.W. Clough - 1973 (PB 226 843)A08

EERC 73-16 "QUAD-4: A Computer Program for Evaluating the Seismic Response of Soil Structures by Variable Damping Finite Element Procedures," by I.M. Idriss, J. Lysmer, R. Hwang and H.B. Seed - 1973 (PB 229 424)A05

EERC 73-17 "Dynamic Behavior of a Multi-Story Pyramid Shaped Building," by R.M. Stephen, J.P. Hollings and J.G. Bouwkamp - 1973 (PB 240 718)A06

EERC 73-18 "Effect of Different Types of Reinforcing on Seismic Behavior of Short Concrete Columns," by V.V. Bertero, J. Hollings, O. Küstü, R.M. Stephen and J.G. Bouwkamp - 1973

EERC 73-19 "Olive View Medical Center Materials Studies, Phase I," by B. Bresler and V.V. Bertero - 1973 (PB 235 986)A06

EERC 73-20 "Linear and Nonlinear Seismic Analysis Computer Programs for Long Multiple-Span Highway Bridges," by W.S. Tseng and J. Penzien - 1973

EERC 73-21 "Constitutive Models for Cyclic Plastic Deformation of Engineering Materials," by J.M. Kelly and P.P. Gillis 1973 (PB 226 024)A03

EERC 73-22 "DRAIN - 2D User's Guide," by G.H. Powell - 1973 (PB 227 016)A05

EERC 73-23 "Earthquake Engineering at Berkeley - 1973," (PB 226 033)A11

EERC 73-24 Unassigned

EERC 73-25 "Earthquake Response of Axisymmetric Tower Structures Surrounded by Water," by C.Y. Liaw and A.K. Chopra 1973 (AD 773 052)A09

EERC 73-26 "Investigation of the Failures of the Olive View Stairtowers During the San Fernando Earthquake and Their Implications on Seismic Design," by V.V. Bertero and R.G. Collins - 1973 (PB 235 106)A13

EERC 73-27 "Further Studies on Seismic Behavior of Steel Beam-Column Subassemblages," by V.V. Bertero, H. Krawinkler and E.P. Popov - 1973 (PB 234 172)A06

EERC 74-1 "Seismic Risk Analysis," by C.S. Oliveira - 1974 (PB 235 920)A06

EERC 74-2 "Settlement and Liquefaction of Sands Under Multi-Directional Shaking," by R. Pyke, C.K. Chan and H.B. Seed 1974

EERC 74-3 "Optimum Design of Earthquake Resistant Shear Buildings," by D. Ray, K.S. Pister and A.K. Chopra - 1974 (PB 231 172)A06

EERC 74-4 "LUSH - A Computer Program for Complex Response Analysis of Soil-Structure Systems," by J. Lysmer, T. Udaka, H.B. Seed and R. Hwang - 1974 (PB 236 796)A05

EERC 74-5 "Sensitivity Analysis for Hysteretic Dynamic Systems: Applications to Earthquake Engineering," by D. Ray 1974 (PB 233 213)A06

EERC 74-6 "Soil Structure Interaction Analyses for Evaluating Seismic Response," by H.B. Seed, J. Lysmer and R. Hwang 1974 (PB 236 519)A04

EERC 74-7 Unassigned

EERC 74-8 "Shaking Table Tests of a Steel Frame - A Progress Report," by R.W. Clough and D. Tang - 1974 (PB 240 869)A03

EERC 74-9 "Hysteretic Behavior of Reinforced Concrete Flexural Members with Special Web Reinforcement," by V.V. Bertero, E.P. Popov and T.Y. Wang - 1974 (PB 236 797)A07

EERC 74-10 "Applications of Reliability-Based, Global Cost Optimization to Design of Earthquake Resistant Structures," by E. Vitiello and K.S. Pister - 1974 (PB 237 231)A06

EERC 74-11 "Liquefaction of Gravelly Soils Under Cyclic Loading Conditions," by R.T. Wong, H.B. Seed and C.K. Chan 1974 (PB 242 042)A03

EERC 74-12 "Site-Dependent Spectra for Earthquake-Resistant Design," by H.B. Seed, C. Ugas and J. Lysmer - 1974 (PB 240 953)A03

EERC 74-13 "Earthquake Simulator Study of a Reinforced Concrete Frame," by P. Hidalgo and R.W. Clough - 1974 (PB 241 944)A13

EERC 74-14 "Nonlinear Earthquake Response of Concrete Gravity Dams," by N. Pal - 1974 (AD/A 006 583)A06

EERC 74-15 "Modeling and Identification in Nonlinear Structural Dynamics - I. One Degree of Freedom Models," by N. Distefano and A. Rath - 1974 (PB 241 548)A06

EERC 75-1 "Determination of Seismic Design Criteria for the Dumbarton Bridge Replacement Structure, Vol. I: Description, Theory and Analytical Modeling of Bridge and Parameters," by F. Baron and S.-H. Pang - 1975 (PB 259 407)A15

EERC 75-2 "Determination of Seismic Design Criteria for the Dumbarton Bridge Replacement Structure, Vol. II: Numerical Studies and Establishment of Seismic Design Criteria," by F. Baron and S.-H. Pang - 1975 (PB 259 408)A11 (For set of EERC 75-1 and 75-2 (PB 259 406))

EERC 75-3 "Seismic Risk Analysis for a Site and a Metropolitan Area," by C.S. Oliveira - 1975 (PB 248 134)A09

EERC 75-4 "Analytical Investigations of Seismic Response of Short, Single or Multiple-Span Highway Bridges," by M.-C. Chen and J. Penzien - 1975 (PB 241 454)A09

EERC 75-5 "An Evaluation of Some Methods for Predicting Seismic Behavior of Reinforced Concrete Buildings," by S.A. Mahin and V.V. Bertero - 1975 (PB 246 306)A16

EERC 75-6 "Earthquake Simulator Study of a Steel Frame Structure, Vol. I: Experimental Results," by R.W. Clough and D.T. Tang - 1975 (PB 243 981)A13

EERC 75-7 "Dynamic Properties of San Bernardino Intake Tower," by D. Rea, C.-Y. Liaw and A.K. Chopra - 1975 (AD/A008 406) A05

EERC 75-8 "Seismic Studies of the Articulation for the Dumbarton Bridge Replacement Structure, Vol. I: Description, Theory and Analytical Modeling of Bridge Components," by F. Baron and R.E. Hamati - 1975 (PB 251 539)A07

EERC 75-9 "Seismic Studies of the Articulation for the Dumbarton Bridge Replacement Structure, Vol. 2: Numerical Studies of Steel and Concrete Girder Alternates," by F. Baron and R.E. Hamati - 1975 (PB 251 540)A10

EERC 75-10 "Static and Dynamic Analysis of Nonlinear Structures," by D.P. Mondkar and G.H. Powell - 1975 (PB 242 434)A08

EERC 75-11 "Hysteretic Behavior of Steel Columns," by E.P. Popov, V.V. Bertero and S. Chandramouli - 1975 (PB 252 365)A11

EERC 75-12 "Earthquake Engineering Research Center Library Printed Catalog," - 1975 (PB 243 711)A26

EERC 75-13 "Three Dimensional Analysis of Building Systems (Extended Version)," by E.L. Wilson, J.P. Hollings and H.H. Dovey - 1975 (PB 243 989)A07

EERC 75-14 "Determination of Soil Liquefaction Characteristics by Large-Scale Laboratory Tests," by P. De Alba, C.K. Chan and H.B. Seed - 1975 (NUREG 0027)A08

EERC 75-15 "A Literature Survey - Compressive, Tensile, Bond and Shear Strength of Masonry," by R.L. Mayes and R.W. Clough - 1975 (PB 246 292)A10

EERC 75-16 "Hysteretic Behavior of Ductile Moment Resisting Reinforced Concrete Frame Components," by V.V. Bertero and E.P. Popov - 1975 (PB 246 388)A05

EERC 75-17 "Relationships Between Maximum Acceleration, Maximum Velocity, Distance from Source, Local Site Conditions for Moderately Strong Earthquakes," by H.B. Seed, R. Murarka, J. Lysmer and I.M. Idriss - 1975 (PB 248 172)A03

EERC 75-18 "The Effects of Method of Sample Preparation on the Cyclic Stress-Strain Behavior of Sands," by J. Mulilis, C.K. Chan and H.B. Seed - 1975 (Summarized in EERC 75-28)

EERC 75-19 "The Seismic Behavior of Critical Regions of Reinforced Concrete Components as Influenced by Moment, Shear and Axial Force," by M.B. Atalay and J. Penzien - 1975 (PB 258 842)A11

EERC 75-20 "Dynamic Properties of an Eleven Story Masonry Building," by R.M. Stephen, J.P. Hollings, J.G. Bouwkamp and D. Jurukovski - 1975 (PB 246 945)A04

EERC 75-21 "State-of-the-Art in Seismic Strength of Masonry - An Evaluation and Review," by R.L. Mayes and R.W. Clough 1975 (PB 249 040)A07

EERC 75-22 "Frequency Dependent Stiffness Matrices for Viscoelastic Half-Plane Foundations," by A.K. Chopra, P. Chakrabarti and G. Dasgupta - 1975 (PB 248 121)A07

EERC 75-23 "Hysteretic Behavior of Reinforced Concrete Framed Walls," by T.Y. Wong, V.V. Bertero and E.P. Popov - 1975

EERC 75-24 "Testing Facility for Subassemblages of Frame-Wall Structural Systems," by V.V. Bertero, E.P. Popov and T. Endo - 1975

EERC 75-25 "Influence of Seismic History on the Liquefaction Characteristics of Sands," by H.B. Seed, K. Mori and C.K. Chan - 1975 (Summarized in EERC 75-28)

EERC 75-26 "The Generation and Dissipation of Pore Water Pressures during Soil Liquefaction," by H.B. Seed, P.P. Martin and J. Lysmer - 1975 (PB 252 648)A03

EERC 75-27 "Identification of Research Needs for Improving Aseismic Design of Building Structures," by V.V. Bertero 1975 (PB 248 136)A05

EERC 75-28 "Evaluation of Soil Liquefaction Potential during Earthquakes," by H.B. Seed, I. Arango and C.K. Chan - 1975 (NUREG 0026)A13

EERC 75-29 "Representation of Irregular Stress Time Histories by Equivalent Uniform Stress Series in Liquefaction Analyses," by H.B. Seed, I.M. Idriss, F. Makdisi and N. Banerjee - 1975 (PB 252 635)A03

EERC 75-30 "FLUSH - A Computer Program for Approximate 3-D Analysis of Soil-Structure Interaction Problems," by J. Lysmer, T. Udaka, C.-F. Tsai and H.B. Seed - 1975 (PB 259 332)A07

EERC 75-31 "ALUSH - A Computer Program for Seismic Response Analysis of Axisymmetric Soil-Structure Systems," by E. Berger, J. Lysmer and H.B. Seed - 1975

EERC 75-32 "TRIP and TRAVEL - Computer Programs for Soil-Structure Interaction Analysis with Horizontally Travelling Waves," by T. Udaka, J. Lysmer and H.B. Seed - 1975

EERC 75-33 "Predicting the Performance of Structures in Regions of High Seismicity," by J. Penzien - 1975 (PB 248 130)A03

EERC 75-34 "Efficient Finite Element Analysis of Seismic Structure - Soil - Direction," by J. Lysmer, H.B. Seed, T. Udaka, R.N. Hwang and C.-F. Tsai - 1975 (PB 253 570)A03

EERC 75-35 "The Dynamic Behavior of a First Story Girder of a Three-Story Steel Frame Subjected to Earthquake Loading," by R.W. Clough and L.-Y. Li - 1975 (PB 248 841)A05

EERC 75-36 "Earthquake Simulator Study of a Steel Frame Structure, Volume II - Analytical Results," by D.T. Tang - 1975 (PB 252 926)A10

EERC 75-37 "ANSR-I General Purpose Computer Program for Analysis of Non-Linear Structural Response," by D.P. Mondkar and G.H. Powell - 1975 (PB 252 386)A08

EERC 75-38 "Nonlinear Response Spectra for Probabilistic Seismic Design and Damage Assessment of Reinforced Concrete Structures," by M. Murakami and J. Penzien - 1975 (PB 259 530)A05

EERC 75-39 "Study of a Method of Feasible Directions for Optimal Elastic Design of Frame Structures Subjected to Earthquake Loading," by N.D. Walker and K.S. Pister - 1975 (PB 257 781)A06

EERC 75-40 "An Alternative Representation of the Elastic-Viscoelastic Analogy," by G. Dasgupta and J.L. Sackman - 1975 (PB 252 173)A03

EERC 75-41 "Effect of Multi-Directional Shaking on Liquefaction of Sands," by H.B. Seed, R. Pyke and G.R. Martin - 1975 (PB 258 781)A03

EERC 76-1 "Strength and Ductility Evaluation of Existing Low-Rise Reinforced Concrete Buildings - Screening Method," by T. Okada and B. Bresler - 1976 (PB 257 906)A11

EERC 76-2 "Experimental and Analytical Studies on the Hysteretic Behavior of Reinforced Concrete Rectangular and T-Beams," by S.-Y.M. Ma, E.P. Popov and V.V. Bertero - 1976 (PB 260 843)A12

EERC 76-3 "Dynamic Behavior of a Multistory Triangular-Shaped Building," by J. Petrovski, R.M. Stephen, E. Gartenbaum and J.G. Bouwkamp - 1976

EERC 76-4 "Earthquake Induced Deformations of Earth Dams," by N. Serff and H.B. Seed - 1976

EERC 76-5 "Analysis and Design of Tube-Type Tall Building Structures," by H. de Clercq and G.H. Powell - 1976 (PB 252 220) A10

EERC 76-6 "Time and Frequency Domain Analysis of Three-Dimensional Ground Motions, San Fernando Earthquake," by T. Kubo and J. Penzien (PB 260 556)A11

EERC 76-7 "Expected Performance of Uniform Building Code Design Masonry Structures," by R.L. Mayes, Y. Omote, S.W. Chen and R.W. Clough - 1976

EERC 76-8 "Cyclic Shear Tests on Concrete Masonry Piers," Part I - Test Results," by R.L. Mayes, Y. Omote and R.W. Clough - 1976 (PB 264 424)A06

EERC 76-9 "A Substructure Method for Earthquake Analysis of Structure - Soil Interaction," by J.A. Gutierrez and A.K. Chopra - 1976 (PB 257 783)A08

EERC 76-10 "Stabilization of Potentially Liquefiable Sand Deposits using Gravel Drain Systems," by H.B. Seed and J.R. Booker - 1976 (PB 258 820)A04

EERC 76-11 "Influence of Design and Analysis Assumptions on Computed Inelastic Response of Moderately Tall Frames," by G.H. Powell and D.G. Row - 1976

EERC 76-12 "Sensitivity Analysis for Hysteretic Dynamic Systems: Theory and Applications," by D. Ray, K.S. Pister and E. Polak - 1976 (PB 262 859)A04

EERC 76-13 "Coupled Lateral Torsional Response of Buildings to Ground Shaking," by C.L. Kan and A.K. Chopra - 1976 (PB 257 907)A09

EERC 76-14 "Seismic Analyses of the Banco de America," by V.V. Bertero, S.A. Mahin and J.A. Hollings - 1976

EERC 76-15 "Reinforced Concrete Frame 2: Seismic Testing and Analytical Correlation," by R.W. Clough and J. Gidwani - 1976 (PB 261 323)A08

EERC 76-16 "Cyclic Shear Tests on Masonry Piers, Part II - Analysis of Test Results," by R.L. Mayes, Y. Omote and R.W. Clough - 1976

EERC 76-17 "Structural Steel Bracing Systems: Behavior Under Cyclic Loading," by E.P. Popov, K. Takanashi and C.W. Roeder - 1976 (PB 260 715)A05

EERC 76-18 "Experimental Model Studies on Seismic Response of High Curved Overcrossings," by D. Williams and W.G. Godden - 1976

EERC 76-19 "Effects of Non-Uniform Seismic Disturbances on the Dumbarton Bridge Replacement Structure," by F. Baron and R.E. Hamati - 1976

EERC 76-20 "Investigation of the Inelastic Characteristics of a Single Story Steel Structure Using System Identification and Shaking Table Experiments," by V.C. Matzen and H.D. McNiven - 1976 (PB 258 453)A07

EERC 76-21 "Capacity of Columns with Splice Imperfections," by E.P. Popov, R.M. Stephen and R. Philbrick - 1976 (PB 260 378)A04

EERC 76-22 "Response of the Olive View Hospital Main Building during the San Fernando Earthquake," by S. A. Mahin, R. Collins, A.K. Chopra and V.V. Bertero - 1976

EERC 76-23 "A Study on the Major Factors Influencing the Strength of Masonry Prisms," by N.M. Mostaghel, R.L. Mayes, R. W. Clough and S.W. Chen - 1976

EERC 76-24 "GADFLEA - A Computer Program for the Analysis of Pore Pressure Generation and Dissipation during Cyclic or Earthquake Loading," by J.R. Booker, M.S. Rahman and H.B. Seed - 1976 (PB 263 947)A04

EERC 76-25 "Rehabilitation of an Existing Building: A Case Study," by B. Bresler and J. Axley - 1976

EERC 76-26 "Correlative Investigations on Theoretical and Experimental Dynamic Behavior of a Model Bridge Structure," by K. Kawashima and J. Penzien - 1976 (PB 263 388)A11

EERC 76-27 "Earthquake Response of Coupled Shear Wall Buildings," by T. Srichatrapimuk - 1976 (PB 265 157)A07

EERC 76-28 "Tensile Capacity of Partial Penetration Welds," by E.P. Popov and R.M. Stephen - 1976 (PB 262 899)A03

EERC 76-29 "Analysis and Design of Numerical Integration Methods in Structural Dynamics," by H.M. Hilber - 1976 (PB 264 410)A06

EERC 76-30 "Contribution of a Floor System to the Dynamic Characteristics of Reinforced Concrete Buildings," by L.J. Edgar and V.V. Bertero - 1976

EERC 76-31 "The Effects of Seismic Disturbances on the Golden Gate Bridge," by F. Baron, M. Arikan and R.E. Hamati - 1976

EERC 76-32 "Infilled Frames in Earthquake Resistant Construction," by R.E. Klingner and V.V. Bertero - 1976 (PB 265 892)A13

UCB/EERC-77/01	"PLUSH - A Computer Program for Probabilistic Finite Element Analysis of Seismic Soil-Structure Interaction," by M.P. Romo Organista, J. Lysmer and H.B. Seed - 1977
UCB/EERC-77/02	"Soil-Structure Interaction Effects at the Humboldt Bay Power Plant in the Ferndale Earthquake of June 7, 1975," by J.E. Valera, H.B. Seed, C.F. Tsai and J. Lysmer - 1977 (PB 265 795)A04
UCB/EERC-77/03	"Influence of Sample Disturbance on Sand Response to Cyclic Loading," by K. Mori, H.B. Seed and C.K. Chan - 1977 (PB 267 352)A04
UCB/EERC-77/04	"Seismological Studies of Strong Motion Records," by J. Shoja-Taheri - 1977 (PB 269 655)A10
UCB/EERC-77/05	"Testing Facility for Coupled-Shear Walls," by L. Li-Hyung, V.V. Bertero and E.P. Popov - 1977
UCB/EERC-77/06	"Developing Methodologies for Evaluating the Earthquake Safety of Existing Buildings," by No. 1 - B. Bresler; No. 2 - B. Bresler, T. Okada and D. Zisling; No. 3 - T. Okada and B. Bresler; No. 4 - V.V. Bertero and B. Bresler - 1977 (PB 267 354)A08
UCB/EERC-77/07	"A Literature Survey - Transverse Strength of Masonry Walls," by Y. Omote, R.L. Mayes, S.W. Chen and R.W. Clough - 1977
UCB/EERC-77/08	"DRAIN-TABS: A Computer Program for Inelastic Earthquake Response of Three Dimensional Buildings," by R. Guendelman-Israel and G.H. Powell - 1977 (PB 270 693)A07
UCB/EERC-77/09	"SUBWALL: A Special Purpose Finite Element Computer Program for Practical Elastic Analysis and Design of Structural Walls with Substructure Option," by D.Q. Le, H. Peterson and E.P. Popov - 1977 (PB 270 567)A05
UCB/EERC-77/10	"Experimental Evaluation of Seismic Design Methods for Broad Cylindrical Tanks," by D.P. Clough
UCB/EERC-77/11	"Earthquake Engineering Research at Berkeley - 1976," - 1977
UCB/EERC-77/12	"Automated Design of Earthquake Resistant Multistory Steel Building Frames," by N.D. Walker, Jr. - 1977
UCB/EERC-77/13	"Concrete Confined by Rectangular Hoops Subjected to Axial Loads," by D. Zallnas, V.V. Bertero and E.P. Popov - 1977
UCB/EERC-77/14	"Seismic Strain Induced in the Ground During Earthquakes," by Y. Sugimura - 1977
UCB/EERC-77/15	"Bond Deterioration under Generalized Loading," by V.V. Bertero, E.P. Popov and S. Viwathanatepa - 1977

UCB/EERC-77/16 "Computer Aided Optimum Design of Ductile Reinforced Concrete Moment Resisting Frames," by S.W. Zagajeski and V.V. Bertero - 1977

UCB/EERC-77/17 "Earthquake Simulation Testing of a Stepping Frame with Energy-Absorbing Devices," by J.M. Kelly and D.F. Tsztoo 1977

UCB/EERC-77/18 "Inelastic Behavior of Eccentrically Braced Steel Frames under Cyclic Loadings," by C.W. Roeder and E.P. Popov - 1977

UCB/EERC-77/19 "A Simplified Procedure for Estimating Earthquake-Induced Deformations in Dams and Embankments," by F.I. Makdisi and H.B. Seed - 1977

UCB/EERC-77/20 "The Performance of Earth Dams during Earthquakes," by H.B. Seed, F.I. Makdisi and P. de Alba - 1977

UCB/EERC-77/21 "Dynamic Plastic Analysis Using Stress Resultant Finite Element Formulation," by P. Lukkunapvasit and J.M. Kelly 1977

UCB/EERC-77/22 "Preliminary Experimental Study of Seismic Uplift of a Steel Frame," by R.W. Clough and A.A. Huckelbridge - 1977

UCB/EERC-77/23 "Earthquake Simulator Tests of a Nine-Story Steel Frame with Columns Allowed to Uplift," by A.A. Huckelbridge - 1977

UCB/EERC-77/24 "Nonlinear Soil-Structure Interaction of Skew Highway Bridges," by M.-C. Chen and Joseph Penzien - 1977

UCB/EERC-77/25 "Seismic Analysis of an Offshore Structure Supported on Pile Foundations," by D.D.-N. Liou - 1977

UCB/EERC-77/26 "Dynamic Stiffness Matrices for Homogeneous Viscoelastic Half-Planes," by G. Dasgupta and A.K. Chopra - 1977

UCB/EERC-77/27 "A Practical Soft Story Earthquake Isolation System," by J.M. Kelly and J.M. Eidinger - 1977

UCB/EERC-77/28 "Seismic Safety of Existing Buildings and Incentives for Hazard Mitigation in San Francisco: An Exploratory Study," by A. J. Meltsner - 1977

UCB/EERC-77/29 "Dynamic Analysis of Electrohydraulic Shaking Tables," by D. Rea, S. Abedi-Hayati and Y. Takahashi - 1977

UCB/EERC-77/30 "An Approach for Improving Seismic-Resistant Behavior of Reinforced Concrete Interior Joints," by B. Galunic, V.V. Bertero and E.P. Popov - 1977

UCB/EERC-78/01 "The Development of Energy-Absorbing Devices for Aseismic Base Isolation Systems," by J.M. Kelly and D.F. Tsztoo 1978

UCB/EERC-78/02 "Effect of Tensile Prestrain on the Cyclic Response of Structural Steel Connections," by J.G. Bouwkamp and A. Mukhopadhyay - 1978

UCB/EERC-78/03 "Experimental Results of an Earthquake Isolation System using Natural Rubber Bearings," by J.M. Eidinger and J.M. Kelly - 1978

UCB/EERC-78/04 "Seismic Behavior of Tall Liquid Storage Tanks," by A. Niwa 1978

UCB/EERC-78/05 "Hysteretic Behavior of Reinforced Concrete Columns Subjected to High Axial and Cyclic Shear Forces," by S.W. Zagajeski, V.V. Bertero and J.G. Bouwkamp - 1978

UCB/EERC-78/06 "Inelastic Beam-Column Elements for the ANSR-I Program," by A. Riahi, D.G. Row and G.H. Powell - 1978

UCB/EERC-78/07 "Studies of Structural Response to Earthquake Ground Motion," by O.A. Lopez and A.K. Chopra - 1978

UCB/EERC-78/08 "A Laboratory Study of the Fluid-Structure Interaction of Submerged Tanks and Caissons in Earthquakes," by R.C. Byrd - 1978

UCB/EERC-78/09 "Models for Evaluating Damageability of Structures," by I. Sakamoto and B. Bresler - 1978

UCB/EERC-78/10 "Seismic Performance of Secondary Structural Elements," by I. Sakamoto - 1978

UCB/EERC-78/11 Case Study--Seismic Safety Evaluation of a Reinforced Concrete School Building," by J. Axley and B. Bresler 1978

UCB/EERC-78/12 "Potential Damageability in Existing Buildings," by T. Blejwas and B. Bresler - 1978

UCB/EERC-78/13 "Dynamic Behavior of a Pedestal Base Multistory Building," by R. M. Stephen, E. L. Wilson, J. G. Bouwkamp and M. Button - 1978